Transcriptional profiling of mRNAs, microRNAs and mitochondrial-nuclear crosstalk in porcine muscle fibers, mitochondrial respiratory and metabolic enzyme activities

Inaugural-Dissertation

zur

Erlangung des Grades

Doktor der Agrarwissenschaft

(Dr. agr.)

der

Landwirtschaftlichen Fakultät

der

Rheinischen Friedrich-Wilhelms-Universität Bonn

von

Xuan Liu

aus

Shandong, China

Bonn 2017

Dedicated to my beloved parents

Abstract

Skeletal muscle is a highly metabolically active tissue and has market value in meat-producing farm animals. The overall aim of this thesis is to deeply investigate the biological functions and pathways associated with muscle fiber types, mitochondrial respiration, glycolytic and oxidative enzyme activities in porcine muscle. Firstly, the transcriptional profile of longissimus biopsies 24h *ante mortem* was investigated in malignant hyperthermia syndrome (MHS)-negative Duroc and Pietrain (PiNN) pigs significantly distinct in muscle fiber types and mitochondrial respiration. Differential gene expression analysis and weighted gene co-expression network analysis (WGCNA) revealed clear differences in muscle metabolic properties between two breeds and identified many biological pathways associated with fiber types and metabolic enzyme activities. To explore the regulatory role of microRNAs (miRNAs) in energy metabolism, the miRNA expression profiles were investigated in the same muscle samples. The miRNA-mRNA regulatory networks related to muscle fiber type, metabolic enzyme activity and ATP production were modelled based on *in silico* prediction of target mRNAs and correlation of expression and phenotypic measurements of muscles in Duroc and PiNN pigs. These complex networks may contribute to the muscle phenotypic variations by fine-tuning gene expressions. Next, the expression profiles of pathway-focused genes related to oxidative and glycolytic pathways were analyzed in conjunction with phenotypic measurements in four pig breeds with distinct metabolic types including Duroc, PiNN, Pietrain homozygous-positive for MHS (PiPP) and an F2 Duroc-Pietrain crossbred homozygous-negative for MHS (DuPi) using longissimus biopsies. At transcript level, lactate dehydrogenase B showed breed specificity, with significantly lower expression in PiPP pigs. A similar mRNA expression pattern was observed for several subunits of oxidative phosphorylation (OXPHOS) complexes, including complex I, complex II, complex IV and ATP synthase. The expressions of these pathway-focused genes were well correlated to their enzyme activities and muscle fiber composition in a breed-dependent manner. These results stressed the importance of transcriptional regulation of genes involved in metabolic pathways especially OXPHOS system in muscle fibers. Finally, in order to address the role of mitochondria, early *post mortem* longissimus samples taken from the same four breeds were used to investigate mitochondrial DNA content, haplotypes and gene expressions of OXPHOS subunits. PiPP pigs carried only one haplotype (Haplotype 8) and showed the lowest absolute mtDNA copy number, the lowest

abundance of transcripts of many mitochondrial and nuclear encoded OXPHOS subunits among all four breeds. The results were informative for the understanding of haplotype and breed-specific mitochondrial content variation and molecular basis of OXPHOS pathway. The co-expression pattern of OXPHOS genes supported the mitochondrial-nuclear crosstalk and their complexity contributed to muscular metabolism. This part of the study highlighted the importance of mitochondrial-nuclear crosstalk, haplotype and copy number variation underlying muscle phenotype differences. In summary, muscle energy metabolism was investigated in this thesis by the whole genome transcriptional profiling of mRNAs and miRNAs followed by a focus on OXPHOS system at the level of both nuclear and mitochondrial DNA contributing to phenotypic variations in different pig breeds. These findings provided insights into the molecular regulatory patterns involved muscular energy metabolism which may be used as biomarkers to predict meat quality and/or diagnose muscular diseases.

Kurzfassung

Skelettmuskel ist ein metabolisch hochgradig aktives Gewebe und ist von Marktwert bei Fleisch produzierenden Nutzieren. Die allgemeine Zielsetzung dieser Arbeit ist die eingehende Untersuchung der biologischen Funktionen und Stoffwechselwege, welche mit Muskelfasertypen, mitochondrieller Atmung, sowie glykolytischen und oxidativen Enzymaktivitäten im Schweinemuskel assoziiert sind. Zunächst wurde das Transkriptionsprofil von Longissimus-Biopsien 24 h ante mortem in malignen Hyperthermie-Syndrom (MHS) –negativen Duroc und Pietrain (PiNN) –Schweinen untersucht, welche sich signifikant hinsichtlich Muskelfasertypen und mitochondrieller Atmung unterscheiden. Differentielle Genexpressionsanalyse und weighted gene co-expression network analysis (WGCNA) offenbarten deutliche Unterschiede hinsichtlich der muskulären Stoffwechseleigenschaften zwischen den beiden Rassen und identifizierten zahlreiche biologische Stoffwechselwege, die mit den Fasertypen und metabolischen Enzymaktivitäten assoziiert waren. Zur Untersuchung der regulatorischen Rolle von MicroRNAs (miRNAs) im Energiestoffwechsel wurden die miRNA-Expressionsprofile in den gleichen Proben untersucht. Die mit Muskelfasertyp, metabolischer Enzymaktivität und ATP-Produktion in Zusammenhang stehenden miRNA-mRNA-regulatorischen Netzwerke wurden durch Korrelation von exprimierten miRNAs und *in silico* identifikation Ziel-mRNAs sowie phänotypischen Messungen von Muskeln bei Duroc- und PiNN-Schweinen modelliert. Diese komplexen Netzwerke könnten durch Feinabstimmung der Genexpression zu den phänotypischen Variationen des Muskels beitragen. Als nächstes wurden die Expressionsprofile von Stoffwechselweg-bezogenen Genen analysiert, welche mit oxidativen und glykolytischen Stoffwechselwegen in Verbindung stehen, zusammen mit phänotypischen Messungen an Longissimus-Biopsien von vier Schweinerassen mit distinkten Stoffwechseltypen, darunter Duroc, PiNN, Pietrain homozygot-positiv für MHS (PiPP) und eine F2-Kreuzung Duroc-Pietrain homozygot-negativ für MHS (DuPi) untersucht. Auf Transkript-Ebene zeigte die Laktat-Dehydrogenase B eine rassespezifische Expression, mit signifikant niedrigeren Werten bei PiPP-Schweinen. Ein ähnliches mRNA-Expressionsmuster konnte für verschiedene Untereinheiten des oxidativen Phosphorylierungskomplexes (OXPHOS-Komplex), einschließlich Komplex I, Komplex II, Komplex IV und ATP-Synthase beobachtet werden. Die Expression dieser Stoffwechselweg-bezogenen Gene korrelierte gut mit ihren enzymatischen Aktivitäten und ihrer Muskelfaser-Zusammensetzung in einer rasseabhängigen Weise. Diese Ergebnisse

betonen die Bedeutung der Transkriptionsregulation von Genen, die an metabolischen Stoffwechselwegen beteiligt sind, insbesondere am OXPHOS-System in Muskelfasern. Schlussendlich wurden frühe post mortem Longissimus-Proben aus den gleichen vier Rassen verwendet, um den mitochondriellen DNA-Gehalt, die Haplotypen sowie die Genexpression von OXPHOS-Untereinheiten zu untersuchen. PiPP-Schweine, die nur einen Haplotyp (Haplotyp 8) trugen, wiesen unter allen vier Rassen die niedrigste absolute mtDNA-Kopienzahl und die am geringste Abundanz von Transkripten von vielen mitochondriell und nuklear kodierter OXPHOS-Untereinheiten auf. Die Ergebnisse helfen beim Verständnis der haplotyp- und rassespezifischen Variation des mitochondriellen DNA-Gehalts sowie der molekularen Basis des OXPHOS-Weges. Das Ko-Expressionsmuster von OXPHOS-Genen unterstützte die mitochondriell-nukleäre Interaktion und ihre Komplexität trug zum muskulären Stoffwechsel bei. Dieser Teil der Studie hebt die grundlegende Bedeutung der Interaktion zwischen Mitochondrien und Zellkern, des Haplotyps sowie der Variation der Kopienzahl für muskuläre Phänotyp-Unterschiede hervor. Zusammenfassend wurde in dieser Arbeit der muskuläre Energiestoffwechsel mittels whole genome transcriptional profiling von mRNAs und miRNAs untersucht, gefolgt von einer Fokussierung auf das OXPHOS-System sowohl auf Ebene der mitochondriellen als auch auf jener der nukleären DNA, welche zur phänotypischen Variation in verschiedenen Schweinerassen beitragen. Diese Erkenntnisse liefern Einblicke in die molekularen Regulationsmuster, die in den muskulären Energiestoffwechsel involviert sind und als Biomarker für die Vorhersage von Fleischqualität und/oder zur Diagnose muskulärer Erkrankungen herangezogen werden können.

Contents

CHAPTER 1

Introduction

1.1 Structure and muscle fiber types of skeletal muscle

Skeletal muscle is a highly metabolically active tissue that both stores and consumes energy. It stores amino acids, carbohydrates and other substances, produces heat for the maintenance of body temperature and consumes the majority of energy during physical activity (Frontera and Ochala 2015). The structure of skeletal muscle is characterized by well-organized muscle fibers and connective tissue. The structure of a single muscle fiber is shown in Figure 1.1. Each muscle fiber is made of thousands of highly organized cylindrical myofibrils. Sarcomere is the basic contractile unit of skeletal muscle. In myofibrils, there are dense protein bands called A-band and less dense bands called I-band. I-bands are bisected by Z-discs in order to form sarcomeres. A-band is made up of thick filaments containing mainly myosin, whereas I-band is made up of thin filaments containing mainly actin, tropomyosin and troponin (Frontera and Ochala 2015). The globular heads of myosin in thick filaments make contact with actin in thin filaments and catalyze the hydrolysis of ATP to release energy during muscle contraction (Huff Lonergan et al. 2010). Other elements in the sarcoplasm of muscle fiber such as mitochondria and sarcoplasmic reticulum (SR) are crucial. For example, mitochondria produce the majority of ATP through oxidative phosphorylation in muscle cells, whereas SR is responsible for the maintaining of calcium homeostasis through the sarcoplasmic reticulum Ca^{2+}-ATPase (SERCA) and calsequestrin. Both ATP production and Ca^{2+} homeostasis are important for muscle contraction, energy metabolism and meat quality (Huff-Lonergan and Lonergan 2005; Shen et al. 2007; Yue et al. 2003).

Muscle fibers are commonly classified into three types including type I slow-twitch oxidative (STO) fibers, type IIA fast-twitch oxidative (FTO) fibers and type IIB fast-twitch glycolytic (FTG) fibers based on their contractile properties and metabolic characteristics (Hocquette et al. 1998). Different criteria could apply to muscle fiber classification such as 1) color of muscle fibers correlates with myoglobin content (red vs white) 2) speed of shortening during a single twitch (slow vs fast) 3) predominance of metabolic pathways (oxidative vs glycolytic) 4) enzyme histochemical stain reactions based on myofibrillar ATPase and Succinate dehydrogenase staining techniques and 5) myosin heavy chain (MHC) isoform expression, etc (Frontera and Ochala 2015). In general, muscle containing high proportion of STO fibers is often associated with high oxidative enzyme activities (Gueguen et al. 2005), large amount of mitochondria, myoglobin and fat, whereas a high ratio of FTG fibers is associated with high glycolytic enzyme activities (Huber et al. 2007;

Ma et al. 2015; Werner et al. 2010b). The FTO fibers have intermediate characteristics between STO and FTG fibers and display both oxidative and glycolytic capacities. The diversity of muscle fibers plays important roles in metabolic properties and muscle development of farm animals. Different pig breeds display distinct muscle fiber compositions. For example, the Berkshire pigs contain a significantly higher percentage of type I fibers than Landrace, Yorkshire and crossbred pigs (Ryu et al. 2008). The mRNA levels of oxidative and intermediate fibers are elevated in Korean native pigs, whereas the glycolytic fibers are highly expressed in Landrace and Yorkshire pigs (Kim et al. 2008).
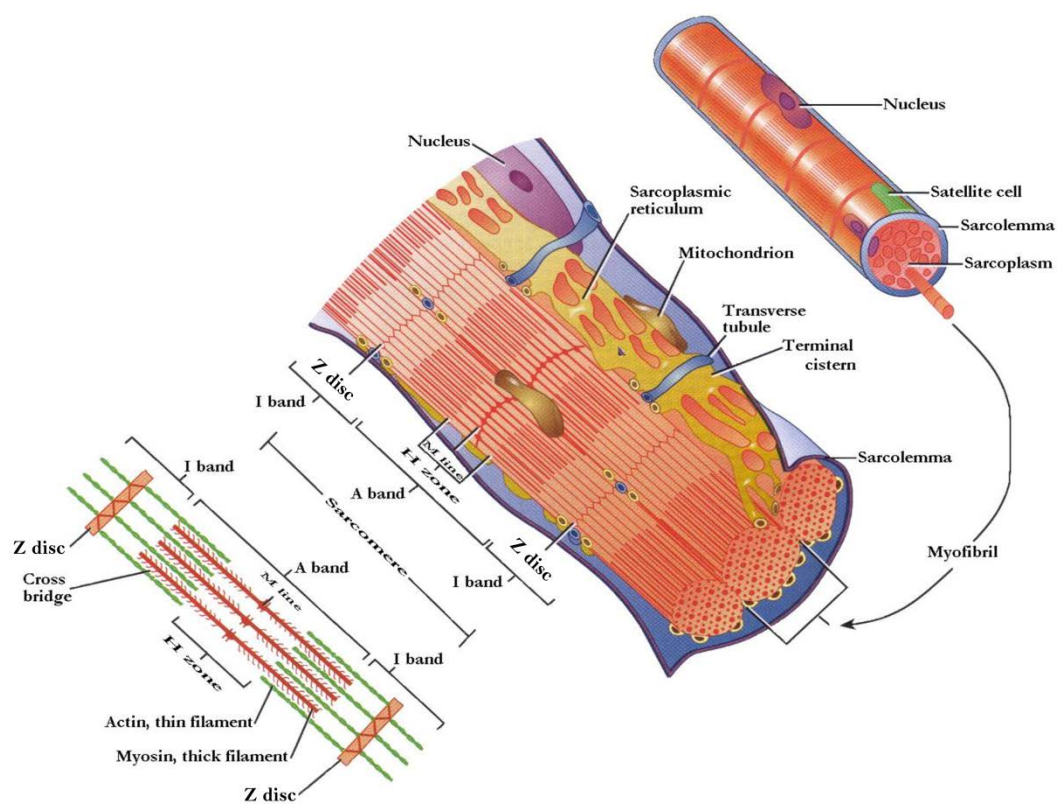
Figure 1.1 The structure of a skeletal muscle fiber (adapted from http://ag.arizona.edu/classes/ans215/lectures/MuscularSystemVI.ppt)

1.2 Overview of energy metabolism in skeletal muscle

The muscle activity requires energy through anabolism and catabolism of glycogen, carbohydrates, and fat, all of which are important resources for energy storage and supply. Adenosine triphosphate (ATP) is the major molecule in energy metabolism. It is produced mainly in mitochondria and used for various energy expenditure processes including muscle contraction, cell maintenance, protein deposition and thermogenesis (Hocquette et

al. 1998). Meat quality parameters such as pH, tenderness, juiciness and water-holding capacity are determined by muscle energy metabolism.

1.2.1 ATP production

Most of ATP is generated through cellular respiration which consists of glycolysis, pyruvate processing, tricarboxylic acid (TCA) cycle (also known as citric acid cycle) and oxidative phosphorylation (OXPHOS) in mitochondria (Figure 1.2). When oxygen is deficient or depleted, such as exhaustive exercise or even death after slaughter in meat-producing animals, anaerobic glycolysis can break down pyruvate into lactate. This process takes place in the cytoplasm with a high cost since the ATP synthesis is less efficient than aerobic metabolism. After slaughter, the oxygen supply of muscle tissues stops. ATP production is shifted from an aerobic environment to an anaerobic environment. The accumulation of end-product lactic acid decreases intracellular pH and hampers the muscle fibers and cells.

1.2.2 Mitochondria and oxidative phosphorylation

Mitochondria are sub-cellular double membrane bound organelles which are involved in many metabolic tasks such as ATP synthesis, calcium signaling, apoptosis, beta-oxidation of fatty acids and the generation of reactive oxygen species. Mitochondria carry their own genetic material. Mitochondrial DNA (mtDNA) is double-stranded and circular. For pigs, the mtDNA is 16,613 base pairs in length and encodes for 37 genes including 12S and 16S rRNAs, 22 tRNAs and 13 subunits of OXPHOS system (Lin et al. 1999). A mitochondrion contains outer membranes (OM) and inner membranes (IM) composed of phospholipid bilayers and proteins. The intermembrane space (IMS) is the space between OM and IM which makes up the electrochemical gradient in mitochondria. Glycolysis splits the glucose into pyruvate in the cytosol. Then TCA cycle is carried out by 8 enzymes that completely oxidize acetyl-coA into two molecules of carbon dioxide together with nicotinamide adenine dinucleotide (NADH) and flavin adenine dinucleotide (FADH2) in the matrix of the mitochondrion. Most of the ATP is produced through oxidative phosphorylation. There are five enzymes complexes locating at the IM in OXPHOS system (Figure 1.3). They are complex I (NADH dehydrogenase), complex II (succinate dehydrogenase), complex III (cytochrome c reductase /cytochrome bc_1), complex IV (cytochrome c oxidase) and complex V (ATP synthase). Subunits of complex I, III, IV and ATP synthase are encoded by both nuclear and mitochondrial DNA. The nuclear encoded OXPHOS complex subunits

need to be processed, imported into mitochondria and assembled with mitochondrial encoded subunits to form a functional OXPHOS system via chaperones, translocases and mitochondrial inner membrane proteins (Bonnefoy et al. 2009; Neupert and Herrmann 2007; Smits et al. 2010; Voos and Rottgers 2002). The electrons are passed from an electron donor such as NADH to an electron acceptor such as oxygen through the electron transport chain (complex I to IV). It is coupled to ATP production by protons pumping into the intermembrane space and moving back to the matrix through ATP synthase complex. ATP synthase is comprised of two subunits, which are membrane extrinsic F1 catalytic part and membrane-embedded F0 part. The two subunits are worked in cooperation to generate ATP through mechanical rotation (Noji and Yoshida 2001). Mitochondrial electron transport chain is an important source of reactive oxygen species (ROS) within most mammalian cells (Grivennikova and Vinogradov 2006; Murphy 2009). Excess amount of ROS could result in oxidative stress, aging, muscle fatigue and dysfunction (Zuo and Pannell 2015). However, the optimal level of ROS is critical for biological function by facilitating glucose uptake or inducing mitochondrial biogenesis (Merry et al. 2010; Powers et al. 2011).

Mitochondrial genetic variation can affect fertility, longevity and metabolic performances in many species such as raccoon dogs, cows and pigs (Camus et al. 2015; Shi et al. 2010). Mitochondrial DNA haplotypes are potential genetic sources for manipulating phenotypes including tolerance to heat, growth and milk quality in farm animals (Tsai and St John 2016). In Drosophila, mtDNA genome variation is proposed to modulate mtDNA copy number (Salminen et al. 2017). Mitochondrial DNA (mtDNA) copy number has been demonstrated to be associated with extensive exercise, age-related hearing impairment, disordered antioxidant capacity and heart failure (Baykara et al. 2016; Falah et al. 2016; Gao et al. 2016; Huang et al. 2016). Therefore, it would be interesting to investigate the influence of mitochondrial haplotypes on mtDNA copy number variation and porcine energy metabolism. Further, the mitochondrial function can be influenced by the transcriptional regulation of OXPHOS subunits and the mitochondrial-nuclear interaction in order to assemble a fully functional OXPHOS system. Unlike nucleus, mitochondrial transcription occurs bidirectionally to produce polycistronic transcript precursors which are cleaved and processed into individual mRNAs, tRNAs and rRNAs (Rebelo et al. 2011). The variations between mRNA levels of mitochondrial encoded genes were caused by post-transcriptional regulation such as miRNAs.

Figure 1.2 Overview of ATP production (adapted from
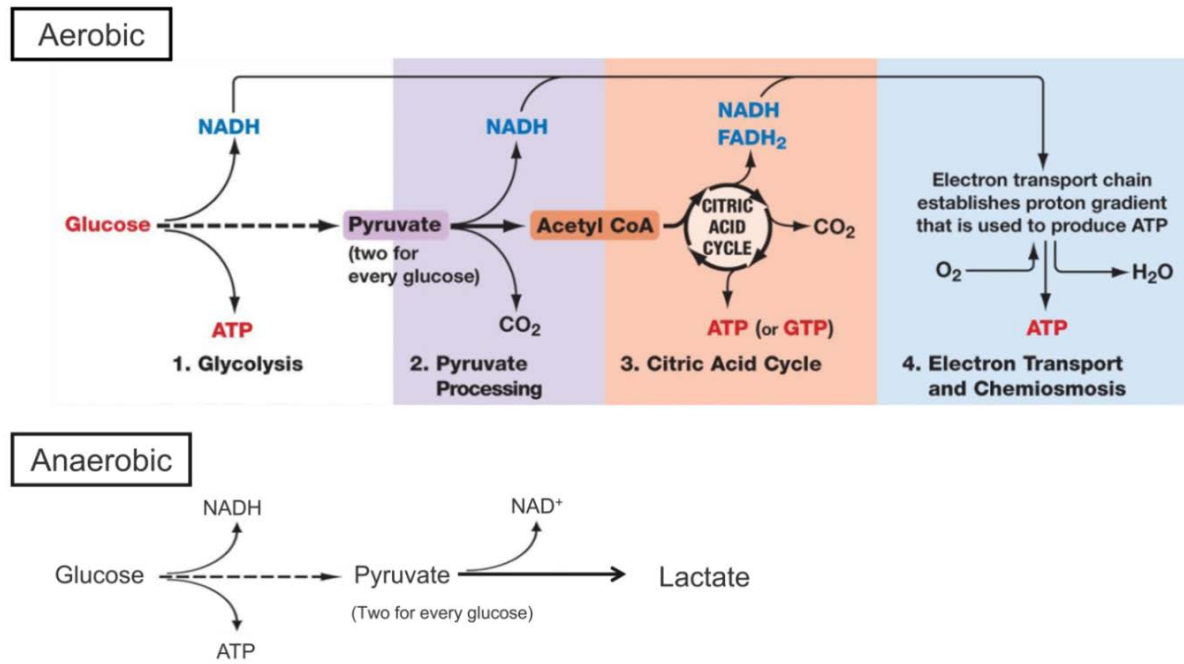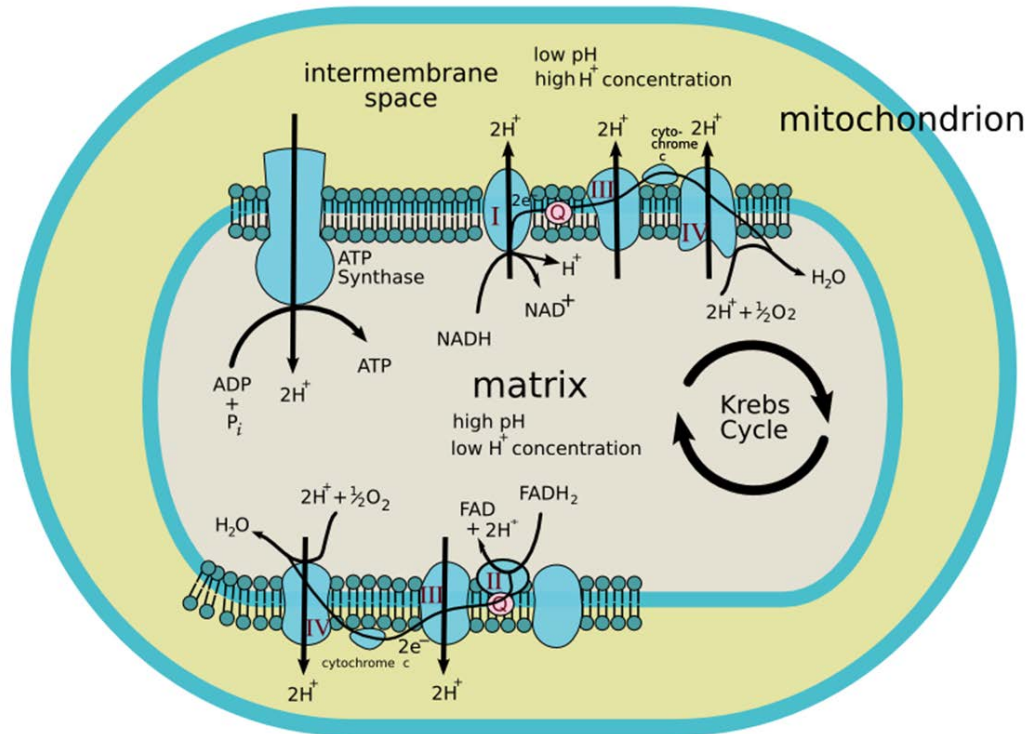http://www.uic.edu/classes/bios/bios100/lectures/respiration.htm)

Figure 1.3 The oxidative phosphorylation system in mitochondria (adapted from
https://commons.wikimedia.org/wiki/File:Mitochondrial_electron_transport_chain.png)

1.3 Relationship between energy metabolism and meat quality

Consumers purchase meat based on meat quality parameters such as the color, flavor, tenderness and juiciness. Muscle fiber composition, metabolic capacities, and fat content are factors that have been found to influence meat quality (Hocquette et al. 1998). In 2004, muscle fiber traits were proposed as additional selection criteria for muscle growth and meat quality in pigs (Fiedler et al. 2004). In general, muscles comprised of more STO fibers are associated with higher oxidative enzyme activities and mitochondrial respiration activity (Gueguen et al. 2005), whereas muscles containing more FTG fibers are associated with higher glycolytic enzyme activities (Huber et al. 2007; Werner et al. 2010b). The oxidative pathways are involved in the determination of meat color. For example, fresh meat color intensity primarily depends on the pigment contents such as hemoglobin and myoglobin which are higher in red muscles than these in white muscles and the oxidation state of the pigments (Pearson and Dutson 1994). Further, lipids are mainly stored in STO fibers (Essen-Gustavsson et al. 1994) which can improve the tenderness and juiciness of the meat. Besides the oxidative metabolism, the glycolytic pathways, such as the conversion from muscle glycogen to lactic acid, could determine the meat ultimate pH and lead to muscle ache, cell damage or impaired tenderness and flavor (Hocquette et al. 1998; Hocquette et al. 2001). Hence the quantities of glycogen content and fat deposition associated with different muscle fiber types are critical for meat quality. Pig breeds such as Pietrain pigs, which contain more FTG fibers, are usually more muscular. Thereby Pietrain pigs are more favorable for meat producer. The selection towards a high percentage of FTG fibers may result in altered meat quality possibly due to lower capillarization, insufficient delivery of oxygen (Karlsson et al. 1999) and glycogen depletion which ultimately cause dry, firm and dark meat (Karlsson et al. 1994). Mitochondria isolated from muscle immediately after slaughter are similar to those found in intact muscle, whereas some mitochondria from pale, soft, exudative (PSE) muscle are already swollen and show a decreased matrix density (Greaser et al. 1969). With an emphasis placed on glycolysis, mitochondrial content and function may be important factors contributing to *post mortem* muscle metabolism (Scheffler et al. 2015). Therefore, energy metabolism has to be properly regulated for optimal metabolic functions related to meat quality. The understanding of the molecular basis of metabolic capacity before and after slaughter is important for the manipulation of muscle metabolism to improve meat quality.

1.4 Roles of microRNAs in skeletal muscle

MicroRNAs (miRNAs) are endogenous small non-coding RNAs ~22 nt in length that post-transcriptionally regulate gene expression (Figure 1.4). In animals, miRNAs are initially generated in nucleus and processed into an approximately 70 nt long stem-loop structure (Pasquinelli 2012). Then it is exported to cytoplasm and further processed by Dicer to generate miRNA/miRNA duplexes. One strand of the duplex is incorporated with Argonaute to form RNA-Induced Silencing Complex (RISC) in order to target mRNAs, whereas the other strand is usually discarded (Shukla et al. 2011). MiRNAs bind mRNAs via complementary base pairing, typically to their 3'UTR with many cases to coding sequences and 5' UTR, and regulate gene expression by either degradation of mRNA or repression of translation (Shukla et al. 2011). Unlike plant miRNAs (Chen 2009), the imperfectly base pairing between miRNA and its target gene is very common in animals. 'Seed sequence' locates at positions 2-8 from the 5'-end of miRNA and it is commonly perfect pairing with target site (Pasquinelli 2012). Several computational prediction tools are available to identify any potential target genes for miRNAs such as TargetScan (http://www.targetscan.org/) (Lewis et al. 2005) and RNAhybrid (http://bibiserv.techfak.uni-bielefeld.de/rnahybrid/) (Rehmsmeier et al. 2004). TargetScan detects targets by searching for the region of transcripts that match the seed sequence of miRNAs whereas RNAhybrid finds the minimum free energy hybridization of a long and a short RNA.

MiRNAs have been shown to play critical roles in various biological processes of skeletal muscle such as myogenesis, adipogenesis and muscle development, etc (Hou et al. 2012; Huang et al. 2008; Li et al. 2012; McDaneld et al. 2009). Further, miRNAs such as miR-133, miR-221 and miR-103 are associated with porcine meat quality (Ponsuksili et al. 2013). The polymorphisms in the porcine miR-133 and miR-208 are proposed as a genetic factor affecting muscle fibers and meat quality traits (Kim et al. 2015; Lee et al. 2013). Since energy metabolism is linked to meat quality, it is helpful to understand the regulatory role of miRNAs in muscle energy metabolism. MiR-499 and miR-130b play a dominant role in the specification of muscle fiber type by promoting the oxidative slow-twitch fiber formation (Chen et al. 2015; Lin et al. 2002; Liu et al. 2015; von Hofsten et al. 2008). MiR-130b, miR-15a and miR-15b could modulate the ATP levels in muscle cells (Nishi et al. 2010; Siengdee et al. 2015). Researchers have shown that miR-210 and miR-338 directly regulate the gene expression level of OXPHOS subunits including complex IV subunits *COX10*, *COXIV* and ATP synthase subunits *ATP5G1* (Aschrafi et al. 2012; Chen

et al. 2010) to alter mitochondrial function and ATP production. In addition, miRNAs such as miR-15a and miR-16 are involved in the regulation of mitochondrial-mediated apoptosis (Gao et al. 2010; Liu et al. 2014; Tang et al. 2015). Moreover, miR-696 is associated with fatty acid oxidation and mitochondrial biogenesis by regulating the expression of the master regulator peroxisome proliferator-activated receptor-gamma coactivator-1alpha (*PGC-1α*) (Aoi et al. 2010). With those miRNAs identified, the lack of a comprehensive and systematic miRNA profiling associated with energy metabolism of porcine skeletal muscle remains unraveled.
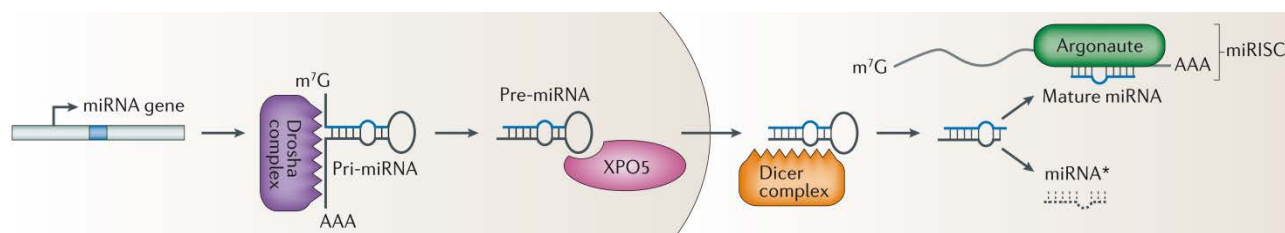
Figure 1.4 The biogenesis of miRNAs (Pasquinelli 2012)

1.5 Research aims

Evidences demonstrate that muscle energy metabolism could influence meat quality parameters such as meat color, flavor and tenderness. The overall objective of this study is to reveal and integrate the mRNA and miRNA expression profiles of porcine skeletal muscle, followed by metabolic pathway focused analysis as well as mitochondrial-nuclear crosstalk in order to identify candidate miRNAs and their target genes which influence muscle fiber type, mitochondrial respiration, metabolic enzyme activity and ATP production. It will provide a better understanding for the molecular mechanism of muscle energy metabolism.

The objectives of the study can further be detailed as following:

Aim 1: to investigate gene expression profile and identify biological functions and pathways associated with muscle fiber, mitochondrial respiratory activity and metabolic enzyme activity in pig skeletal muscle

Aim 2: to investigate microRNA expression profile and construct regulatory miRNA-mRNA network associated with mitochondrial respiratory and metabolic enzyme activity in muscle

Aim 3: to identify molecular changes in mitochondrial respiratory activity and metabolic enzyme activity via a pathway-focused gene expression profiling in muscle of four pig breeds with distinct metabolic types

Aim 4: to investigate mitochondrial-nuclear crosstalk, haplotype and copy number variation in porcine muscle fiber type, mitochondrial respiratory and metabolic enzyme activities

CHAPTER 2

Materials and methods

2.1 Experimental design

This study used longissimus muscle samples taken from four pig breeds including Duroc, Pietrain homozygous-negative for malignant hyperthermia susceptibility (MHS) (PiNN), Pietrain homozygous-positive for MHS (PiPP) and an F2 Duroc-Pietrain crossbred homozygous-negative for MHS (DuPi) at 24h *ante mortem*, 0min and 30min *post mortem*. The measurements of phenotypes were performed previously (Krischek et al. 2011; Werner et al. 2010a; Werner et al. 2010b). The phenotypic traits included porcine muscle fiber composition (STO, FTO and FTG), mitochondrial respiratory activity, metabolic enzyme activities and adenine nucleotide concentration (IMP, AMP, ADP and ATP). Metabolic enzymes contained glycogen phosphorylase (GP), phosphofructokinase (PFK), lactate dehydrogenase (LDH), citrate synthase (CS), complex I, complex II, complex IV and ATP synthase.

The experimental design in this thesis is shown in Figure 2.1. It consists of four parts including 1) dissection of mRNA profile of biopsies in Duroc and PiNN pigs, 2) construction of energy metabolism associated miRNA-mRNA network using biopsies of Duroc and PiNN pigs, 3) pathway-focused gene expression profiling using biopsies of four pig breeds Duroc, DuPi, PiNN and PiPP, and 4) quantification of mtDNA copy number, mitochondrial and nuclear encoded OXPHOS gene expression using muscle samples collected from two *post mortem* time points in all four pig breeds harboring different mitochondrial haplotypes. The absolute mtDNA copy number was quantified by the standard curve method without co-amplification of nuclear mitochondrial DNA sequences. The first two parts were achieved using whole genome approaches Affymetrix porcine snowball array and Affymetrix genechip miRNA 3.0 array by weighted gene co-expression network analysis, ANOVA and pairwise correlation to analyze the global mRNA and miRNA expressions. In the last two parts, porcine OXPHOS system were deeply investigated via haplotypes, mitochondrial DNA content, OXPHOS gene expression and their association with phenotypes of interest at both nuclear and mitochondrial genome levels before and after slaughter. Hence in this thesis, the molecular basis of muscle energy metabolism was investigated from whole genome to pathway specific, from nuclear genome to mitochondrial genome, from *ante mortem* to *post mortem*. The detailed methodological information can be found in the published scientific paper (see Annex A.1, A.2, A.3, A.4). The main methods with descriptions are briefly summarized in this chapter.
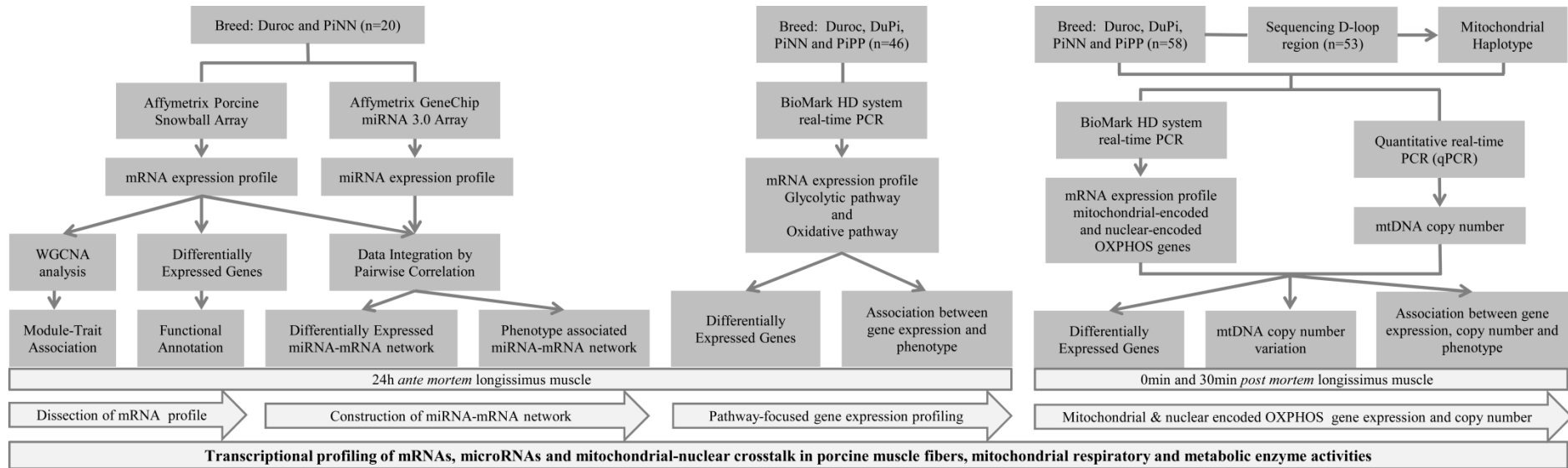
Figure 2.1 An overview of experimental design

2.2 Sample collection and phenotypic measurement

The experiment and muscle collection were approved and authorized under the German and European animal welfare regulations for animal husbandry, transport, and slaughter (Krischek et al. 2011; Werner et al. 2010a; Werner et al. 2010b). All experimental procedures, including animal care and tissue sample collection, followed guidelines for safeguarding and good scientific practice in accordance with the German Law of Animal Protection, officially authorized by the Animal Care Committee and authorities [Niedersächsischen Landesamt für Verbraucherschutz und Lebensmittelsicherheit (LAVES) 33.42502/01-47.05]. Duroc, PiNN, PiPP, and DuPi pigs were raised to the age of 180 days at the University of Bonn. Muscle samples from each breed were collected one day before slaughter (24h *ante mortem*), immediately (0min *post mortem*) and 30min after stunning (30min *post mortem*) from longissimus muscle (LM) between the 13th and 14th thoracic vertebrae. Samples were frozen in liquid nitrogen and stored at –80 °C until analysis. The applied methods for all phenotypical traits were measured as described previously (Krischek et al. 2011; Werner et al. 2010a; Werner et al. 2010b) and described in publications (see Annex A.1, A.2, A.3, A.4).

2.3 Approaches for Aim 1

2.3.1 DNA microarray analysis

The microarray-based transcription profiling was performed in longissimus muscle samples obtained 24h before slaughter from Duroc and Pietrain pigs using Porcine Snowball Array (Affymetrix) containing 47,880 probe-sets. Expression Console software was used for robust multichip average (RMA) normalization and the detection of present genes by applying the DABG (detection above background) algorithm. Further filtering was done by excluding transcripts with low signals and probes that were present in less than 80% of the samples within each breed. 17,820 probes passed the quality filtering and were used for further analysis. Differential expression analysis was performed using the ANOVA procedure in JMP genomics 7 (SAS Institute). The breed was treated as a fixed effect. False discovery rate (FDR) was used to control an error rate of a multiple-hypothesis testing according to Benjamini and Hochberg (Benjamini and Hochberg 1995).

2.3.2 Weighted gene co-expression network analysis (WGCNA)

WGCNA is a powerful approach to identify genes sharing similar functions and/or involved in related molecular events. It was used to identify pathways associated with muscle fiber types and activities of glycolytic and oxidative enzymes. Post-filter, 17,820 probes were utilized in the construction of weighted gene co-expression networks using the blockwise modules function in the WGCNA R package as described previously (Langfelder and Horvath 2008; Ponsuksili et al. 2013; Zhang and Horvath 2005). The analysis was applied separately for each breed. It firstly grouped genes into a module based on their co-expression pattern. To achieve this, the WGCNA procedure calculated a Pearson correlation matrix for all genes and then an adjacency matrix was calculated by raising all values to power β from the correlation matrix. By inspecting the scale-free topology model fit, the minimal β value giving a coefficient of determination R^2 higher than 90% was selected as the power β. The adjacency matrix was converted to a topological overlap matrix (TOM) and the TOM-based dissimilarity matrix for hierarchical clustering. The gene co-expression modules were identified from the hierarchical cluster tree using a dynamic tree cut procedure. The formula of topological overlap matrix (TOM) $\Omega = [\omega_{ij}]$ was as follows,

$$\omega_{ij} = \frac{a_{ij} + \sum_u a_{iu} a_{uj}}{min\{\sum_u a_{iu}, \sum_u a_{ju}\} + 1 - a_{ij}}, \; a_{ij} = \left|cor(x_i, x_j)\right|^{\beta} \tag{1}$$

where x_i and x_j were the gene expression profile of the x_i-th and x_j-th gene and a_{ij} was the adjacency. Modules were further merged based on the dissimilarity between their eigengenes, which were defined as the first principle component of each module. Eigengene acts as the representative for each module. Module-trait relationships were estimated using the correlation between module eigengene and phenotype to identify any gene co-expression module which was highly correlated to the phenotype.

2.3.3 Gene functional annotation and pathway analysis

The differentially expressed genes (DEGs) between Duroc and PiNN pigs were analyzed using the IPA software (Ingenuity Systems, http://www.ingenuity.com) to identify pathways related to phenotypic differences of the muscle between these two breeds. IPA categorizes genes based on annotated gene functions and statistical tests for over-representation of functional terms within the gene list using Fisher's Exact Test. Further, a gene list of each significant module-trait correlation was analyzed to obtain biologically meaningful represented pathways based on an enrichment score and p-value threshold

using IPA and the DAVID online-tool (Database for Annotation, Visualization and Integrated Discovery; https://david.ncifcrf.gov/).

2.4 Approaches for Aim 2

2.4.1   MicroRNA microarray analysis

The miRNA expression profile of the longissimus muscle samples 24h *ante mortem* from Duroc and PiNN pigs was determined by the Affymetrix GeneChip miRNA 3.0 Array (Affymetrix). It is comprised of 16,772 entries representing hairpin precursor, total 19,724 probe sets for detection of most miRNA from 153 species (miRBase V.17). Expression Console software was used for robust multichip average (RMA) normalization and the detection of present miRNAs by applying the DABG (detection above background) algorithm. Further filtering was done by excluding probes that were present in less than 70 % of the samples within each breed and annotated miRNAs that had sequence greater than or equal to 30nt in length. 3,587 probes passed the quality filtering and were used for further analysis.

2.4.2   Statistical and bioinformatics analysis

Differential expression analysis for miRNA was performed using the ANOVA procedure in JMP genomics 7 (SAS Institute). Breed was treated as a fixed effect. False discovery rate (FDR) was used to control an error rate of a multiple-hypothesis testing according to Benjamin & Hochberg (Benjamini and Hochberg 1995). The previous microarray-based mRNA expression data was used to integrate with the differentially expressed miRNAs and scan for potential target genes. Pearson correlation between miRNA and mRNA expression levels was calculated. RNAhybrid 2.1.2 and TargetScan 7.0 were used to predict targets of miRNAs. RNAhybrid (http://bibiserv.techfak.uni-bielefeld.de/rnahybrid) is computational software that detects the most energetically favorable hybridization sites of a small RNA within a large RNA (Kruger and Rehmsmeier 2006; Rehmsmeier et al. 2004). The miRNA probe sets were tested with the following parameters: number of hits per target = 1 and energy cutoff = −25 kcal/mol and maximal bulge loop size per side = 4. TargetScan (http://targetscan.org/) was used to predict the target genes based on complementarity of the miRNA seed sequence (position 2-8 of the miRNA 5´end) and target binding site on the 5´UTR, 3´UTR and protein coding region of the porcine mRNA sequences (Sus scrofa 10.2 download from NCBI: http://www.ncbi.nlm.nih.gov on 1.9.2015) (Lewis et al. 2005). Transcripts negatively correlated with miRNA and predicted

as potential targets were passed to functional analysis using IPA software as described previously.

In addition to the identification of differentially expressed miRNA-mRNA regulatory network, the correlation between individual miRNAs and phenotypical traits including muscle fiber type, mitochondrial respiratory activity, metabolic enzymes activity and adenosine phosphate concentrations were analyzed. Then the miRNA and mRNA profile were integrated based on their pairwise correlations and computational target prediction to construct the miRNA-mRNA networks associated with energy metabolism. The miRNA-mRNA network were constructed using the following criteria: 1) the expressions of both miRNAs and target mRNAs were significantly correlated to the phenotypical traits; 2) the gene expression level was negatively correlated with the expression of its miRNA regulator; 3) the gene was computationally predicted as a target gene of the corresponding miRNA.

2.5 Approaches for Aim 3

2.5.1   Quantitative real-time PCR (qPCR)

qPCR of all RNA samples (n = 46) was performed using fastgene expression analysis with EvaGreen dye on a BioMark HD real-time PCR system according to manufacturer's recommendations (Fluidigm). Briefly, cDNAwas synthesized from 2 μg of total RNA using Superscript II reverse transcriptase and oligo-dT (Invitrogen) with specific target amplification and exonuclease I (New England Biolabs) treatment. qPCR reactions were performed using a 48 × 48 dynamic array and integrated fluidic circuit. For each sample inlet, 2.5 μL of 2 × SsoFast EvaGreen supermix with low ROX (Biorad), 0.25 μL of 20 × DNA-binding dye sample loading reagent, and 2.25 μL of specific target amplification and exonuclease-I-treated sample were loaded. For each assay inlet, 2.5 μL of 2 × assay loading reagent, 2.25 μL of 1×DNA suspension buffer, and 0.25 μL of 100 μM mixed (forward and reverse) primers were loaded. All measurements were performed in duplicate. Thermal parameters were: 95 °C for 60 s, followed by 30 cycles of 95 °C for 5 s and 60 °C for 20 s.

2.5.2   Statistical analysis

Data were analyzed using SAS 9.3 statistical software (SAS Institute) and the GLM procedure. The statistical model included effects of breed, gender, and breed–gender

interaction. Post hoc Tukey–Kramer method was used for multiple comparison adjustments. Results were reported as least-squares means (Lsmeans) with standard error (SE) and considered to be statistically significant if $p < 0.05$. Correlation coefficient (r) between gene expression and phenotypic measurement was calculated separately for each breed and in combination of all breeds together.

2.6 Approaches for Aim 4

2.6.1 Mitochondrial-specific primer design

Primers for detecting mitochondrial DNA (mtDNA) copy number were carefully designed to avoid the co-amplification of the mitochondrial duplicated regions in nuclear genome. The duplication of the mitochondrial genome in the nuclear genome was detected using BLASTN (http://www.ncbi.nlm.nih.gov) (Altschul et al. 1990). The mitochondrial sequence (Sus scrofa 10.2 download from NCBI: http://www.ncbi.nlm.nih.gov/ on 1.9.2015) was split into fragments of 150 bps in length with a 50 bps overlap. Each fragment was blasted against both strands of chromosomes across the entire porcine genome to identify the 'unique' mitochondrial fragments which were not mapped to any chromosomes. Mapping results were considered to be significant if E-value < 0.1 and length >100 bps. Figure of duplicated regions in nuclear genomes was generated using R package IdeoViz (Pai and Ren 2014) and cytogenetic map of pig chromosomes was extracted from ArkDB (http://www.thearkdb.org/arkdb) (Hu et al. 2001).

2.6.2 Absolute quantification of mtDNA copy number

The amount of mtDNA and nuclear DNA were determined by quantitative real-time PCR (qPCR). The mitochondrial genes *ND1*, *ND2* and *COX1* were used to quantify mtDNA copy number, whereas the nuclear gene glucagon gene (*GCG*), which is highly conserved among species and presents as a single copy in animals, was used as the single-copy reference gene (Wang et al. 2012; Xie et al. 2015). MtDNA standards and nuclear DNA standards were prepared separately using PCR products in seven serial dilutions with a dilution factor of 10. The copy number was calculated according to the following equations (Chan et al. 2013):

$$copies/\mu l = \frac{ng/\mu l}{m} \qquad (2)$$

$$m = n \times [1.096 \times 10^{-12}] \qquad (3)$$

Where m is the mass of a single copy and n is the target size in base pairs.

The absolute copy numbers of *ND1*, *ND2*, *COX1* and *GCG* were calculated based on their standard curves, the equation was as following:

$$copies = 10^{(Ct-b)/a} \tag{4}$$

Where a is the slope and b is the intercept of the regression line.

Since GCG is a single copy nuclear gene, the mtDNA copies per nuclear genome was calculated as following:

$$mtDNA\ copies/\ nuclear\ genome\ = \frac{mtDNA\ copies}{nuclearDNA\ copies} \tag{5}$$

The mtDNA copy number per nuclear genome was calculated separately using ND1, ND2 and COX1. The data was recorded as their mean.

2.6.3 Measurement of gene expression

Fast gene expression analysis with EvaGreen dye on a BioMark HD real-time PCR system was used to measure gene expressions of all RNA samples as previously described in 2.5.1 with modifications. The qPCR reaction was performed using a 96×96 dynamic array instead of a 48×48 dynamic array.

2.6.4 Sequencing and Haplotype analysis

DNA from muscle samples of 53 animals (Duroc: N=15, DuPi: N=15, PiNN: N=9, PiPP: N=14) were sequenced using an ABI 3500 sequencer (Applied Biosystems Inc, Foster City, CA, USA). The D-loop region was amplified using forward primer 5'-CTCCGCCATCAGCACCCAAAG-3' and reverse primer 5'-GCACCTTGTTTGGATTRTCG-3' (Jin et al. 2012). All sequences were aligned using Clustal X2.1 (Thompson et al. 1997). DNASP 5.1 software was used to analyze the haplotypes of all sequences (Librado and Rozas 2009). The detailed information of haplotypes was shown in Annex A.4. Only the haplotypes which contained at least three animals were included in the subsequent statistical analysis.

2.6.5 Statistical analysis

Data were analyzed using SAS 9.4 statistical software (SAS Institute) and the MIXED procedure. The statistical model included effects of breed (Duroc, PiNN, PiPP and DuPi), gender (male and female), time (0 and 30min *post mortem*) and haplotype (Haplotype1, 4, 6, 7, 8). The model was combined with a repeated statement for the time component to take into account correlations among measurements made on the same animal at time 0 and 30min *post mortem*. Post hoc Tukey–Kramer method was used for multiple comparison adjustments. By applying the Lsmean with SE, results were considered to be statistically significant if p-value < 0.05. Correlation coefficient between gene expression and phenotypic measurement (r) was calculated for all individuals.

CHAPTER 3

Results and discussion

The metabolic characteristics of skeletal muscle have influences on meat production in farm animals. For example, a higher fat content and more STO fibers can improve the tenderness and juiciness of meat (Essen-Gustavsson et al. 1994). Further, the proportion of glycolytic and oxidative fibers are associated with meat color intensity (Pearson and Dutson 1994). Therefore, muscular energy metabolism needs to be properly regulated and optimized to improve meat quality.

Two common commercial pig breeds Duroc and Pietrain are divergent for different muscle characteristics and meat quality. Duroc pigs are fattier and their skeletal muscle contains more STO fibers which are generally associated with higher oxidative enzyme activities, whereas Pietrain pigs are more muscular and their muscles are more lean and contain higher percentage of FTG fibers which are associated with higher glycolytic enzyme activities (Gueguen et al. 2005; Huber et al. 2007; Werner et al. 2010a; Werner et al. 2010b). Although Pietrain pigs may be more favorable for meat industry due to their higher carcass yield, more FTG fibers may result in lower capillarization, insufficient delivery of oxygen and glycogen depletion, which lead to dry, firm and dark meat (Karlsson et al. 1994; Karlsson et al. 1999). Hence they are great models to investigate the regulation of energy metabolism in order to improve meat quality.

Muscle transcriptional profile based on muscle fiber, mitochondrial respiratory activity and metabolic enzymes

In this part, porcine snowball microarrays were performed to investigate the mRNA expression profiles of longissimus muscle samples obtained 24h before slaughter of Duroc and PiNN pigs, using differential gene expression and weighted gene co-expression network analysis (WGCNA) to dissect pathways associated with different muscle fiber types and activities of glycolytic and oxidative enzymes. Duroc and PiNN pigs were significantly differed for the muscle fiber types (STO and FTO) and mitochondrial respiration activity (succinate-dependent state 3 respiration rate). Duroc pigs had a higher percentage of STO (16.08 vs 9.99 %) and a lower percentage of FTO (8.62 vs 15.13 %) compared to PiNN pigs with p-value <0.05. The succinate-dependent state 3 respiration rate was significantly higher in Duroc than PiNN pigs with p<0.05.

Firstly, ANOVA analysis identified 2,345 differentially expressed probes between two breeds. Differentially expressed genes (DEGs) were analyzed using ingenuity IPA to identify any potential pathways and biological functions. The identified DEGs between the

muscles of breed Duroc and PiNN were highly associated with protein ubiquitination, stem cell pluripotency, amyloid processing, 3-phosphoinositide biosynthesis and degradation pathways. Ubiquitin protein system (UPS) has been known to regulate muscle atrophy and implicate on meat quality such as water holding capacity (Huynh et al. 2013; Lecker et al. 1999; Loan et al. 2014; Murton et al. 2008). In the results, the protein ubiquitination pathway was the top canonical pathway up-regulated in Duroc whereas amyloid processing was listed as the top canonical pathway in up-regulated DEGs of PiNN. In myotubes, amyloid processing is associated with glucose uptake and oxidation in energy metabolism (Hamilton et al. 2014). Amyloid beta (Abeta) could inhibit the 26S proteasome activity. The interplay between UPS and Abeta has been shown to be associated with Alzheimer's disease (Hong et al. 2014). Differentially expressed genes in amyloid processing such as *PSENEN*, *AKT1* and *CAPN3* have implications in muscle biology of pigs involved in calcium homeostasis, muscular leanness and muscle mass (Chan et al. 2000; Cheng et al. 2015; Izumiya et al. 2008; Richard et al. 1995). Further, DEGs also revealed differences in functions of muscle development and carbohydrate metabolism. The proposed candidate genes include both Duroc up-regulated (*PPARGC1A*, *PPP3CA* and *CD36*) and PiNN up-regulated (*SRL*, *ATP2A1*, *PEKFB2*, *GSK3A* and *GYS1*). Peroxisome proliferator-activated receptor gamma coactivator 1 alpha (*PPARGC1A)* acts as a master regulator to control mitochondrial biogenesis and oxidative phosphorylation. Further, its activation can promote the formation of slow-twitch oxidative fibers (LeBleu et al. 2014; Lin et al. 2002). *PPP3CA* is differentially expressed in muscles comprised of different proportions of fast and slow muscle fibers (Wan et al. 2014). *CD36* plays a significant role in lipid accumulation and fatty acid homeostasis (Angin et al. 2012; Samovski et al. 2015). On the other hand, PiNN up-regulated genes were well agreed with the higher percentage of fast-twitch glycolytic muscle fibers. For example, sarcalumenin (*SRL*) and fast twitch Ca2+ ATPase (*ATP2A1*) have been reported as fast-type muscle genes (Wu et al. 2013). Fructose 2, 6-bisphosphatase 2 (PEKFB2) can promote glycolysis (Ros and Schulze 2013). Glycogen synthase kinase 3 alpha (GSK3A) and glycogen synthase 1 (GYS1) are essential for glycogen storage and they can influence muscle-to-meat transition via glycolysis and reduced pH (Monin and Sellier 1985). Therefore, the comparison of transcriptome profiling for longissimus biopsies between Duroc and PiNN pigs revealed differences in their muscular metabolic characteristics.

Next, WGCNA analysis was performed to dissect gene expression profiles for these two breeds. It is a powerful tool to group genes into a co-expression network/module based on their expression pattern. For breed Duroc, a total of 21 modules were examined for their relationships with all measurements of phenotypical traits which included muscle fiber composition, mitochondrial respiratory activity, metabolic enzyme activities and adenine nucleotide concentration. Results revealed strong correlations between mitochondrion-associated co-expression modules and phenotypes of STO, FTG and cytochrome c oxidase (COX) activity. For example, module blue and green yellow were positively correlated with STO and negatively correlated with FTG. These two modules were enriched for 'mitochondrion' and mitochondrial part' GO terms respectively. The containing genes are involved in functions of adenine nucleotide transport (*SLC25A4* or *ANT1*) (Kawamata et al. 2011), mitochondrial (mt) translation (*GFM1*) (Coenen et al. 2004), OXPHOS subunits formation [*NDUFV2, NDUFV3, NDUFS1, NDUFS4, NDUFS6, NDUFS7, NDUFB2, NDUFB3, NDUFB4, NDUFB8, NDUFB11, NDUFA5, NDUFA10,* and *NDUFA11* (encode for Complex I); *SDHA* and *SDHB* (encode for Complex II); *COX7A1* and *COX4l1* (encode for COX); *ATP5L, ATP5J, ATP5G2, ATP5G3, ATP5A1*, and *ATP5C1* (encode for ATP synthase)] and mt oxidation of fatty acids (*ACSL1, ACSL3, ACSL4, ACSL5, HADH* and *HADHB*) (Ellis et al. 2010; Zhou et al. 2012). These co-expression modules linked mitochondrial functions to the oxidative capacity of skeletal muscle. It would be interesting to see whether those genes in Duroc pigs imply a predominant role of oxidative capacity and respiration over PiNN. A total of 20 co-expression modules were identified for a trait correlation in PiNN pigs. Overall, fewer significant module-trait relationships were observed for PiNN. The identified modules were enriched in macromolecule catabolic process, actin cytoskeleton and transcription activator activity. These results highlighted the importance of mitochondria for the oxidative capacity in porcine muscle.

Further, the identified co-expression modules in WGCNA could link to mitochondrial respiratory activity and ATP synthesis. In Duroc pigs, 4 modules which included dark red, green yellow, dark orange and purple were enriched for energy production. Their containing genes are potential factors to regulate ATP production. They encoded the components of respiration chain (*NDUFS1* and *ATP5A1*) (Hejzlarova et al. 2014; Martin et al. 2005; Rybalka et al. 2014) and the receptor of hormones such as insulin and thyroid hormone (*INSR*, *IRS2* and *THRB*) (Short et al. 2001; Stump et al. 2003). In PiNN pigs, 5 modules (module dark green, green yellow, grey 60, light steel blue and medium orchid)

were enriched for energy production. Some genes in these modules are proposed as potential factors regulating respiratory chain (*ATP5B* and *ATP5C1*), hormones (*THRB*) and transcription factors (*PPARGC1A* and *NRFs*) (Kang and Li Ji 2012; Lehman et al. 2000; Wu et al. 1999). Molecule LRPPRC influences the stability of most mitochondrial mRNAs and its deficiency leads to COX deficiency and ATP synthase deficiency associated with reduced ATP production (Mourier et al. 2014).

Collectively, in this part, a comparative transcriptome profiling of 24h *ante mortem* longissimus muscle for Duroc and PiNN pigs revealed clear differences in their muscle metabolic properties. Gene co-expression network analysis stressed the importance of mitochondria in the oxidative capacity of skeletal muscle. In particular, the Duroc breed showed more clearly molecular function involved in oxidative capacity and respiratory activity than PiNN. In PiNN pigs, co-expression modules enriched in macromolecule catabolic process, actin cytoskeleton, and transcription activator activity were associated with muscle fiber composition, mitochondrial respiration, and metabolic enzyme activities. Therefore these results highlighted the importance of mitochondria for the oxidative capacity of the porcine skeletal muscle and provided breed-specific pathways in muscle fibers.

MicroRNA-mRNA regulatory networking fine-tunes the porcine muscular mitochondrial respiratory and metabolic enzyme activities

This part of the project focused on the microRNA profiling of the same porcine muscle samples. The construction of miRNA-mRNA network allows investigating how miRNAs are involved in energy metabolism by fine-tuning gene expression.

Firstly, the differentially expressed miRNAs between breed Duroc and PiNN pigs were identified using ANOVA, followed by integration with differentially expressed mRNAs based on the miRNA-mRNA pairwise correlation and computational target prediction. The identified target genes were enriched for protein ubiquitination pathway, stem cell pluripotency, geranylgeranyl diphosphate biosynthesis, skeletal and muscular system development. Many identified miRNAs and their target genes have been shown to play a role in diverging muscle characteristics. For example, ubiquitination pathway including Duroc up-regulated genes *USP45* and *USP28* were predicted as a direct target of miR-133 and miR-310 respectively. MiR-133 are proposed as a genetic factor affecting muscle fibers and meat quality traits (Lee et al. 2013), whereas a loss function of miR-310 can

cause defects in energy metabolism and deregulation of nutritional homeostasis-associated genes (Cicek et al. 2016). Other Duroc up-regulated genes such as *CMYA5*, *AR*, *RB1* and *BMPR2* in functional category of skeletal and muscular development were predicted to be regulated by miR-4787, miR-877 and miR-4687 etc. These genes, not only are associated to water loss, intramuscular fat and marbling traits, but also are involved in promoting slow-twitch muscle fiber formation and adipogenesis (Altuwaijri et al. 2004; Lim et al. 2013; Schleinitz et al. 2011; Xu et al. 2011). Hence the identified Duroc up-regulated genes and their corresponding miRNAs could contribute to the higher percentage of oxidative muscle fibers and fat content in Duroc pigs. On the other hand, PiNN up-regulated genes such as *SMAD3* and *PFKEB2* were predicted as a target of miR-423. These two genes have been shown to play a role in both muscle fiber specificity and glycolysis in skeletal muscle (LeBleu et al. 2014; Lin et al. 2002; Ros and Schulze 2013; Tiano et al. 2015). Therefore, our assembled miRNA-mRNA regulatory network may fine-tune the expression of genes within the pathways and shape the related phenotypes among pig breeds.

Next, the association between miRNA profiles and the phenotypes from the same animal set was assessed. Based on the identified miRNAs that highly correlated with the phenotypes, we integrated the miRNA and mRNA expression profiles to identify miRNA regulated genes that influence energy metabolism. In the network, MiR-25, its targets *BMPR2* and *IRS1* were significantly correlated to STO and FTO muscle fibers. MiR-25 is abundant in cardiomyocytes and it can target both the mitochondrial calcium uniporter (*MCU*) and Ca^{2+} transporting ATPase (*ATP2A2*) (Pan et al. 2015; Wahlquist et al. 2014). In the present study, miR-25 was proposed to target genes of *BMPR2* and *IRS1*. *BMPR2* is essential for BMP signaling and may be involved in the regulation of adipogenesis and obesity (Schleinitz et al. 2011). Whereas *IRS1* is a major molecule mediating insulin-signaling pathway, which affects the mitochondrial function, ATP production and muscle oxidative capacity by increasing the mRNA level of complex I and complex IV (Cheng et al. 2010; Stump et al. 2003). MiR-210 and its predicted targets *ATP5I*, *ME3*, *MTCH1* and *CPT2* were highly correlated to ADP and ATP concentration. MiR-210 modulates mitochondrial function, decreases *COX10* expression and activates the generation of reactive oxygen species (ROS) (Chen et al. 2010). Its proposed target genes *ATP5I*, *ME3*, *MTCH1* and *CPT2* in the current study are involved in ATP production, apoptosis and beta-oxidation of long fatty acids in mitochondria (Kerner and Hoppel 2000; Pickova et al.

2005; Xu et al. 2002; Yang et al. 2002). There were more identified miRNA-mRNA pairs in the present study such as miR-27 targeting *CYP24A1* in the vitamin D metabolism highly correlated to phenotype of PFK activity and miR-363 targeting *USP24* in ubiquitin pathway highly correlated to phenotypes of STO fibers, mitochondrial respiration and AMP concentration.

Up to now we have shown that the identified miRNA-mRNA network could be linked to muscle fiber types, oxidative enzyme activities and ATP production. Interestingly, a tight relationship between mitochondria and ubiquitin proteasome system (UPS) at the level of gene expression was observed. It revealed a link between these two systems contributing to energy metabolism of skeletal muscle via fine-tuning the gene expression by miRNAs under physiological conditions. However, further detailed information of the interaction between mitochondria and UPS still remains elusive.

In this study, we assembled the miRNA-mRNA regulatory networks related to muscle fiber type, mitochondrial respiration, metabolic enzyme activities and ATP production based on the correlation information between expression of miRNAs and target genes following computational target prediction, and as well as phenotypical measurements of Duroc and PiNN pigs. These complex networks could make contributions to the muscle phenotypic variations by fine-tuning gene expression. These results provided an insight into the regulatory role of miRNAs in energy metabolism in porcine muscle.

Molecular changes in mitochondrial respiratory activity and metabolic enzyme activity in muscle of four pig breeds with distinct metabolic types

In part one and part two of this study, the investigation of both transcriptional mRNA and miRNA profiling of skeletal muscle identified various biological pathways associated with energy metabolism and highlighted the importance of mitochondria for the oxidative capacity of porcine muscle fibers. Mitochondria play an important role in cellular ATP production through oxidative phosphorylation. Oxidative pathway components include complex I, complex II, complex IV and ATP synthase etc. Further, glycolytic pathway components such as muscle-specific glycogen phosphorylase, phosphofructokinase and lactate dehydrogenase also contribute to ATP generation. Understanding the genotype-phenotype correlation within these pathways can offer valuable insight for muscle metabolism and meat quality.

In the current part of this project, we analyzed expression profiles of pathway-focused genes related to both oxidative and glycolytic pathways, in conjunction with muscle fiber typing and metabolic enzyme activities to further understand the molecular basis of muscle properties and functions that affect meat quality, using four distinct metabolic types of pig breeds including Duroc, PiNN, PiPP and DuPi. We included both PiPP and PiNN pigs to better distinguish possible associated effects of a single nucleotide mutation in ryanodine receptor 1(*RYR1*). Although this genetic defect leads to the abnormality of cellular calcium homeostasis and results in pale, soft, and exudative meat (Fujii et al. 1991; Shen et al. 2007), the MHS homozygous genotype is still retained in pork production because of its advantageous carcass yield and lean percentage, which is associated with higher FTG fiber ratio (Werner et al. 2010a; Werner et al. 2010b).

For the metabolic phenotypes of the four breeds, each breed displayed a distinct muscle fiber composition. Duroc pigs had the highest percentage of STO fibers, with the most contrast between Duroc (13.91%) and PiPP (6.48%) breeds. PiPP pigs had a significant higher percentage of FTG fibers (81.57%) compared to PiNN pigs (74.95%), while that of Duroc and DuPi were in between these two Pietrain genotypes. Mitochondrial respiration and the activities of the most investigated metabolic enzymes were comparable among genotypes, except for significant lower complex I activity in PiPP pigs.

At the transcriptional level, lactate dehydrogenase B showed breed specificity, with significantly lower expression in PiPP pigs. The results showed no breed specific differences for LDHA at transcript level. Lactate has been identified as an intermediate substance in metabolic processes to provide fuel for aerobic metabolism rather than a dead-end waste product of glycolysis due to hypoxia (Gladden 2004). LDH catalyzes interconversion of pyruvate to lactate and NADH to NAD^+. Its two common subunits, M and H, are encoded by LDHA and LDHB, respectively. LDHA encoded subunit M catalyzes the conversion of pyruvate to lactate, whereas LDHB encoded LDH subunit H oxidizes lactate back to pyruvate and thus can generate mitochondrial energy via aerobic metabolism in the TCA cycle (Gabriel-Costa et al. 2015). The results demonstrated the lowest gene expression of LDHB in PiPP pigs, which also had the lowest percentage of STO muscle fibers. Different LDH isoforms have been shown to be associated with different muscle fiber-types such as the predominant distribution of H-subunit in type I fibers and M-subunit in type IIA and IIB fibers (Leberer and Pette 1984; Peter et al. 1971).

Therefore, LDH may function as a key mediator of lactate oxidation via its H subunit and this process seems to be reduced in pigs with low STO fiber percentage like the PiPP pigs.

A similar expression pattern was shown for many subunits of oxidative phosphorylation complexes including complex I, complex II, complex IV and ATP synthase, with lower expression in PiPP pigs. There are several possible explanations. PiPP pigs are positive for the *RYR1* point mutation (Fujii et al. 1991). Defective RYR1 leads to abnormally elevated Ca^{2+} levels in cytoplasm and causes excess muscle contraction and high energy consumption, followed by a faster shift of energy generation from aerobic to anaerobic glycolysis accompanied by acidosis (Werner et al. 2005). The Ca^{2+} homeostasis abnormality can influence mitochondrial Ca^{2+} concentrations and affect mitochondrial function. MHS knock-in mice showed a clear overload in the mitochondrial matrix and a switch to a compromised bioenergetics state characterized by low OXPHOS under a non-triggered state (Giulivi et al. 2011). Next, the larger amount of FTG fibers in PiPP pigs which have the characteristics of low capillarization and inefficient oxygen delivery could possibly lead to the lower OXPHOS gene expression. Another possible causation could be the significantly lower AMP: ATP ratio in PiPP pigs. AMP activates AMP-activated protein kinase (AMPK) which further activates PGC-1α by phosphorylation to control OXPHOS (Jager et al. 2007; O'Neill et al. 2013). Further, the higher glycogen levels in FTG fibers (Fernandez et al. 1995) could also repress the activation of AMPK signaling pathway and result in the lower expression of OXPHOS in PiPP pigs (Wojtaszewski et al. 2002; Wojtaszewski et al. 2003).

Next part of the results showed the most significant correlations between mRNA level and enzyme activity were breed-dependent, such as complex IV in Duroc, complex II and IV in DuPi, complex I in PiNN and complex I and IV in PiPP. Complex gene regulations at post-transcriptional and post-translational levels in association with different genetic backgrounds may roughly explain the results. Molecules such as LRPPRC affect RNA stability and thus influence complex IV and ATP synthase as well as ATP production (Mili and Pinol-Roma 2003; Mourier et al. 2014). Moreover, events such as the import of nuclear-encoded OXPHOS subunits into mitochondria and OXPHOS complex assembly could also contribute to the disparity between mRNA levels and enzyme activity for OXPHOS complex. Last but not least, a strong association between STO fibers and gene expression of OXPHOS complex subunits was observed especially in Duroc pigs. It may be explained by the high percentage of STO fibers in Duroc compared to other breeds. The

Duroc-Pietrain crossbred DuPi showed significant correlation between OXPHOS expression and FTO fibers, which belong to intermediate muscle fiber type.

Therefore, this part revealed differential gene expression of glycolytic and oxidative enzymes in skeletal muscle of Duroc, DuPi, PiNN and PiPP pigs. PiPP pigs exhibited the lowest LDHB expression supporting a role of LDH in aerobic respiration via its H subunit. PiPP pigs also showed the lower gene expression for many subunits of OXPHOS complexes including complex I, II, IV and ATP synthase. Within different pig breeds, OXPHOS was highly regulated and optimized to meet different energy requirement via fine-tuning breed-specific genetic differences. Finally, this study also linked the OXPHOS system to different muscle fiber types. All these results highlighted the importance of OXPHOS system in oxidative capacity of muscle fibers and provided valuable breed-specific information for the molecular basis of metabolic enzyme activities, which directly impact meat quality.

Mitochondrial-nuclear crosstalk, haplotype and copy number variation distinct in muscle fiber type, mitochondrial respiratory and metabolic enzyme activities

Mitochondria, as double membrane-bound organelles with their own DNA, are involved in many key cellular processes such as calcium homeostasis, reactive oxygen species production and ATP generation by oxidative phosphorylation (OXPHOS). With most emphasis placed on glycolysis, mitochondrial content and function may be important factors that contribute to *post mortem* muscular metabolism and may improve our ability to predict pH decline and meat quality. In this part, we investigated the mitochondrial content, followed by the expressions of both mitochondrial and nuclear encoded genes involved in energy metabolism together with muscle fiber typing and metabolic enzyme activities at time 0 and 30min *post mortem* in longissimus muscles (LM) of pig breeds Duroc, PiNN, PiPP and DuPi. Since mitochondrial DNA haplotypes are potential genetic sources for manipulating phenotypes including tolerance to heat, growth and milk quality in farm animals (Tsai and St John 2016), it is of interest to investigate haplotypes within these animals and their effect on energy metabolism.

Among all pig breeds, Duroc pigs had the highest percentage of STO fibers whereas PiPP pigs had the largest amount of FTG fibers. Duroc pigs had the highest complex I activity compared to other breeds, especially to DuPi and PiPP. PiPP pigs had the lowest pH than all other three breeds. The enzyme activities of PFK and LDH were increased, whereas

oxidative enzyme activities of CS, complex I and complex II were decreased at 30min *post mortem* compared to immediately slaughter.

At molecular level, PiPP pigs showed the least absolute mitochondrial DNA (mtDNA) copy number and the lowest transcript abundance of mitochondrial-encoded subunits *ND1*, *ND6*, *ATP6* and nuclear-encoded subunits *NDUFA11*, *NDUFB8*, *NDUFS8*, *NDUFV1*, *ATP5G1* and *ATP5L*. The muscle of PiPP pigs contained the largest amount of FTG fibers which in general possess a fewer number of mitochondria compared to oxidative fibers, whereas there were the most STO fibers in the muscle of Duroc pigs. The results showed a strong association between mitochondrial content and muscle fiber composition. MtDNA copy number variation is dependent on a balance between mtDNA synthesis and degradation, the elevated removal of mitochondria and the alteration of mtDNA replication via factors such as mitochondrial transcription factor A (TFAM) could contribute to this variation (Pohjoismaki et al. 2006). The abnormal Ca^{2+} homeostasis in PiPP pigs may result in oxidative stress associated with elevated ROS production, which induces mitophagy to remove damaged mitochondria. The excess ROS to a sufficient degree could result in damaged organelle and trigger non-selective autophagy (Deffieu et al. 2013). Unlike replication and transcription of nuclear DNA are two distinct processes, the mtDNA replication and mitochondrial transcription have been proposed to be associated (Kasiviswanathan et al. 2012). The transcription machinery generates nascent RNA which is processed to serve as primer for mtDNA replication (Fuste et al. 2010; Xu and Clayton 1996). Hence the observed variation of mitochondrial gene expression between different pig breeds was very likely to be associated with the fluctuated mtDNA copy number between breeds. Indeed, our results showed significant correlations between mtDNA copy number and expressions of several mitochondrial encoded OXPHOS genes. In some cancer types, mtDNA content is correlated with the expression of respiratory electron transport genes (Reznik et al. 2016). The down regulation of nuclear encoded OXPHOS subunits in PiPP pigs is very likely caused by the abnormal Ca^{2+} homeostasis of PiPP pigs as described in previous part. Glucocorticoid receptor (GR) binds to the D-loop control region and so that stress and corticosteroids have a direct influence on rat hippocampal mtDNA gene expression (Hunter et al. 2016). Since *RYR1* mutated PiPP pigs are stress susceptible, it is likely that mtDNA transcription would be influenced in those pigs. The methylation of mtDNA may be another mechanism altering mitochondrial transcription in PiPP pigs. Under conditions of oxidative stress, upregulated DNMT1 suppresses the expression of

ND6 through methylation (Shock et al. 2011). It is consistent with our result of the lower expressed ND6 expression in PiPP pigs likely with mutant RYR1 induced mitochondrial injury and oxidative stress (Jin et al. 2014).

With the identification of mitochondrial haplotypes in these animals, all PiPP pigs belonged to haplotype 8 and this haplotype showed the lowest mtDNA copy number and the lowest gene expression of mitochondrial-encoded subunits *ND1, ND6, CYB, COX1, ATP6* and nuclear-encoded subunits *NDUFA11, NDUFA13* and *NDUFB8*. Mitochondrial haplotype is proposed to modulate global DNA methylation and methylation status of various signaling pathways (Atilano et al. 2015; Bellizzi et al. 2012). The DNA methylation of nuclear encoded DNA polymerase gamma A regulates mtDNA copy number (Kelly et al. 2012). Since haplotype was identified based on the sequence of D-loop, which belonged to mtDNA control region, different haplotype might result in different methylation pattern of D-loop and leads to altered mitochondrial gene expression profile. The de-methylation of D-loop is likely to be involved in regulation of mtDNA copy number and *ND2* expression (Gao et al. 2015). All these supported the possibility that the effect of mitochondrial haplotype on mitochondrial content and OXPHOS system might be exerted via DNA methylation at both mitochondrial and nuclear genome. In this part, we showed pig breeds and mtDNA haplotype, in other words, mitochondrial and nuclear genetic background could influence mitochondrial content and OXPHOS system. This effect might be exerted via D-loop by glucocorticoid stress hormone and DNA methylation. However, this assumption needs further investigation.

The mtDNA copy number in longissimus muscle was decreased from 420 copies per nuclear genome at 0min *post mortem* to 389 copies at 30min *post mortem* with p-value of 0.02. No mitochondrial-encoded genes were differently expressed between 0 and 30min *post mortem*. Only three nuclear-encoded genes *NDUFB8, COX7A2* and *ATP5L* showed significantly lower mRNA levels at 30min *post mortem* than 0min. Hence we concluded early *post mortem* time influenced mitochondrial content but had only minor effect on OXPHOS gene expression.

The observation of significant correlations between mitochondrial and nuclear encoded OXPHOS gene expressions in our results strongly supported the theory of mitochondrial-nuclear crosstalk which may involve transcription factors such as TFAM which are encoded by nuclear genome for mitochondrial gene expression. The nuclear-encoded

subunits need to be imported into mitochondria together with mitochondrial-encoded subunits to form a fully assembled functional OXPHOS system in the mitochondrial inner membrane. On the other hand, mitochondria are communicating to nucleus via retrograde communication such as signaling molecule Ca^{2+}. The mitochondria-to-nucleus stress signaling occurs through the disrupted Ca^{2+} homeostasis (Biswas et al. 1999). The absence of mtDNA-encoded subunits COX1 and COX2 affect the stability of some subunits of nuclear encoded respiratory chain proteins (Marusich et al. 1997). The mRNA level of master regulator mediating mitochondrial biogenesis and oxidative phosphorylation (LeBleu et al. 2014) PPARG coactivator 1 alpha (*PGC-1α*) showed significant correlations to all investigated mitochondrial encoded OXPHOS subunits and six nuclear encoded subunits in our results. Hence PGC-1α may be one of the factors contributing to the coordination of mitochondrial-nuclear genome in porcine OXPHOS system. The expression of *PGC-1α* was also highly correlated to enzyme activities of complex I, II and IV in traits. It reinforces the functional role of *PGC-1α* in mitochondrial energy metabolism. The high association between nuclear encoded OXPHOS gene expression and oxidative enzyme activities suggested these genes have dominant contributions to the complex activities over the mitochondrial encoded subunits. Whereas the mitochondrial encoded OXPHOS genes were more associated with muscle fiber types which were consistent with STO muscle fibers in general contain more mitochondria (Gueguen et al. 2005). Our measured mtDNA copy number was correlated positively to STO fibers and oxidative enzyme activities but negatively to FTG fibers. It has been demonstrated that the mtDNA copy number is related to oxidative capacity and adipocyte lipogenesis (Kaaman et al. 2007). Since lipids are stored mainly in STO fibers to improve the tenderness and juiciness of meat (Essen-Gustavsson et al. 1994), mtDNA copy number is possible linked to meat quality.

In brief, PiPP pigs (haplotype 8) showed the lowest mtDNA copy number, the most reduced gene expressions of many mitochondrial and nuclear encoded OXPHOS subunits among all four breeds. It provided valuable information of haplotype and breed-specific mitochondrial content variation and molecular basis of mitochondrial respiration, which improve our ability to predict pH decline and meat quality. Finally, the expression pattern of these OXPHOS genes supported the mitochondrial-nuclear crosstalk and their complexity contributed to muscular phenotypes.

CHAPTER 4

Conclusions and perspectives

Conclusions

In this thesis, the mRNA and miRNA transcriptome profiling of *ante mortem* skeletal muscle for Duroc and PiNN pigs were comprehensively investigated. The comparative transcriptome profiling between these two breeds revealed clear differences in their muscle metabolic properties. Gene co-expression network analysis grouped genes into different co-expression modules and identified various biological pathways associated with fiber types, mitochondrial respiratory activity and metabolic enzyme activities. It highlighted the importance of mitochondria in the oxidative capacity of muscle particularly in breed Duroc. Next, the miRNA-mRNA regulatory networks associated to the phenotypes of interest were constructed using the correlation information between expressed miRNAs and target mRNAs with computational target prediction and phenotypical measurements of Duroc and PiNN pigs. These complex networks may make contributions to the muscle energy metabolism in porcine by fine-tuning gene expressions. In the end, the comparative pathway-focused gene expression profiling was performed in muscles of four pig breeds (Duroc, DuPi, PiNN and PiPP) with distinct metabolic types. These results stressed the importance of gene expression related to oxidative and glycolytic pathways in the metabolic capacity of muscle fibers. It furthered the breed-specific understanding of the molecular basis of metabolic enzyme activities, which directly impact meat quality. The last part of the thesis focused on the mitochondrial genome and its interaction with nuclear genome. The results provided valuable information of haplotype and breed-specific mitochondrial content variation and molecular basis of mitochondrial respiration, which improve the prediction of many muscle pathologic processes. The study highlighted the importance of mitochondrial-nuclear crosstalk, haplotype and copy number variation underlying muscle phenotype differences.

Future perspectives

Holistic approaches of transcriptomics, proteomics and metabolomics have the potential to reveal pathways and functional networks related to important traits. Integrative approaches facilitate the identification of hub or key genes. However functional validation is required. To validate any candidate gene playing a functional role in energy metabolism, an *in vitro* model system can be set up to perform enzymatic functional assay by mutation or silencing certain genes. Tools such as clustered regularly interspaced short palindromic repeat (CRISPR) could be used for gene editing. CRISPR associated protein 9 nuclease (CRISPR/Cas9) system consists of two key molecules that result in insertions or deletions into the DNA. The guided RNA (gRNA) is designed to find and bind to a specific sequence in the DNA and Cas9 cuts the two strands of DNA at a specific location so that nucleotides can be added or removed (Sander and Joung 2014). Recently, CRISPR/Cas9 has been used to edit mitochondrial genome in addition to nuclear genome (Jo et al. 2015). Most recently, CRISPR/Cas9 has been shown to robustly and specifically reduce the expressions of miRNAs up to 96% (Chang et al. 2016). The application of CRISPR/Cas9 in miRNA editing will strengthen the ability to study miRNAs underlying functions in energy metabolism. The validation of candidate miRNAs and their target genes could be performed *in vitro* model system, firstly to confirm whether it is a direct target using luciferase assay by constructing miRNA and gene expressing plasmids, then to investigate the role of miRNA-mRNA pairs in energy metabolism using functional assay such as the measurement of ATP production and oxygen consumption via knock in and knock down gene expression by miRNA. The confirmation of miRNAs and target genes as potential biomarkers for energy metabolism may improve the meat production and quality. The identification and confirmation of miRNAs and their target genes could be extended to mitochondrial genome rather than being limited to nuclear level. It has been proposed that miR-133a targets mitochondrial-encoded complex I subunit *ND1*, miR-130a targets complex IV *COX3*, miR-181c translocates into mitochondria and regulates complex IV *COX1* and miR-151a-5p reduces cellular ATP production by targeting *CYB* in various tissues or cells (Barrey et al. 2011; Das et al. 2012; Kren et al. 2009; Zhou et al. 2015). Furthermore, a few miRNAs are predicted to originate from the mitochondrial genome (Barrey et al. 2011; Shinde and Bhadra 2015), suggesting the existence of mitochondrial-encoded miRNAs and their possible functions.

This thesis has shown the effect of mitochondrial haplotype and breed on mitochondrial content and OXPHOS system, speculatively via DNA methylation at both mitochondrial and nuclear genome. To test this hypothesis, DNA methylation pattern of mitochondrial and nuclear genome could be investigated by whole genome bisulfite sequencing (WGBS). Next generation sequencing based WGBS can provide a comprehensive view of methylation patterns across the whole genome at single nucleotide resolution. In library preparation, bisulfite conversion changes unmethylated cytosine to uracil and the converted based are then identified as thymine in the sequencing data and read counts are used to determine the percentage of methylated cytosines. It can detect the methylation patterns of cytosine-guanine dinucleotides (CpG), CHH (where H correspond to A, T or C) and CHG regions across the entire genome. A better understanding of epigenetic variations and mitochondrial-nuclear crosstalk could provide valuable information for detection and diagnosis of diseases. Mitochondrial replacement therapy (MRT) has been merged as a promising tool that has the potential to treat mitochondrial diseases with the concern of whether mitochondrial-nuclear interactions are likely to pose a problem for MRT (Eyre-Walker 2017).

Mitochondrial stress induced mitochondrial-to-nucleus retrograde signaling (MtRS) regulates histone acetylation and alters nuclear gene expression (Guha et al. 2016). Hence it would be of interest to investigate the transcription and epigenetic reprogramming at both mitochondrial and nuclear genome where mitochondrial stress is induced by the depletion of mtDNA copy number via ethidium bromide treatment, mtDNA mutation and /or the disruption of OXPHOS complex via knockout certain subunits in a porcine cell model. There are mouse models of complex I, II and IV deficiency by knockout and or knock down nuclear-encoded OXPHOS subunits (Torraco et al. 2015). And mouse models carrying mutations in the mtDNA such as genes of *Cox1, Nd6* and *Cox1/Nd6* are associated with phenotypes of complex IV deficiency, age associated disorders and cardiomyopathy (Torraco et al. 2015). Knock down of these candidate genes are expected to induce mitochondrial stress in *in vitro* cell model. The severity of mitochondrial stress could be measured by ROS production, ATP generation, oxygen consumption and cell viability etc. Further, glucocorticoids have been shown to influence mitochondrial transcription in HepG2 cells and rat brain via mitochondrial localized glucocorticoid receptor (GR) (Hunter et al. 2016; Psarra and Sekeris 2011). The dose-response effects of glucocorticoid and thyroid hormones on mitochondria of porcine cells could also be

investigated since mitochondrion acts as a primary site of the action of steroid and thyroid hormone (Psarra et al. 2006).

Moreover, the establishment of transmitochondrial cytoplasmic hybrid (cybrids) cells from porcine could allow the analysis of cells containing different haplotype with identical nuclear background and evaluate the specific effect of haplotype on energy metabolism. This setup will provide a precise insight for unravel the contributions of mitochondrial and nuclear genes as well as the interplay of two genomes.

CHAPTER 5

Summary

Summary

Skeletal muscle activity requires ATP as the major currency molecule of energy that is produced mainly through oxidative phosphorylation in mitochondria. Important factors of meat quality such as tenderness and juiciness are associated with muscle fiber proportion and energy metabolism in meat-producing animals. In this thesis, pig breed Duroc and Pietrain differing for the slow-twitch-oxidative (STO) fibers and fast-twitch-oxidative (FTO) fibers as well as mitochondrial activity have been used to identify potential biological pathways related to energy metabolism. Based on the transcriptomic profiling of the *ante mortem* longissimus muscle, differential gene expression between Duroc and PiNN samples were associated with protein ubiquitination, stem cell pluripotency, amyloid processing, 3-phosphoinositide biosynthesis and degradation pathways. In weighted gene co-expression network analysis, Duroc revealed strong correlations between mitochondrion-enriched co-expression modules and STO (r = 0.78), FTO (r = -0.98), complex I (r = 0.72) and complex IV activity (r = 0.86). In contrast, co-expression modules enriched in macromolecule catabolic process, actin cytoskeleton and transcription activator activity were associated to fiber types, mitochondrial respiration and metabolic enzymes in PiNN. The results revealed the importance of mitochondria and raised our interests to deeply investigate mitochondria and oxidative phosphorylation (OXPHOS) system. A comparative analysis of the miRNA expression profile between Duroc and PiNN was performed to construct the miRNA-mRNA regulatory networks based on their pairwise correlation and computational target prediction. The identified target genes were enriched in protein ubiquitination pathway, stem cell pluripotency, skeletal and muscular system development. By integrating the correlation with phenotypical traits, the constructed miRNA-mRNA networks associated with energy metabolism suggest their essential roles in modulating the mitochondrial energy expenditure in porcine muscle. For example, miR-25 targeting *BMPR2* and *IRS1*, miR-363 targeting *USP24*, miR-28 targeting *HECW2* and miR-210 targeting *ATP5I, ME3, MTCH1* and *CPT2* were highly associated with STO fibers, FTO fibers, ADP and ATP concentration. These complex networks may contribute to the divergent muscle phenotypes by fine-tuning gene expressions. The confirmation of miRNAs and their target genes and their functions in muscle energy metabolism become very important in the further. The expression profiles of pathway-focused genes related to oxidative ad glycolytic pathways were analyzed to further understand the molecular basis of muscle properties. This part also included a F2 Duroc-Pietrain crossbred DuPi and MHS

homozygous-positive breed PiPP carrying *RYR1* mutation in addition to Duroc and PiNN. Each breed type displayed a distinct muscle fiber composition. PiPP pigs showed a significant lower complex I activity than three other breeds. At transcript level, lactate dehydrogenase B showed breed specificity, with significantly lower expression in PiPP pigs. PiPP pigs showed the lowest gene expression for several subunits of oxidative phosphorylation (OXPHOS) complexes, including complex I, complex II, complex IV and ATP synthase. This study also linked the OXPHOS system to different muscle fiber types. Duroc pigs had the strongest association between OXPHOS expression and STO fibers, whereas DuPi pigs had significant correlation between OPXHOS expression and FTO fibers. Therefore, the transcriptional regulation of OXPHOS subunits is essential for the oxidative capacity of muscle fibers. Since OXPHOS subunits are encoded by both the nuclear and mitochondrial genome, the two genome systems interact intricately to form the fully assembled functional OXPHOS complexes. The last part of the thesis is focused on mitochondrial genome activity of early *post mortem* longissimus muscle of the same four pig breeds harboring different mitochondrial haplotypes and muscle fiber types, mitochondrial respiratory activities, and fat content. PiPP carried only haplotype 8 and showed the lowest absolute mtDNA copy number accompanied by the lowest transcript abundance of mitochondrial encoded subunits *ND1, ND6*, *ATP6*, nuclear encoded subunits *NDUFA11* and *NDUFB8*. Haplotype 4 of Duroc pigs had significantly higher mtDNA copy number and higher mRNA levels of mitochondrial encoded subunits *ND1, ND6*, and *ATP6*. These results revealed that the mitochondrial and nuclear genetic backgrounds have an effect on mitochondrial content and the expressions of OXPHOS subunits in porcine. The co-expression pattern of OXPHOS genes supported the mitochondrial-nuclear crosstalk and their complexity contributed to muscle metabolism. An important transcription factor *PGC-1α* may contribute to the coordination of the mitochondrial-nuclear genome in building the OXPHOS system. Hence mitochondrial-nuclear crosstalk, haplotype, and copy number variation may play important roles in muscle phenotypic variations in farm animals. In summary, this thesis carried out transcriptional profiling of mRNAs and miRNAs across the whole genome in porcine muscles. Many biological pathways were identified to be associated with muscle fibers, mitochondrial respiration and metabolic enzyme activities, especially the results highlighted the significance of OXPHOS system in energy metabolism. OXPHOS system was then intensively investigated at the level of both nuclear and mitochondrial DNA in early *post mortem* and *ante mortem* (nucleus only) muscles of four pig breeds harboring different mitochondrial

haplotypes and divergent phenotypes. Different pig breeds and haplotypes showed different mitochondrial content and OXPHOS gene expression pattern, which were linked to phenotypical variations. All these findings provided insights into the molecular regulatory patterns involved in muscle fibers and energy metabolism which may be used as biomarkers to predict meat quality and/or diagnose muscular diseases.

Zusammenfassung

Skelettmuskelaktivität ist auf ATP als hauptsächliche Energiewährung, welche vorwiegend durch oxidative Phosphorylierung in den Mitochondrien produziert wird, angewiesen. Wichtige Faktoren bei der Fleischqualität wie Zartheit und Saftigkeit sind mit dem Muskelfaserverhältnis und Energiestoffwechsel der Fleisch produzierenden Tiere assoziiert. In der vorliegenden Arbeit wurden die Schweinerassen Duroc und Pietrain, welche sich hinsichtlich ihrer slow-twitch-oxidative (STO) und fast-twitch-oxidative (FTO) –Fasern, wie auch ihrer mitochondriellen Aktivität unterscheiden, genutzt, um potenzielle biologische Stoffwechselwege im Zusammenhang mit dem Energiestoffwechsel zu identifizieren. Basierend auf holistischen Transkriptionsprofilen des ante mortem Longissimus-Muskels war die differentielle Genexpression zwischen Duroc und PiNN-Proben mit Protein-Ubiquitinierungs-, Stammzell-Pluripotenz-, Amyloid-Prozessierungs- und 3-Phosphoinositid-Biosynthese und –degradations-Stoffwechselwegen assoziiert. In der weighted gene co-expression network analysis zeigte Duroc starke Korrelationen zwischen Mitochondrien-annotierten Ko-Expressionsmodulen und STO (r = 0.78), FTO (r = -0.98), Komplex I (r = 0.72) und Komplex IV Aktivität (r = 0.86). Im Gegensatz dazu waren Ko-Expressionsmodule, die im Makromolekül-Katabolismus, im Aktin-Zytoskelett und in der Transkriptions-Aktivator-Aktivität annotiert waren, mit den Faserarten, der mitochondriellen Atmung und metabolischen Enzymen in PiNN assoziiert. Diese Ergebnisse deckten die wichtige Rolle der Mitochondrien auf und lenkten unser Interesse auf eine tiefgehende Untersuchung dieser Organellen und des Systems der oxidativen Phosphorylierung (OXPHOS). Eine vergleichende Analyse des miRNA-Expressionsprofils zwischen Duroc und PiNN wurde durchgeführt, um die miRNA-mRNA regulatorischen Netzwerke basierend auf ihrer paarweisen Korrelation sowie rechnergestützter Target-Vorhersage konstruieren zu können. Die identifizierten Zielgene wurden in den Stoffwechselwegen Protein-Ubiquitinierung, Stammzell-Pluripotenz, Skelett- und Muskelsystem-Entwicklung annotiert. Durch Integration der Korrelation mit phänotypischen Merkmalen legen die mit dem Energiestoffwechsel assoziierten miRNA-mRNA-Netzwerk-Konstrukte ihre unentbehrliche Rolle bei der Modulation des mitochondriellen Energieverbauchs im Schweinemuskel nahe. Zum Beispiel sind miR-25 mit den Zielgenen *BMPR2* und *IRS1*, miR-363 mit dem Zielgen *USP24*, miR-28 mit dem Zielgen *HECW2* sowie miR-210 mit den Zielgenen *ATP51, ME3, MTCH1* und *CPT2* hochgradig assoziiert mit STO-Fasern, FTO-Fasern sowie der ADP- und ATP-

Konzentration. Diese komplexen Netzwerke könnten durch Feinabstimmung der Genexpression zu den unterschiedlichen Muskel-Phänotypen beitragen. Die Bestätigung von miRNAs, ihrer Zielgene und ihrer Funktionen im Muskelenergiestoffwechsel werden im Weiteren sehr wichtig werden. Die Expressionsprofile von Stoffwechselweg-bezogenen Genen, welche im Zusammenhang mit oxidativen und glykolytischen Stoffwechselwegen stehen, wurden für ein weitergehendes Verständnis der molekularen Basis von Muskeleigenschaften analysiert. Dieser Teil umfasste des Weiteren eine F2-Kreuzung Duroc-Pietrain (DuPi) sowie eine MHS-homozygot-positive Rasse PiPP, welche in Ergänzung zu Duroc und PiNN Trägerin einer *RYR1*-Mutation ist. Jeder Zuchttyp wies eine individuelle Muskelfaserzusammensetzung auf. PiPP-Schweine zeigten eine signifikant niedrige Komplex-I-Aktivität als die drei anderen Schweinerassen. Auf Transkript-Ebene wies die Laktat-Dehydrogenase B eine Rassespezifität mit signifikant niedrigerer Expression in PiPP-Schweinen auf. PiPP-Schweine zeigten die niedrigste Genexpression für verschiedene Untereinheiten des oxidativen Phosphorylierungs-Komplexes (OXPHOS-Komplex), darunter Komplex I, Komplex II, Komplex IV und für die ATP-Synthase. Diese Studie verknüpfte zudem das OXPHOS-System mit verschiedenen Muskelfasertypen. Duroc-Schweine wiesen die stärkste Assoziation zwischen der OXPHOS-Expression und STO-Fasern auf, wohingegen DuPi-Schweine eine signifikante Korrelation zwischen der OXPHOS-Expression und FTO-Fasern zeigten. Aus diesem Grund ist die Transkriptions-Regulation der OXPHOS-Untereinheiten für die oxidative Kapazität der Muskelfasern essentiell. Da OXPHOS-Untereinheiten sowohl vom nukleären als auch vom mitochondriellen Genom kodiert werden, kommt es zu einer komplizierten Interaktion der beiden Genomsysteme beim Aufbau des vollständig funktionalen OXPHOS-Komplexes. Der letzte Teil der Arbeit legte den Fokus auf die mitochondrielle Genom-Aktivität des frühen *post mortem* Longissimus-Muskels der gleichen vier Schweinerassen, mit jeweils individuellen mitochondriellen Haplotypen, Muskelfasertypen, mitochondriellen Atmungsketten-Aktivitäten und Fettgehalten. PiPP trug ausschließlich Haplotyp 8 und wies die niedrigste absolute mtDNA-Kopienzahl in Begleitung der geringsten Abundanz von Transkripten der mitochondriell kodierten Untereinheiten *ND1*, *ND6, ATP6* sowie der nukleär kodierten Untereinheiten *NDUFA11* und *NDUFB8* auf. Haplotyp 4 der Duroc-Schweine hatte eine signifikant höhere mtDNA-Kopienzahl und eine höhere Genexpression für die mitochondriell kodierten Untereinheiten *ND1, ND6* und *ATP6*. Diese Ergebnisse zeigten, dass die mitochondriellen und nukleären genetischen Hintergründe eine Auswirkung auf den mitochondriellen Gehalt

und die Expression von OXPHOS-Untereinheiten bei Schweinen haben. Das Ko-Expressionsmuster von OXPHOS-Genen unterstützte die mitochondriell-nukleäre Interaktion und ihre Komplexität trug zum muskulären Stoffwechsel bei. Ein wichtiger Transkriptionsfaktor, *PGC-1α*, könnte zur Koordination des mitochondriell-nukleären Genoms beim Aufbau des OXPHOS-Systems beitragen. Infolgedessen könnten die mitochondriell-nukleäre Interaktion, der Haplotyp und die Variation der Kopienzahl wichtige Rollen bei der phänotypischen Variation des Muskels bei Nutztieren spielen. Zusammengefasst wurde in dieser Arbeit ein Transkriptionsprofil der mRNAs und miRNAs über das gesamte Genom des Schweinemuskels hinweg erstellt. Es konnten viele biologische Stoffwechselwege, die im Zusammenhang mit Muskelfasern, der mitochondriellen Atmung und metabolischen Enzymaktivitäten stehen, identifiziert werden, insbesondere hoben die Ergebnisse die Bedeutung des OXPHOS-Systems für den Energiestoffwechsel hervor. Anschließend wurde das OXPHOS-System intensiv auf sowohl nukleärer als auch mitochondrieller DNA-Ebene für den frühen *post mortem*-Muskel bzw. ausschließlich nukleär für den ante mortem-Muskel bei vier Schweinerassen mit verschiedenen mitochondriellen Haplotypen und unterschiedlichen Phänotypen untersucht. Verschiedene Schweinerassen und Haplotypen wiesen einen unterschiedlichen mitochondriellen Gehalt und ein unterschiedliches OXPHOS-Gen-Expressionsmuster auf, beides war ebenfalls mit phänotypischen Variationen verknüpft. All diese Ergebnisse liefern Einblicke in die molekularen regulatorischen Muster, die in Muskelfasereigenschaften und Energiestoffwechsel involviert sind und welche als Biomarker zur Vorhersage der Fleischqualität und/oder zur Diagnose muskulärer Erkrankungen genutzt werden könnten.

CHAPTER 6

References

References

Altschul SF, Gish W, Miller W, Myers EW, Lipman DJ (1990) Basic local alignment search tool. Journal of Molecular Biology 215:403-410

Altuwaijri S et al. (2004) Androgen receptor regulates expression of skeletal muscle-specific proteins and muscle cell types. Endocrine 25:27-32

Angin Y et al. (2012) CD36 inhibition prevents lipid accumulation and contractile dysfunction in rat cardiomyocytes. The Biochemical journal 448:43-53

Aoi W, Naito Y, Mizushima K, Takanami Y, Kawai Y, Ichikawa H, Yoshikawa T (2010) The microRNA miR-696 regulates PGC-1{alpha} in mouse skeletal muscle in response to physical activity. American journal of physiology Endocrinology and metabolism 298:E799-806

Aschrafi A, Kar AN, Natera-Naranjo O, MacGibeny MA, Gioio AE, Kaplan BB (2012) MicroRNA-338 regulates the axonal expression of multiple nuclear-encoded mitochondrial mRNAs encoding subunits of the oxidative phosphorylation machinery. Cellular and molecular life sciences : CMLS 69:4017-4027

Atilano SR et al. (2015) Mitochondrial DNA variants can mediate methylation status of inflammation, angiogenesis and signaling genes. Human molecular genetics 24:4491-4503

Barrey E, Saint-Auret G, Bonnamy B, Damas D, Boyer O, Gidrol X (2011) Pre-microRNA and mature microRNA in human mitochondria. PloS one 6:e20220

Baykara O, Sahin SK, Akbas F, Guven M, Onaran I (2016) The effects of mitochondrial DNA deletion and copy number variations on different exercise intensities in highly trained swimmers. Cellular and molecular biology (Noisy-le-Grand, France) 62:109-115

Bellizzi D, D'Aquila P, Giordano M, Montesanto A, Passarino G (2012) Global DNA methylation levels are modulated by mitochondrial DNA variants. Epigenomics 4:17-27

Benjamini Y, Hochberg Y (1995) Controlling the False Discovery Rate: A Practical and Powerful Approach to Multiple Testing. Journal of the Royal Statistical Society Series B (Methodological) 57:289-300

Biswas G et al. (1999) Retrograde Ca2+ signaling in C2C12 skeletal myocytes in response to mitochondrial genetic and metabolic stress: a novel mode of inter-organelle crosstalk. The EMBO journal 18:522-533

Bonnefoy N, Fiumera HL, Dujardin G, Fox TD (2009) Roles of Oxa1-related inner-membrane translocases in assembly of respiratory chain complexes. Biochimica et biophysica acta 1793:60-70

Camus MF, Wolf JB, Morrow EH, Dowling DK (2015) Single Nucleotides in the mtDNA Sequence Modify Mitochondrial Molecular Function and Are Associated with Sex-Specific Effects on Fertility and Aging. Current biology : CB 25:2717-2722

Chan SL, Mayne M, Holden CP, Geiger JD, Mattson MP (2000) Presenilin-1 mutations increase levels of ryanodine receptors and calcium release in PC12 cells and cortical neurons. The Journal of biological chemistry 275:18195-18200

Chan SW, Chevalier S, Aprikian A, Chen JZ (2013) Simultaneous quantification of mitochondrial DNA damage and copy number in circulating blood: a sensitive approach to systemic oxidative stress. BioMed research international 2013:157547

Chang H, Yi B, Ma R, Zhang X, Zhao H, Xi Y (2016) CRISPR/cas9, a novel genomic tool to knock down microRNA in vitro and in vivo. Scientific reports 6:22312

Chen X (2009) Small RNAs and their roles in plant development. Annual review of cell and developmental biology 25:21-44

Chen Z, Li Y, Zhang H, Huang P, Luthra R (2010) Hypoxia-regulated microRNA-210 modulates mitochondrial function and decreases ISCU and COX10 expression. Oncogene 29:4362-4368

Chen Z et al. (2015) MiR130b-Regulation of PPARgamma Coactivator-1alpha Suppresses Fat Metabolism in Goat Mammary Epithelial Cells. PloS one 10:e0142809

Cheng KK, Akasaki Y, Lecommandeur E, Lindsay RT, Murfitt S, Walsh K, Griffin JL (2015) Metabolomic analysis of akt1-mediated muscle hypertrophy in models of diet-induced obesity and age-related fat accumulation. Journal of proteome research 14:342-352

Cheng Z, Tseng Y, White MF (2010) Insulin signaling meets mitochondria in metabolism. Trends in endocrinology and metabolism: TEM 21:589-598

Cicek IO, Karaca S, Brankatschk M, Eaton S, Urlaub H, Shcherbata HR (2016) Hedgehog Signaling Strength Is Orchestrated by the mir-310 Cluster of MicroRNAs in Response to Diet. Genetics 202:1167-1183

Coenen MJ et al. (2004) Mutant mitochondrial elongation factor G1 and combined oxidative phosphorylation deficiency. The New England journal of medicine 351:2080-2086

Das S et al. (2012) Nuclear miRNA regulates the mitochondrial genome in the heart. Circulation research 110:1596-1603

Deffieu M, Bhatia-Kissova I, Salin B, Klionsky DJ, Pinson B, Manon S, Camougrand N (2013) Increased levels of reduced cytochrome b and mitophagy components are required to trigger nonspecific autophagy following induced mitochondrial dysfunction. Journal of cell science 126:415-426

Ellis JM et al. (2010) Adipose acyl-CoA synthetase-1 directs fatty acids toward beta-oxidation and is required for cold thermogenesis. Cell metabolism 12:53-64

Essen-Gustavsson B, Karlsson A, Lundstrom K, Enfalt AC (1994) Intramuscular fat and muscle fibre lipid contents in halothane-gene-free pigs fed high or low protein diets and its relation to meat quality. Meat science 38:269-277

Eyre-Walker A (2017) Mitochondrial Replacement Therapy: Are Mito-nuclear Interactions Likely To Be a Problem? Genetics 205:1365-1372

Falah M et al. (2016) The potential role for use of mitochondrial DNA copy number as predictive biomarker in presbycusis. Therapeutics and clinical risk management 12:1573-1578

Fernandez X, Lefaucheur L, Candek M (1995) Comparative study of two classifications of muscle fibres: Consequences for the photometric determination of glycogen according to fibre type in red and white muscle of the pig. Meat science 41:225-235

Fiedler I, Dietl G, Rehfeldt C, Wegner J, Ender K (2004) Muscle fibre traits as additional selection criteria for muscle growth and meat quality in pigs – results of a simulated selection. Journal of Animal Breeding and Genetics 121:331-344

Frontera WR, Ochala J (2015) Skeletal muscle: a brief review of structure and function. Calcified tissue international 96:183-195

Fujii J et al. (1991) Identification of a mutation in porcine ryanodine receptor associated with malignant hyperthermia. Science (New York, NY) 253:448-451

Fuste JM et al. (2010) Mitochondrial RNA polymerase is needed for activation of the origin of light-strand DNA replication. Molecular cell 37:67-78

Gabriel-Costa D et al. (2015) Lactate up-regulates the expression of lactate oxidation complex-related genes in left ventricular cardiac tissue of rats. PloS one 10:e0127843

Gao J, Wen S, Zhou H, Feng S (2015) De-methylation of displacement loop of mitochondrial DNA is associated with increased mitochondrial copy number and

nicotinamide adenine dinucleotide subunit 2 expression in colorectal cancer. Molecular medicine reports 12:7033-7038

Gao SM et al. (2010) Synergistic apoptosis induction in leukemic cells by miR-15a/16-1 and arsenic trioxide. Biochemical and biophysical research communications 403:203-208

Gao Y et al. (2016) Changes of the mitochondrial DNA copy number and the antioxidant system in the PBMC of hepatocellular carcinoma. Chinese journal of applied physiology 32:1-5

Giulivi C et al. (2011) Basal bioenergetic abnormalities in skeletal muscle from ryanodine receptor malignant hyperthermia-susceptible R163C knock-in mice. The Journal of biological chemistry 286:99-113

Gladden LB (2004) Lactate metabolism: a new paradigm for the third millennium. The Journal of physiology 558:5-30

Greaser ML, Cassens RG, Briskey EJ, Hoekstra WG (1969) Post-Mortem Changes in Subcellular Fractions from Normal and Pale, Soft, Exudative Porcine Muscle. 1. Calcium Accumulation and Adenosine Triphosphatase Activities. Journal of Food Science 34:120-124

Grivennikova VG, Vinogradov AD (2006) Generation of superoxide by the mitochondrial Complex I. Biochimica et biophysica acta 1757:553-561

Gueguen N, Lefaucheur L, Fillaut M, Vincent A, Herpin P (2005) Control of skeletal muscle mitochondria respiration by adenine nucleotides: differential effect of ADP and ATP according to muscle contractile type in pigs. Comparative biochemistry and physiology Part B, Biochemistry & molecular biology 140:287-297

Guha M et al. (2016) HnRNPA2 is a novel histone acetyltransferase that mediates mitochondrial stress-induced nuclear gene expression. Cell discovery 2:16045

Hamilton DL, Findlay JA, Montagut G, Meakin PJ, Bestow D, Jalicy SM, Ashford ML (2014) Altered amyloid precursor protein processing regulates glucose uptake and oxidation in cultured rodent myotubes. Diabetologia 57:1684-1692

Hejzlarova K et al. (2014) Nuclear genetic defects of mitochondrial ATP synthase. Physiological research / Academia Scientiarum Bohemoslovaca 63 Suppl 1:S57-71

Hocquette JF, Ortigues-Marty I, Pethick D, Herpin P, Fernandez X (1998) Nutritional and hormonal regulation of energy metabolism in skeletal muscles of meat-producing animals. Livestock Production Science 56:115-143

Hocquette JF, Ortigues-Marty I, Vermorel M (2001) Manipulation of Tissue Energy Metabolism in Meat-Producing Ruminants - Review. Asian-Australasian journal of animal sciences 14:720-732

Hong L, Huang HC, Jiang ZF (2014) Relationship between amyloid-beta and the ubiquitin-proteasome system in Alzheimer's disease. Neurological research 36:276-282

Hou X, Tang Z, Liu H, Wang N, Ju H, Li K (2012) Discovery of MicroRNAs associated with myogenesis by deep sequencing of serial developmental skeletal muscles in pigs. PloS one 7:e52123

Hu J et al. (2001) The ARKdb: genome databases for farmed and other animals. Nucleic acids research 29:106-110

Huang J, Tan L, Shen R, Zhang L, Zuo H, Wang DW (2016) Decreased Peripheral Mitochondrial DNA Copy Number is Associated with the Risk of Heart Failure and Long-term Outcomes. Medicine 95:e3323

Huang TH, Zhu MJ, Li XY, Zhao SH (2008) Discovery of porcine microRNAs and profiling from skeletal muscle tissues during development. PloS one 3:e3225

Huber K, Petzold J, Rehfeldt C, Ender K, Fiedler I (2007) Muscle energy metabolism: structural and functional features in different types of porcine striated muscles. Journal of muscle research and cell motility 28:249-258

Huff-Lonergan E, Lonergan SM (2005) Mechanisms of water-holding capacity of meat: The role of postmortem biochemical and structural changes. Meat science 71:194-204

Huff Lonergan E, Zhang W, Lonergan SM (2010) Biochemistry of postmortem muscle - lessons on mechanisms of meat tenderization. Meat science 86:184-195

Hunter RG et al. (2016) Stress and corticosteroids regulate rat hippocampal mitochondrial DNA gene expression via the glucocorticoid receptor. Proceedings of the National Academy of Sciences of the United States of America 113:9099-9104

Huynh TP, Murani E, Maak S, Ponsuksili S, Wimmers K (2013) UBE3B and ZRANB1 polymorphisms and transcript abundance are associated with water holding capacity of porcine M. longissimus dorsi. Meat science 95:166-172

Izumiya Y et al. (2008) Fast/Glycolytic muscle fiber growth reduces fat mass and improves metabolic parameters in obese mice. Cell metabolism 7:159-172

Jager S, Handschin C, St-Pierre J, Spiegelman BM (2007) AMP-activated protein kinase (AMPK) action in skeletal muscle via direct phosphorylation of PGC-1alpha. Proceedings of the National Academy of Sciences of the United States of America 104:12017-12022

Jin L et al. (2012) Mitochondrial DNA evidence indicates the local origin of domestic pigs in the upstream region of the Yangtze River. PloS one 7:e51649

Jin O et al. (2014) RyR1 mutation associated with malignant hyperthermia facilitates catecholaminergic stress-included arrhythmia via mitochondrial injury and oxidative stress (893.8). The FASEB Journal 28:893.898

Jo A et al. (2015) Efficient Mitochondrial Genome Editing by CRISPR/Cas9. BioMed research international 2015:305716

Kaaman M, Sparks LM, van Harmelen V, Smith SR, Sjolin E, Dahlman I, Arner P (2007) Strong association between mitochondrial DNA copy number and lipogenesis in human white adipose tissue. Diabetologia 50:2526-2533

Kang C, Li Ji L (2012) Role of PGC-1alpha signaling in skeletal muscle health and disease. Annals of the New York Academy of Sciences 1271:110-117

Karlsson A, Essen-Gustavsson B, Lundstrom K (1994) Muscle glycogen depletion pattern in halothane-gene-free pigs at slaughter and its relation to meat quality. Meat science 38:91-101

Karlsson AH, Klont RE, Fernandez X (1999) Skeletal muscle fibres as factors for pork quality. Livestock Production Science 60:255-269

Kasiviswanathan R, Collins TR, Copeland WC (2012) The interface of transcription and DNA replication in the mitochondria. Biochimica et biophysica acta 1819:970-978

Kawamata H, Tiranti V, Magrane J, Chinopoulos C, Manfredi G (2011) adPEO mutations in ANT1 impair ADP-ATP translocation in muscle mitochondria. Human molecular genetics 20:2964-2974

Kelly RD, Mahmud A, McKenzie M, Trounce IA, St John JC (2012) Mitochondrial DNA copy number is regulated in a tissue specific manner by DNA methylation of the nuclear-encoded DNA polymerase gamma A. Nucleic acids research 40:10124-10138

Kerner J, Hoppel C (2000) Fatty acid import into mitochondria. Biochimica et biophysica acta 1486:1-17

Kim JM, Lim KS, Hong JS, Kang JH, Lee YS, Hong KC (2015) A polymorphism in the porcine miR-208b is associated with microRNA biogenesis and expressions of SOX-6 and MYH7 with effects on muscle fibre characteristics and meat quality. Animal genetics 46:73-77

Kim NK et al. (2008) Comparisons of longissimus muscle metabolic enzymes and muscle fiber types in Korean and western pig breeds. Meat science 78:455-460

Kren BT, Wong PY, Sarver A, Zhang X, Zeng Y, Steer CJ (2009) MicroRNAs identified in highly purified liver-derived mitochondria may play a role in apoptosis. RNA biology 6:65-72

Krischek C, Natter R, Wigger R, Wicke M (2011) Adenine nucleotide concentrations and glycolytic enzyme activities in longissimus muscle samples of different pig genotypes collected before and after slaughter. Meat science 89:217-220

Kruger J, Rehmsmeier M (2006) RNAhybrid: microRNA target prediction easy, fast and flexible. Nucleic acids research 34:W451-454

Langfelder P, Horvath S (2008) WGCNA: an R package for weighted correlation network analysis. BMC bioinformatics 9:559

Leberer E, Pette D (1984) Lactate dehydrogenase isozymes in type I, IIA and IIB fibres of rabbit skeletal muscles. Histochemistry 80:295-298

LeBleu VS et al. (2014) PGC-1alpha mediates mitochondrial biogenesis and oxidative phosphorylation in cancer cells to promote metastasis. Nature cell biology 16:992-1003, 1001-1015

Lecker SH, Solomon V, Mitch WE, Goldberg AL (1999) Muscle protein breakdown and the critical role of the ubiquitin-proteasome pathway in normal and disease states. The Journal of nutrition 129:227S-237S

Lee JS, Kim JM, Lim KS, Hong JS, Hong KC, Lee YS (2013) Effects of polymorphisms in the porcine microRNA MIR206 / MIR133B cluster on muscle fiber and meat quality traits. Animal genetics 44:101-106

Lehman JJ, Barger PM, Kovacs A, Saffitz JE, Medeiros DM, Kelly DP (2000) Peroxisome proliferator-activated receptor gamma coactivator-1 promotes cardiac mitochondrial biogenesis. The Journal of clinical investigation 106:847-856

Lewis BP, Burge CB, Bartel DP (2005) Conserved seed pairing, often flanked by adenosines, indicates that thousands of human genes are microRNA targets. Cell 120:15-20

Li HY et al. (2012) Identification and comparison of microRNAs from skeletal muscle and adipose tissues from two porcine breeds. Animal genetics 43:704-713

Librado P, Rozas J (2009) DnaSP v5: a software for comprehensive analysis of DNA polymorphism data. Bioinformatics (Oxford, England) 25:1451-1452

Lim D, Lee SH, Kim NK, Cho YM, Chai HH, Seong HH, Kim H (2013) Gene Co-expression Analysis to Characterize Genes Related to Marbling Trait in Hanwoo (Korean) Cattle. Asian-Australasian journal of animal sciences 26:19-29

Lin CS et al. (1999) Complete nucleotide sequence of pig (Sus scrofa) mitochondrial genome and dating evolutionary divergence within Artiodactyla. Gene 236:107-114

Lin J et al. (2002) Transcriptional co-activator PGC-1 alpha drives the formation of slow-twitch muscle fibres. Nature 418:797-801

Liu J, Liang X, Gan Z (2015) Transcriptional regulatory circuits controlling muscle fiber type switching. Science China Life sciences 58:321-327

Liu L et al. (2014) MicroRNA-15b enhances hypoxia/reoxygenation-induced apoptosis of cardiomyocytes via a mitochondrial apoptotic pathway. Apoptosis : an international journal on programmed cell death 19:19-29

Loan HT, Murani E, Maak S, Ponsuksili S, Wimmers K (2014) UBXN1 polymorphism and its expression in porcine M. longissimus dorsi are associated with water holding capacity. Molecular biology reports 41:1411-1418

Ma J et al. (2015) The miRNA Transcriptome Directly Reflects the Physiological and Biochemical Differences between Red, White, and Intermediate Muscle Fiber Types. International journal of molecular sciences 16:9635-9653

Martin MA et al. (2005) Leigh syndrome associated with mitochondrial complex I deficiency due to a novel mutation in the NDUFS1 gene. Archives of neurology 62:659-661

Marusich MF, Robinson BH, Taanman JW, Kim SJ, Schillace R, Smith JL, Capaldi RA (1997) Expression of mtDNA and nDNA encoded respiratory chain proteins in chemically and genetically-derived Rho0 human fibroblasts: a comparison of subunit proteins in normal fibroblasts treated with ethidium bromide and fibroblasts from a patient with mtDNA depletion syndrome. Biochimica et biophysica acta 1362:145-159

McDaneld TG et al. (2009) MicroRNA transcriptome profiles during swine skeletal muscle development. BMC genomics 10:77

Merry TL, Steinberg GR, Lynch GS, McConell GK (2010) Skeletal muscle glucose uptake during contraction is regulated by nitric oxide and ROS independently of AMPK. American journal of physiology Endocrinology and metabolism 298:E577-585

Mili S, Pinol-Roma S (2003) LRP130, a pentatricopeptide motif protein with a noncanonical RNA-binding domain, is bound in vivo to mitochondrial and nuclear RNAs. Molecular and cellular biology 23:4972-4982

Monin G, Sellier P (1985) Pork of low technological quality with a normal rate of muscle pH fall in the immediate post-mortem period: The case of the Hampshire breed. Meat science 13:49-63

Mourier A, Ruzzenente B, Brandt T, Kuhlbrandt W, Larsson NG (2014) Loss of LRPPRC causes ATP synthase deficiency. Human molecular genetics 23:2580-2592

Murphy MP (2009) How mitochondria produce reactive oxygen species. The Biochemical journal 417:1-13

Murton AJ, Constantin D, Greenhaff PL (2008) The involvement of the ubiquitin proteasome system in human skeletal muscle remodelling and atrophy. Biochimica et biophysica acta 1782:730-743

Neupert W, Herrmann JM (2007) Translocation of proteins into mitochondria. Annual review of biochemistry 76:723-749

Nishi H et al. (2010) MicroRNA-15b modulates cellular ATP levels and degenerates mitochondria via Arl2 in neonatal rat cardiac myocytes. The Journal of biological chemistry 285:4920-4930

Noji H, Yoshida M (2001) The rotary machine in the cell, ATP synthase. The Journal of biological chemistry 276:1665-1668

O'Neill HM, Holloway GP, Steinberg GR (2013) AMPK regulation of fatty acid metabolism and mitochondrial biogenesis: implications for obesity. Molecular and cellular endocrinology 366:135-151

Pai S, Ren J (2014) IdeoViz: Plots data (continuous/discrete) along chromosomal ideogram, R package version 1.6.0 edn.,

Pan L et al. (2015) MiR-25 protects cardiomyocytes against oxidative damage by targeting the mitochondrial calcium uniporter. International journal of molecular sciences 16:5420-5433

Pasquinelli AE (2012) MicroRNAs and their targets: recognition, regulation and an emerging reciprocal relationship. Nature reviews Genetics 13:271-282

Pearson AM, Dutson TR (1994) Quality Attributes and Their Measurement in Meat, Poultry and Fish Products. Blackie Academic,

Peter JB, Sawaki S, Barnard RJ, Edgerton VR, Gillespie CA (1971) Lactate dehydrogenase isoenzymes: distribution in fast-twitch red, fast-twitch white, and slow-twitch intermediate fibers of guinea pig skeletal muscle. Archives of biochemistry and biophysics 144:304-307

Pickova A, Potocky M, Houstek J (2005) Assembly factors of F1FO-ATP synthase across genomes. Proteins 59:393-402

Pohjoismaki JL, Wanrooij S, Hyvarinen AK, Goffart S, Holt IJ, Spelbrink JN, Jacobs HT (2006) Alterations to the expression level of mitochondrial transcription factor A, TFAM, modify the mode of mitochondrial DNA replication in cultured human cells. Nucleic acids research 34:5815-5828

Ponsuksili S, Du Y, Hadlich F, Siengdee P, Murani E, Schwerin M, Wimmers K (2013) Correlated mRNAs and miRNAs from co-expression and regulatory networks affect porcine muscle and finally meat properties. BMC genomics 14:533

Powers SK, Talbert EE, Adhihetty PJ (2011) Reactive oxygen and nitrogen species as intracellular signals in skeletal muscle. The Journal of physiology 589:2129-2138

Psarra AM, Sekeris CE (2011) Glucocorticoids induce mitochondrial gene transcription in HepG2 cells: role of the mitochondrial glucocorticoid receptor. Biochimica et biophysica acta 1813:1814-1821

Psarra AM, Solakidi S, Sekeris CE (2006) The mitochondrion as a primary site of action of steroid and thyroid hormones: presence and action of steroid and thyroid hormone receptors in mitochondria of animal cells. Molecular and cellular endocrinology 246:21-33

Rebelo AP, Dillon LM, Moraes CT (2011) Mitochondrial DNA transcription regulation and nucleoid organization. Journal of inherited metabolic disease 34:941-951

Rehmsmeier M, Steffen P, Hochsmann M, Giegerich R (2004) Fast and effective prediction of microRNA/target duplexes. RNA (New York, NY) 10:1507-1517

Reznik E et al. (2016) Mitochondrial DNA copy number variation across human cancers. eLife 5

Richard I et al. (1995) Mutations in the proteolytic enzyme calpain 3 cause limb-girdle muscular dystrophy type 2A. Cell 81:27-40

Ros S, Schulze A (2013) Balancing glycolytic flux: the role of 6-phosphofructo-2-kinase/fructose 2,6-bisphosphatases in cancer metabolism. Cancer & metabolism 1:8

Rybalka E, Timpani CA, Cooke MB, Williams AD, Hayes A (2014) Defects in mitochondrial ATP synthesis in dystrophin-deficient mdx skeletal muscles may be caused by complex I insufficiency. PloS one 9:e115763

Ryu YC et al. (2008) Comparing the histochemical characteristics and meat quality traits of different pig breeds. Meat science 80:363-369

Salminen TS, Oliveira MT, Cannino G, Lillsunde P, Jacobs HT, Kaguni LS (2017) Mitochondrial genotype modulates mtDNA copy number and organismal phenotype in Drosophila. Mitochondrion

Samovski D et al. (2015) Regulation of AMPK activation by CD36 links fatty acid uptake to beta-oxidation. Diabetes 64:353-359

Sander JD, Joung JK (2014) CRISPR-Cas systems for editing, regulating and targeting genomes. Nature biotechnology 32:347-355

Scheffler TL, Matarneh SK, England EM, Gerrard DE (2015) Mitochondria influence postmortem metabolism and pH in an in vitro model. Meat science 110:118-125

Schleinitz D et al. (2011) Genetic and evolutionary analyses of the human bone morphogenetic protein receptor 2 (BMPR2) in the pathophysiology of obesity. PloS one 6:e16155

Shen QW, Underwood KR, Means WJ, McCormick RJ, Du M (2007) The halothane gene, energy metabolism, adenosine monophosphate-activated protein kinase, and glycolysis in postmortem pig longissimus dorsi muscle. Journal of animal science 85:1054-1061

Shi Y, Buffenstein R, Pulliam DA, Van Remmen H (2010) Comparative studies of oxidative stress and mitochondrial function in aging. Integrative and comparative biology 50:869-879

Shinde S, Bhadra U (2015) A complex genome-microRNA interplay in human mitochondria. BioMed research international 2015:206382

Shock LS, Thakkar PV, Peterson EJ, Moran RG, Taylor SM (2011) DNA methyltransferase 1, cytosine methylation, and cytosine hydroxymethylation in mammalian mitochondria. Proceedings of the National Academy of Sciences of the United States of America 108:3630-3635

Short KR, Nygren J, Barazzoni R, Levine J, Nair KS (2001) T(3) increases mitochondrial ATP production in oxidative muscle despite increased expression of UCP2 and -3. American journal of physiology Endocrinology and metabolism 280:E761-769

Shukla GC, Singh J, Barik S (2011) MicroRNAs: Processing, Maturation, Target Recognition and Regulatory Functions. Molecular and cellular pharmacology 3:83-92

Siengdee P, Trakooljul N, Murani E, Schwerin M, Wimmers K, Ponsuksili S (2015) MicroRNAs Regulate Cellular ATP Levels by Targeting Mitochondrial Energy Metabolism Genes during C2C12 Myoblast Differentiation. PloS one 10:e0127850

Smits P, Smeitink J, van den Heuvel L (2010) Mitochondrial translation and beyond: processes implicated in combined oxidative phosphorylation deficiencies. Journal of biomedicine & biotechnology 2010:737385

Stump CS, Short KR, Bigelow ML, Schimke JM, Nair KS (2003) Effect of insulin on human skeletal muscle mitochondrial ATP production, protein synthesis, and mRNA transcripts. Proceedings of the National Academy of Sciences of the United States of America 100:7996-8001

Tang J, Wang Z, Chen L, Huang G, Hu X (2015) Gossypol acetate induced apoptosis of pituitary tumor cells by targeting the BCL-2 via the upregulated microRNA miR-15a. International journal of clinical and experimental medicine 8:9079-9085

Thompson JD, Gibson TJ, Plewniak F, Jeanmougin F, Higgins DG (1997) The CLUSTAL_X windows interface: flexible strategies for multiple sequence alignment aided by quality analysis tools. Nucleic acids research 25:4876-4882

Tiano JP, Springer DA, Rane SG (2015) SMAD3 negatively regulates serum irisin and skeletal muscle FNDC5 and peroxisome proliferator-activated receptor gamma coactivator 1-alpha (PGC-1alpha) during exercise. The Journal of biological chemistry 290:7671-7684

Torraco A, Peralta S, Iommarini L, Diaz F (2015) Mitochondrial Diseases Part I: mouse models of OXPHOS deficiencies caused by defects in respiratory complex subunits or assembly factors. Mitochondrion 21:76-91

Tsai T, St John JC (2016) The role of mitochondrial DNA copy number, variants, and haplotypes in farm animal developmental outcome. Domestic animal endocrinology 56 Suppl:S133-146

von Hofsten J, Elworthy S, Gilchrist MJ, Smith JC, Wardle FC, Ingham PW (2008) Prdm1- and Sox6-mediated transcriptional repression specifies muscle fibre type in the zebrafish embryo. EMBO reports 9:683-689

Voos W, Rottgers K (2002) Molecular chaperones as essential mediators of mitochondrial biogenesis. Biochimica et biophysica acta 1592:51-62

Wahlquist C et al. (2014) Inhibition of miR-25 improves cardiac contractility in the failing heart. Nature 508:531-535

Wan L, Ma J, Xu G, Wang D, Wang N (2014) Molecular cloning, structural analysis and tissue expression of protein phosphatase 3 catalytic subunit alpha isoform (PPP3CA)

gene in Tianfu goat muscle. International journal of molecular sciences 15:2346-2358

Wang J, Jiang J, Fu W, Jiang L, Ding X, Liu JF, Zhang Q (2012) A genome-wide detection of copy number variations using SNP genotyping arrays in swine. BMC genomics 13:273

Werner C, Natter R, Schellander K, Wicke M (2010a) Mitochondrial respiratory activity in porcine longissimus muscle fibers of different pig genetics in relation to their meat quality. Meat science 85:127-133

Werner C, Natter R, Wicke M (2010b) Changes of the activities of glycolytic and oxidative enzymes before and after slaughter in the longissimus muscle of Pietrain and Duroc pigs and a Duroc-Pietrain crossbreed. Journal of animal science 88:4016-4025

Werner C, Opalka JR, Gellerich FN, Wicke M (2005) The influence of mitochondrial function on meat quality in turkey and swine. Arch Anim Breed 48:106-114

Wojtaszewski JF, Jorgensen SB, Hellsten Y, Hardie DG, Richter EA (2002) Glycogen-dependent effects of 5-aminoimidazole-4-carboxamide (AICA)-riboside on AMP-activated protein kinase and glycogen synthase activities in rat skeletal muscle. Diabetes 51:284-292

Wojtaszewski JF et al. (2003) Regulation of 5'AMP-activated protein kinase activity and substrate utilization in exercising human skeletal muscle. American journal of physiology Endocrinology and metabolism 284:E813-822

Wu W, Ren Z, Zhang L, Liu Y, Li H, Xiong Y (2013) Overexpression of Six1 gene suppresses proliferation and enhances expression of fast-type muscle genes in C2C12 myoblasts. Molecular and cellular biochemistry 380:23-32

Wu Z et al. (1999) Mechanisms controlling mitochondrial biogenesis and respiration through the thermogenic coactivator PGC-1. Cell 98:115-124

Xie YM et al. (2015) Quantitative changes in mitochondrial DNA copy number in various tissues of pigs during growth. Genetics and molecular research : GMR 14:1662-1670

Xu B, Clayton DA (1996) RNA-DNA hybrid formation at the human mitochondrial heavy-strand origin ceases at replication start sites: an implication for RNA-DNA hybrids serving as primers. The EMBO journal 15:3135-3143

Xu X et al. (2002) The novel presenilin-1-associated protein is a proapoptotic mitochondrial protein. The Journal of biological chemistry 277:48913-48922

Xu X, Xu X, Yin Q, Sun L, Liu B, Wang Y (2011) The molecular characterization and associations of porcine cardiomyopathy asssociated 5 (CMYA5) gene with carcass trait and meat quality. Molecular biology reports 38:2085-2090

Yang Z, Lanks CW, Tong L (2002) Molecular mechanism for the regulation of human mitochondrial NAD(P)+-dependent malic enzyme by ATP and fumarate. Structure (London, England : 1993) 10:951-960

Yue G et al. (2003) Linkage and QTL mapping for Sus scrofa chromosome 6. Journal of Animal Breeding and Genetics 120:45-55

Zhang B, Horvath S (2005) A general framework for weighted gene co-expression network analysis. Statistical applications in genetics and molecular biology 4:Article17

Zhou R et al. (2015) Mitochondria-related miR-151a-5p reduces cellular ATP production by targeting CYTB in asthenozoospermia. Scientific reports 5:17743

Zhou Z, Zhou J, Du Y (2012) Estrogen receptor alpha interacts with mitochondrial protein HADHB and affects beta-oxidation activity. Molecular & cellular proteomics : MCP 11:M111 011056

Zuo L, Pannell BK (2015) Redox Characterization of Functioning Skeletal Muscle. Frontiers in physiology 6:338

ANNEX A

Publications

List of publications

A.1 Muscle transcriptional profile based on muscle fiber, mitochondrial respiratory activity and metabolic enzymes

Xuan Liu, Yang Du, Nares Trakooljul, Bodo Brand, Eduard Muráni, Carsten Krischek, Michael Wicke, Manfred Schwerin, Klaus Wimmers, Siriluck Ponsuksili

Published in: International Journal of Biological Sciences (2015) 11(12):1348-1362

DOI: 10.7150/ijbs.13132

A.2 MicroRNA-mRNA regulatory networking fine-tunes the porcine muscular mitochondrial respiratory and metabolic enzyme activities

Xuan Liu, Nares Trakooljul, Frieder Hadlich, Eduard Muráni, Klaus Wimmers, Siriluck Ponsuksili

Published in: BMC Genomics (2016) 17:531

DOI: 10.1186/s12864-016-2850-8

A.3 Molecular changes in mitochondrial respiratory activity and metabolic enzyme activity in muscle of four pig breeds with distinct metabolic types

Xuan Liu, Nares Trakooljul, Eduard Muráni, Carsten Krischek, Karl Schellander, Michael Wicke, Klaus Wimmers, Siriluck Ponsuksili

Published in: Journal of Bioenergetics and Biomembranes (2016) 48(1):55-65

DOI: 10.1007/s10863-015-9639-3

A.4 Mitochondrial-nuclear crosstalk, haplotype and copy number variation distinct in muscle fiber type, mitochondrial respiratory and metabolic enzyme activities

Xuan Liu, Nares Trakooljul, Frieder Hadlich, Eduard Muráni, Klaus Wimmers, Siriluck Ponsuksili

Published in: Scientific Reports (2017) 7: 14024

DOI: 10.1038/s41598-017-14491-w

Research Paper

Muscle Transcriptional Profile Based on Muscle Fiber, Mitochondrial Respiratory Activity, and Metabolic Enzymes

Xuan Liu[1], Yang Du[1], Nares Trakooljul[1], Bodo Brand[1], Eduard Muráni[1], Carsten Krischek[2], Michael Wicke[3], Manfred Schwerin[1], Klaus Wimmers[1], Siriluck Ponsuksili[1] ✉

1. Leibniz Institute for Farm Animal Biology (FBN), Institute for Genome Biology, Wilhelm-Stahl-Allee 2, D-18196 Dummerstorf, Germany
2. 2 Institute of Food Quality and Food Safety, University of Veterinary Medicine Hannover, D-30173 Hannover, Germany.
3. 3 Department of Animal Science, Quality of Food of Animal Origin, Georg-August-University Goettingen, D-37075 Goettingen, Germany.

✉ Corresponding author: Siriluck Ponsuksili, Leibniz Institute for Farm Animal Biology Wilhelm-Stahl-Allee 2, 18196 Dummerstorf, Germany. Phone: +49 38208 68700; Fax: +49 38208 68702; Email: s.wimmers@fbn-dummertorf.de

Abstract

Skeletal muscle is a highly metabolically active tissue that both stores and consumes energy. Important biological pathways that affect energy metabolism and metabolic fiber type in muscle cells may be identified through transcriptomic profiling of the muscle, especially ante mortem. Here, gene expression was investigated in malignant hyperthermia syndrome (MHS)-negative Duroc and Pietrian (PiNN) pigs significantly differing for the muscle fiber types slow-twitch-oxidative fiber (STO) and fast-twitch-oxidative fiber (FTO) as well as mitochondrial activity (succinate-dependent state 3 respiration rate). Longissimus muscle samples were obtained 24 h before slaughter and profiled using cDNA microarrays. Differential gene expression between Duroc and PiNN muscle samples were associated with protein ubiquitination, stem cell pluripotency, amyloid processing, and 3-phosphoinositide biosynthesis and degradation pathways. In addition, weighted gene co-expression network analysis within both breeds identified several co-expression modules that were associated with the proportion of different fiber types, mitochondrial respiratory activity, and ATP metabolism. In particular, Duroc results revealed strong correlations between mitochondrion-associated co-expression modules and STO (r = 0.78), fast-twitch glycolytic fiber (r = -0.98), complex I (r=0.72) and COX activity (r = 0.86). Other pathways in the protein-kinase-activity enriched module were positively correlated with STO (r=0.93), while negatively correlated with FTO (r = -0.72). In contrast to PiNN, co-expression modules enriched in macromolecule catabolic process, actin cytoskeleton, and transcription activator activity were associated with fiber types, mitochondrial respiratory activity, and metabolic enzyme activities. Our results highlight the importance of mitochondria for the oxidative capacity of porcine muscle and for breed-dependent molecular pathways in muscle cell fibers.

Key words: microarray; muscle; muscle fiber; mitochondrial Respiratory Activity

Introduction

Skeletal muscle activity requires energy through anabolism and catabolism of glycogen, carbohydrates, and fat, all of which are important for energy storage and supply [1]. The major currency molecule of energy, adenosine triphosphate (ATP), is produced mainly through oxidative phosphorylation in mitochondria. In oxygen-deficient or oxygen-depleted conditions, like exhaustive exercise or even death after slaughter in meat-producing animals, anaerobic glycolysis produces an accumulation of lactic acid and lowers the muscle pH, both of which ultimately lead to muscle ache and cell damage or to impaired meat

tenderness and flavor [1, 2]. Further, factors like the proportion of glycolytic and oxidative fibers are associated with meat characteristics such as color [3]. Generally, a higher fat content and more oxidative fibers than glycolytic fibers can improve the juiciness and tenderness of meat. Therefore, energy metabolism in the muscle cells needs to be properly regulated for optimal metabolic functions for different muscle fibers and can ultimately influence meat quality [2].

Two well-studied commercial pig breeds, Duroc and Pietrain, exhibit distinct muscle phenotypes and meat quality. For example, Duroc pigs are fattier and have lower muscle mass but a higher percentage of slow-twitch oxidative muscle fibers compared to Pietrain pigs, which are more muscular and have a higher lean meat percentage and more fast-twitch glycolytic fibers. These differences may be attributed to differences in gene expression profiles of the muscle in these two breeds, which arise as early as the prenatal stages [4, 5]. Although mitochondrial respiratory and metabolic enzyme activities have been well studied in the different muscle fiber types of these two breeds [6-8], the underlying molecular basis of their differences remains to be unraveled.

In the present study, microarray-based transcription profiling, differential gene expression and weighted gene co-expression network analysis (WGCNA) were used to dissect pathways associated with muscle fiber types and activities of glycolytic and oxidative enzymes in longissimus muscle samples obtained 24 h before slaughter of Duroc and Pietrain. WGCNA groups genes into a co-expression network/module based on their similarity of expression patterns. This approach has been demonstrated to identify genes sharing similar functions and/or involved in related molecular events [9]. Results from the present study shed light on biological pathways related to energy metabolism and mitochondrial respiratory activity in muscle cell, and this may have implications for pork quality.

Materials and Methods

Sample collection and phenotypic measurement

This experiment and muscle biopsy collection have been approved and authorized by the German and European animal welfare regulations for animal husbandry, transport, and slaughter [6-8]. Animal care and tissue collection procedures followed the guidelines of the German Law of Animal Protection, and the experimental protocol was approved by the Animal Care Committee of the research institutions and with an official permission from the responsible authorities (Niedersächsischen Landesamt für Ver-

braucherschutz und Lebensmittelsicherheit (LAVES) 33.42502/01-47.05). The experimental protocol was carried out in accordance with the approved guidelines for safeguarding good scientific practice

As previously described [6-8], Duroc and Pietrain (PiNN) pigs, which are a subset of animals from our previous study, were raised until 180 days of age. To avoid the effects of the malignant hyperthermia syndrome (MHS) locus, only muscle samples from MHS-negative genotype pigs were investigated. Muscle biopsies were collected from five female and male pigs of each breed (n=20) for DNA microarray analysis and phenotypic measurements. Biopsies were collected from the longissimus muscle (LM) between the 13/14th thoracic vertebrae (Th) 24 h before slaughter. Phenotypic measurements of muscle fiber types, mitochondrial respiratory activity, and activities of glycolytic and oxidative enzymes were performed as described previously [6-8]. A short definition and a brief description of the applied methods for all phenotypic traits are provided in Supplemental Table S1.

Total RNA isolation

Total RNA was isolated from the LM biopsies kept at -80 °C (Duroc n=10, PiNN n=10) using Tri-Reagent and RNeasy Mini kit (Qiagen) with an on-column DNase treatment according to the manufacturer's protocol. The RNA integrity was assessed on a 1% agarose gel by electrophoresis. The RNA concentration was measured by a Nano Drop ND-1000 Spectrophotometer (PEQLAB).

DNA microarray analysis

Porcine Snowball Microarray (Affymetrix) containing 47,880 probe-sets was used to determine the expression profile of the LM 24 h ante mortem of Duroc and PiNN pigs. 500 ng total RNA isolated from each biopsy were used for cDNA synthesis and subsequent biotin labeling using the Affymetrix WT plus Expression kit and Genechip WT terminal labeling and hybridization kit according to the manufacturer's instructions. Each of the labeled cRNA samples was hybridized on the array (n=20). The hybridization, washing, and scanning of the arrays was performed in accordance with the manufacturer's recommendations. Affymetrix GCOC1.1.1 software was used for quality control. Expression Console software was used for robust multichip average (RMA) normalization and the detection of present genes by applying the DABG (detection above background) algorithm. Further filtering was done by excluding transcripts with low signals and probes that were present in less than 80% of the samples within each breed. 17,820 probes passed the quality filtering and were used for

further analyses. Differential expression analysis was performed using the ANOVA procedure in JMP genomics 7 (SAS Institute). The breed was treated as a fixed effect. False discovery rate (FDR) was used to control an error rate of a multiple-hypothesis testing according to Benjamini & Hochberg [10]. The expression data are available in the Gene Expression Omnibus public repository with the GEO accession number GSE69840: GSM1709900 – GSM1709919.

Weighted gene co-expression network analysis (WGCNA)

Post-filter, 17,820 probes were utilized in the construction of weighted gene co-expression networks using the blockwise modules function in the WGCNA R package as described previously [9, 11, 12]. The analysis was applied separately for each breed. The WGCNA procedure calculated a Pearson correlation matrix for all genes then an adjacency matrix was calculated by raising all values to a power ß from the correlation matrix. The adjacency matrix was converted to a topological overlap matrix (TOM) and the TOM-based dissimilarity matrix for hierarchical clustering. The gene co-expression modules were identified from the hierarchical cluster tree using a dynamic tree cut procedure. The formula of topological overlap matrix (TOM) $\Omega = [\omega_{ij}]$ was as follows,

$$\omega_{ij} = \frac{a_{ij} + \sum_u a_{iu} a_{uj}}{min\{\sum_u a_{iu}, \sum_u a_{ju}\} + 1 - a_{ij}}, \; a_{ij} = \left| cor(x_i, x_j) \right|^{ß}$$

where x_i and x_j were the gene expression profile of the x_i-th and x_j-th gene and a_{ij} was the adjacency. By inspecting the scale-free topology model fit, the power ß was selected as the minimal ß value giving a coefficient of determination R^2 higher than 90%. Modules were further merged based on the dissimilarity between their eigengenes, which were defined as the first principle component of each module. Genes that were not assigned to another module were assigned to module grey. Eigengenes act as the representative for each module. To identify gene co-expression modules highly correlated to the phenotype, module-trait relationships were estimated using the correlation between the module eigengene and the phenotype.

Gene functional annotation and pathway analysis

To identify pathways related to phenotypic differences of the muscle between Duroc and PiNN pigs, differentially expressed genes (DEGs) between these two breeds were analyzed using the IPA software (Ingenuity Systems, http://www.ingenuity.com). IPA categorizes genes based on annotated gene functions and statistically tests for over-representation of functional terms within the gene list using Fisher's

Exact Test. Moreover, we used WGCNA to identify gene network modules based on their co-expression patterns and correlated them with phenotypic measurements or traits for both pig breeds separately. A gene list of each significant module-trait correlation was analyzed to obtain biologically meaningful represented pathways based on an enrichment score and p-value threshold using IPA and the DAVID online-tool (Database for Annotation, Visualization and Integrated Discovery; http://david.abcc.ncifcrf.gov/home.jsp).

Quantitative real time PCR (qPCR) for microarray validation

qPCR of each individual RNA sample (n=20) was performed using a fast gene expression analysis, EvaGreen, and the BioMark HD Real-time PCR System according to manufacturer's recommendation (Fluidigm). Briefly, cDNA was synthesized from 2 μg of total RNA using Superscript II reverse transcriptase and Oligo dT with a specific target amplification (STA) and Exonuclease I treatment. The qPCR reaction was performed using a 48X48 Dynamic Array and integrated fluidic circuit (IFC). For each sample inlet, 2.5 uL SsoFast EvaGreen supermix with low ROX (Biorad), 0.25 uL DNA binding dye sample loading reagent, and 2.25 uL STA and Exo-I treated sample were loaded. For each assay inlet, 2.5 uL assay loading reagent, 2.25 uL DNA suspension buffer, and 0.25 uL 100 uM mixed (forward and reverse) primers were loaded. All measurements were performed in duplicate. The thermal parameters were 95 °C for 60 s, followed by 30 cycles of 95 °C for 5 s and 60 °C for 20s. The primer sequence information is accessible in Supplemental Table S2. *ATP6V1C1, ATP6V1E1, COX10, COX7A2, CYB5A, NDUFS1, NDUFS6* and *PPA1* were selected for a qPCR validation based on their functions related to energy metabolism. Three reference genes, *ACTB, RPL32*, and *RPS11* were used to normalize the expression value. Correlation coefficient analysis between the microarray and qPCR was calculated using SAS 9.3 (SAS Institute).

Results

Phenotypic traits

Definitions for all phenotype traits are listed in Supplemental Table S1 and the results are depicted in Figure 1. Muscle fiber composition analysis indicated that Duroc pigs had a higher percentage of slow-twitch-oxidative fiber (STO) (16.08 vs 9.99 %; p-value=0.032) and a smaller percentage of fast-twitch-oxidative fiber (FTO) (8.62 vs 15.13 %, p=0.019) compared to PiNN pigs. No difference between breeds was observed for the

fast-twitch-glycolytic fiber (FTG). The succinate-dependent state 3 respiration rate, a measure of mitochondrial activity, was significantly higher in Duroc than PiNN pigs ($p<0.05$). Other mitochondrial respiratory activity (MRA) and respiratory control index (RCI) parameters such as pyruvate-dependent state 3 respiration and state 4 respiration tended to be higher in Duroc than PiNN but did not reach the significance threshold. Metabolic enzymes such as glycogen phosphorylase (GP), phosphofructokinase (PFK), and lactate dehydrogenase (LDH) had comparable enzyme activities between breeds, while Duroc pigs had slightly higher activities of citrate synthase (CS), complex I, and complex II. There were no differences for adenine nucleotide concentrations of inosine 5'-monophosphate (IMP), adenosine 5'-monophosphate (AMP), adenosine diphosphate (ADP), and adenosine triphosphate (ATP) between these two breeds.
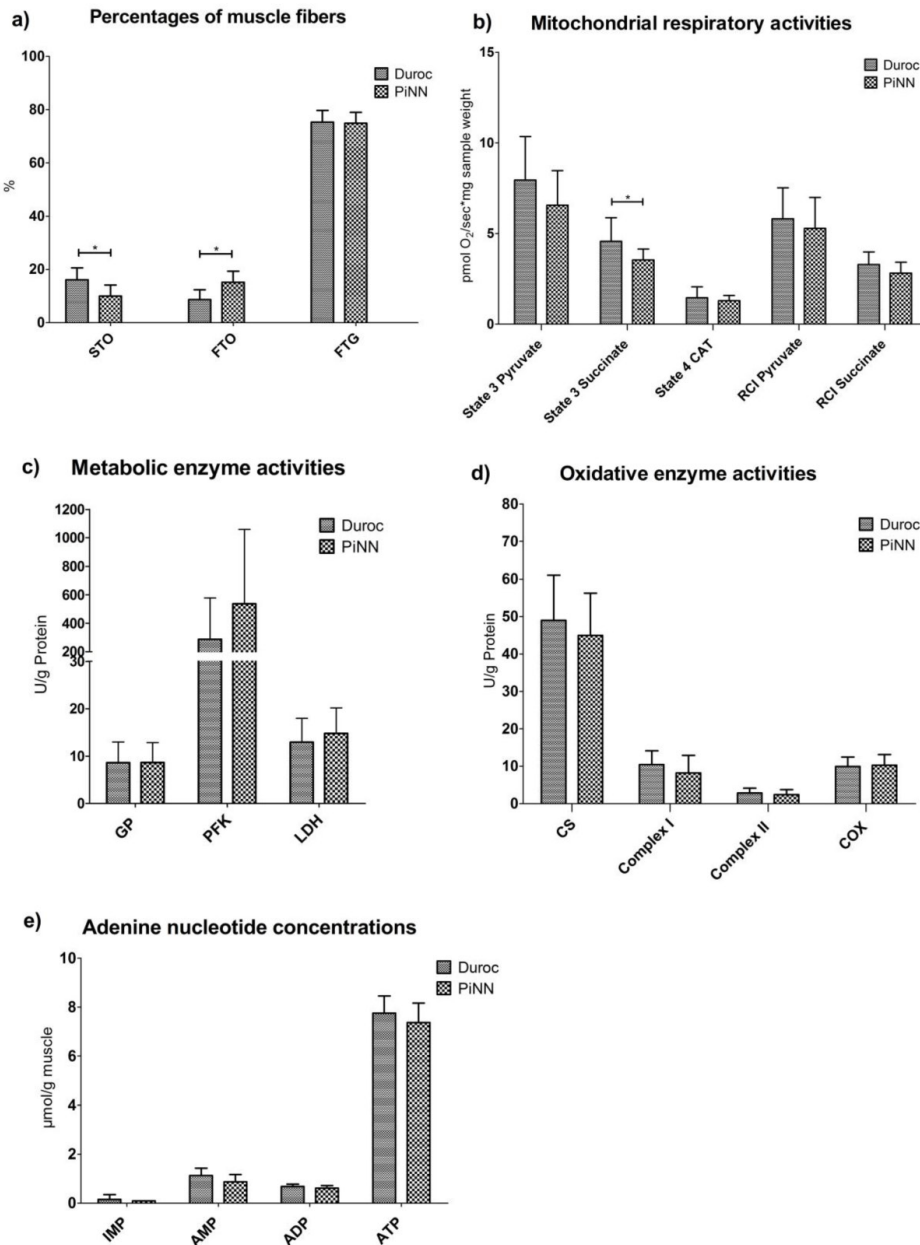

Figure 1. Least squares means and SD of a) muscle fiber percentage b) mitochondrial respiration activities c) metabolic enzyme activities d) oxidative enzyme activities and e) adenine nucleotide concentrations depending on pig breeds Duroc and PiNN 24h antemortem.

Table 1. Differentially expressed genes (DEGs) in the top three canonical pathways derived from Ingenuity Pathway Analysis (IPA) for Duroc and Pietrain (PiNN) pigs

DEGs	Ingenuity Canonical Pathways	p-value	No. of genes	Genes
Duroc-up	Protein Ubiquitination Pathway	3.15E-08	33	*USP45, UBE2D2, FBXW7, DNAJC3, DNAJC13, DNAJC10, SKP1, USO1, USP8, USP7, DNAJC28, HSP90B1, USP13, BIRC3, USP28, USP15, USP38, BIRC6, DNAJC1, MDM2, USP1, UBE2D1, DNAJB14, UBE3A, XIAP, SKP2, UCHL3, DNAJC21, CUL2, UBR1, USP34, USP25, BIRC2*
	Mouse Embryonic Stem Cell Pluripotency	3.08E-06	16	*IL6ST, PIK3CA, TCF4, JAK1, PIK3C2A, PIK3R1, SOS2, BMPR2, XIAP, NANOG, PTPN11, BMPR1A, SOS1, MAP3K7, SMAD4, GSK3B*
	HIPPO signaling	4.62E-06	15	*DLG1, TJP2, PPP2R2A, PPP1R11, STK3, SKP1, PPP2R5A, SKP2, ITCH, PPP1CC, PPP1R12A, PPP2R3A, SMAD4, PPP2R5E, INADL*
PiNN-up	Amyloid Processing	2.07E-04	8	*CSNK1E, CAPN6, AKT1, CDK5, APH1A, MAPT, PSENEN, CAPN3*
	3-phosphoinositide Bio-synthesis	2.91E-04	15	*PPFIA1, PPAPDC3, EPHX2, MDP1, PIP4K2B, PPP4C, MTMR6, CDC25B, PPP1R16B, DUSP1, CDIP, PPM1H, CILP, THTPA, PI4KB*
	3-phosphoinositide Deg-radation	3.12E-04	14	*CDC25B, MTMR6, PPFIA1, INPP4A, PPAPDC3, DUSP1, PPP1R16B, EPHX2, PPM1H, MDP1, CILP, PPP4C, THTPA, MTMR3*

Table 2. Differentially expressed genes (DEGs) in interesting functional categories derived from Ingenuity Pathway Analysis (IPA) for Duroc and Pietrain (PiNN) pigs

DEGs	Functions	p-value	No. of genes	Genes
Duroc-up	Skeletal and muscular system development and function	1.48E-03 - 5.48E-03	26	*AR, NEB, PPARGC1A, CHSY1, CHUK, PBX1, PDS5B, RBL1, RBL2, BNIP2, HSP90B1, MSTN, RB1, SSPN, DMD, GABPA, UTRN, CMYA5, PPP3CA, FMN1, HIF1A, KIAA1715, LRP6, MECOM, NIPBL, RPGRIP1L*
	Carbohydrate metabolism	5.48E-03 - 5.48E-03	23	*ABCC9, APPL1, CD36, DPP4, HIF1A, LNPEP, PIK3C2A, PIK3CA, PIK3R1, PPM1A, PREX2, PRKAA1, PRKAA2, PRKD3, PTEN, PTPN11, RHOQ, SEPT7, SKP2, SLC1A3, SSFA2, STEAP4, WWP1*
PiNN-up	Skeletal and muscular system development and function	1.77E-06 - 1.24E-02	80	*ACVR2B, AKT1, ANXA6, ASB2, ATP2A1, ATP6V0C, BECN1, CAND2, CAPN3, CAPN6, CAV3, CDK5, CDK9, CEBPB, CLCN1, COL6A1, COL6A3, CRYAB, CSF1, CXCL12, DDR1, DISP1, DNAJC5, DUSP1, ENG, ENO1, ERBB2, ERRFI1, ESR1, FADD, FLII, FZD4, GAA, GAB2, GSK3A, HEXIM1, HSPB2, HSPG2, ICMT, ILK, JMJD6, JSRP1, KCNJ11, KCNJ12, KREMEN1, LMNA, LTBP1, MEF2D, MMP2, MPRIP, MTOR, MYH14, NOL3, NPNT, NPRL3, P2RX6, PLOD1, PRKCA, RAB35, RRAGA, RXRA, SCARB2, SCN1B, SCN4B, SF3B4, SLC6A8, SMAD3, SPEG, SPRY2, SRF, SRL, SRPK3, STIM1, SUFU, SYPL2, THRA, TLR5, TNFRSF11B, USP19, VCAM1*
	Carbohydrate metabolism	4.66E-05 - 1.23E-02	50	*AKT1, ALG2, AP2M1, APOD, CDIPT, CEBPB, CLN6, CSF1, DPM3, ERBB2, FITM2, GAA, GAPDH, GSK3A, GYS1, HLAA, INPP4A, KCNJ11, LPIN1, MAN2B2, MDP1, MECP2, MMP2, MTMR3, MTOR, NF2, NISCH, NR1D1, PCYT2, PFKFB2, PI4KB, PIGB, PIGC, PIGL, PIGO, PIGQ, PIP4K2B, PLA2G15, PLCD1, RAB35, SCAP, SERINC2, SMAD3, SMARCB1, SPI1, TFEB, USP2, WDTC1, XYLT1, ZFYVE1*

Differentially expressed genes and pathway analysis

Out of 47,880 probe-sets on the snowball micro-array, 17,820 quality-filtered probes were further an-alyzed for differential expression between Duroc and PiNN muscle samples using ANOVA on JMP Genomics 7. In total, 2,345 probes were differentially expressed (FDR<0.05) between Duroc and PiNN pigs. Among these, 1,402 probes were up-regulated in Duroc pigs, while 943 probes were up-regulated in PiNN pigs (Table S3). Differentially expressed genes were analyzed with IPA to identify prominent pathways and biological functions. The top three canonical pathways and related genes are shown in Table 1. Protein ubiquitination, embryonic stem cell pluripotency, and HIPPO signaling pathways were over-represented in Duroc, while amyloid processing, and 3-phosphoinositide biosynthesis and degradation were enriched in PiNN. Since our phenotypic data showed tendencies of differential muscle trait measurements in these pigs (Table S1 and Figure 1), we also looked into differentially expressed genes between Duroc and PiNN that are assigned to the functional categories related to skeletal and muscular system development and function as well as carbohydrate metabolism to obtain insight into candidate genes for meat quality, as shown in Table 2.

Weighted gene co-expression network analysis

Due to considerable differences in genetics and phenotypes between Duroc and PiNN, the weighted gene co-expression network analysis (WGCNA) was performed using post quality-filtered data of 17,820 probes separately for each breed. WGCNA grouped genes into 21 modules for Duroc and 20 modules for PiNN based on their co-expression patterns. The number of genes in each module is listed in Supplemental Tables S4 and S5 for Duroc and PiNN, respectively. Further, the representative of each module, an eigengene that is the 1st principle component, was tested for a significant correlation between each module with all 19 traits related to muscle fiber composition, mitochondrial respiration activity, en-

zyme activities, and adenine nucleotide concentration. The co-expression transcripts in each module and associated gene ontology (GO) terms were identified using DAVID functional annotation for Duroc (Table S4) and PiNN (Table S5) separately. In addition, modules that were associated with the function 'energy production' were also identified using IPA.

Muscle fiber composition-related gene co-expression modules

For Duroc pigs, a total of 21 modules were examined for their relationship with all measured traits. Of them, 13, 10, and 9 modules were correlated with the percentage of STO, FTO, and FTG muscle fibers, respectively (p<0.05). Among these, modules blue and green-yellow (each co-expression module was arbitrarily color-coded) were positively correlated with STO fibers (blue/STO, r=0.87, *p*=0.001; green-yellow/STO, r=0.78, *p*=0.008), while negatively correlated with FTG fibers (blue/FTG, r= -0.94, p=5E-05; green-yellow/FTG, r= -0.98 p=7E-07) as shown in Figure 2. Functional analysis showed that the blue and green-yellow modules were associated with GO terms 'mitochondrion' and 'mitochondrial part' (Table 3). Interestingly, modules dark-orange and cyan showed the inverse relationship to STO and FTG; they were negatively correlated with STO while positively correlated with FTG (dark-orange/STO, r= -0.72, p=0.02; cyan/STO, r= -0.82, p=0.004; dark-orange/FTG r=0.89 p=6E-04; cyan/FTG, r=0.73, p=0.02). Modules dark-orange and cyan were associated with 'intracellular organelle lumen' and 'regulation of phosphorylation', respectively. Furthermore, modules saddle-brown, black, and white were positively correlated with STO with correlation coefficients (r) ranging from 0.76 to 0.93 (p<0.01), while negatively correlated with FTO (r= -0.72 to -0.83, p<0.02). The related genes within the modules were associated with GO-terms 'protein kinase activity', 'phosphorus metabolic process', and 'cytoskeleton', respectively. In addition, module cyan was also highly correlated with MRA measurements including state 3 pyruvate (r= -0.92, p=2E-04), state 3 succinate (r= -0.8, p=0.005), and state 4 CAT (r= -0.65, p=0.04). Module green-yellow, dark-grey, and white were all positively correlated with oxidative enzyme Complex I and COX with the correlation coefficients ranging between 0.66 to 0.86 (p<0.04), also shown in Figure 2, and their gene members were enriched for GO terms 'mitochondrial part', 'cytoplasmic vesicle', and 'cytoskeleton', respectively.

A total of 20 gene co-expression modules were tested for a trait correlation in PiNN pigs. Overall, fewer significant module-trait relationships were observed in PiNN (Figure 3) compared to Duroc pigs

(Figure 2). Modules pale-violet-red 1 and green-yellow were positively correlated with STO (r=0.66 to 0.82, p<0.04). Module black was negatively correlated with FTG (r= -0.75, p=0.01). Modules green-yellow and black were enriched for 'actin cytoskeleton' and 'cellular macromolecule catabolic process', respectively, while no significant enrichment term for module pale violet-red was identified. For glycolytic enzyme measurements, module green, enriched for 'transcription activator activity', was positively correlated with GP and LDH with (r ranged from 0.67 to 0.8 with p<0.03) as shown in Figure 3. Modules significantly correlated with mitochondrial activities included module white, which showed a negative correlation with state-3-pyruvate (r= -0.81, p=0.004), state-3-succinate (r= -0.71, p=0.02), and AMP (r= -0.85, p=0.002), but a positive correlation with ADP (r=0.71, p=0.02). Gene members of this module were over-represented in 'enzyme binding'. Module blue 2, associated with 'macromolecule catabolic process', was negatively correlated with ADP (r= -0.72, p=0.02) and ATP (r= -0.65, p=0.04).

Several gene members of these significant trait-correlated modules were also differentially expressed between Duroc and PiNN as shown in Supplemental Table S4 and S5.

Energy production-related gene co-expression modules

To identify potential candidate genes that may play important roles in energy metabolism in the muscle, the co-expression modules that were significantly correlated with the trait measurements of mitochondrial respiration activity, enzyme activities, and adenine nucleotide concentration (p<0.05) were associated to the functional category 'energy production' using the IPA enrichment. In Duroc pigs, 4 out of 11 modules were linked to 'energy production' together with its functions annotation network, as shown in Table 5. Of these, module dark-red was correlated with RCI pyruvate (r= -0.68, p=0.03); green-yellow with Complex I (r=0.72, p=0.02) and COX (r=0.86 p=0.002); dark-orange with GP (r= -0.68, p=0.03) and AMP (r= -0.66, p=0.04); and purple with LDH (r= -0.75, p=0.01). In PiNN pigs, 5 out of 11 modules were associated with 'energy production' together with its functions annotation network (Table 6). These were (module/trait) dark-green/CS (r=0.66, p=0.04), green-yellow/State 3 Succinate (r=0.7, p=0.03), grey 60/CS (r=0.71, p= 0.02), light-steel-blue/RCI pyruvate (r= 0.67, p=0.03), light-steel-blue/CS (r=0.72, p=0.02), and medium-orchid/GP (r=0.67, p=0.03). Several gene members of these significant trait-correlated modules were

also differentially expressed between Duroc and PiNN: *LRPPRC, PPARGC,* (see also Tables 5 and 6).

qRT-PCR validation

The expression of *ATP6V1C1, ATP6V1E1, COX10, COX7A2, CYB5A, NDUFS1, NDUFS6,* and *PPA1* were validated by qPCR. The correlation coefficient between qPCR and microarray data ranged from 0.59 (p<0.006) to 0.81 (p<0.0001), suggesting a good concordance between microarray and qPCR results, as shown in Figure 4.

Table 3. Gene ontology (GO) terms for significant trait-correlated modules in Duroc

Module	Top Term	Count[1]	Percent[2]	P-value of Top Term
saddlebrown	GO:0004672~protein kinase activity	18	7.76	4.78E-03
black	GO:0006793~phosphorus metabolic process	44	9.40	3.61E-04
blue	GO:0005739~mitochondrion	182	9.20	5.98E-10
green-yellow	GO:0044429~mitochondrial part	45	6.86	5.81E-06
light cyan	GO:0044420~extracellular matrix part	9	2.72	1.57E-03
dark grey	GO:0031410~cytoplasmic vesicle	17	6.77	2.10E-02
white	GO:0005856~cytoskeleton	31	11.92	6.49E-03
dark orange	GO:0070013~intracellular organelle lumen	33	13.41	7.40E-03
cyan	GO:0042325~regulation of phosphorylation	23	6.74	9.28E-05

[1] No. of genes in term
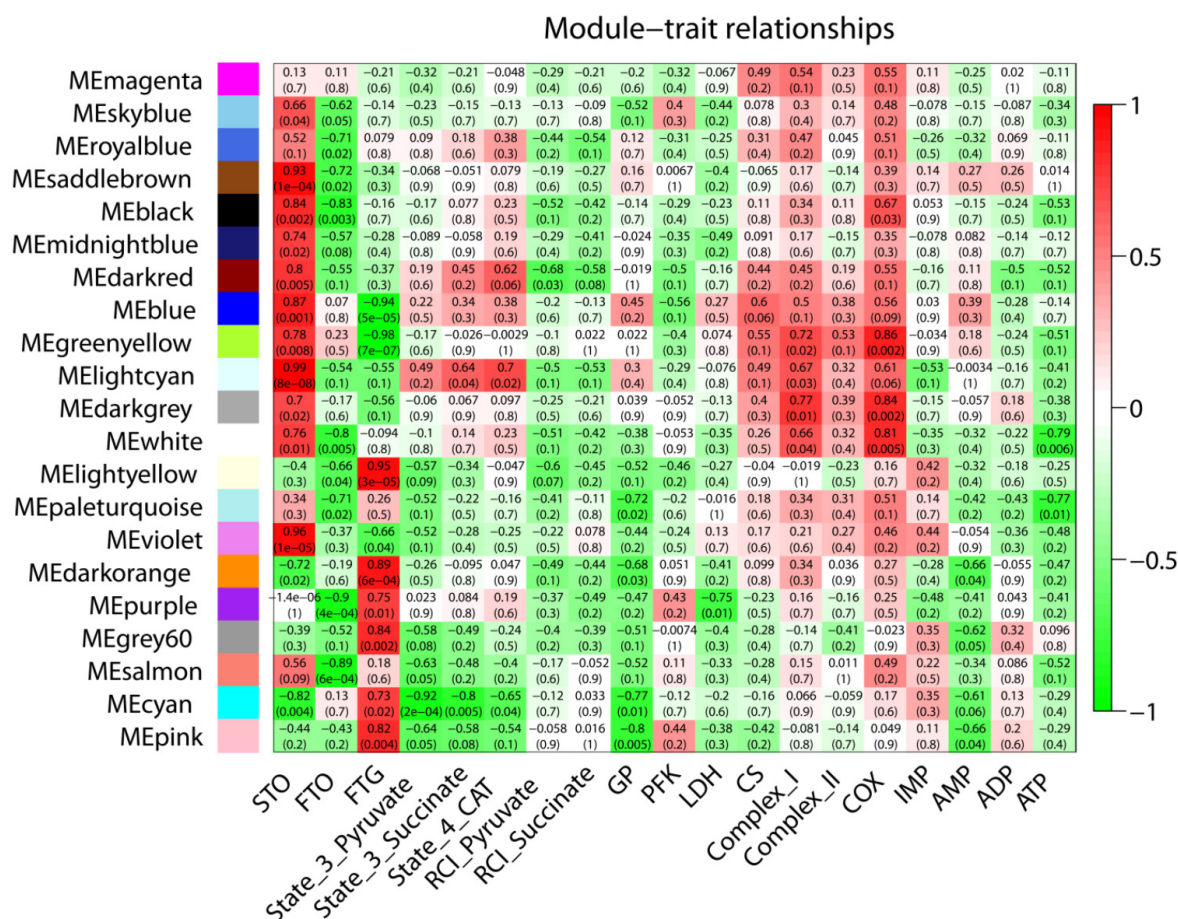[2] (No. of genes in term/No. of genes in module)×100

Figure 2. Correlation matrix between each module and trait for Duroc pigs. Weighted gene co-expression network analysis (WGCNA) was used to group genes into 21 different modules based on their co-expression pattern. Each module is assigned arbitrarily to a color. The respective colors are shown on the left. The eigengene of each module, as a representative of the corresponding module, was tested for correlation with each trait. Shown are the correlation coefficients and the corresponding p-values in brackets. Cell color encodes correlation (red, positive correlation; green, negative correlation).

Table 4. Gene ontology (GO) terms for significant trait-correlated modules in Pietrain (PiNN)

Module	Top Term	Count[1]	Percent[2]	P-value of Top Term
white	GO:0019899~enzyme binding	8	7.14	3.96E-02
blue 2	GO:0009057~macromolecule catabolic process	159	7.93	2.75E-15
green-yellow	GO:0015629~actin cytoskeleton	16	12.50	1.93E-10
green	GO:0016563~transcription activator activity	35	5.47	2.61E-06

[1] No. of genes in term
[2] (No. of genes in term/No. of genes in module)×100

Table 5. Gene co-expression modules associated with energy production in Ingenuity Pathway Analysis (IPA) for Duroc

Function	Module	Correlated Phenotype (p-value)	Functions Annotation Network*
Energy production	Dark red	STO RCI pyruvate (0.03 - 0.005)	
	Green yellow	STO FTG Complex I COX (0.02 - <0.0001)	
	Dark orange	STO FTG GP AMP (0.02 - <.0001)	
	Purple	FTO FTG LDH (0.01 - <0.0001)	

*the bold genes in the network are members of the respective trait-associated modules and differentially expressed between Duroc and PiNN.

Table 6. Gene co-expression modules associated with energy production in Ingenuity Pathway Analysis (IPA) for Pietrain (PiNN)

Function	Module	Correlated Phenotype (*p-value*)	Functions Annotation Network*
Energy production	Dark green	CS (0.04)	
	Green yellow	STO State3 succinate (0.03-0.004)	
	Grey 60	CS (0.02)	
	Light steel blue	RCI pyruvate CS (0.03-0.02)	
	Medium orchid	GP (0.03)	

Enzyme		Transmembrane Receptor		Transporter	
Unknown		Function		G-protein Coupled Receptor	
Kinase		Ligand-dependent Nuclear Receptor		Peptidase	
Transcription Regulator		– – Relationship			

* the bold genes in the network are members of the respective trait-associated modules and differentially expressed between Duroc and PiNN.
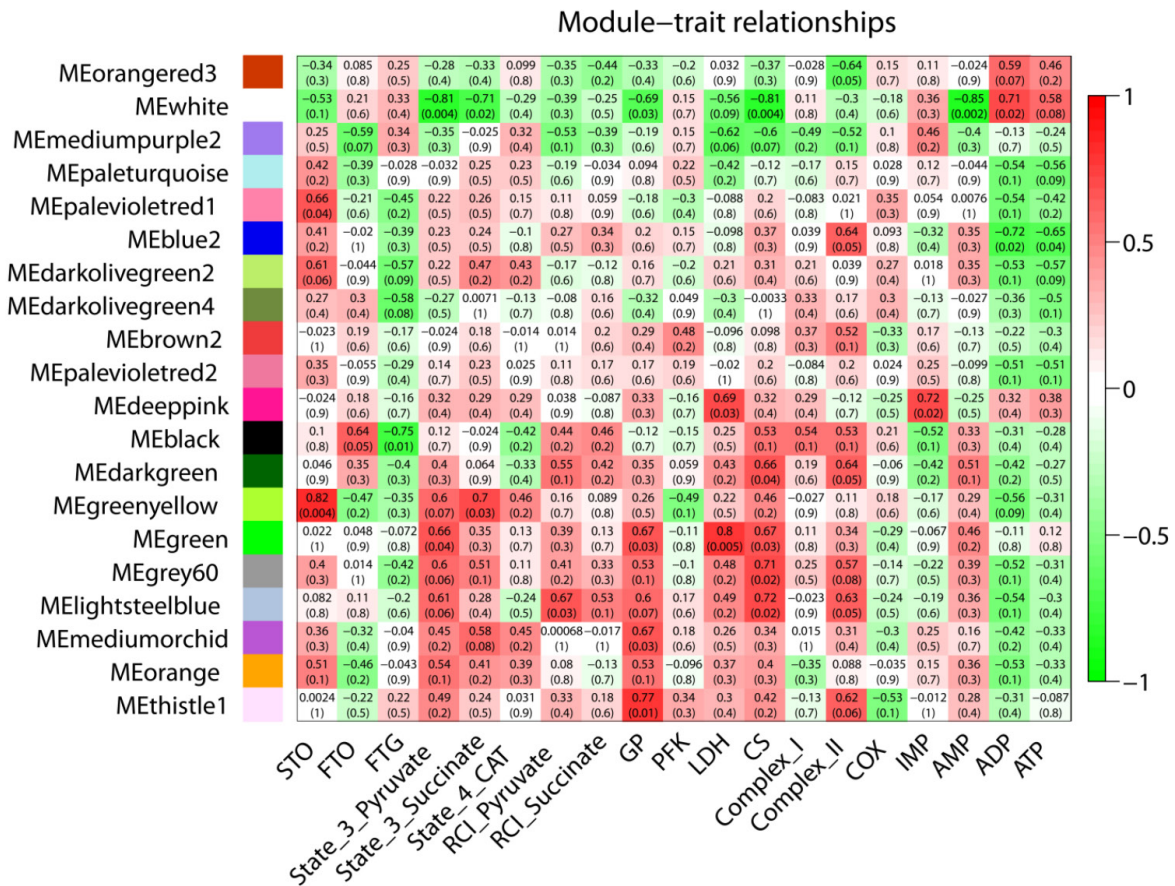
Module−trait relationships

Figure 3. Correlation matrix between each module and trait for PiNN pigs. Weighted gene co-expression network analysis (WGCNA) is used to group genes into 20 different modules based on their co-expression pattern. Each module is assigned arbitrarily to a color. The respective colors are shown on the left. The eigengene of each module, as a representative of the corresponding module, was tested for correlation with each trait. Shown are correlation coefficients (upper value) and the corresponding p-values (lower value). Cell color encodes correlation (red, positive correlation; green, negative correlation).

Discussion

Duroc and Pietrain breeds are divergent for muscle characteristics and meat quality. Pietrain pigs are more muscular and lean, whereas Duroc pigs are fattier and preferable for marbling. Mutations in the ryanodine receptor (*RYR1*), frequently carried in Pietrain pigs, have impacts on meat quality, stress resistance, and carcass composition. RYR1 is a calcium channel expressed primarily in skeletal muscle. The *RYR1* mutation c.1840C>T (p.Arg614Cys) in pigs causes a dysregulation of the calcium-flux leading to early energy depletion, AMPK activation, accelerated glycolysis and an increased incidence of pale, soft, exudative (PSE) meat [13, 14]. In this study, MHS homozygous-negative pigs were used avoid an effect from the *RYR1* locus. The muscle samples from Duroc pigs showed a higher percentage of STO and lower percentage of FTO fibers, with no difference for FTG fibers compared to PiNN pigs. This observation agrees well with previous reports with a bigger sample size, except for the percentage of FTG fibers, which was higher in PiNN pigs [6, 8, 15, 16]. Muscles containing more STO fibers are associated with higher oxidative enzyme activities and mitochondrial respiration activity [17]; muscles comprised of more FTG fibers are associated with higher glycolytic enzyme activities [6, 18]. Lipids are stored mainly in STO fibers [19], which can improve the tenderness and juiciness of the meat. Selection towards a high percentage of FTG fibers for meat production may therefore result in altered meat quality possibly due to lower capillarization and insufficient delivery of oxygen [20] or glycogen depletion, which ultimately influence meat toward dry, firm, and dark [21]. The understanding of the molecular basis of muscle fiber type and metabolic capacity is important and may have implications on meat production and meat quality.
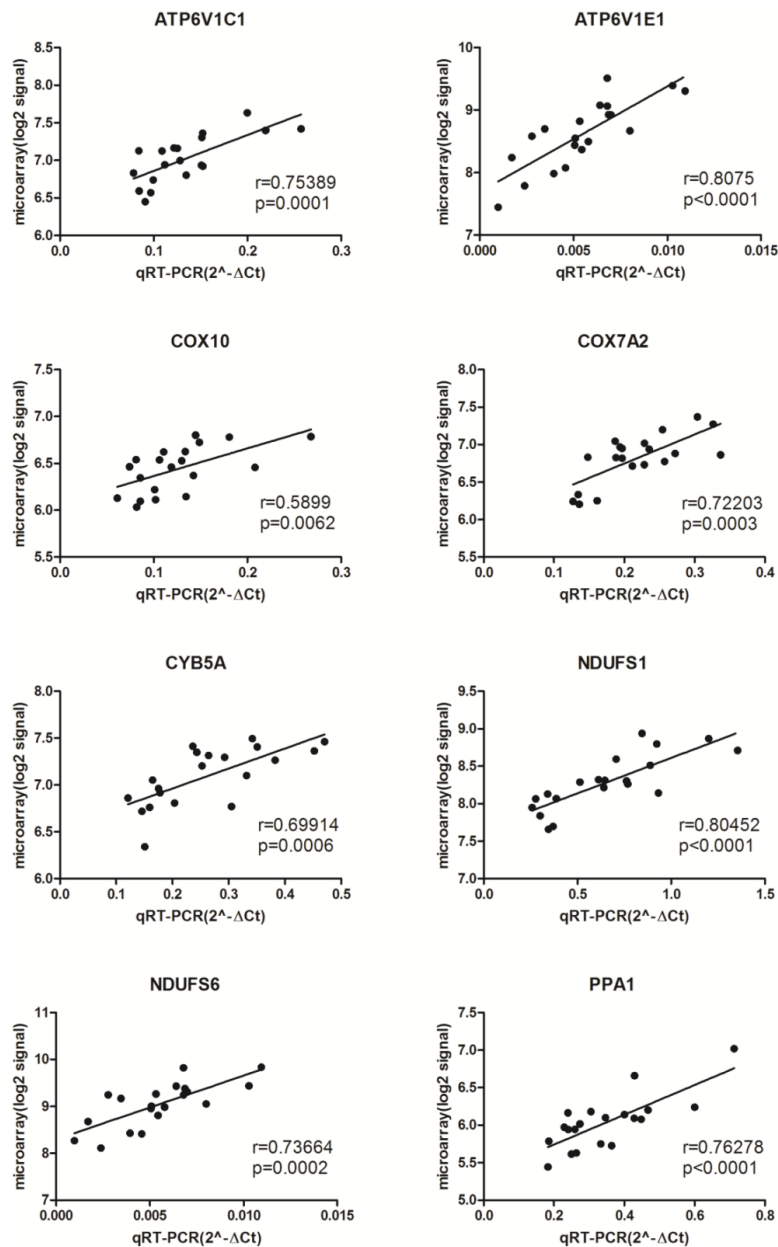
Figure 4. qPCR validation of microarray results for eight genes: *ATP6V1C1*, *ATP6V1E1*, *COX10*, *COX7A2*, *CYB5A*, *NDUFS1*, *NDUFS6*, and *PPA1*. Plot between qPCR (2^-ΔCt on the x-axis) and microarray (log2 signals on the y-axis) for each gene. The corresponding correlation coefficient (r) and p values are shown.

DEGs revealed differences in the canonical pathways between Duroc and PiNN

Protein turnover is essential to gaining muscle mass. Three major proteolytic mechanisms in muscle are the ATP-dependent ubiquitin proteasome system (UPS), Ca^{2+}-dependent-calpain system, and lysosomal proteasomes. In our present results, the protein ubiquitination pathway was among the top canonical pathways up-regulated in Duroc. The UPS is known as a principle regulator of muscle atrophy [22]. Protein ubiquitination is an ATP-dependent process mediated by ubiquitin-activating enzyme E1, specific ubiquitin-conjugating-enzyme E2, and ubiquitin protein ligase E3, which promote protein degradation via the 26s proteasome and has implications on meat quality [23-26]. Interestingly, amyloid processing was listed as a top canonical pathway in up-regulated DEGs of PiNN. Amyloid processing has been associ-

ated with glucose uptake, and oxidation in myotubes [27, 28]. DEGs in amyloid processing, like *CSNK1E, CAPN6, AKT1, CDK5, APH1A, MAPT, PSENEN*, and *CAPN3* have implications in muscle biology of the pig. *PSENEN* encodes Presenilin, a component of the gamma-secretase protein complex that is required for the processing of the beta-amyloid precursor protein to generate amyloid beta (Abeta). Abeta inhibits the proteolytic activities of the 26S proteasome and the interplay of Abeta and UPS is associated with Alzheimer's disease [27]. Mutations in *PSENEN* disrupt cellular Ca^{2+} homeostasis via the regulation of ryanodine receptors (RYR), sarcoendoplasmic reticulum Ca^{2+} transport ATPase (SERCA), and/or inositol 1,4,5-trisphosphate channels, all of which are crucial regulators of Ca^{2+} release [29-32]. *PSENEN* has been identified as a potential candidate gene for meat quality [33, 34].

AKT1, a serine threonine protein kinase, is a critical mediator of cell growth and survival. AKT1 transgene activation promotes type IIb fiber hypertrophy and increases glycolysis while reducing fat accumulation [35, 36]. The up-regulation of *AKT1* in PiNN may have a functional link to its leanness. The calpain system target proteins are involved in assembly and scaffolding of myofibrillar proteins such as titin [37]. Its activation promotes disassembly of myofilaments from intact myofibrillar proteins and permits the degradation of these sarcomeric proteins by UPS [38]; it is also involved in the regulation of muscle mass [39]. Calpain-3 (*CAPN3*) is a calcium-dependent cysteine protease expressed in muscle. Mutations in calpain-3 cause Limb-Girdle Muscular Dystrophy Type 2A (LGMD2A) [40]. Immature muscle observed in calpain-3 overexpressing transgenic mice suggests a role for this protein in muscle maturation [41]. Calpain-3 may play a role in sarcomere maintenance and organization by acting upstream of the UPS; its absence results in death of muscle fibers [42, 43]. Calpain-6 (*CAPN6*) is a suppressor of muscle cell differentiation, and its deficiency promotes skeletal muscle development and regeneration [44].

DEGs revealed differences in the functional categories of muscle metabolism between Duroc and PiNN

Peroxisome proliferator-activated receptor gamma coactivator 1 alpha (*PPARGC1A*) and protein phosphatase 3 catalytic subunit alpha isoform (*PPP3CA*) were up-regulated in Duroc compared to PiNN. *PPARGC1A* activation promotes the slow, oxidative myogenic program in mice [45] and drives the formation of slow-twitch muscle fibers in cultured muscle cells [46]. It also acts as a master coordinator to control mitochondrial biogenesis and oxidative

phosphorylation [47]. Hence, *PPARGC1A* may provide a link between muscle fiber type and energy metabolism. *PPP3CA* is differentially expressed in muscles comprised of different proportions of fast and slow muscle fibers [48]. *CD36* mediates uptake of long-chain fatty acid and thus plays a role in lipid accumulation and fatty acid homeostasis [49, 50]. Sarcalumenin (*SRL*) and fast twitch Ca^{2+} ATPase (*ATP2A1*) have been reported as fast-type muscle genes [51]. The up-regulation of these two genes support the high percentage of fast-twitch glycolytic muscle fibers in PiNN. Fructose 2, 6–bisphosphatase 2 (*PEKFB2*), up-regulated in PiNN, can promote glycolysis by controlling the level of Fructose 2, 6 – bisphosphate, which is an allosteric activator of phosphofructokinase (PFK-1) [52]. Glycogen synthase kinase 3 alpha (*GSK3A*) and glycogen synthase 1 (*GYS1*) are crucial for glycogen storage and can influence the muscle-to-meat process via glycolysis, reduced pH, and pale color [53, 54]. Moreover, a high level of glycogen has been associated with a higher percentage of fast-twitch glycolytic fibers [55].

Gene co-expression networks link to oxidative capacity of skeletal muscle

Transcriptional network analysis identified 13 co-expression modules correlated with STO muscle fibers in Duroc pigs ($p<0.05$). Among these, module light-cyan showed a strong correlation with STO (Figure 2) and its members (9 genes) were enriched for 'extracellular matrix part' (Table 3). Of these *COL3A1, COL5A2, COL6A1*, and *COL12A1* encode for type III, V, VI, and XII collagen, respectively. Collagens are major components of the extracellular matrix (ECM). Collagen-VI deficient *Col6a1-/-* mice show myopathic disorder and, most important, mitochondrial dysfunction [56]. Modules blue and green-yellow were positively correlated with STO, while negatively with correlated with FTG. These modules were enriched for 'mitochondrion' and 'mitochondrial part' GO terms. Mitochondria play a prominent role in ATP production and oxidative phosphorylation. Oxidative capacity of the muscle cells has been associated with muscle fiber types via mitochondrial volume and density [57], which is typically higher in slow-twitch type I fibers than fast-twitch type II fibers [58]. 182 genes of module blue and 45 genes of module green-yellow were enriched for 'mitochondrion' and 'mitochondrial part', respectively (Table 3). These genes are not only involved in mitochondrial biogenesis and functional maintenance, but also in the mitochondrial oxidation of fatty acids. *SLC25A4* or *ANT1* is a muscle-specific isoform. Adenine nucleotide translocators (*ANT*) regulates the adenine nucleotide concentration by trans-

locating ADP and ATP between mitochondrial matrix and cytoplasm. It provides ADP for oxidative phosphorylation and is essential for mitochondrial function [59]. *GFM1* (mitochondrial translation elongation factor G1) is involved in oxidative phosphorylation disorder [60]. Many genes in modules blue and green-yellow are major components of the electron transport chain and important for oxidative phosphorylation to produce ATP [*NDUFV2, NDUFV3, NDUFS1, NDUFS4, NDUFS6, NDUFS7, NDUFB2, NDUFB3, NDUFB4, NDUFB8, NDUFB11, NDUFA5, NDUFA10,* and *NDUFA11* (encode for Complex I); *SDHA* and *SDHB* (encode for Complex II); *COX7A1* and *COX4l1* (encode for COX); *ATP5L, ATP5J, ATP5G2, ATP5G3, ATP5A1*, and *ATP5C1* (encode for ATP synthase)]. Moreover, many genes were associated with lipid metabolism and mitochondrial oxidation of fatty acids like acyl-CoA synthetase long-chain family member *ACSL1*, *ACSL3*, *ACSL4*, and *ACSL5*, which encode the long-chain fatty-acid-coenzyme A ligase family members. Particularly, ACSL1 interacts with carnitine palmitoyltransferase 1a (CPT1a) and voltage-dependent anion channel (VDAC) to transfer the activated fatty acids through the mitochondrial outer membrane and to catalyze fatty acid oxidation [61]. It contributes 80% of total ACSL activity and is important for mitochondrial beta-oxidation of long-chain fatty acids in adipose tissue, liver, and skeletal muscle [62-64]. *HADH* and *HADHB* are members of the 3-hydroxyacyl-CoA dehydrogenase gene family. The encoded proteins catalyze the oxidation of straight-chain 3-CoAs as part of the beta-oxidation pathway in the mitochondrial matrix. Beta-oxidation of FAs could be influenced by the interaction between estrogen receptor alpha and HADHB [65]. Altogether, genes in these modules are involved in various functions including nucleotide transport, mitochondrial (mt) translation, OXPHOS subunits formation, mt membrane biogenesis, and mt oxidation of fatty acids. Overall, these gene modules link mitochondrial functions to oxidative capacity of the skeletal muscle. It is of interest whether the up-regulation of these genes in Duroc pigs also implies a predominant role of oxidative capacity and respiration activity in Duroc over PiNN.

Gene co-expression networks link to mitochondrial respiration activity and ATP synthesis

In Duroc pigs, 4 modules were enriched for energy production. Genes belonging to these modules are potential factors that control mitochondrial respiration and ATP synthesis, components of the respiratory chain, hormones and transcription factors. *NDUFS1* encodes NADH dehydrogenase involved in the mitochondrial respiration chain. *ATP5A1* encodes alpha unit of ATP synthase F1 unit. Deficiency of these genes affects functional complex I and/or ATP synthase and results in decreased ATP production [66-68]. Insulin regulates stimulation of protein synthesis and lipid and glucose storage [69]. Insulin receptor (INSR) and insulin receptor substrate 2 (IRS2) are major molecules mediating insulin-signaling pathways. The effect of insulin on skeletal muscle mitochondrial function and oxidative capacity has been shown. Insulin increases ATP production as well as the mRNA level and enzyme activities of complex I and COX [70]. Thyroid hormone receptor beta (*THRB*) encodes one of the nuclear hormone receptors for thyroid hormone. The overexpression of thyroid hormone receptor in myoblast stimulates both cytochrome oxidase and citrate synthase activities [71]. Thyroid hormone has been shown to increase ATP production as well as citrate synthase and cytochrome c oxidase activities in muscle tissue [72] and influences both nuclear and mitochondrial genes in respiratory functions [73, 74].

In PiNN pigs, 5 modules were enriched for energy production. Some genes belonging to these modules are regarded as potentially regulating the respiratory chain, hormones, and transcription factors. *ATP5B* and *ATP5C1* encode the beta and gamma units of ATP synthase F1. They are essential for the fully assembled and functional ATP synthase and, therefore, ATP production. *PPARGC1A*, as a transcriptional co-activator regulating genes in energy metabolism, activates the expression of nuclear respiratory factors (NRFs), promotes mitochondrial biogenesis, and stimulates coupled respiration [75]. In cultured myotubes, *PGC-1* activates the expression of mitochondrial respiratory chain COXIV and ATP synthase as well as mtTFA through the induction of *NRF-1* and *NRF-2* expression [76, 77]. The activated mtTFA translocates into mitochondria and directly activates the transcription and replication of mtDNA [76, 77]. Leucine-rich pentatricopeptide repeat containing (*LRPPRC*) deficiency affects the stability of most mitochondrial mRNAs and leads to COX deficiency and ATP synthase deficiency associated with reduced ATP production in conditional knockout mouse heart [78].

Gene expression profiling by microarray is restricted on transcript level. Events such as post-transcriptional regulation and protein modification could contribute to molecular mechanisms. Proteome and metabolome analysis could provide insight on the molecular basis related to energy metabolism in muscle. To further validate whether any candidate gene plays a role in energy metabolism, an in vitro model system can be set up to perform enzymatic

functional assay by mutation or silencing certain genes.

Conclusions

In the present study, a comparative transcriptome profiling of ante mortem skeletal muscle between Duroc and PiNN revealed clear differences in their muscle metabolic properties. Gene co-expression network analysis highlights the importance of mitochondria in the oxidative capacity of muscle. In particular, the Duroc breed showed more clear molecular function involved in oxidative capacity and respiration activity than PiNN. In contrast to PiNN, co-expression modules enriched in macromolecule catabolic process, actin cytoskeleton, and transcription activator activity were associated with fiber types, mitochondrial respiratory activity, and metabolic enzyme activities. Our results highlight the importance of mitochondria for the oxidative capacity of the porcine muscle, particularly in providing breed-specific processes for the molecular pathways in muscle cell fibers, and muscle biology.

Abbreviations

STO: slow-twitch oxidative; FTO: fast-twitch oxidative; FTG: fast-twitch glycolytic; ATP: adenosine triphosphate; WGCNA: weighted gene co-expression network analysis; PiNN: malignant hyperthermia syndrome (MHS)-negative Pietrain; LM: longissimus muscle; Th: thoracic vertebrae; RMA: robust multichip average; DABG: detection above background; FDR: false discovery rate; TOM: topological overlap matrix; qPCR: quantitative polymerase chain reaction; MRA: mitochondrial respiratory activity; RCI: respiratory control index; GO: gene ontology.

Supplementary Material

Tables S1-S5. http://www.ijbs.com/v11p1348s1.pdf

Acknowledgements

Competing Interests

The authors have declared that no competing interest exists.

References

1. Hocquette JF, Ortigues-Marty I, Pethick D, Herpin P, Fernandez X. Nutritional and hormonal regulation of energy metabolism in skeletal muscles of meat-producing animals. Livest Pro Sci. 1998; 56: 115-43.
2. Hocquette J, Ortigues-Marty I, Vermorel M. Manipulation of tissue energy metabolism in meat-producing ruminants. Asian Australas J AnimSci. 2001; 14: 720-32.
3. Pearson A. Introduction to quality attributes and their measurement in meat, poultry and fish products. Quality attributes and their measurement in meat, poultry and fish products. Springer; 1994: 1-33.
4. Davoli R, Braglia S, Russo V, Varona L, te Pas MF. Expression profiling of functional genes in prenatal skeletal muscle tissue in Duroc and Pietrain pigs. J Anim Breed Genet. 2011; 128: 15-27. doi:10.1111/j.1439-0388.2010.00867.x.
5. Murani E, Muraniova M, Ponsuksili S, Schellander K, Wimmers K. Identification of genes differentially expressed during prenatal development of skeletal muscle in two pig breeds differing in muscularity. BMC Dev Biol. 2007; 7: 109. doi:10.1186/1471-213x-7-109.
6. Werner C, Natter R, Wicke M. Changes of the activities of glycolytic and oxidative enzymes before and after slaughter in the longissimus muscle of Pietrain and Duroc pigs and a Duroc-Pietrain crossbreed. J Anim Sci. 2010; 88: 4016-25.
7. Krischek C, Natter R, Wigger R, Wicke M. Adenine nucleotide concentrations and glycolytic enzyme activities in longissimus muscle samples of different pig genotypes collected before and after slaughter. Meat Sci. 2011; 89: 217-20.
8. Werner C, Natter R, Schellander K, Wicke M. Mitochondrial respiratory activity in porcine longissimus muscle fibers of different pig genetics in relation to their meat quality. Meat Sci. 2010; 85: 127-33.
9. Langfelder P, Horvath S. WGCNA: an R package for weighted correlation network analysis. BMC Bioinformatics. 2008; 9: 559.
10. Benjamini Y, Hochberg Y. Controlling the false discovery rate: a practical and powerful approach to multiple testing. J R Stat Soc Series B Stat Methodol. 1995; 57: 289-300.
11. Ponsuksili S, Du Y, Hadlich F, Siengdee P, Murani E, Schwerin M, et al. Correlated mRNAs and miRNAs from co-expression and regulatory networks affect porcine muscle and finally meat properties. BMC Genomics. 2013; 14: 533.
12. Zhang B, Horvath S. A general framework for weighted gene co-expression network analysis. Stat Appl Genet Mol Biol. 2005; 4: Article17.
13. Yue G, Stratil A, Kopecny M, Schröffelova D, Schröffel J, Hojny J, et al. Linkage and QTL mapping for Sus scrofa chromosome 6. J Anim Breed Genet. 2003; 120: 45-55.
14. Shen Q, Underwood K, Means W, McCormick R, Du M. The halothane gene, energy metabolism, adenosine monophosphate-activated protein kinase, and glycolysis in postmortem pig longissimus dorsi muscle. J Anim Sci. 2007; 85: 1054-61.
15. Chang KC, da Costa N, Blackley R, Southwood O, Evans G, Plastow G, et al. Relationships of myosin heavy chain fibre types to meat quality traits in traditional and modern pigs. Meat Sci. 2003; 64: 93-103.
16. Wimmers K, Ngu NT, Jennen DG, Tesfaye D, Murani E, Schellander K, et al. Relationship between myosin heavy chain isoform expression and muscling in several diverse pig breeds. J Anim Sci. 2008; 86: 795-803.
17. Gueguen N, Lefaucheur L, Fillaut M, Vincent A, Herpin P. Control of skeletal muscle mitochondria respiration by adenine nucleotides: differential effect of ADP and ATP according to muscle contractile type in pigs. Comp Biochem Physiol B Biochem Mol Biol. 2005; 140: 287-97.
18. Huber K, Petzold J, Rehfeldt C, Ender K, Fiedler I. Muscle energy metabolism: structural and functional features in different types of porcine striated muscles. J Muscle Res Cell Motil. 2007; 28: 249-58.
19. Essen-Gustavsson B, Karlsson A, Lundstrom K, Enfalt AC. Intramuscular fat and muscle fibre lipid contents in halothane-gene-free pigs fed high or low protein diets and its relation to meat quality. Meat Sci. 1994; 38: 269-77.
20. Karlsson AH, Klont RE, Fernandez X. Skeletal muscle fibres as factors for pork quality. Livest Prod Sci. 1999; 60: 255-69.
21. Karlsson A, Essen-Gustavsson B, Lundstrom K. Muscle glycogen depletion pattern in halothane-gene-free pigs at slaughter and its relation to meat quality. Meat Sci. 1994; 38: 91-101.
22. Lecker SH, Solomon V, Mitch WE, Goldberg AL. Muscle protein breakdown and the critical role of the ubiquitin-proteasome pathway in normal and disease states. J Nutr. 1999; 129: 227S-37S.
23. Murton AJ, Constantin D, Greenhaff PL. The involvement of the ubiquitin proteasome system in human skeletal muscle remodelling and atrophy. Biochim Biophys Acta. 2008; 1782: 730-43.
24. Huynh TP, Murani E, Maak S, Ponsuksili S, Wimmers K. UBE3B and ZRANB1 polymorphisms and transcript abundance are associated with water holding capacity of porcine M. longissimus dorsi. Meat Sci. 2013; 95: 166-72.
25. Loan H, Murani E, Maak S, Ponsuksili S, Wimmers K. Novel SNPs of the porcine TRIP12 are associated with water holding capacity of meat. Czech Journal of Animal Science. 2013; 58: 525-33.
26. Loan HT, Murani E, Maak S, Ponsuksili S, Wimmers K. UBXN1 polymorphism and its expression in porcine M. longissimus dorsi are associated with water holding capacity. Mol Biol Rep. 2014; 41: 1411-8.
27. Hong L, Huang HC, Jiang ZF. Relationship between amyloid-beta and the ubiquitin-proteasome system in Alzheimer's disease. Neurol Res. 2014; 36: 276-82.
28. Hamilton DL, Findlay JA, Montagut G, Meakin PJ, Bestow D, Jalicy SM, et al. Altered amyloid precursor protein processing regulates glucose uptake and oxidation in cultured rodent myotubes. Diabetologia. 2014; 57: 1684-92.
29. Chan SL, Mayne M, Holden CP, Geiger JD, Mattson MP. Presenilin-1 mutations increase levels of ryanodine receptors and calcium release in PC12 cells and cortical neurons. J Biol Chem. 2000; 275: 18195-200.
30. Green KN, Demuro A, Akbari Y, Hitt BD, Smith IF, Parker I, et al. SERCA pump activity is physiologically regulated by presenilin and regulates amyloid beta production. J Cell Biol. 2008; 181: 1107-16.
31. Landman N, Jeong SY, Shin SY, Voronov SV, Serban G, Kang MS, et al. Presenilin mutations linked to familial Alzheimer's disease cause an imbalance in

phosphatidylinositol 4,5-bisphosphate metabolism. Proc Natl Acad Sci U S A. 2006; 103: 19524-9.

32. Ferreira IL, Bajouco LM, Mota SI, Auberson YP, Oliveira CR, Rego AC. Amyloid beta peptide 1-42 disturbs intracellular calcium homeostasis through activation of GluN2B-containing N-methyl-d-aspartate receptors in cortical cultures. Cell Calcium. 2012; 51: 95-106.

33. MacLennan DH, Phillips MS. Malignant hyperthermia. Science. 1992; 256: 789-94.

34. Ponsuksili S, Murani E, Trakooljul N, Schwerin M, Wimmers K. Discovery of candidate genes for muscle traits based on GWAS supported by eQTL-analysis. Int J Biol Sci. 2014; 10: 327-37.

35. Cheng KK, Akasaki Y, Lecommandeur E, Lindsay RT, Murfitt S, Walsh K, et al. Metabolomic analysis of akt1-mediated muscle hypertrophy in models of diet-induced obesity and age-related fat accumulation. J Proteome Res. 2015; 14: 342-52.

36. Izumiya Y, Hopkins T, Morris C, Sato K, Zeng L, Viereck J, et al. Fast/Glycolytic muscle fiber growth reduces fat mass and improves metabolic parameters in obese mice. Cell Metab. 2008; 7: 159-72.

37. Huang J, Forsberg NE. Role of calpain in skeletal-muscle protein degradation. Proc Natl Acad Sci U S A. 1998; 95: 12100-5.

38. Powers SK, Kavazis AN, DeRuisseau KC. Mechanisms of disuse muscle atrophy: role of oxidative stress. Am J Physiol Regul Integr Comp Physiol. 2005; 288: R337-44.

39. Otani K, Han DH, Ford EL, Garcia-Roves PM, Ye H, Horikawa Y, et al. Calpain system regulates muscle mass and glucose transporter GLUT4 turnover. J Biol Chem. 2004; 279: 20915-20.

40. Richard I, Broux O, Allamand V, Fougerousse F, Chiannilkulchai N, Bourg N, et al. Mutations in the proteolytic enzyme calpain 3 cause limb-girdle muscular dystrophy type 2A. Cell. 1995; 81: 27-40.

41. Spencer MJ, Guyon JR, Sorimachi H, Potts A, Richard I, Herasse M, et al. Stable expression of calpain 3 from a muscle transgene in vivo: immature muscle in transgenic mice suggests a role for calpain 3 in muscle maturation. Proc Natl Acad Sci U S A. 2002; 99: 8874-9.

42. Duguez S, Bartoli M, Richard I. Calpain 3: a key regulator of the sarcomere? FEBS J. 2006; 273: 3427-36.

43. Kramerova I, Kudryashova E, Venkatraman G, Spencer MJ. Calpain 3 participates in sarcomere remodeling by acting upstream of the ubiquitin-proteasome pathway. Hum Mol Genet. 2005; 14: 2125-34.

44. Tonami K, Hata S, Ojima K, Ono Y, Kurihara Y, Amano T, et al. Calpain-6 deficiency promotes skeletal muscle development and regeneration. PLoS Genet. 2013; 9: e1003668.

45. Ljubicic V, Burt M, Lunde JA, Jasmin BJ. Resveratrol induces expression of the slow, oxidative phenotype in mdx mouse muscle together with enhanced activity of the SIRT1-PGC-1alpha axis. Am J Physiol Cell Physiol. 2014; 307: C66-82.

46. Lin J, Wu H, Tarr PT, Zhang CY, Wu Z, Boss O, et al. Transcriptional co-activator PGC-1 alpha drives the formation of slow-twitch muscle fibres. Nature. 2002; 418: 797-801.

47. LeBleu VS, O'Connell JT, Gonzalez Herrera KN, Wikman H, Pantel K, Haigis MC, et al. PGC-1alpha mediates mitochondrial biogenesis and oxidative phosphorylation in cancer cells to promote metastasis. Nat Cell Biol. 2014; 16: 992-1003, 1-15.

48. Wan L, Ma J, Xu G, Wang D, Wang N. Molecular cloning, structural analysis and tissue expression of protein phosphatase 3 catalytic subunit alpha isoform (PPP3CA) gene in Tianfu goat muscle. Int J Mol Sci. 2014; 15: 2346-58.

49. Angin Y, Steinbusch LK, Simons PJ, Greulich S, Hoebers NT, Douma K, et al. CD36 inhibition prevents lipid accumulation and contractile dysfunction in rat cardiomyocytes. Biochem J. 2012; 448: 43-53.

50. Samovski D, Sun J, Pietka T, Gross RW, Eckel RH, Su X, et al. Regulation of AMPK activation by CD36 links fatty acid uptake to beta-oxidation. Diabetes. 2015; 64: 353-9.

51. Wu W, Ren Z, Zhang L, Liu Y, Li H, Xiong Y. Overexpression of Six1 gene suppresses proliferation and enhances expression of fast-type muscle genes in C2C12 myoblasts. Mol Cell Biochem. 2013; 380: 23-32.

52. Ros S, Schulze A. Balancing glycolytic flux: the role of 6-phosphofructo-2-kinase/fructose 2,6-bisphosphatases in cancer metabolism. Cancer Metab. 2013; 1: 8.

53. Monin G, Sellier P. Pork of low technological quality with a normal rate of muscle pH fall in the immediate post-mortem period: The case of the Hampshire breed. Meat Sci. 1985; 13: 49-63.

54. Bowker B, Grant A, Forrest J, Gerrard D. Muscle metabolism and PSE pork. J Anim Sci. 2000; 79: 1-8.

55. Fernandez X, Lefaucheur L, Candek M. Comparative study of two classifications of muscle fibres: Consequences for the photometric determination of glycogen according to fibre type in red and white muscle of the pig. Meat Sci. 1995; 41: 225-35.

56. Irwin WA, Bergamin N, Sabatelli P, Reggiani C, Megighian A, Merlini L, et al. Mitochondrial dysfunction and apoptosis in myopathic mice with collagen VI deficiency. Nat Genet. 2003; 35: 367-71.

57. Schwerzmann K, Hoppeler H, Kayar SR, Weibel ER. Oxidative capacity of muscle and mitochondria: correlation of physiological, biochemical, and morphometric characteristics. Proc Natl Acad Sci U S A. 1989; 86: 1583-7.

58. Picard M, Hepple RT, Burelle Y. Mitochondrial functional specialization in glycolytic and oxidative muscle fibers: tailoring the organelle for optimal function. Am J Physiol Cell Physiol. 2012; 302: C629-41.

59. Kawamata H, Tiranti V, Magrane J, Chinopoulos C, Manfredi G. adPEO mutations in ANT1 impair ADP-ATP translocation in muscle mitochondria. Hum Mol Genet. 2011; 20: 2964-74.

60. Coenen MJ, Antonicka H, Ugalde C, Sasarman F, Rossi R, Heister JG, et al. Mutant mitochondrial elongation factor G1 and combined oxidative phosphorylation deficiency. N Engl J Med. 2004; 351: 2080-6.

61. Lee K, Kerner J, Hoppel CL. Mitochondrial carnitine palmitoyltransferase 1a (CPT1a) is part of an outer membrane fatty acid transfer complex. J Biol Chem. 2011; 286: 25655-62.

62. Ellis JM, Li LO, Wu PC, Koves TR, Ilkayeva O, Stevens RD, et al. Adipose acyl-CoA synthetase-1 directs fatty acids toward beta-oxidation and is required for cold thermogenesis. Cell Metab. 2010; 12: 53-64.

63. Li LO, Ellis JM, Paich HA, Wang S, Gong N, Altshuller G, et al. Liver-specific loss of long chain acyl-CoA synthetase-1 decreases triacylglycerol synthesis and beta-oxidation and alters phospholipid fatty acid composition. J Biol Chem. 2009; 284: 27816-26.

64. Li LO, Grevengoed TJ, Paul DS, Ilkayeva O, Koves TR, Pascual F, et al. Compartmentalized acyl-CoA metabolism in skeletal muscle regulates systemic glucose homeostasis. Diabetes. 2015; 64: 23-35.

65. Zhou Z, Zhou J, Du Y. Estrogen receptor alpha interacts with mitochondrial protein HADHB and affects beta-oxidation activity. Mol Cell Proteomics. 2012; 11: M111 011056.

66. Martin MA, Blazquez A, Gutierrez-Solana LG, Fernandez-Moreira D, Briones P, Andreu AL, et al. Leigh syndrome associated with mitochondrial complex I deficiency due to a novel mutation in the NDUFS1 gene. Arch Neurol. 2005; 62: 659-61.

67. Rybalka E, Timpani CA, Cooke MB, Williams AD, Hayes A. Defects in mitochondrial ATP synthesis in dystrophin-deficient mdx skeletal muscles may be caused by complex I insufficiency. PLoS One. 2014; 9: e115763.

68. Hejzlarova K, Mracek T, Vrbacky M, Kaplanova V, Karbanova V, Nuskova H, et al. Nuclear genetic defects of mitochondrial ATP synthase. Physiol Res. 2014; 63 Suppl 1: S57-71.

69. Cheng Z, Tseng Y, White MF. Insulin signaling meets mitochondria in metabolism. Trends Endocrinol Metab. 2010; 21: 589-98.

70. Stump CS, Short KR, Bigelow ML, Schimke JM, Nair KS. Effect of insulin on human skeletal muscle mitochondrial ATP production, protein synthesis, and mRNA transcripts. Proc Natl Acad Sci U S A. 2003; 100: 7996-8001.

71. Rochard P, Rodier A, Casas F, Cassar-Malek I, Marchal-Victorion S, Daury L, et al. Mitochondrial activity is involved in the regulation of myoblast differentiation through myogenin expression and activity of myogenic factors. J Biol Chem. 2000; 275: 2733-44.

72. Short KR, Nygren J, Barazzoni R, Levine J, Nair KS. T(3) increases mitochondrial ATP production in oxidative muscle despite increased expression of UCP2 and -3. Am J Physiol Endocrinol Metab. 2001; 280: E761-9.

73. Pillar TM, Seitz HJ. Thyroid hormone and gene expression in the regulation of mitochondrial respiratory function. Eur J Endocrinol. 1997; 136: 231-9.

74. Garesse R, Vallejo CG. Animal mitochondrial biogenesis and function: a regulatory cross-talk between two genomes. Gene. 2001; 263: 1-16.

75. Lehman JJ, Barger PM, Kovacs A, Saffitz JE, Medeiros DM, Kelly DP. Peroxisome proliferator-activated receptor gamma coactivator-1 promotes cardiac mitochondrial biogenesis. J Clin Invest. 2000; 106: 847-56.

76. Kang C, Li Ji L. Role of PGC-1alpha signaling in skeletal muscle health and disease. Ann N Y Acad Sci. 2012; 1271: 110-7.

77. Wu Z, Puigserver P, Andersson U, Zhang C, Adelmant G, Mootha V, et al. Mechanisms controlling mitochondrial biogenesis and respiration through the thermogenic coactivator PGC-1. Cell. 1999; 98: 115-24.

78. Mourier A, Ruzzenente B, Brandt T, Kuhlbrandt W, Larsson NG. Loss of LRPPRC causes ATP synthase deficiency. Hum Mol Genet. 2014; 23: 2580-92.

CrossMark

MicroRNA-mRNA regulatory networking fine-tunes the porcine muscle fiber type, muscular mitochondrial respiratory and metabolic enzyme activities

Xuan Liu, Nares Trakooljul, Frieder Hadlich, Eduard Muráni, Klaus Wimmers and Siriluck Ponsuksili[*]

Abstract

Background: MicroRNAs (miRNAs) are small non-coding RNAs that play critical roles in diverse biological processes via regulation of gene expression including in skeletal muscles. In the current study, miRNA expression profile was investigated in longissimus muscle biopsies of malignant hyperthermia syndrome-negative Duroc and Pietrain pigs with distinct muscle metabolic properties in order to explore the regulatory role of miRNAs related to mitochondrial respiratory activity and metabolic enzyme activity in skeletal muscle.

Results: A comparative analysis of the miRNA expression profile between Duroc and Pietrain pigs was performed, followed by integration with mRNA profiles based on their pairwise correlation and computational target prediction. The identified target genes were enriched in protein ubiquitination pathway, stem cell pluripotency and geranylgeranyl diphosphate biosynthesis, as well as skeletal and muscular system development. Next, we analyzed the correlation between individual miRNAs and phenotypical traits including muscle fiber type, mitochondrial respiratory activity, metabolic enzyme activity and adenosine phosphate concentrations, and constructed the regulatory miRNA-mRNA networks associated with energy metabolism. It is noteworthy that miR-25 targeting *BMPR2* and *IRS1*, miR-363 targeting *USP24*, miR-28 targeting *HECW2* and miR-210 targeting *ATP5I*, *ME3*, *MTCH1* and *CPT2* were highly associated with slow-twitch oxidative fibers, fast-twitch oxidative fibers, ADP and ATP concentration suggesting an essential role of the miRNA-mRNA regulatory networking in modulating the mitochondrial energy expenditure in the porcine muscle. In the identified miRNA-mRNA network, a tight relationship between mitochondrial and ubiquitin proteasome system at the level of gene expression was observed. It revealed a link between these two systems contributing to energy metabolism of skeletal muscle under physiological conditions.

Conclusions: We assembled miRNA-mRNA regulatory networks based on divergent muscle properties between different pig breeds and further with the correlation analysis of expressed genes and phenotypic measurements. These complex networks relate to muscle fiber type, metabolic enzyme activity and ATP production and may contribute to divergent muscle phenotypes by fine-tuning the expression of genes. Altogether, the results provide an insight into a regulatory role of miRNAs in muscular energy metabolisms and may have an implication on meat quality and production.

Keywords: Muscle, Mitochondrial respiratory activity, miRNA-mRNA network

BioMed Central

Background

MicroRNAs (miRNAs) are endogenous small non-coding RNAs ~22 nt in length that play critical roles in diverse biological processes via epigenetic regulation of gene expression. Precursor miRNAs (pre-miRNA) are initially generated in nucleus and processed into an approximately 70 nt long stem-loop structure. It is then exported to cytoplasm and processed by Dicer to generate miRNA/miRNA duplexes. One strand of which is incorporated with Agonaute to form RNA-Induced Silencing Complex (RISC) that targets mRNAs via base-pair complementary, typically to their 3′ untranslated regions (3′UTR) or CDs and downregulates gene expression by either degradation of mRNA or repression of translation, while the other strand is usually discarded [1].

Skeletal muscle is highly metabolically active and valuable for meat-producing animals. Slow-twitch-oxidative (STO), fast-twitch-oxidative (FTO), and fast-twitch-glycolytic (FTG) fiber were the three major muscle fiber types in pigs. Muscle fibers have strong association with muscle metabolic activities and meat quality such as tenderness, juiciness and color. Muscle containing a high proportion of oxidative fibers is often associated with higher fat content, oxidative enzyme activities and mitochondrial density [2–4]; a high ratio of FTG fibers is associated with high glycolytic enzyme activities. Previous research has identified several miRNAs are associated with meat quality such as miR-133, miR-221 and miR-103 etc. in porcine skeletal muscle [5]. The polymorphisms in the porcine miR-133 and miR-208 are proposed as a genetic factor affecting muscle fibers and meat quality traits [6, 7]. Since the critical roles of miRNAs such as myogenesis, adipogenesis and muscle development have been discovered in pig skeletal muscle [8–11], the understanding of the miRNA regulation in metabolic properties of skeletal muscle fibers could be key to improvement of meat quality [12]. MiR-210 and miR-338 could regulate the gene expression of oxidative phosphorylation (OXPHOS) machinery including complex IV subunits COX10, COXIV and ATP synthase subunits ATP5G1 [13, 14]. MiR-15a and miR-15b modulate the cellular ATP levels [15, 16]. MiR-696 regulates the fatty acid oxidation and mitochondrial biogenesis through targeting peroxisome proliferator-activated receptor-gamma coactivator-1alpha (PGC-1α) [17]. With those miRNAs identified, the lack of a comprehensive and systematic miRNA profiling associated with energy metabolism of skeletal muscle remains unraveled.

Our previous research on muscle transcriptional profile has revealed numerous biological pathways significantly associated with muscle fiber type, mitochondrial respiratory activity and metabolic enzymes [18]. It is of interesting to further investigate how miRNAs are involved in energy metabolism by fine-turning gene expression. In the present study, the miRNA transcriptome profiling of longissimus muscle (LM) samples obtained 24 h before slaughter of two pig breeds Duroc and Pietrain exhibiting divergent meat quality and muscle phenotypes provided a comprehensive insight into the discovery of miRNAs associated with muscle fiber, mitochondrial respiratory activity and metabolic enzyme activity. Muscle of Duroc pigs contains higher percentage of STO fibers, mitochondrial respiratory activity and higher fat content to improve the tenderness and juiciness of the meat. In comparison, PiNN pigs are more muscular and favorable for meat industry. Their skeletal muscles are leaner and contain more FTG fibers [18–20]. Hence Duroc and Pietrain pigs are great models to study energy metabolism of skeletal muscle. The miRNA and mRNA expression profile was then integrated based on their pairwise correlations and computational target prediction to construct the regulatory miRNA-mRNA networks which could potentially affect metabolic properties of skeletal muscle and hence meat quality. The illumination of miRNA-based regulatory metabolism could enrich our knowledge of the roles of miRNAs in achieving phenotypic diversity of skeletal muscle in different breeds.

Methods

Animals and sample collection

The experiment and muscle biopsy collection were approved and authorized by the German and European animal welfare regulations for animal husbandry, transport, and slaughter [19–21]. All experimental procedures, including animal care and tissue sample collection, followed guidelines for safeguarding and good scientific practice in accordance with the German Law of Animal Protection, officially authorized by the Animal Care Committee and authorities [Niedersächsischen Landesamt für Verbraucherschutz und Lebensmittelsicherheit (LAVES) 33.42502/01-47.05].

As previously described [19–21], Duroc and Pietrain (PiNN) pigs were raised until 180 days of age. To rule out the effects of the maglinant hyperthermia syndrome (MHS) locus, only muscle samples from MHS-negative genotype pigs were investigated. Muscle biopsies were collected from five female and male pigs of each breed ($n = 20$) for phenotypic measurements (see Additional file 1 for detailed phenotype definition and measurement) [18–21]. Biopsies were collected 24 h before slaughter from the longissimus muscle between 13th and 14th thoracic vertebrae. Muscle samples were frozen in liquid nitrogen and stored at −80 °C until analysis.

RNA isolation

Small RNAs were isolated and enriched from longissimus muscle biopsies using a miReasy Mini kit and an

RNeasy MinElute Cleanup kit (Qiagen) according to manufacturer's protocols. The quality and quantity of small RNA were assessed with an Agilent 2100 Bioanalyzer (Agilent) using an Agilent small RNA kit.

MicroRNA microarray analysis

The Affymetrix GeneChip miRNA 3.0 Array (Affymetrix) was used to determine the miRNA expression profile of the LM 24 h ante mortem of Duroc and PiNN pigs. It is comprised of 16,772 entries representing hairpin precursor, total probe set 19,724 for detection of most miRNA from 153 species (miRBase V.17). 200 ng of small RNA were used in sample preparation using a FlashTag Biotin HSR RNA Labeling kit (Genisphere) for Affymetrix GeneChip miRNA Arrays. Each of the labeled RNA ($n = 20$) was then hybridized for 16 h to an Affymetrix GeneChip miRNA array according to manufacturer's recommendation (Affymetrix), washed and stained in the Affymetrix Fluidics Station 450, and scanned on the Affymetrix G3000 Gene Array Scanner. Expression Console software was used for robust multichip average (RMA) normalization and the detection of present miRNAs by applying the DABG (detection above background) algorithm. Further filtering was done by excluding probes that were present in less than 70 % of the samples within each breed and annotated miRNAs that had sequence greater than or equal to 30 nt in length. Three thousand five hundred eighty seven probes passed the quality filtering and were used for further analysis. The availability of expression data are in the Gene Expression Omnibus public repository with the GEO accession number GSE80198: GSM2120718-GSM2120737.

Statistics and bioinformatics analyses

Differential expression analysis for miRNA was performed using the ANOVA procedure in JMP genomics 7(SAS Institute). Breed was treated as a fixed effect. False discovery rate (FDR) was used to control an error rate of a multiple-hypothesis testing according to Benjamin & Hochberg [22]. We used our previous microarray-based mRNA expression data to integrate with the differentially expressed miRNAs and scan for potential target genes. Pearson correlation of miRNA and mRNA expression levels was calculated.

Both RNAhybrid 2.1.2 and TargetScan 7.0 were used to predict targets of miRNAs. RNAhybrid (http://bibiserv.techfak.uni-bielefeld.de/rnahybrid) is computational software that detects the most energetically favorable hybridization sites of a small RNA within a large RNA [23, 24]. The miRNA probe sets were tested with the following parameters: number of hits per target = 1 and energy cutoff = –25 kcal/mol and maximal internal or bulge loop size per side = 4. TargetScan (http://targetscan.org/) was used to predict the target gene

candidates based on complementarity of the miRNA seed sequence (position 2-8 of the miRNA 5′-end) and target binding site on the 5′ UTR, 3′ UTR and protein coding region of the porcine mRNA sequences (Sus scrofa 10.2 download from NCBI: http://www.ncbi.nlm.nih.gov/ on 1.9.2015) [25]. Hafner et al. and Chi et al. have found that Argonaute-bound target sites in coding sequences (CDs) are as numerous as those located in 3′ UTR in both HEK293 cells (50 % CDs vs 46 % 3′UTR) [26] and mouse brain (25 % CDs vs 32 % 3′UTR) [27]. Other research suggests that miRNA target sites in 3′ UTR are more efficient at triggering mRNAs degradation while CDs and 5′UTR located sites can effectively repress translation [28, 29]. Xu et al. develop novel computational approach for target prediction with sites located along the entire gene sequences to increase the percentage of true positive targets [30]. Hence 5′ UTR, CDs and 3′UTR were included in this study to improve the sensitivity of miRNA target identification and avoid a substantial number of missing targets. Transcripts that negatively correlated with miRNA and predicted as potential targets were further passed to functional analysis.

IPA software (Ingenuity System, https://www.ingenuity.com) was used for functional analysis of potential miRNA target genes. It categorizes genes based on annotated gene functions and statistically tests for overrepresentation of functional terms within the gene list using Fisher's Exact Test. The miRNA-mRNA regulatory networks were visualized using Cytoscape V3.2.1 (http://cytoscape.org) [31].

Quantitative real time PCR (qPCR) for microRNA microarray (miChip) validation

Four miRNAs (ssc-miR-24-3p, ssc-miR-30a-5p, ssc-miR-126 and ssc-miR-145) related to energy metabolism were validated by qPCR of each individual sample ($n = 20$). The same samples were used for both qPCR validation and miRNA-chips. The cDNA was synthesized from 250 ng isolated miRNAs using an NCode™ VILO™ miRNA cDNA Synthesis Kit (Invitrogen) according to manufacturer's protocols. Real-time PCR was performed using the EXPRESS SYBR GreenER™ miRNA qRT-PCR Kit with premixed ROX (Invitrogen) according to manufacturer's protocols. All measurements were performed in duplicates. The thermal parameters were 50 °C for 2 min, 95 °C for 2 min, followed by 45 cycles of 95 °C for 15 s and 60 °C for 1 min. The universal qPCR primer was provided in the kit and the miRNA-specific forward primers were designed for the miRNAs of interest. The designed primer sequence information is accessible in Additional file 2. Geometric mean of the 5S and U6 transcription levels was used as an internal standard to normalize the miRNA expression value. Correlation

coefficient analysis between the miChip and qPCR data was calculated using SAS 9.3 (SAS Institute).

Results

Differentially expressed miRNAs between Duroc and Pietrain

Out of 3587 probes quality-filtered probes, 58 probes belonged to 27 unique mature miRNA sequences were differentially expressed ($p < 0.05$, FDR < 0.2) between Duroc and PiNN using ANOVA on JMP Genomics 7. Among these, 33 probes belonged to 8 mature miRNA sequences were up-regulated in Duroc pigs, while 25 probes belonged to 19 different mature miRNA sequences were up-regulated in PiNN pigs (Additional file 3). Among these, miR-363, miR-423 and miR-34 were the top three upregulated miRNAs in Duroc pigs with fold change ranging from 3.29 to 1.68. Whereas the top three upregulated miRNAs in PiNN were miR-4687, miR-3619 and miR-22 with fold change ranging from 3.45 to 2.71.

Correlation between differentially expressed miRNAs and target mRNAs

The mRNA expression data of matched samples from our previous study (GEO accession number GSE69840: GSM1709900 - GSM1709919) were used for a pairwise correlation analysis [18]. In total, 2345 mRNA probes were differentially expressed ($p < 0.05$, FDR < 0.05) between two breeds. A pairwise correlation coefficient analysis was computed between 58 miRNA probes and 2345 mRNA probes. Among the 136,010 Pearson correlation coefficients, 12,408 negative correlated miRNA-mRNA pairs were detected at $p < 0.05$ and FDR < 0.05 for correlation between miRNA and mRNA. Computational target prediction was performed using Targetscan and RNA hybrid. After combining the correlation analysis and target prediction results, 598 miRNA-mRNA pairs containing 340 genes and 11 mature miRNA sequences were retained (Additional file 4). The heat map and hierarchical clustering of miRNA-mRNA pairs based on their expression levels (lsmeans) shown in Fig. 1 demonstrates an inverse relationship between mRNAs and mRNA target candidates. All the target genes were further analyzed with IPA to identify prominent functions and pathways that may contribute to divergent muscle metabolic properties between the two breed types. Target genes assigned to the functional categories related to skeletal and muscular system development and function as well as carbohydrate metabolism were focused on. The top three canonical pathways for Duroc up-regulated target genes were protein ubiquitination pathway, p70S6K signaling and mouse embryonic stem cell pluripotency, while

geranylgeranyl diphosphate biosynthesis, phagosome maturation and urate biosynthesis/Inosine 5′-phosphate degradation for PiNN up-regulated target genes. A representative miRNA-mRNA regulatory network of focused biological pathways depicted in Fig. 2 illustrates a complex relationship and networking of the two biomolecule types.

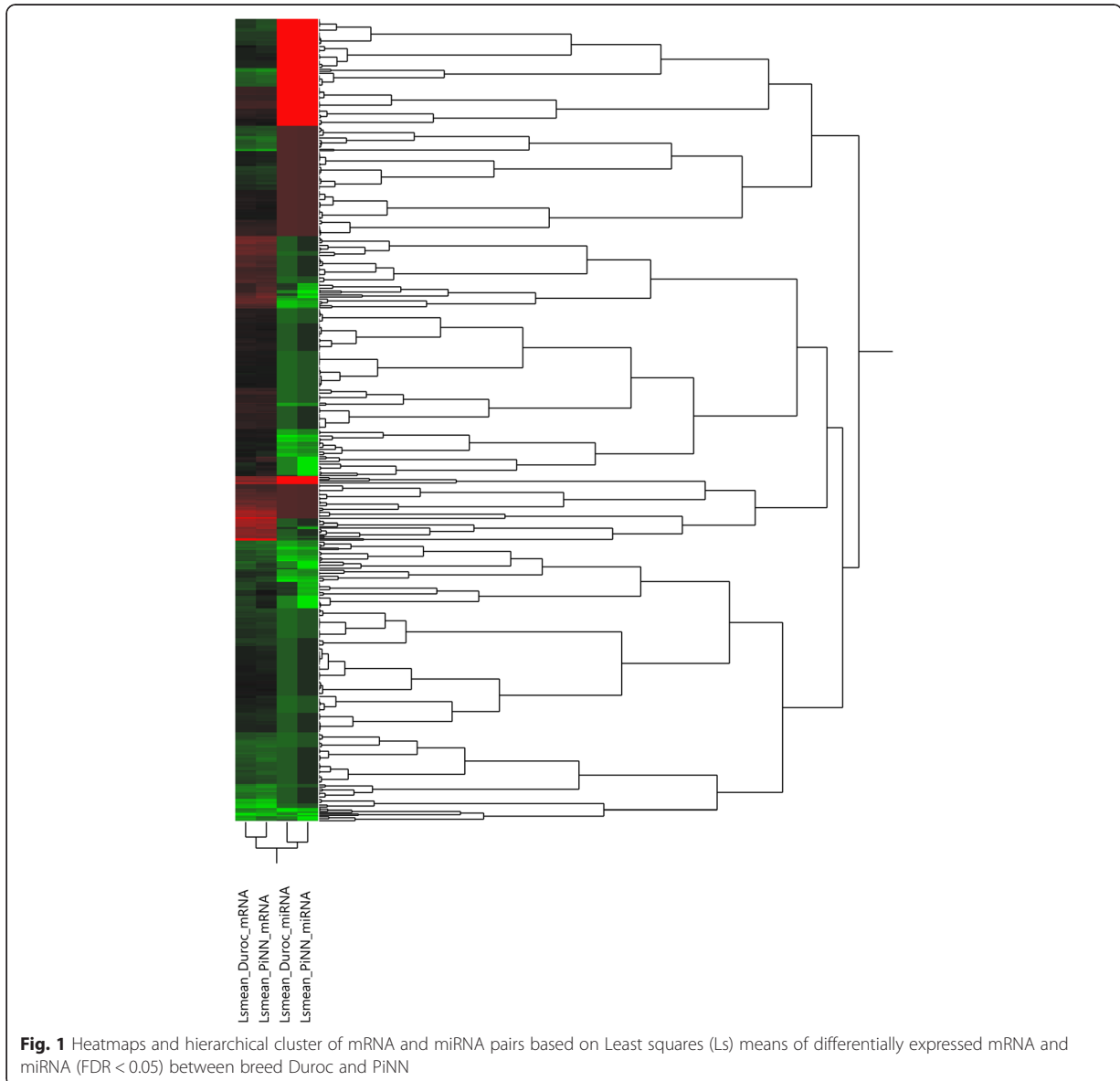### Correlation between miRNA expression and phenotypic traits

The expression of 3587 miRNA probes was calculated for the correlation with traits of muscle fiber composition, mitochondrial respiratory activity and metabolic enzyme activity in both Duroc and PiNN pigs. In total, 3263 miRNA-phenotype pairs containing 1864 miRNA probes belonged to 757 mature miRNA sequences were identified at $p < 0.05$ shown correlation between miRNA and at least one of the 19 phenotypes. The top 100 significant miRNAs correlated to phenotypes were shown in Additional file 5 ($p < \sim0.001$). Table 1 showed the top five miRNAs significantly correlated to each phenotype.

Integration of correlated miRNAs, mRNAs and phenotypic traits

Correlations between gene expression derived from post quality-filtered 17,820 mRNA probes and each phenotypic- trait were calculated for both Duroc and PiNN pigs. In total, 24,374 mRNA-phenotype pairs containing 11,091 mRNA probes belonging to 7489 genes were identified at $p < 0.05$. The top 100 significant mRNAs correlated with phenotypes are accessible in Additional file 6 ($p < 0.0002$). Pairwise correlation coefficient analysis was then performed between the identified 1864 miRNA probes and 11,091 mRNA probes which correlated with at least one of the 19 phenotypes. After combining with the target prediction results, 26,861 miRNA-mRNA pairs containing 3182 genes and 387 miRNAs ($p < 0.05$) were identified to correlate with at least one phenotype. The top ten miRNA-mRNA pairs for each phenotype were shown in Fig. 3 and Additional file 7 ($p < 0.05$, FDR < 0.24).

Correlation relationship between mitochondrial and UPS related genes

From all identified top 10 miRNA-mRNA pairs associated with each phenotypic trait (Fig. 3), the expression correlation between 9 selected nuclear-encoded mitochondrial-related genes and 7 selected UPS-related genes were calculated. In Table 2, mitochondria related genes: ATP synthase, mitochondrial F0 complex, subunit E (*ATP5I*), Malic enzymes 3 (*ME3*), mitochondrial carrier 1 (*MTCH1*), cytochrome P450, family 24, subfamily A, peptide 1 (*CYP24A1*), kinesin family member 1

Fig. 1 Heatmaps and hierarchical cluster of mRNA and miRNA pairs based on Least squares (Ls) means of differentially expressed mRNA and miRNA (FDR < 0.05) between breed Duroc and PiNN

binding protein (*KIAA1279*), prohibitin 2 (*PHB2*), pyruvate dehydrogenase alpha 1 (*PDHA1*) and ubiquinol-cytochrome c reductase complex chaperone (*UQCC*) were significantly correlated with at least one of the six UPS-related genes: Sus scrofa similar to E3 ubiquitin-protein ligase HECW2 (*HECW2*), ubiquitin specific peptidase 24 (*USP24*), ubiquitin family domain containing 1 (*UBFD1*), mitochondrial ubiquitin ligase activator of NFKB 1-like (*MUL1*), amyloid beta (A4) precursor protein (*APP*) and heat shock 70 kDa protein 2 (*HSPA2*) at $p < 0.05$.

qRT-PCR validation

The expression of ssc-miR-24-3p, ssc-miR-30a-5p, ssc-miR-126 and ssc-miR-145 were random selected for validation by qRT-PCR. The correlation coefficient between qPCR and miChip data ranged from 0.543 ($p = 0.0134$) to 0.6833 ($p = 0.0009$), suggesting a good concordance between miChip and qPCR results, as shown in Fig. 4.

Discussion

Duroc and Pietrain are divergent for different muscle characteristics and meat quality. Duroc pigs are fattier and their skeletal muscle contains larger amount STO fibers which are generally associated with higher oxidative enzyme activities, mitochondrial respiratory activity and the storage of lipid to improve the tenderness and juiciness of the meat, whereas Pietrain pigs are more
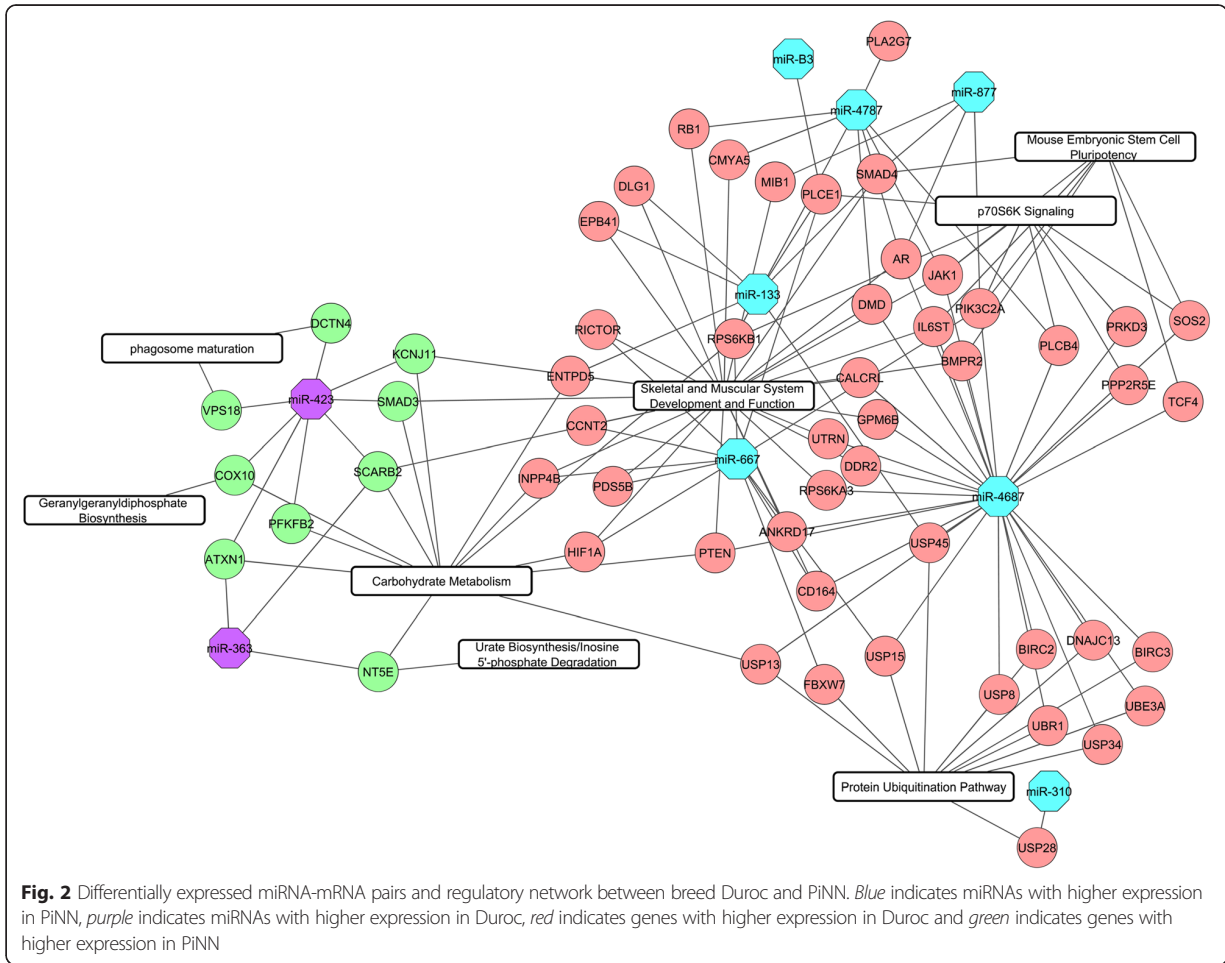
Fig. 2 Differentially expressed miRNA-mRNA pairs and regulatory network between breed Duroc and PiNN. *Blue* indicates miRNAs with higher expression in PiNN, *purple* indicates miRNAs with higher expression in Duroc, *red* indicates genes with higher expression in Duroc and *green* indicates genes with higher expression in PiNN

muscular and their muscles are more lean and contain higher percentage of FTG fibers which are associated with higher glycolytic enzyme activities [2, 18–20, 32, 33]. The higher percentage of FTG fibers may result in lower capillarization, insufficient delivery of oxygen and glycogen depletion, which ultimately lead to dry, firm, and dark meat [34, 35]. Since microRNAs have been known as critical regulators in energy metabolism of skeletal muscle, in the present study, miRNA expression profiling and functional analysis may shed light on miRNA-based epigenetic regulatory mechanism of muscle fiber type and metabolic enzyme activity and hence may be translated to improvement of meat quality.

The miRNA profile of porcine skeletal muscle has been investigated in several studies and the miRNA-mRNA networks are constructed [36–38]. Hou et al. analyzes the miRNA and mRNA profile for Landrace (lean-type) and Tongcheng (obese-type) pigs [36]. In both the study of Hou et al. and our present study, biological process of muscle development was shown in

the identified differentially expressed miRNA-mRNA network and it highlights the importance of the regulatory role of miRNAs in diverging porcine muscle development between obese-type and lean-type pigs. Further, some miRNAs such as miR-363, miR-133 and miR-423 were identified in the network of both studies. Tang et al. investigated the miRNA and mRNA expressions of skeletal muscle for Landrace and Tongcheng pigs at 33, 65 and 90 days to explore prenatal muscle development while Jing et al. construct differentially expressed miRNA-mRNA network between different residual feed intake in pigs [37, 38].

Roles of the differentially expressed miRNAs and their target genes in divergent muscle characteristics
To understand the regulatory role of miRNAs that may contribute to phenotypic variation of the skeletal muscle in different pig breeds, differentially expressed miRNAs and mRNAs between the two breeds were integrated, so that the key target genes regulated by key miRNAs were identified. Functional analysis results showed that the

target genes were significantly enriched for various muscle related bio-functions suggesting biological related results rather than random noise. The top canonical pathway for Duroc-up regulated genes was protein ubiquitination pathway containing genes of *USP28*, *USP8*, *USP45*, *USP15*, *USP13*, *UBR1*, *DNAJC13*, *FBXW7*, *BIRC3*, *USP34*, *UBE3A*, BIRC2. The ATP-dependent ubiquitin is mediated by ubiquitin-activating enzyme E1, specific ubiquitin-conjugating-enzyme E2 and ubiquitin protein E3 to promote protein degradation via the 26 s proteasome and has implications on meat quality and muscle atrophy [39–42]. In our study, *USP45* and *USP28* were predicted as a direct target of miR-133 and miR-310 respectively. MiR-133b could influence both major apoptosis pathways and wound healing [43, 44], and most importantly, the polymorphisms in the porcine MiR206/MiR133b cluster are proposed as a genetic factor affecting muscle fibers and meat quality traits [6]. MiR-311-3p belongs to miR-310 miRNA family and its loss of function can cause defects in energy metabolism and deregulation of nutritional homeostasis-associated genes [45]. MiR-363 has been discovered as a negative regulator of adipogenesis in adipose tissue-derived stromal cells by directly targeting the 3′UTR of E2F3 [46]. This is in line with our study that the expression level of miR-363 is higher in Duroc than PiNN with average fold change more than 3. Other Duroc up-regulated genes such as *CMYA5*, *AR*, *RB1* and *BMPR2* in functional

category of skeletal and muscular system development and function were regulated by miR-4787, miR-877 and miR-4687 etc. Cardiomyopathy associated 5 (*CMYA5*) also called TRIM76 belongs to the tripartite motif super family of proteins (TRIM). Its interaction with both M-band Titin and Calpain 3 suggests its relevance to Limb-girdle Muscular Dystrophies [47]. One SNP (A7189C) of *CMYA5* is significantly associated with water loss and intramuscular fat, which proposes the porcine *CMYA5* as a potential candidate gene for meat quality [48]. Androgen Receptor (AR) is a steroid-hormone activated transcriptional factor. The androgen-AR signaling pathway promotes the slow-twitch muscle fiber formation in skeletal muscle by increasing the expression of slow-twitch-specific genes and suppressing the fast-twitch-specific genes [49].. Moreover, retinoblastoma 1 (RB1) has been identified to be related to Marbling trait in cattle via gene co-expression analysis [50]. Bone Morphogenetic Protein Receptor type II (*BMPR2*) encodes a member of the bone morphogenetic protein receptor family of transmembrane serine/threonine kinases. It is essential for BMP signaling and may be involved in the regulation of adipogenesis and hence in Obesity [51]. All the above Duroc-up regulated genes with their corresponding down regulated miRNAs could contribute to the higher amount of oxidative muscle fibers and fat content. On the other hand, PiNN-up regulated genes *SMAD3* and *PFKFB2* were regulated by miR-423. These

Table 1 The top five significant miRNAs correlated to phenotypes in both Duroc and PiNN pigs

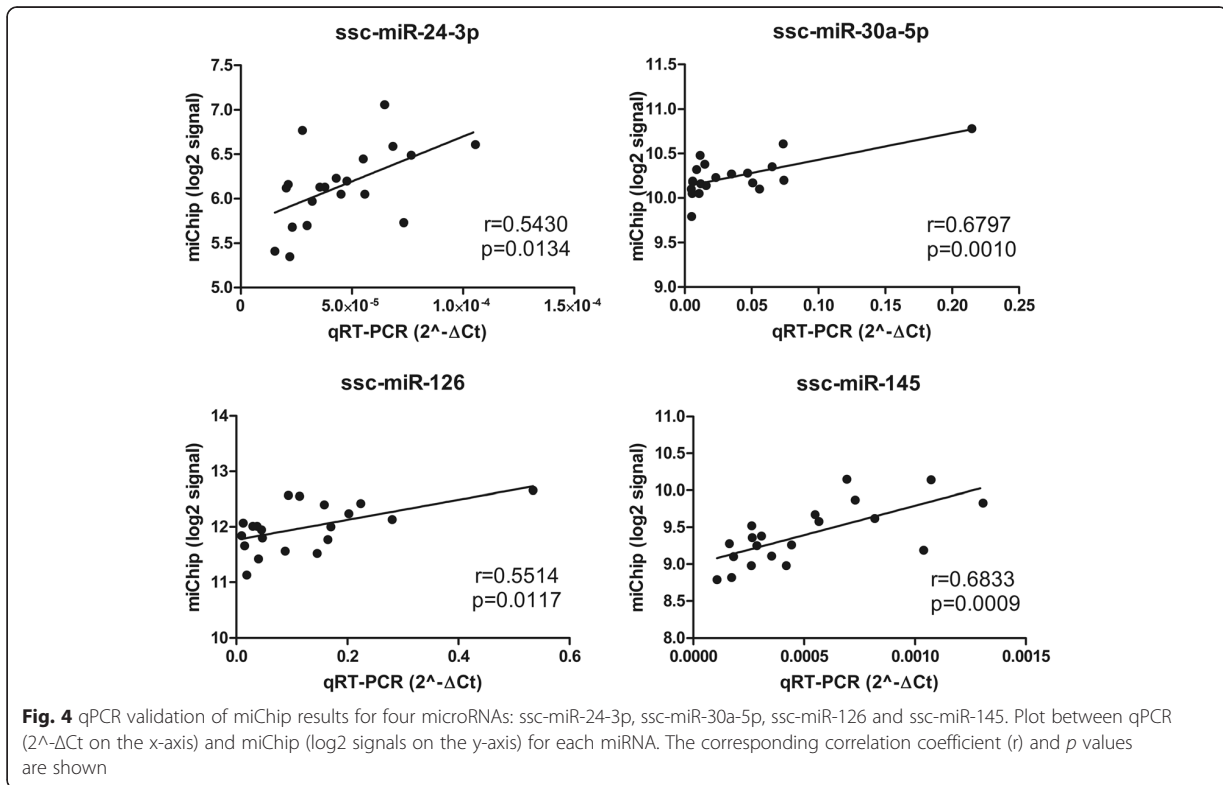| Phenotype	Top five significant miRNAs	*P*-value	|Correlation|
STO	miR-130, miR-208, miR-363, miR-24, miR-126	3.123E-04–1.195E-03	0.803–0.753
FTO	miR-22, miR-166, miR-1892, miR-1343, miR-143	1.222E-03–4.514E-03	0.752–0.689
FTG	miR-99, miR-499, let-7, miR-181, miR-154	1.577E-04–3.337E-04	0.824–0.801
State3_pyruvate	miR-30, miR-196, miR-190, miR-363, miR-95	1.508E-03–7.169E-03	0.661–0.581
State3_succinate	miR-126, miR-196, miR-363, miR-1892, miR-30	7.329E-04–4.205E-03	0.691–0.611
State4_CAT	miR-196, miR-2012, miR-192, miR-202, miR-17	2.484E-04–1.360E-02	0.731–0.542
RCI_pyruvate	miR-17, miR-182, miR-203, miR-27, miR-378	6.558E-03–1.258E-02	0.587–0.547
RCI_succinate	miR-182, miR-203, miR-17, miR-27, miR-542	3.630E-04–4.034E-03	0.718–0.613
GP	miR-148, let-7, miR-194, miR-7, miR-25	3.063E-03–1.477E-02	0.627–0.536
PFK	miR-130, miR-208, miR-193, miR-32, miR-24	5.944E-04–1.455E-03	0.700–0.663
LDH	miR-17, miR-58, miR-15, miR-769, miR-345	1.090E-04–4.384E-03	0.758–0.609
CS	miR-338, miR-30, miR-17, miR-182, miR-455	3.970E-05–1.959E-03	0.786–0.649
ComplexI	miR-182, miR-181, miR-143, miR-28, miR-765	2.691E-04–1.620E-03	0.743–0.672
ComplexII	miR-182, miR-1, miR-1307, miR-203, miR-499	2.557E-03–2.458E-02	0.666–0.527
ComplexIV	miR-196, let-7, miR-451, miR-128, miR-99	3.668E-03–7.785E-03	0.618–0.577
IMP	miR-168, miR-166, miR-58, miR-223, let-7	3.908E-04–1.382E-02	0.745–0.569
AMP	miR-10, miR-126, let-7, miR-27, miR-450	9.860E-05–5.804E-04	0.789–0.730
ADP	miR-15, miR-885, miR-322, miR-450, miR-338	1.316E-04–4.540E-03	0.781–0.636
ATP	miR-15, miR-450, miR-210, miR-885, miR-451	4.811E-04–9.562E-03	0.737–0.593
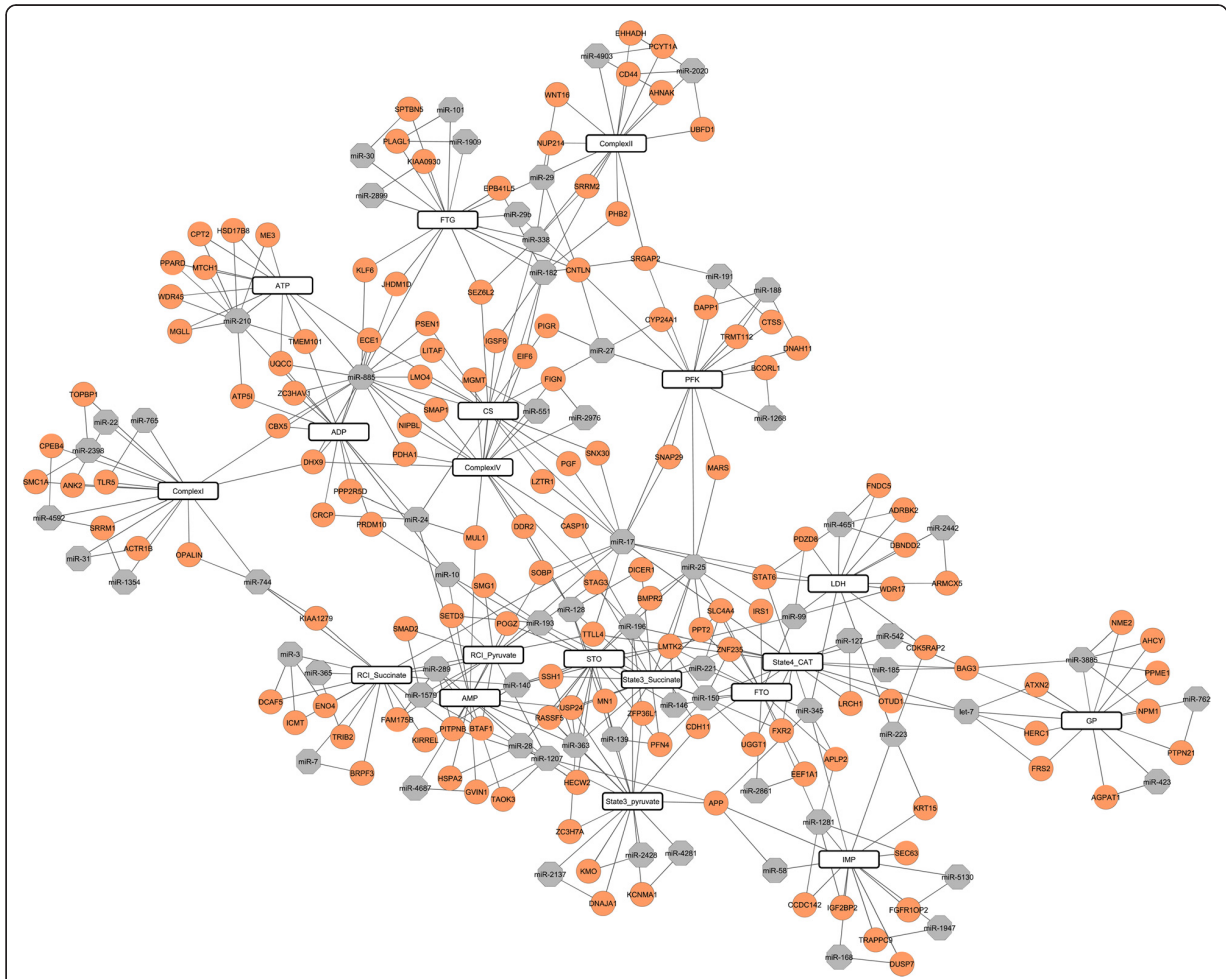
Fig. 3 Regulatory network of miRNA-mRNA associated with muscle fiber composition, mitochondrial respiratory activity, metabolic enzyme activity and adenine nucleotide concentration for breed Duroc and PiNN. Genes were colored with *orange* while miRNAs with *grey*

Table 2 Correlation between mitochondrial and UPS related gene expressions

Genes			Mitochondria related genes							
			ATP5I	ME3	MTCH1	CYP24A1	KIAA1279	PHB2	PDHA1	UQCC
UPS related genes	HECW2	r	0.386	0.623	0.494	−0.318	−0.392	−0.306	0.586	0.509
		p	0.093	**0.003**	**0.027**	0.171	0.087	0.189	**0.007**	**0.022**
	USP24	r	−0.285	−0.284	−0.376	0.160	0.542	0.478	−0.422	−0.281
		p	0.224	0.226	0.102	0.501	**0.014**	**0.033**	0.064	0.231
	UBFD1	r	0.512	0.501	0.746	0.069	−0.512	−0.669	0.477	0.515
		p	**0.021**	**0.024**	**0.0002**	0.772	**0.021**	**0.001**	**0.034**	**0.020**
	MUL1	r	0.336	0.083	0.131	0.657	0.460	0.224	−0.375	0.051
		p	0.147	0.726	0.583	**0.002**	**0.041**	0.341	0.103	0.832
	APP	r	0.214	0.486	0.463	−0.368	−0.300	−0.292	0.214	0.327
		p	0.365	**0.030**	**0.040**	0.110	0.199	0.211	0.364	0.159
	HSPA2	r	0.414	0.484	0.566	−0.212	−0.502	−0.474	0.537	0.274
		p	0.070	**0.031**	**0.009**	0.369	**0.024**	**0.035**	**0.015**	0.242

numbers in bold are *p*-values < significance threshold of 0.05

Fig. 4 qPCR validation of miChip results for four microRNAs: ssc-miR-24-3p, ssc-miR-30a-5p, ssc-miR-126 and ssc-miR-145. Plot between qPCR (2^-ΔCt on the x-axis) and miChip (log2 signals on the y-axis) for each miRNA. The corresponding correlation coefficient (r) and *p* values are shown

two genes are involved in not only muscle fiber specificity but also the promotion of glycolysis in skeletal muscle. SMAD family member 3 (SMAD3) promotes muscle atrophy in vivo by regulating atrogin-1, mTOR and protein synthesis [52]. It suppresses the expression of peroxisome proliferator-activated receptor γ coactivator 1-α (*PGC-1α*) [53], which is a master coordinator to control mitochondrial biogenesis and drives the formation of slow-twitch muscle fibers [54, 55]. Fructose -2, 6- biphosphatase 2 (*PFKFB2*) can promote glycolysis by controlling the level of Fructose 2, 6- bisphosphate, which is an allosteric activator of phosphofructokinase (PFK-1) [56]. Collectively, we demonstrate that differential miRNAs and target gene candidates assemble regulatory networks that may fine-tune the expression of genes within the pathways and shape the related phenotypes among pig breeds.

Phenotype-correlated microRNAs link to various processes in energy metabolism
Numerous studies have revealed the critical roles of miRNAs in skeletal muscle development and the irregular miRNA expression contributes to various muscular disorders [57]. Table 1 shows the top five miRNAs significantly correlated to each phenotypic trait including muscle fiber type, mitochondrial respiratory activity (MRA) and metabolic enzyme activities for Duroc and

PiNN pigs. Both positive and negative correlations were included to discover any potential links between miRNAs and phenotypes. STO, FTO, and FTG fibers were three major muscle fiber types in pigs which are strong associated with muscle metabolic activities and meat quality. MiRNAs such as miR-208, miR-499, miR-130 and miR-363 showed highly significant correlation with muscle fiber types. MiR-208 and miR-499 play a dominant role in the specification of muscle fiber identity by inducing the type I fiber program via targeting Sox6 which acts as a repressor of slow-twitch genes [58–60]. MiR-130b belongs to miR-130 family directly targets gene PGC-1α, which is a master regulator for mitochondrial biogenesis and its activation promotes the slow, oxidative myogenic program in mice and drives the formation of slow-twitch muscle fibers in cultured muscle cells [54, 61]. In C2C12 cells, miR-130b could modulate cellular ATP levels by targeting electron transport chain subunits Ndufb7 and Cox6a2 [16]. As previously mentioned, miR-363 has been discovered as a negative regulator of adipogenesis in adipose tissue-derived stromal cells by directly targeting the 3′UTR of E2F3 [46]. Since lipids are stored mainly in STO muscle fibers to improve tenderness and juiciness of the meat [33], and muscles containing more STO fibers are associated with higher oxidative enzyme activities and mitochondrial respiratory activity [2], it is expected that miR-363 shows high

correlation with STO muscle fiber type and mitochondrial respiratory activity including state 3 pyruvate and state 3 succinate. MiR-30 family members haven been demonstrated to control calcium signaling by directly inhibiting a Ca^{2+} transporter *TRPC6* etc. [62]. Considering the crucial regulatory role of calcium signaling in mitochondrial ATP production, it was not unexpected that miR-30 was associated with mitochondrial respiratory activity including state3 pyruvate and state3 succinate and TCA involved CS enzyme activity. Furthermore, miR-30 directly targets Prdm1 to promote fast muscle formation since Prdm1 regulates muscle fiber differentiation by repressing the transcription factor Sox6 which acts as a repressor of slow-twitch-specific gene expression [60, 63]. All these reinforced the association between STO fiber, mitochondrial respiratory activity and fat content. MiR-196 was highly correlated to mitochondrial state 3 and state 4 respiration rate and Complex IV activity. MiR-196a displays a tissue-specific expression pattern in porcine and plays a role in porcine adipose development via inducing the expression of adipocyte specific markers, lipid accumulation and triglyceride content [64]. MiR-542 was significantly correlated to RCI succinate. MiR-542-3p directly targets bone morphogenetic protein 7 (BMP7), which induces differentiation of adipose derived mesenchymal stem cells into brown adipocytes and increases mitochondrial activity in mature brown adipocytes [65–67]. MiR-1 was correlated to Complex II activity in the present study. MiR-1 family is abundantly expressed in cardiac and skeletal muscle. It post-transcriptionally represses the expression of genes in antioxidant network and thus influences susceptibility to cardiac oxidative stress of miR-1 transgenic mice [68]. Moreover, it was proposed as a candidate gene associated with muscle fiber type composition [69]. MiR-7, miR-194 and miR-25 were identified to correlate with GP activity. Both miR-7 and miR-194 could directly target and suppress the expression of insulin-like growth factor 1 receptor (IGF-1R) whereas miR-25 regulates insulin synthesis at its mRNA level [70–72]. Since insulin and insulin-like growth factor system are crucial for normal glucose homeostasis [73, 74], it is likely that miR-7 and miR-194 could play a role in glucose metabolism via IGF-1R and insulin. MiR-210, miR-15 and miR-338 were highly correlated to the concentration of ADP and ATP in muscle cells. MiR-210 and miR-338 regulate the expression of oxidative phosphorylation (OXPHOS) machinery including complex IV subunits *COX10*, *COXIV* and ATP synthase subunits *ATP5G1* correspondingly [13, 14]. The fully assemble of OXPHOS system could directly contribute to the ATP production. Furthermore, the modulation of cellular ATP levels by miR-15b was supported by other work as well [15]. Overall, our results and previous reports functionally link miRNAs to muscle fiber specificity, mitochondrial respiration, adipogenesis, glucose metabolism and ATP production and further suggest an essential role of miRNAs in energy metabolism.

Phenotype-correlated miRNA-mRNA regulatory network link to energy metabolism

Based on the identified miRNAs that highly correlated with the phenotypes, we further integrated the miRNA and mRNA expression profiles to identify miRNAs regulated genes that influence energy metabolism. The microRNA-mRNA regulatory network was constructed using the following criteria: 1) The expressions of both miRNAs and target mRNAs were correlated to the phenotypical traits 2) The gene expression level was negatively correlated with the expression of its miRNA regulator 3) The gene was computationally predicted as a target gene of the corresponding miRNA. It is noteworthy that miR-25 together with its target genes Bone Morphogenetic Protein Receptor type II (*BMPR2*) and insulin receptor substrate 1 (*IRS1*) were correlated to STO and FTO muscle fibers. MiR-25 has been documented to be abundant in cardiomyocytes. It targets the mitochondrial calcium uniporter (MCU) and Ca^{2+} transporting ATPase (ATP2A2) and plays a role in cardiac contractility [75, 76]. In the present study, miR-25 was proposed to target both genes *BMPR2* and *IRS1*. *BMPR2* encodes a member of the bone morphogenetic protein receptor family of transmembrane serine/threonine kinases. It is essential for BMP signaling and may be involved in the regulation of adipogenesis and hence in obesity [51]. IRS1 is a major molecule mediating insulin-signaling pathways. Insulin not only regulates stimulation of protein synthesis and glucose storage [77], but also has effect on mitochondrial function and oxidative capacity of skeletal muscle via increasing the expression level of complex I and complex IV and hence ATP production [78]. MiR-363 and its target gene ubiquitin specific peptidase 24 (*USP24*) were correlated to STO fibers, mitochondrial respiratory activity including state 3 pyruvate and state 3 succinate, and AMP concentration in muscle cells, while miR-28 and its target gene *HECW2* were correlated to STO muscle fibers. USP24 belongs to a large family of cysteine proteases that function as deubiquitinating enzymes. *HECW2* encodes HECT, C2 and WW domain containing E3 ubiquitin protein ligase 2 which is a major component of ubiquitin proteasome system (UPS). UPS utilizes ATP to promote protein degradation and regulate muscle mass. Accumulated ubiquitin proteins in fast- to slow- transforming rabbit muscle revealed a possible role of UPS in muscle fiber specificity [79]. Interestingly, miR-363 has been discovered as a negative regulator of adipogenesis as described previously [46]. Misregulation of miRNAs

belonging to miR-23a/27a/24-2 cluster has been recently associated to hypertrophic cardiomyopathy and skeletal muscle atrophy [80]. MiR-27 was almost sixfold greater in slow-twitch than in fast-twitch muscle in vivo. It posttranscriptionally regulates fast-specific myostatin (MSTN) expression, which mature mRNA level is sixfold greater in fast vs slow muscle [81]. In this study, miR-27 was identified to be associated with PFK activity – a rate-limiting enzyme in glycolysis and potentially target cytochrome P450, family 24, subfamily A, polypeptide 1 (*CYP24A1*), which catalyzes the side-chain oxidation of vitamin D [82]. The vitamin D pathway has the suppressive effect on brown adipocyte differentiation and mitochondrial respiration [83]. MiR-210 and its predicted targets *ATP5I*, *ME3*, *MTCH1* and *CPT2* were highly correlated to ADP and ATP concentration in present study. MiR-210 modulates mitochondrial function, decreases COX10 expression and activates the generation of reactive oxygen species (ROS) [14]. *ATP5I* encodes ATP synthase mitochondrial F0 complex subunit E and it is required for the full assembly of the ATP synthase and ATP production [84]. *ME3* encodes mitochondrial NADP (+)-dependent malic enzyme 3. The regulation of human mitochondrial NADP (+)-dependent malic enzyme by ATP and fumarate may be crucial for the metabolism of glutamine for energy production [85]. *MTCH1* and *CPT2* encode for mitochondrial carrier 1 and carnitine palmitoyltransferase 2 respectively. MTCH1 also known as Presenilin 1-associated protein (PSAP) which acts as a proapoptotic mitochondrial protein induce apoptosis independent of the proapoptotic proteins Bax and Bak [86]. The two isoforms of MTCH1 share two proapoptotic domains and multiple internal signals for import into the mitochondrial outer membrane [87]. Fatty acid is a major energy source for the heat and skeletal muscle. CPT2 together with CPT1 are involved in beta-oxidation of long chain fatty acids in the mitochondria [88]. Altogether suggests that miR-210 and its target genes *ATP5I*, *ME3*, *MTCH1* and *CPT2* are likely to be involved in ATP production, apoptosis and beta-oxidation of long fatty acids in mitochondria. We have demonstrated that correlation relationship between miRNA and target mRNA can be used to functionally link to phenotypes of interest such as muscle fiber type specification, mitochondrial respiration activity and metabolic enzymes related to ATP production.

Crosstalk between mitochondria and UPS in skeletal muscle

Up to now we have shown that the identified miRNA-mRNA networks are linked to muscle fiber types, oxidative enzyme activities and ATP generation. Some of these target genes are involved in mitochondrial function and UPS. An interesting finding was the significant correlation between mitochondrial and UPS related gene expressions. More specifically, mitochondrial related genes including *ATP5I*, *ME3*, *MTCH1*, *CYP24A KIAA1279*, *PHB2*, *PDHA1* and *UQCC* were highly correlated to at least one of the UPS-related genes including *HECW2*, *USP24*, *UBFD1*, *MUL1*, *APP* and *HSPA2*.

The tightly interdependent relationship between mitochondria and UPS system has been described in many age-related diseases such as Alzheimer's and Parkinson's disease [89–91]. Our present study revealed a link between these two systems at the level of gene expression under normal state, since all the investigated animals were healthy. In other words, both mitochondria and UPS might contribute to energy metabolism of skeletal muscle via fine-turning the gene expression by miRNAs under physiological conditions.

The HECT, C2 and WW domain containing E3 ubiquitin protein ligase 2 (HECW2), ubiquitin specific peptidase 24 (USP24), ubiquitin family domain containing 1 (UBFD1) and mitochondrial ubiquitin ligase activator of NFKB 1-like (MUL1), Amyloid beta precursor protein (APP) and Heat shock 70 kDa protein 2 (HSPA2) are either the major components or associated with the UPS system [92, 93]. Those genes targeted by several miRNAs including miR-28, miR-363, miR-2020, miR-24, miR-1207, miR-345 and miR-58 may be the cause of fluctuation of the UPS degradation for ubiquitin proteasome-dependent molecules [94] such as transcriptional coactivator PGC-1α which acts as a master regulator for mitochondrial biogenesis, to control mitochondrial gene expression indirectly. On the other side, miR-210 and miR-885 targeted genes of ATP synthase mitochondrial F0 complex subunit E (ATP5I), Pyruvate dehydrogenase alpha 1 (PDHA1) and Ubiquinol-cytochrome c reductase complex chaperone (UQCC) [95] could affect cellular ATP generation, followed by influencing the ATP-dependent UPS system [96]. However, further detail information of the interaction between mitochondria and UPS still remains elusive.

Conclusion

In this study, we modelled the miRNA-mRNA regulatory networks related to muscle fiber type, metabolic enzyme activity and ATP production using the correlation information between expressed miRNAs and target mRNAs as well as muscular phenotypic measurements of Duroc and PiNN pigs. These complex networks may contribute to the muscle phenotypic variations by fine-tuning the expression of genes. Altogether, the results provide an insight into a regulatory role of miRNAs in muscular energy metabolisms.

Additional files

Abbreviations
miRNA, microRNA; STO, slow-twitch-oxidative; FTO, fast-twitch-oxidative; FTG, fast-twitch-glycolytic; PiNN: pietrain; UPS, ubiquitin proteasome system.

Availability of data and material
The availability of expression data are in the Gene Expression Omnibus public repository with the GEO accession number GSE80198: GSM2120718-GSM2120737.

Authors' contributions
XL analysed the microarray data and drafted the manuscript; FH helped in target prediction analysis. NT, EM, and KW helped in sampling and data collection and drafting the manuscript; SP discussed and contributed to data interpretation and helped in drafting the manuscript. All authors have read and approved the final manuscript.

Competing interests
The authors declare that they have no competing interests.

Consent for publication
Not applicable.

Ethics approval and consent to participate
All experimental procedures, including animal care and tissue sample collection, followed guidelines for safeguarding and good scientific practice in accordance with the German Law of Animal Protection, officially authorized by the Animal Care Committee and authorities [Niedersächsischen Landesamt für Verbraucherschutz und Lebensmittelsicherheit (LAVES) 33.42502/01-47.05].

References
1. Shukla GC, Singh J, Barik S. MicroRNAs: processing, maturation, target recognition and regulatory functions. Mol Cell Pharmacol. 2011;3:83–92.
2. Gueguen N, Lefaucheur L, Fillaut M, Vincent A, Herpin P. Control of skeletal muscle mitochondria respiration by adenine nucleotides: differential effect of ADP and ATP according to muscle contractile type in pigs. Comp Biochem Physiol B Biochem Mol Biol. 2005;140:287–97.
3. Picard M, Hepple RT, Burelle Y. Mitochondrial functional specialization in glycolytic and oxidative muscle fibers: tailoring the organelle for optimal function. Am J Physiol Cell Physiol. 2012;302:C629–41.
4. Schwerzmann K, Hoppeler H, Kayar SR, Weibel ER. Oxidative capacity of muscle and mitochondria: correlation of physiological, biochemical, and morphometric characteristics. Proc Natl Acad Sci U S A. 1989;86:1583–7.
5. Ponsuksili S, Du Y, Hadlich F, Siengdee P, Murani E, Schwerin M, Wimmers K. Correlated mRNAs and miRNAs from co-expression and regulatory networks affect porcine muscle and finally meat properties. BMC Genomics. 2013;14:533.
6. Lee JS, Kim JM, Lim KS, Hong JS, Hong KC, Lee YS. Effects of polymorphisms in the porcine microRNA MIR206 / MIR133B cluster on muscle fiber and meat quality traits. Anim Genet. 2013;44:101–6.
7. Kim JM, Lim KS, Hong JS, Kang JH, Lee YS, Hong KC. A polymorphism in the porcine miR-208b is associated with microRNA biogenesis and expressions of SOX-6 and MYH7 with effects on muscle fibre characteristics and meat quality. Anim Genet. 2015;46:73–7.
8. Hou X, Tang Z, Liu H, Wang N, Ju H, Li K. Discovery of MicroRNAs associated with myogenesis by deep sequencing of serial developmental skeletal muscles in pigs. PLoS One. 2012;7, e52123.
9. Huang TH, Zhu MJ, Li XY, Zhao SH. Discovery of porcine microRNAs and profiling from skeletal muscle tissues during development. PLoS One. 2008; 3, e3225.
10. McDaneld TG, Smith TP, Doumit ME, Miles JR, Coutinho LL, Sonstegard TS, Matukumalli LK, Nonneman DJ, Wiedmann RT. MicroRNA transcriptome profiles during swine skeletal muscle development. BMC Genomics. 2009;10: 77.
11. Li HY, Xi QY, Xiong YY, Liu XL, Cheng X, Shu G, Wang SB, Wang LN, Gao P, Zhu XT, et al. Identification and comparison of microRNAs from skeletal muscle and adipose tissues from two porcine breeds. Anim Genet. 2012;43: 704–13.
12. Hocquette JF, Ortigues-Marty I, Vermorel M. Manipulation of tissue energy metabolism in meat-producing ruminants - review. Asian Australas J Anim Sci. 2001;14:720–32.
13. Aschrafi A, Kar AN, Natera-Naranjo O, MacGibeny MA, Gioio AE, Kaplan BB. MicroRNA-338 regulates the axonal expression of multiple nuclear-encoded mitochondrial mRNAs encoding subunits of the oxidative phosphorylation machinery. Cell Mol Life Sci. 2012;69:4017–27.
14. Chen Z, Li Y, Zhang H, Huang P, Luthra R. Hypoxia-regulated microRNA-210 modulates mitochondrial function and decreases ISCU and COX10 expression. Oncogene. 2010;29:4362–8.
15. Nishi H, Ono K, Iwanaga Y, Horie T, Nagao K, Takemura G, Kinoshita M, Kuwabara Y, Mori RT, Hasegawa K, et al. MicroRNA-15b modulates cellular ATP levels and degenerates mitochondria via Arl2 in neonatal rat cardiac myocytes. J Biol Chem. 2010;285:4920–30.
16. Siengdee P, Trakooljul N, Murani E, Schwerin M, Wimmers K, Ponsuksili S. MicroRNAs regulate cellular ATP levels by targeting mitochondrial energy metabolism genes during C2C12 myoblast differentiation. PLoS One. 2015; 10, e0127850.
17. Aoi W, Naito Y, Mizushima K, Takanami Y, Kawai Y, Ichikawa H, Yoshikawa T. The microRNA miR-696 regulates PGC-1{alpha} in mouse skeletal muscle in response to physical activity. Am J Physiol Endocrinol Metab. 2010;298: E799–806.
18. Liu X, Du Y, Trakooljul N, Brand B, Murani E, Krischek C, Wicke M, Schwerin M, Wimmers K, Ponsuksili S. Muscle transcriptional profile based on muscle fiber, mitochondrial respiratory activity, and metabolic enzymes. Int J Biol Sci. 2015;11:1348–62.
19. Werner C, Natter R, Schellander K, Wicke M. Mitochondrial respiratory activity in porcine longissimus muscle fibers of different pig genetics in relation to their meat quality. Meat Sci. 2010;85:127–33.
20. Werner C, Natter R, Wicke M. Changes of the activities of glycolytic and oxidative enzymes before and after slaughter in the longissimus muscle of Pietrain and Duroc pigs and a Duroc-Pietrain crossbreed. J Anim Sci. 2010;88:4016–25.
21. Krischek C, Natter R, Wigger R, Wicke M. Adenine nucleotide concentrations and glycolytic enzyme activities in longissimus muscle samples of different pig genotypes collected before and after slaughter. Meat Sci. 2011;89:217–20.
22. Benjamini Y, Hochberg Y. Controlling the false discovery rate: a practical and powerful approach to multiple testing. J R Stat Soc Ser B Methodol. 1995;57:289–300.
23. Rehmsmeier M, Steffen P, Hochsmann M, Giegerich R. Fast and effective prediction of microRNA/target duplexes. RNA. 2004;10:1507–17.

24. Kruger J, Rehmsmeier M. RNAhybrid: microRNA target prediction easy, fast and flexible. Nucleic Acids Res. 2006;34:W451–4.

25. Lewis BP, Burge CB, Bartel DP. Conserved seed pairing, often flanked by adenosines, indicates that thousands of human genes are microRNA targets. Cell. 2005;120:15–20.

26. Hafner M, Landthaler M, Burger L, Khorshid M, Hausser J, Berninger P, Rothballer A, Ascano Jr M, Jungkamp AC, Munschauer M, et al. Transcriptome-wide identification of RNA-binding protein and microRNA target sites by PAR-CLIP. Cell. 2010;141:129–41.

27. Chi SW, Zang JB, Mele A, Darnell RB. Argonaute HITS-CLIP decodes microRNA-mRNA interaction maps. Nature. 2009;460:479–86.

28. Hausser J, Syed AP, Bilen B, Zavolan M. Analysis of CDS-located miRNA target sites suggests that they can effectively inhibit translation. Genome Res. 2013;23:604–15.

29. Lytle JR, Yario TA, Steitz JA. Target mRNAs are repressed as efficiently by microRNA-binding sites in the 5′ UTR as in the 3′ UTR. Proc Natl Acad Sci U S A. 2007;104:9667–72.

30. Xu W, San Lucas A, Wang Z, Liu Y. Identifying microRNA targets in different gene regions. BMC Bioinformatics. 2014;15 Suppl 7:S4.

31. Cline MS, Smoot M, Cerami E, Kuchinsky A, Landys N, Workman C, Christmas R, Avila-Campilo I, Creech M, Gross B, et al. Integration of biological networks and gene expression data using Cytoscape. Nat Protoc. 2007;2:2366–82.

32. Huber K, Petzold J, Rehfeldt C, Ender K, Fiedler I. Muscle energy metabolism: structural and functional features in different types of porcine striated muscles. J Muscle Res Cell Motil. 2007;28:249–58.

33. Essen-Gustavsson B, Karlsson A, Lundstrom K, Enfalt AC. Intramuscular fat and muscle fibre lipid contents in halothane-gene-free pigs fed high or low protein diets and its relation to meat quality. Meat Sci. 1994;38:269–77.

34. Karlsson AH, Klont RE, Fernandez X. Skeletal muscle fibres as factors for pork quality. Livest Prod Sci. 1999;60:255–69.

35. Karlsson A, Essen-Gustavsson B, Lundstrom K. Muscle glycogen depletion pattern in halothane-gene-free pigs at slaughter and its relation to meat quality. Meat Sci. 1994;38:91–101.

36. Hou X, Yang Y, Zhu S, Hua C, Zhou R, Mu Y, Tang Z, Li K. Comparison of skeletal muscle miRNA and mRNA profiles among three pig breeds. Mol Genet Genomics. 2016;291:559–73.

37. Tang Z, Yang Y, Wang Z, Zhao S, Mu Y, Li K. Integrated analysis of miRNA and mRNA paired expression profiling of prenatal skeletal muscle development in three genotype pigs. Sci Rep. 2015;5:15544.

38. Jing L, Hou Y, Wu H, Miao Y, Li X, Cao J, Brameld JM, Parr T, Zhao S. Transcriptome analysis of mRNA and miRNA in skeletal muscle indicates an important network for differential Residual Feed Intake in pigs. Sci Rep. 2015;5:11953.

39. Lecker SH, Solomon V, Mitch WE, Goldberg AL. Muscle protein breakdown and the critical role of the ubiquitin-proteasome pathway in normal and disease states. J Nutr. 1999;129:227S–37S.

40. Murton AJ, Constantin D, Greenhaff PL. The involvement of the ubiquitin proteasome system in human skeletal muscle remodelling and atrophy. Biochim Biophys Acta. 2008;1782:730–43.

41. Huynh TP, Murani E, Maak S, Ponsuksili S, Wimmers K. UBE3B and ZRANB1 polymorphisms and transcript abundance are associated with water holding capacity of porcine M. longissimus dorsi. Meat Sci. 2013;95:166–72.

42. Loan HT, Murani E, Maak S, Ponsuksili S, Wimmers K. UBXN1 polymorphism and its expression in porcine M. longissimus dorsi are associated with water holding capacity. Mol Biol Rep. 2014;41:1411–8.

43. Patron JP, Fendler A, Bild M, Jung U, Muller H, Arntzen MO, Piso C, Stephan C, Thiede B, Mollenkopf HJ, et al. MiR-133b targets antiapoptotic genes and enhances death receptor-induced apoptosis. PLoS One. 2012;7, e35345.

44. Robinson PM, Chuang TD, Sriram S, Pi L, Luo XP, Petersen BE, Schultz GS. MicroRNA signature in wound healing following excimer laser ablation: role of miR-133b on TGFbeta1, CTGF, SMA, and COL1A1 expression levels in rabbit corneal fibroblasts. Invest Ophthalmol Vis Sci. 2013;54:6944–51.

45. Cicek IO, Karaca S, Brankatschk M, Eaton S, Urlaub H, Shcherbata HR. Hedgehog signaling strength is orchestrated by the mir-310 cluster of microRNAs in response to diet. Genetics. 2016;202:1167–83.

46. Chen L, Cui J, Hou J, Long J, Li C, Liu L. A novel negative regulator of adipogenesis: microRNA-363. Stem Cells. 2014;32:510–20.

47. Sarparanta J, Blandin G, Charton K, Vihola A, Marchand S, Milic A, Hackman P, Ehler E, Richard I, Udd B. Interactions with M-band titin and calpain 3 link myospryn (CMYA5) to tibial and limb-girdle muscular dystrophies. J Biol Chem. 2010;285:30304–15.

48. Xu X, Xu X, Yin Q, Sun L, Liu B, Wang Y. The molecular characterization and associations of porcine cardiomyopathy asssociated 5 (CMYA5) gene with carcass trait and meat quality. Mol Biol Rep. 2011;38:2085–90.

49. Altuwaijri S, Lee DK, Chuang KH, Ting HJ, Yang Z, Xu Q, Tsai MY, Yeh S, Hanchett LA, Chang HC, et al. Androgen receptor regulates expression of skeletal muscle-specific proteins and muscle cell types. Endocrine. 2004;25:27–32.

50. Lim D, Lee SH, Kim NK, Cho YM, Chai HH, Seong HH, Kim H. Gene co-expression analysis to characterize genes related to marbling trait in Hanwoo (Korean) cattle. Asian-Australas J Anim Sci. 2013;26:19–29.

51. Schleinitz D, Kloting N, Bottcher Y, Wolf S, Dietrich K, Tonjes A, Breitfeld J, Enigk B, Halbritter J, Korner A, et al. Genetic and evolutionary analyses of the human bone morphogenetic protein receptor 2 (BMPR2) in the pathophysiology of obesity. PLoS One. 2011;6, e16155.

52. Goodman CA, McNally RM, Hoffmann FM, Hornberger TA. Smad3 induces atrogin-1, inhibits mTOR and protein synthesis, and promotes muscle atrophy in vivo. Mol Endocrinol. 2013;27:1946–57.

53. Tiano JP, Springer DA, Rane SG. SMAD3 negatively regulates serum irisin and skeletal muscle FNDC5 and peroxisome proliferator-activated receptor gamma coactivator 1-alpha (PGC-1alpha) during exercise. J Biol Chem. 2015;290:7671–84.

54. Lin J, Wu H, Tarr PT, Zhang CY, Wu Z, Boss O, Michael LF, Puigserver P, Isotani E, Olson EN, et al. Transcriptional co-activator PGC-1 alpha drives the formation of slow-twitch muscle fibres. Nature. 2002;418:797–801.

55. LeBleu VS, O'Connell JT, Gonzalez Herrera KN, Wikman H, Pantel K, Haigis MC, de Carvalho FM, Damascena A, Domingos Chinen LT, Rocha RM, et al. PGC-1alpha mediates mitochondrial biogenesis and oxidative phosphorylation in cancer cells to promote metastasis. Nat Cell Biol. 2014;16:992–1003. 1001–1015.

56. Ros S, Schulze A. Balancing glycolytic flux: the role of 6-phosphofructo-2-kinase/fructose 2,6-bisphosphatases in cancer metabolism. Cancer Metab. 2013;1:8.

57. Williams AH, Liu N, van Rooij E, Olson EN. MicroRNA control of muscle development and disease. Curr Opin Cell Biol. 2009;21:461–9.

58. Liu J, Liang X, Gan Z. Transcriptional regulatory circuits controlling muscle fiber type switching. Sci China Life Sci. 2015;58:321–7.

59. van Rooij E, Quiat D, Johnson BA, Sutherland LB, Qi X, Richardson JA, Kelm Jr RJ, Olson EN. A family of microRNAs encoded by myosin genes governs myosin expression and muscle performance. Dev Cell. 2009;17:662–73.

60. von Hofsten J, Elworthy S, Gilchrist MJ, Smith JC, Wardle FC, Ingham PW. Prdm1- and Sox6-mediated transcriptional repression specifies muscle fibre type in the zebrafish embryo. EMBO Rep. 2008;9:683–9.

61. Ljubicic V, Burt M, Lunde JA, Jasmin BJ. Resveratrol induces expression of the slow, oxidative phenotype in mdx mouse muscle together with enhanced activity of the SIRT1-PGC-1alpha axis. Am J Physiol Cell Physiol. 2014;307:C66–82.

62. Wu J, Zheng C, Wang X, Yun S, Zhao Y, Liu L, Lu Y, Ye Y, Zhu X, Zhang C, et al. MicroRNA-30 family members regulate calcium/calcineurin signaling in podocytes. J Clin Invest. 2015;125:4091–106.

63. Wang X, Wang K, Han L, Zhang A, Shi Z, Zhang K, Zhang H, Yang S, Pu P, Shen C, et al. PRDM1 is directly targeted by miR-30a-5p and modulates the Wnt/beta-catenin pathway in a Dkk1-dependent manner during glioma growth. Cancer Lett. 2013;331:211–9.

64. Ning X, Liu S, Qiu Y, Li G, Li Y, Li M, Yang G. Expression profiles and biological roles of miR-196a in swine. Genes (Basel). 2016;7:5.

65. Kureel J, Dixit M, Tyagi AM, Mansoori MN, Srivastava K, Raghuvanshi A, Maurya R, Trivedi R, Goel A, Singh D. miR-542-3p suppresses osteoblast cell proliferation and differentiation, targets BMP-7 signaling and inhibits bone formation. Cell Death Dis. 2014;5:e1050.

66. Zheng L, Liu JM, Wang JX, Li MZ, Lian WG, Xie P, Liu SF. Effect of bone morphogenetic protein 7 on differentiation of adipose derived mesenchymal stem cells into brown adipocytes in rats. Zhongguo Yi Xue Ke Xue Yuan Xue Bao. 2014;36:654–9.

67. Townsend KL, An D, Lynes MD, Huang TL, Zhang H, Goodyear LJ, Tseng YH. Increased mitochondrial activity in BMP7-treated brown adipocytes, due to increased CPT1- and CD36-mediated fatty acid uptake. Antioxid Redox Signal. 2013;19:243–57.

68. Wang L, Yuan Y, Li J, Ren H, Cai Q, Chen X, Liang H, Shan H, Fu ZD, Gao X, et al. MicroRNA-1 aggravates cardiac oxidative stress by post-transcriptional modification of the antioxidant network. Cell Stress Chaperones. 2015;20:411–20.

69. Hong JS, Noh SH, Lee JS, Kim JM, Hong KC, Lee YS. Effects of polymorphisms in the porcine microRNA miR-1 locus on muscle fiber type composition and miR-1 expression. Gene. 2012;506:211–6.

70. Wang B, Sun F, Dong N, Sun Z, Diao Y, Zheng C, Sun J, Yang Y, Jiang D. MicroRNA-7 directly targets insulin-like growth factor 1 receptor to inhibit cellular growth and glucose metabolism in gliomas. Diagn Pathol. 2014;9:211.

71. Yu Y, Chai J, Zhang H, Chu W, Liu L, Ma L, Duan H, Li B, Li D. miR-194 promotes burn-induced hyperglycemia via attenuating IGF-IR expression. Shock. 2014;42:578–84.

72. Setyowati Karolina D, Sepramaniam S, Tan HZ, Armugam A, Jeyaseelan K. miR-25 and miR-92a regulate insulin I biosynthesis in rats. RNA Biol. 2013;10:1365–78.

73. Rajpathak SN, Gunter MJ, Wylie-Rosett J, Ho GY, Kaplan RC, Muzumdar R, Rohan TE, Strickler HD. The role of insulin-like growth factor-I and its binding proteins in glucose homeostasis and type 2 diabetes. Diabetes Metab Res Rev. 2009;25:3–12.

74. Clemmons DR. Role of insulin-like growth factor iin maintaining normal glucose homeostasis. Horm Res. 2004;62 Suppl 1:77–82.

75. Pan L, Huang BJ, Ma XE, Wang SY, Feng J, Lv F, Liu Y, Liu Y, Li CM, Liang DD, et al. MiR-25 protects cardiomyocytes against oxidative damage by targeting the mitochondrial calcium uniporter. Int J Mol Sci. 2015;16:5420–33.

76. Wahlquist C, Jeong D, Rojas-Munoz A, Kho C, Lee A, Mitsuyama S, van Mil A, Park WJ, Sluijter JP, Doevendans PA, et al. Inhibition of miR-25 improves cardiac contractility in the failing heart. Nature. 2014;508:531–5.

77. Cheng Z, Tseng Y, White MF. Insulin signaling meets mitochondria in metabolism. Trends Endocrinol Metab. 2010;21:589–98.

78. Stump CS, Short KR, Bigelow ML, Schimke JM, Nair KS. Effect of insulin on human skeletal muscle mitochondrial ATP production, protein synthesis, and mRNA transcripts. Proc Natl Acad Sci U S A. 2003;100:7996–8001.

79. Sultan KR, Dittrich BT, Leisner E, Paul N, Pette D. Fiber type-specific expression of major proteolytic systems in fast- to slow-transforming rabbit muscle. Am J Physiol Cell Physiol. 2001;280:C239–47.

80. Hernandez-Torres F, Aranega AE, Franco D. Identification of regulatory elements directing miR-23a-miR-27a-miR-24-2 transcriptional regulation in response to muscle hypertrophic stimuli. Biochim Biophys Acta. 2014;1839:885–97.

81. Allen DL, Loh AS. Posttranscriptional mechanisms involving microRNA-27a and b contribute to fast-specific and glucocorticoid-mediated myostatin expression in skeletal muscle. Am J Physiol Cell Physiol. 2011;300:C124–37.

82. Annalora AJ, Goodin DB, Hong WX, Zhang Q, Johnson EF, Stout CD. Crystal structure of CYP24A1, a mitochondrial cytochrome P450 involved in vitamin D metabolism. J Mol Biol. 2010;396:441–51.

83. Ricciardi CJ, Bae J, Esposito D, Komarnytsky S, Hu P, Chen J, Zhao L. 1,25-Dihydroxyvitamin D3/vitamin D receptor suppresses brown adipocyte differentiation and mitochondrial respiration. Eur J Nutr. 2015;54:1001–12.

84. Pickova A, Potocky M, Houstek J. Assembly factors of F1FO-ATP synthase across genomes. Proteins. 2005;59:393–402.

85. Yang Z, Lanks CW, Tong L. Molecular mechanism for the regulation of human mitochondrial NAD(P) + −dependent malic enzyme by ATP and fumarate. Structure. 2002;10:951–60.

86. Xu X, Shi YC, Gao W, Mao G, Zhao G, Agrawal S, Chisolm GM, Sui D, Cui MZ. The novel presenilin-1-associated protein is a proapoptotic mitochondrial protein. J Biol Chem. 2002;277:48913–22.

87. Lamarca V, Sanz-Clemente A, Perez-Pe R, Martinez-Lorenzo MJ, Halaihel N, Muniesa P, Carrodeguas JA. Two isoforms of PSAP/MTCH1 share two proapoptotic domains and multiple internal signals for import into the mitochondrial outer membrane. Am J Physiol Cell Physiol. 2007;293:C1347–61.

88. Kerner J, Hoppel C. Fatty acid import into mitochondria. Biochimica et Biophysica Acta (BBA) - Molecular and Cell Biology of Lipids. 2000;1486:1–17.

89. Branco DM, Arduino DM, Esteves AR, Silva DF, Cardoso SM, Oliveira CR. Cross-talk between mitochondria and proteasome in Parkinson's disease pathogenesis. Front Aging Neurosci. 2010;2:17.

90. Ross JM, Olson L, Coppotelli G. Mitochondrial and ubiquitin proteasome system dysfunction in ageing and disease: two sides of the same coin? Int J Mol Sci. 2015;16:19458–76.

91. Duke DC, Moran LB, Kalaitzakis ME, Deprez M, Dexter DT, Pearce RK, Graeber MB. Transcriptome analysis reveals link between proteasomal and mitochondrial pathways in Parkinson's disease. Neurogenetics. 2006;7:139–48.

92. Hong L, Huang HC, Jiang ZF. Relationship between amyloid-beta and the ubiquitin-proteasome system in Alzheimer's disease. Neurol Res. 2014;36:276–82.

93. Shiber A, Ravid T. Chaperoning proteins for destruction: diverse roles of Hsp70 chaperones and their co-chaperones in targeting misfolded proteins to the proteasome. Biomolecules. 2014;4:704–24.

94. Trausch-Azar J, Leone TC, Kelly DP, Schwartz AL. Ubiquitin proteasome-dependent degradation of the transcriptional coactivator PGC-1{alpha} via the N-terminal pathway. J Biol Chem. 2010;285:40192–200.

95. Tucker EJ, Wanschers BF, Szklarczyk R, Mountford HS, Wijeyeratne XW, van den Brand MA, Leenders AM, Rodenburg RJ, Reljic B, Compton AG, et al. Mutations in the UQCC1-interacting protein, UQCC2, cause human complex III deficiency associated with perturbed cytochrome b protein expression. PLoS Genet. 2013;9, e1004034.

96. Huang H, Zhang X, Li S, Liu N, Lian W, McDowell E, Zhou P, Zhao C, Guo H, Zhang C, et al. Physiological levels of ATP negatively regulate proteasome function. Cell Res. 2010;20:1372–85.

Molecular changes in mitochondrial respiratory activity and metabolic enzyme activity in muscle of four pig breeds with distinct metabolic types

Xuan Liu[1], Nares Trakooljul[1], Eduard Muráni[1], Carsten Krischek[2], Karl Schellander[3], Michael Wicke [4†], Klaus Wimmers[1], Siriluck Ponsuksili[1]*

[1] *Leibniz Institute for Farm Animal Biology (FBN), Institute for Genome Biology, D-18196 Dummerstorf, Germany*

[2] *Institute of Food Quality and Food Safety, University of Veterinary Medicine Hannover, D-30173 Hannover, Germany*

[3] *Insititute of Animal Science, Animal Breeding and Husbandry Group, University of Bonn, Bonn, Germany*

[4]*Department of Animal Sciences, Quality of Food of Animal Origin, Georg-August-University Goettingen, Germany*

†Deceased

*Corresponding author:

Siriluck Ponsuksili

Leibniz Institute for Farm Animal Biology

Wilhelm-Stahl-Allee 2

18196 Dummerstorf, Germany

Phone: +49 38208 68700

Fax: +49 38208 68702

Email: s.wimmers@fbn-dummertorf.de
(Manuscript version)

1

Abstract

Skeletal muscles are metabolically active and have market value in meat-producing farm animals. A better understanding of biological pathways affecting energy metabolism in skeletal muscle could advance the science of skeletal muscle. In this study, comparative pathway-focused gene expression profiling in conjunction with muscle fiber typing were analyzed in skeletal muscles from Duroc, Pietrain, and Duroc–Pietrain crossbred pigs. Each breed type displayed a distinct muscle fiber-type composition. Mitochondrial respiratory activity and glycolytic and oxidative enzyme activities were comparable among genotypes, except for significantly lower complex I activity in Pietrain pigs homozygous-positive for malignant hyperthermia syndrome. At the transcriptional level, lactate dehydrogenase B showed breed specificity, with significantly lower expression in Pietrain pigs homozygous-positive for malignant hyperthermia syndrome. A similar mRNA expression pattern was shown for several subunits of oxidative phosphorylation complexes, including complex I, complex II, complex IV, and ATP synthase. Significant correlations were observed between mRNA expression of genes in focused pathways and enzyme activities in a breed-dependent manner. Moreover, expression patterns of pathway-focused genes were well correlated with muscle fiber-type composition. These results stress the importance of regulation of transcriptional rate of genes related to oxidative and glycolytic pathways in the metabolic capacity of muscle fibers. Overall, the results further the breed-specific understanding of the molecular basis of metabolic enzyme activities, which directly impact meat quality.

Keywords: muscle fiber;metabolic enzymes;expression pattern; pig

Introduction

Tenderness and juiciness are important factors of meat quality and are associated with percentage of oxidative and glycolytic muscle fibers in meat-producing animals. Selection for fast-growing breeds not only affects meat quality, but also composition of muscle fiber-type (Karlsson et al. 1994). Duroc and Pietrain are two common commercial pig breeds known for divergent meat quality and muscular energy metabolism. Duroc pigs contain a higher proportion of slow-twitch oxidative (STO) fibers. In comparison, Pietrain pigs are muscular and lean, and their muscles contain more fast-twitch glycolytic (FTG) fibers. Muscle containing a high proportion of STO fibers is often associated with high oxidative

2

enzyme activities (Gueguen et al. 2005); a high ratio of FTG fibers is associated with high glycolytic enzyme activities (Huber et al. 2007; Werner et al. 2010b). Because these factors affect properties of meat, understanding the metabolic properties of skeletal muscle fibers could be key to improvement of meat quality (Hocquette et al. 2001).

Mitochondria play an important role in cellular ATP generation through oxidative phosphorylation. Oxidative capacity of muscle is proportional to mitochondrial volume and density, with higher capacity in slow-twitch fibers and lower in fast-twitch fibers (Picard et al. 2012; Schwerzmann et al. 1989). Beside ATP production mitochondria also influence Ca^{2+} homeostasis by uptake and efflux of Ca^{2+} across the mitochondrial membrane. The latter is important, as the Ca^{2+} in turn has an impact on the mitochondrial ATP production (Griffiths and Rutter 2009). Mutations within ryanodine receptor 1 (*RYR1*), a calcium release channel in the sarcoplasmic reticulum (SR), are frequently detected in Pietrain pigs and result in membrane leakage and increased Ca^{2+} outflow from the SR to the cytoplasm. This leads to increased excitability of the muscle associated with malignant hyperthermia susceptibility (MHS) (Fujii et al. 1991), a calcium regulation disorder characterized by skeletal muscle hypermetabolism. This genetic defect consequently leads to reduced water holding capacity; loss of stress resistance; and pale, soft, and exudative meat (Fujii et al. 1991; Huff-Lonergan and Lonergan 2005; Shen et al. 2007; Yue et al. 2003). Thus, oxidative pathways are influenced as heritable traits, and understanding the genotype-phenotype correlation within these pathways can offer valuable insight for metabolism as well as meat production.

In this study, we analyzed expression profiles of pathway-focused genes related to oxidative and glycolytic pathways in conjunction with muscle fiber typing and metabolic enzyme activities to further understand the molecular basis of muscle properties and functions that affect meat quality. We analyzed and compared four distinct metabolic types of pig breeds: Duroc, Pietrain homozygous-negative for MHS (PiNN), Pietrain homozygous-positive for MHS (PiPP), and an F2 crossbred Duroc–Pietrain homozygous-negative for MHS (DuPi).

Materials and methods

Sample collection and phenotypic measurement

3

The experiment and muscle biopsy collection were approved and authorized by the German and European animal welfare regulations for animal husbandry, transport, and slaughter (Krischek et al. 2011; Werner et al. 2010a; Werner et al. 2010b). All experimental procedures, including animal care and tissue sample collection, followed guidelines for safeguarding and good scientific practice in accordance with the German Law of Animal Protection, officially authorized by the Animal Care Committee and authorities [Niedersächsischen Landesamt für Verbraucherschutz und Lebensmittelsicherheit (LAVES) 33.42502/01-47.05].

As previously described (Krischek et al. 2011; Werner et al. 2010a; Werner et al. 2010b), Duroc, PiNN, PiPP, and DuPi pigs from a resource population of the University of Bonn were raised until 180 days of age. Muscle biopsies of each breed (Duroc, n = 12; DuPi, n = 12; PiNN, n = 10; PiPP, n = 12) were collected 24 h before slaughter from the longissimus muscle between 13th and 14th thoracic vertebrae for quantitative real-time PCR (qPCR) and muscle-related phenotyping. Muscle samples were frozen in liquid nitrogen and stored at – 80 °C until analysis. Measurements of muscle fiber-type composition, mitochondrial respiratory activity, glycolytic and oxidative enzyme activities and concentrations of ATP, ADP and and AMP were performed as described previously (Krischek et al. 2011; Werner et al. 2010a; Werner et al. 2010b). Definitions and brief descriptions of applied methods for all phenotypic traits are provided in Online Resource 1.

Total RNA isolation

Total RNA was isolated from longissimus muscle biopsies using Tri-reagent and RNeasy Minikit (Qiagen) with an on-column DNase treatment according to the manufacturer's protocol. RNA integrity was assessed by 1% agarose gel electrophoresis. RNA concentration was measured on a NanoDrop ND-1000 spectrophotometer (Peqlab).

Quantitative real-time PCR (qPCR)

qPCR of all RNA samples (n = 46) was performed using fast gene expression analysis with EvaGreen dye on a BioMark HD real-time PCR system according to manufacturer's recommendations (Fluidigm). All reagents were purchased from Fluidigm unless otherwise indicated. Briefly, cDNA was synthesized from 2 µg of total RNA using Superscript II reverse transcriptase and oligo-dT (Invitrogen) with specific target amplification and exonuclease I (New England Biolabs) treatment. qPCR reactions were performed using a

4

48x48 dynamic array and integrated fluidic circuit. For each sample inlet, 2.5 µL of 2×SsoFast EvaGreen supermix with low ROX (Biorad), 0.25 µL of 20×DNA-binding dye sample loading reagent, and 2.25 µL of specific target amplification and exonuclease-I-treated sample were loaded. For each assay inlet, 2.5 µL of 2×assay loading reagent, 2.25 µL of 1×DNA suspension buffer, and 0.25 µL of 100 µM mixed (forward and reverse) primers were loaded. All measurements were performed in duplicate. Thermal parameters were: 95 ^{o}C for 60 s, followed by 30 cycles of 95 ^{o}C for 5 s and 60 ^{o}C for 20 s. Assays were performed for genes encoding glycolytic enzymes including muscle-specific glycogen phosphorylase (*PYGM*) and phosphofructokinase (*PFKM*) and four subunits of lactate dehydrogenase (*LDH*): *LDHA, LDHB, LDHC*, and *LDHD*. Oxidative pathway components including *CS*, 35 complex I subunits (Online Resource 2), four subunits of complex II (*SDHA, SDHB, SDHC*, and *SDHD*), nine subunits of complex IV (*COX10, COX15, COX17, COX5B, COX6A1, COX6C, COX7A1, COX7A2,* and *COX7C*), and six ATP synthase subunits (*ATP5B, ATP5G1, ATP5G2, ATP5J2, ATP5L,* and *ATP7A*) were also addressed. Primer sequence information is accessible in Online Resource 2. Reference genes *ACTB, RPL32*, and *RPS11* were used to normalize expression values.

Statistical analysis

Data were analyzed using SAS 9.3 statistical software (SAS Institute) and the GLM procedure. The statistical model included effects of breed, gender, and breed–gender interaction. Post hoc Tukey–Kramer method was used for multiple comparison adjustments. Results were reported as least-squares means (Lsmeans) with standard error (SE) and considered to be statistically significant if $p < 0.05$. Data were plotted using GraphPad Prism 5. Correlation coefficient (r) between gene expression and phenotypic measurement was calculated separately for each breed and in combination of all breeds together.

Results

Muscle phenotyping and breed differences

To illuminate breed differences in muscle metabolic and functional capacities and properties, fiber-type compositions were compared among the four breeds. Duroc pigs had the highest percentage of STO fibers, with the most contrast between Duroc (13.91%) and

5

PiPP (6.48%) breeds (Online Resource 3). However, the percentage of fast-twitch oxidative (FTO) fibers was significantly lower in Duroc (8.81%) than other breeds, especially in comparison to PiNN pigs (15.11%; $p = 0.011$). Interestingly, PiPP pigs had a significantly higher percentage of FTG fibers (81.57%) compared with PiNN counterparts (74.95%; $p = 0.035$), while that of Duroc and DuPi were in between these two Pietrain genotypes.

All mitochondrial respiratory activities measured were comparable across all four genotypes, with a tendency for lower state 3 and state 4 respiration in PiNN and lower respiratory control index in DuPi pigs (Online Resource 3). No significant differences among breeds were detected for glycolytic enzyme activity of glycogen phosphorylase (GP), phosphofructokinase (PFK), or lactate dehydrogenase (LDH). Complex I activity was significantly lower in PiPP (5.07%) compared to Duroc (9.79%; $p = 0.009$) and PiNN (9.26%; $p = 0.037$) pigs. However, other oxidative enzyme activities, including citrate synthase (CS), complex II, and complex IV, were not significantly different among breeds. For adenine nucleotide concentration, AMP was significantly lower in PiPP than Duroc ($p < 0.01$) and DuPi ($p < 0.05$), but not PiNN, pigs. In addition, ADP concentration was significantly lower in DuPi compared to Duroc and PiPP pigs ($p < 0.01$).

Expression profiling of pathway-focused genes

To further examine breed differences in muscle at a molecular level, pathway-focused gene expression profiling was performed using qPCR. Our pathway-focused panel included nuclear-encoded genes involved in both glycolytic and oxidative pathways. In addition, expression of genes encoding 10 V-ATPase lysosomal subunits were measured to analyze lysosomal-related energy metabolism. Out of 71 genes investigated, 48 genes showed significant differences among breeds ($p < 0.05$). One gene showed a significant effect of gender, and seven genes demonstrated a significant interaction effect of breed and gender (Online Resource 4).

Differential genes in the glycolytic pathway

For the glycolytic pathway, no differential expression was detected among breeds for *PYGM* and *PFKM* (Fig. 1). Likewise, there was no difference among breeds for mRNA levels of *LDHA* and *LDHC*. However, transcription of *LDHB* was significantly lower in

6

PiPP than Duroc ($p < 0.05$) and DuPi ($p < 0.01$) pigs. In addition, mRNA level of *LDHD* was lower in PiPP than PiNN pigs ($p < 0.05$) (Fig. 1).

Differential genes in the oxidative pathway

Assessment of 35 nuclear genes encoding for subunits of mitochondrial complex I showed that 24 genes were significantly different for at least one pairwise comparison of relative mRNA expression for each gene and pig breed (Table 1). Overall, PiPP pigs demonstrated the most differentially expressed genes in complex I. PiPP pigs differentially expressed 8, 10, and 13 genes compared to Duroc, DuPi, and PiNN pigs, respectively. All differentially expressed genes except *NDUFA12* were down-regulated in PiPP. Similar patterns of downregulation were observed in PiPP compared to other genotypes for most subunits of complex II (*SDHA, SDHC,* and *SDHD*) and complex IV (*COX1, COX5B, COX6C, COX 7A1,* and *COX7A2*) (Fig. 2) and all subunits of ATP synthase (Fig. 3). *CS* showed no breed difference.

Correlation between gene expression and enzyme activity

We further performed correlation analyses between gene transcript level and enzyme activity to identify genes that may influence the pathways. Correlation analyses were calculated for each breed separately as well as for all breeds combined. Overall, most significant correlations were breed-dependent. For example, only PiNN exhibited high correlation for complex I subunits with *NDUFA2, NDURFA11, NDUFA12, NDUFA13, and NDUFB8* (Table 2). Alternatively, Duroc pigs had high correlation between complex IV mRNA levels and enzyme activity for *COX5B* (r = 0.66; $p = 0.021$) and *COX7A1* (r = 0.59; $p = 0.041$). DuPi pigs had high correlations for complex II subunit with *SDHC* (r = 0.65; $p = 0.031$) and complex IV subunits with *COX10* (r = 0.58; $p = 0.047$), *COX6C* (r = 0.65; $p = 0.023$), and *COX7A2* (r = 0.79; $p = 0.002$). PiPP pigs had significant correlations for complex I subunit *NDUFS5* (r = –0.69; $p = 0.029$) and complex IV subunit *COX7A1* (r = –0.6; $p = 0.049$). When all breed data were combined, most genes were still significantly correlated with enzyme activity. Eleven genes were significantly correlated with complex I activity. *NDUFA4L2* (r = 0.45; $p = 0.003$), *NDUFA9* (r = 0.45; $p = 0.003$), and *NDUFA13* (r = 0.45; $p = 0.003$) encoded for subunit A of complex I were the top three significant genes that correlated with complex I activity. Four genes were significantly correlated

7

with complex IV activity, with *COX7A2* (r = 0.63; *p* < 0.0001) showing the highest significance (Table 2).

Correlation between gene expression and fiber-type

Since each breed showed a distinct fiber-type composition, we performed correlation analyses between gene expression and muscle fiber-type for each breed separately (Table 3). In Duroc pigs, percentage of STO muscle fiber significantly correlated with expression of several genes of oxidative phosphorylation complexes, including 10 subunits of complex I, two subunits of complex II, one subunit of complex IV, and one subunit of ATP synthase. In DuPi pigs, significant correlations were observed between FTO muscle fiber and genes coding for four subunits of complex I and one subunit of complex II. For PiNN pigs, a negative correlation was detected between FTG fiber composition and ATP synthase as well as V-ATPase.

Discussion

In this study, we compared mitochondrial respiratory activity, metabolic enzyme activity, muscle fiber-type component, and expression of pathway-focused genes of four metabolically distinct pig breeds differing in muscularity, and muscle structure. The lean-type Pietrain breed is known for muscularity, muscle fiber density, and a higher proportion of glycolytic muscle fibers, while Duroc pigs are less muscular, and have a higher proportion of slow-twitch muscle fibers. This study also included a crossbred F_2 Duroc–Pietrain breed. Although a single nucleotide mutation within *RYR1* causes an abnormality of cellular calcium homeostasis, resulting in pale, soft, and exudative meat as well as MHS (Fujii et al. 1991; Shen et al. 2007), the MHS homozygous genotype is still retained in pork production because of its advantageous carcass yield and lean percentage, which is associated with higher FTG fiber ratios (Werner et al. 2010a). Therefore, we investigated both MHS homozygous-positive (PiPP) and MHS homozygous-negative (PiNN) Pietrain pigs to better distinguish possible associated effects of *RYR1*.

Downregulation of LDHB in PiPP pigs

LDH catalyzes interconversion of pyruvate to lactate as well as interconversion of NADH to NAD$^+$. LDH is a tetramer of four subunits. The two common subunits, M and H, are encoded by *LDHA* and *LDHB*, respectively. LDHC is a testis-specific protein, while

8

LDHD can metabolize D-lactate (de Bari et al. 2013). Lactate is an intermediate in numerous metabolic processes and provides fuel for aerobic metabolism rather than a dead-end waste product of glycolysis due to hypoxia (Gladden 2004). Evidence has shown that reduced LDHA activity stimulates mitochondrial respiration, suggesting a link between glycolysis and mitochondrial physiology (Fantin et al. 2006). However, our results showed no breed-specific differences in *LDHA* transcript levels, consistent with comparable LDH activities measured among the four breeds. Interestingly, our results indicated downregulation of *LDHB* in PiPP pigs, which also had the least percentage of STO muscle fibers. *LDHB* encodes LDH subunit H, which oxidizes lactate back to pyruvate and thus can generate mitochondrial energy via aerobic metabolism in the TCA cycle (Gabriel-Costa et al. 2015). Different LDH isoforms have been associated with different muscle fiber-types. LDH1 isoenzyme, consisting of four H-subunits, is predominantly distributed in type I STO fibers; LDH5, containing four M-subunits, is distributed mainly in type IIA and IIB fibers in rabbit and guinea pig skeletal muscles (Leberer and Pette 1984; Peter et al. 1971). Therefore, LDH may function as a key mediator of lactate oxidation via its H subunit and this process seems to be reduced in pigs with low STO fiber percentages like the PiPP.

OXPHOS complexes in PiPP pigs

Complex I, complex II, complex IV, and ATP synthase are major components of oxidative phosphorylation (OXPHOS). They locate in mitochondrial inner membranes and generate ATP via OXPHOS. Each complex consists of different subunits that are assembled into a functional complex. We examined all nuclear-encoded genes of subunits for the OXPHOS pathway by qPCR and found that PiPP pigs transcriptionally downregulated complex I, complex II, complex IV, and ATP synthase for most subunits compared to PiNN, Duroc, and DuPi pigs.

PiPP pigs are positive for the *RYR1* point mutation (Fujii et al. 1991). Defective RYR1 leads to increased release of Ca^{2+} from the SR to the cytoplasm. In normal conditions, accumulation of Ca^{2+} in cytoplasm initiates muscle contraction. Ca^{2+} then must be pumped back to the SR by SR Ca^{2+} ATPase (SERCA) to initiate muscle relaxation (Fill and Copello 2002; Lanner et al. 2010). In PiPP pigs, abnormally elevated Ca^{2+} levels in cytoplasm cause excess muscle contraction and high energy consumption, leading to a faster shift of energy generation from aerobic to anaerobic glycolysis and resulting in

9

acidosis (Werner et al. 2005). The Ca^{2+} homeostasis abnormality can also influence mitochondrial Ca^{2+} concentrations, as the mitochondrial membranes contain different calcium in- and efflux systems. Since Ca^{2+} plays a pivotal role in the mitochondria of muscle cells, the elevated Ca^{2+} concentrations can affect the mitochondrial function and probably the meat quality like in the PiPP pigs. This assumption is supported by a study in MHS knock-in mice that showed a clear Ca^{2+} overload in the mitochondrial matrix and a switch to a compromised bioenergetic state characterized by low OXPHOS under a non-triggered state (Giulivi et al. 2011). Extreme conditions, such as Ca^{2+} concentrations >100 µM, could dephosphorylate complex IV and decrease affinity for cytochrome C through a cAMP-dependent tyrosine phosphorylation site in liver complex IV subunit I (Gellerich et al. 2010). Moreover, our results indicate that muscle of PiPP pigs contains a high percentage of FTG fibers, which have characteristic low capillarisation and inefficient oxygen delivery and yet are accompanied by downregulated OXPHOS.

Significantly higher AMP concentrations, such as in Duroc pigs, and the AMP:ATP ratio activate AMP-activated protein kinase (AMPK) via allosteric AMP binding. AMPK binds to and activates PGC-1α by direct phosphorylation to control OXPHOS (Jager et al. 2007; O'Neill et al. 2013). Knockout of both β1 and β2 isoforms of AMPK in transgenic mice reduces mitochondrial biogenesis, revealing the essential role of AMPK in maintaining mitochondrial capacity (O'Neill et al. 2011). This is in line with a reduced AMP:ATP ratio and transcriptional downregulation of OXPHOS-related enzymes, including complex I, complex II, complex IV, and ATP synthase, in PiPP pigs. Further, it is reinforced by higher glycogen levels in FTG fibers (Fernandez et al. 1995) and repressed activation of AMPK in the presence of high levels of muscle glycogen (Wojtaszewski et al. 2002; Wojtaszewski et al. 2003). Gene expression of v-ATPase subunits was included in this study because the v-ATPase-regulator complex acts as a switch between anabolic and catabolic metabolism depending on the status of nutrient supply (Zhang et al. 2014). However, no breed difference was observed for the v-ATPase complex.

Breed-specific OXPHOS complexes

Our results show that most significant correlations between mRNA level and enzyme activity was breed-dependent, such as complex IV in Duroc, complex II and IV in DuPi, complex I in PiNN, and complex I and IV in PiPP. Complex gene regulations at posttranscriptional and posttranslational levels in association with different genetic

10

backgrounds may roughly explain the results. Other evidence has shown that LRPPRC can influence complex IV and ATP synthase as well as ATP production by affecting RNA stability (Cannino et al. 2007; Mili and Pinol-Roma 2003; Mourier et al. 2014). This should be investigated in our further study.

Since oxidative phosphorylation occurrs in mitochondria, the nuclear-encoded OXPHOS complex subunits need to be processed, imported into mitochondria and then together with mitochondrial-encoded subunits to form a fully assembled functional OXPHOS system in the mitochondrial inner membrane via chaperones, translocases and mitochondrial inner membrane proteins (Bonnefoy et al. 2009; Neupert and Herrmann 2007; Smits et al. 2010; Voos and Rottgers 2002). The most advanced proposed OXPHOS system organization is the 'plasticity model', which is the coexisting of single complexes and supercomplexes (Acín-Pérez et al. 2008; Schon and Dencher 2009). There are several favorable combinations of supercomplexes which are the combination of complex I and III, the combination of complex III and IV, the combination of complex I, III and IV and the ATP synthase is present as a single complex (Dudkina et al. 2014). Events such as importation of molecules into mitochondria and OXPHOS complex assemblization could also contribute to the disparity between mRNA levels and enzyme activity for OXPHOS complex. Therefore, within the pig breeds, the OXPHOS system is differently regulated and optimized to meet appropriate energy requirements via fine-turning various genetic controls. Further investigations are under progress to clarify this assumption.

OXPHOS complexes are linked to oxidative capacity of muscle fibers

We show a positive correlation between STO fibers and gene expression of OXPHOS complex subunits, which play an essential role in mitochondrial respiration, especially in Duroc pigs. The strong association between gene expression of OXPHOS complexes and STO fibers may be explained by the high percentage of STO fibers in Duroc pigs compared to other breeds. Interestingly, DuPi pigs, which are a crossbreed of Duroc and Pietrain, also showed significant correlation between OXPHOS expression and FTO fibers, which are intermediate between STO and FTG fibers. This suggests that muscle fiber-type composition, which is unique for muscle types and breeds, may play a determinant role for oxidative capacity of OXPHOS complexes.

11

OXPHOS complexes I-IV are also known as electron transport chains and are embedded within inner mitochondrial membranes. The complexes are important to muscle fidelity, because mitochondrial electron transport chain disorders can cause muscle abnormalities (Enns et al. 2005). It has been reported that type IIB fibers have unique properties compared to type I and IIA fibers, which involve complex I and complex II substrates (Anderson and Neufer 2006). Moreover, transcription factor PGC-1α may provide a link between muscle fiber-type and energy production because it can drive formation of slow-twitch muscle fibers in cultured muscle cells and also activate expression of nuclear respiratory factors, which influence transcription of OXPHOS complexes (Arany et al. 2007; Kang and Li Ji 2012; Lin et al. 2002; Wu et al. 1999). In addition, expression of NADH dehydrogenase subunit 1 and ATPase subunit 6 is associated with oxidative fiber and fat content (Kim et al. 2008).

Conclusion

Our study revealed differential gene expression of both glycolytic and oxidative enzymes in skeletal muscle of Duroc, PiPP, PiNN, and DuPi pigs. LDH subunits showed differential expression patterns across pig breeds. Significantly, PiPP pigs exhibited the lowest *LDHB* and *LDHD* expression, supporting a role for LDH in aerobic respiration rather than as a dead-end waste product of glycolysis due to hypoxia. Many subunits of OXPHOS complexes displayed significantly different expression between PiPP pigs and the three other breeds. Within different pig breeds, OXPHOS was regulated and optimized to meet different energy requirements via fine-turning breed-specific genetic differences. This study also linked the OXPHOS system to different types of muscle fibers. For example, Duroc pigs had the strongest association between OXPHOS complex expression and STO muscle fibers, whereas DuPi pigs had significant correlation between OXPHOS complex expression and FTO fibers. These results highlight the importance of the OXPHOS system in oxidative capacity of muscle fibers. Our results provide valuable breed-specific information for the molecular basis of metabolic enzyme activities, which directly impact meat quality.

12

in a project initiated and led by Prof. Dr. Michael Wicke (Department of Animal Science, Quality of Food of Animal Origin, Georg-August-University Goettingen) who has left us forever.

Competing interests

The authors declare that they have no competing interests.

Reference

Acín-Pérez R, Fernández-Silva P, Peleato ML, Pérez-Martos A, Enriquez JA (2008) Respiratory active mitochondrial supercomplexes Molecular cell 32:529-539

Anderson EJ, Neufer PD (2006) Type II skeletal myofibers possess unique properties that potentiate mitochondrial H(2)O(2) generation American journal of physiology Cell physiology 290:C844-851

Arany Z et al. (2007) The transcriptional coactivator PGC-1beta drives the formation of oxidative type IIX fibers in skeletal muscle Cell Metab 5:35-46

Bonnefoy N, Fiumera HL, Dujardin G, Fox TD (2009) Roles of Oxa1-related inner-membrane translocases in assembly of respiratory chain complexes Biochim Biophys Acta 1793:60-70

Cannino G, Di Liegro CM, Rinaldi AM (2007) Nuclear-mitochondrial interaction Mitochondrion 7:359-366

de Bari L, Moro L, Passarella S (2013) Prostate cancer cells metabolize d-lactate inside mitochondria via a D-lactate dehydrogenase which is more active and highly expressed than in normal cells FEBS Lett 587:467-473

Dudkina N, Boekema E, Braun H-P (2014) Respiratory Chain Supercomplexes in Mitochondria. In: Hohmann-Marriott MF (ed) The Structural Basis of Biological Energy Generation. Springer Netherlands, pp 217-229

Enns GM et al. (2005) Relationship of primary mitochondrial respiratory chain dysfunction to fiber type abnormalities in skeletal muscle Clinical genetics 68:337-348

Fantin VR, St-Pierre J, Leder P (2006) Attenuation of LDH-A expression uncovers a link between glycolysis, mitochondrial physiology, and tumor maintenance Cancer Cell 9:425-434

Fernandez X, Lefaucheur L, Candek M (1995) Comparative study of two classifications of muscle fibres: Consequences for the photometric determination of glycogen according to fibre type in red and white muscle of the pig Meat Sci 41:225-235

Fill M, Copello JA (2002) Ryanodine receptor calcium release channels Physiological reviews 82:893-922

Fujii J et al. (1991) Identification of a mutation in porcine ryanodine receptor associated with malignant hyperthermia Science 253:448-451

Gabriel-Costa D et al. (2015) Lactate up-regulates the expression of lactate oxidation complex-related genes in left ventricular cardiac tissue of rats PLoS One 10:e0127843

Gellerich FN et al. (2010) The regulation of OXPHOS by extramitochondrial calcium Biochim Biophys Acta 1797:1018-1027

Giulivi C et al. (2011) Basal bioenergetic abnormalities in skeletal muscle from ryanodine receptor malignant hyperthermia-susceptible R163C knock-in mice J Biol Chem 286:99-113

Gladden LB (2004) Lactate metabolism: a new paradigm for the third millennium J Physiol 558:5-30

Griffiths EJ, Rutter GA (2009) Mitochondrial calcium as a key regulator of mitochondrial ATP production in mammalian cells Biochim Biophys Acta 1787:1324-1333

Gueguen N, Lefaucheur L, Fillaut M, Vincent A, Herpin P (2005) Control of skeletal muscle mitochondria respiration by adenine nucleotides: differential effect of ADP and ATP according to muscle contractile type in pigs Comp Biochem Physiol B Biochem Mol Biol 140:287-297

Hocquette JF, Ortigues-Marty I, Vermorel M (2001) Manipulation of tissue energy metabolism in meat-producing ruminants Asian Australas J Anim Sci 14:720-732

Huber K, Petzold J, Rehfeldt C, Ender K, Fiedler I (2007) Muscle energy metabolism: structural and functional features in different types of porcine striated muscles J Muscle Res Cell Motil 28:249-258

Huff-Lonergan E, Lonergan SM (2005) Mechanisms of water-holding capacity of meat: The role of postmortem biochemical and structural changes Meat Sci 71:194-204

13

Jager S, Handschin C, St-Pierre J, Spiegelman BM (2007) AMP-activated protein kinase (AMPK) action in skeletal muscle via direct phosphorylation of PGC-1alpha Proc Natl Acad Sci U S A 104:12017-12022

Kang C, Li Ji L (2012) Role of PGC-1alpha signaling in skeletal muscle health and disease Ann N Y Acad Sci 1271:110-117

Karlsson A, Essen-Gustavsson B, Lundstrom K (1994) Muscle glycogen depletion pattern in halothane-gene-free pigs at slaughter and its relation to meat quality Meat Sci 38:91-101

Kim NK et al. (2008) Comparisons of longissimus muscle metabolic enzymes and muscle fiber types in Korean and western pig breeds Meat Sci 78:455-460

Krischek C, Natter R, Wigger R, Wicke M (2011) Adenine nucleotide concentrations and glycolytic enzyme activities in longissimus muscle samples of different pig genotypes collected before and after slaughter Meat Sci 89:217-220

Lanner JT, Georgiou DK, Joshi AD, Hamilton SL (2010) Ryanodine receptors: structure, expression, molecular details, and function in calcium release Cold Spring Harb Perspect Biol 2:a003996

Leberer E, Pette D (1984) Lactate dehydrogenase isozymes in type I, IIA and IIB fibres of rabbit skeletal muscles Histochemistry 80:295-298

Lin J et al. (2002) Transcriptional co-activator PGC-1 alpha drives the formation of slow-twitch muscle fibres Nature 418:797-801 doi:10.1038/nature00904

Mili S, Pinol-Roma S (2003) LRP130, a pentatricopeptide motif protein with a noncanonical RNA-binding domain, is bound in vivo to mitochondrial and nuclear RNAs Mol Cell Biol 23:4972-4982

Mourier A, Ruzzenente B, Brandt T, Kuhlbrandt W, Larsson NG (2014) Loss of LRPPRC causes ATP synthase deficiency Hum Mol Genet 23:2580-2592

Neupert W, Herrmann JM (2007) Translocation of proteins into mitochondria Annu Rev Biochem 76:723-749

O'Neill HM, Holloway GP, Steinberg GR (2013) AMPK regulation of fatty acid metabolism and mitochondrial biogenesis: implications for obesity Mol Cell Endocrinol 366:135-151

O'Neill HM et al. (2011) AMP-activated protein kinase (AMPK) beta1beta2 muscle null mice reveal an essential role for AMPK in maintaining mitochondrial content and glucose uptake during exercise Proc Natl Acad Sci U S A 108:16092-16097

Peter J, Sawaki S, Barnard R, Edgerton V, Gillespie C (1971) Lactate dehydrogenase isoenzymes: distribution in fast-twitch red, fast-twitch white, and slow-twitch intermediate fibers of guinea pig skeletal muscle Arch Biochem Biophys 144:304-307

Picard M, Hepple RT, Burelle Y (2012) Mitochondrial functional specialization in glycolytic and oxidative muscle fibers: tailoring the organelle for optimal function American journal of physiology Cell physiology 302:C629-641

Schon EA, Dencher NA (2009) Heavy breathing: energy conversion by mitochondrial respiratory supercomplexes Cell Metab 9:1-3

Schwerzmann K, Hoppeler H, Kayar SR, Weibel ER (1989) Oxidative capacity of muscle and mitochondria: correlation of physiological, biochemical, and morphometric characteristics Proc Natl Acad Sci U S A 86:1583-1587

Shen Q, Underwood K, Means W, McCormick R, Du M (2007) The halothane gene, energy metabolism, adenosine monophosphate-activated protein kinase, and glycolysis in postmortem pig longissimus dorsi muscle J Anim Sci 85:1054-1061

Smits P, Smeitink J, van den Heuvel L (2010) Mitochondrial Translation and Beyond: Processes Implicated in Combined Oxidative Phosphorylation Deficiencies J Biomed Biotechnol 2010:737385

Voos W, Rottgers K (2002) Molecular chaperones as essential mediators of mitochondrial biogenesis Biochim Biophys Acta 1592:51-62

Werner C, Natter R, Schellander K, Wicke M (2010a) Mitochondrial respiratory activity in porcine longissimus muscle fibers of different pig genetics in relation to their meat quality Meat Sci 85:127-133

Werner C, Natter R, Wicke M (2010b) Changes of the activities of glycolytic and oxidative enzymes before and after slaughter in the longissimus muscle of Pietrain and Duroc pigs and a Duroc-Pietrain crossbreed J Anim Sci 88:4016-4025

Werner C, Opalka JR, Gellerich FN, Wicke M (2005) The influence of mitochondrial function on meat quality in turkey and swine Arch Tierz Dummenstorf 48:106-111

Wojtaszewski JF, Jorgensen SB, Hellsten Y, Hardie DG, Richter EA (2002) Glycogen-dependent effects of 5-aminoimidazole-4-carboxamide (AICA)-riboside on AMP-activated protein kinase and glycogen synthase activities in rat skeletal muscle Diabetes 51:284-292

Wojtaszewski JF et al. (2003) Regulation of 5'AMP-activated protein kinase activity and substrate utilization in exercising human skeletal muscle Am J Physiol Endocrinol Metab 284:E813-822

14

Wu Z et al. (1999) Mechanisms Controlling Mitochondrial Biogenesis and Respiration through the Thermogenic Coactivator PGC-1 Cell 98:115-124

Yue G et al. (2003) Linkage and QTL mapping for Sus scrofa chromosome 6 J Anim Breed Genet 120:45-55

Zhang CS et al. (2014) The lysosomal v-ATPase-Ragulator complex is a common activator for AMPK and mTORC1, acting as a switch between catabolism and anabolism Cell Metab 20:526-540

Figure legends
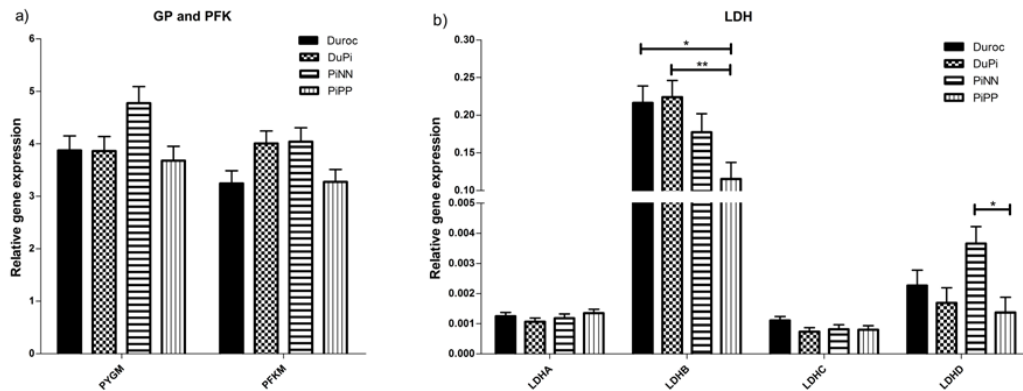
Fig. 1 Relative mRNA expression of a) muscle glycogen phosphorylase (*PYGM*), phosphofructokinase (*PFKM*), and b) lactate dehydrogenase (*LDH*) isoforms (*LDHA, LDHB, LDHC*, and *LDHD*) in longissimus muscles of Duroc, DuPi, PiNN, and PiPP pig breeds was determined using quantitative real time PCR (qPCR). Relative gene expression was normalized to reference genes *ACTB*, *RPL32*, and *RPS11* using 2^ (-ΔCt). Each column represents the least square means with standard error represented by bars. *$p < 0.05$; **$p < 0.01$

15
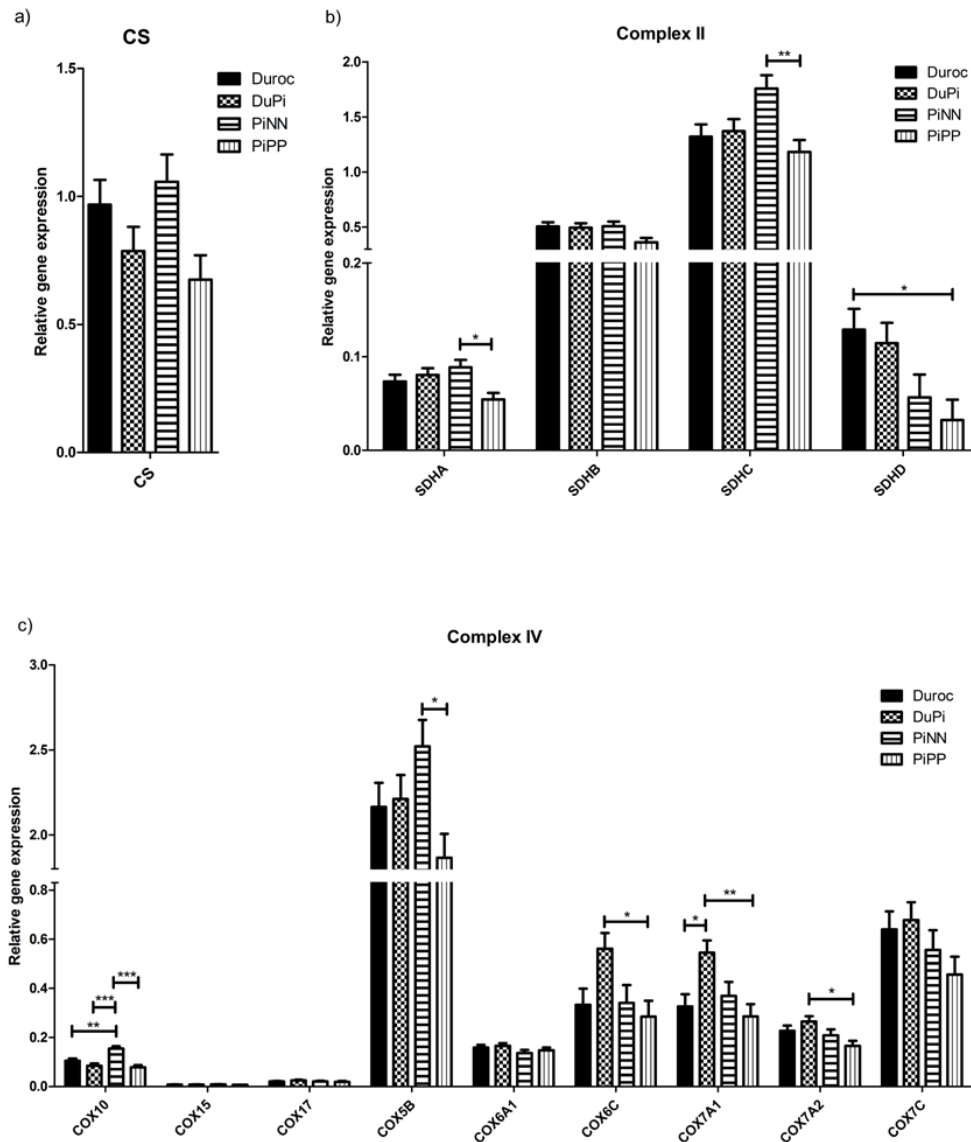
Fig. 2 Relative mRNA expression of a) citrate synthase (*CS*), b) complex II (SDH) isoforms (*SHDA, SDHB, SDHC*, and *SDHD*), and c) complex IV isoforms (*COX10, COX15, COX17, COX5B, COX6A1, COX6C, COX7A1, COX7A2*, and *COX7C*) in longissimus muscles of Duroc, DuPi, PiNN, and PiPP pig breeds was determined using quantitative real time PCR (qPCR). Relative gene expression was normalized to reference genes *ACTB, RPL32*, and *RPS11* using $2^{\wedge}$ (-ΔCt). Each column represents the least square means with standard error represented by bars. *$p < 0.05$; **$p < 0.01$; ***$p < 0.001$

16
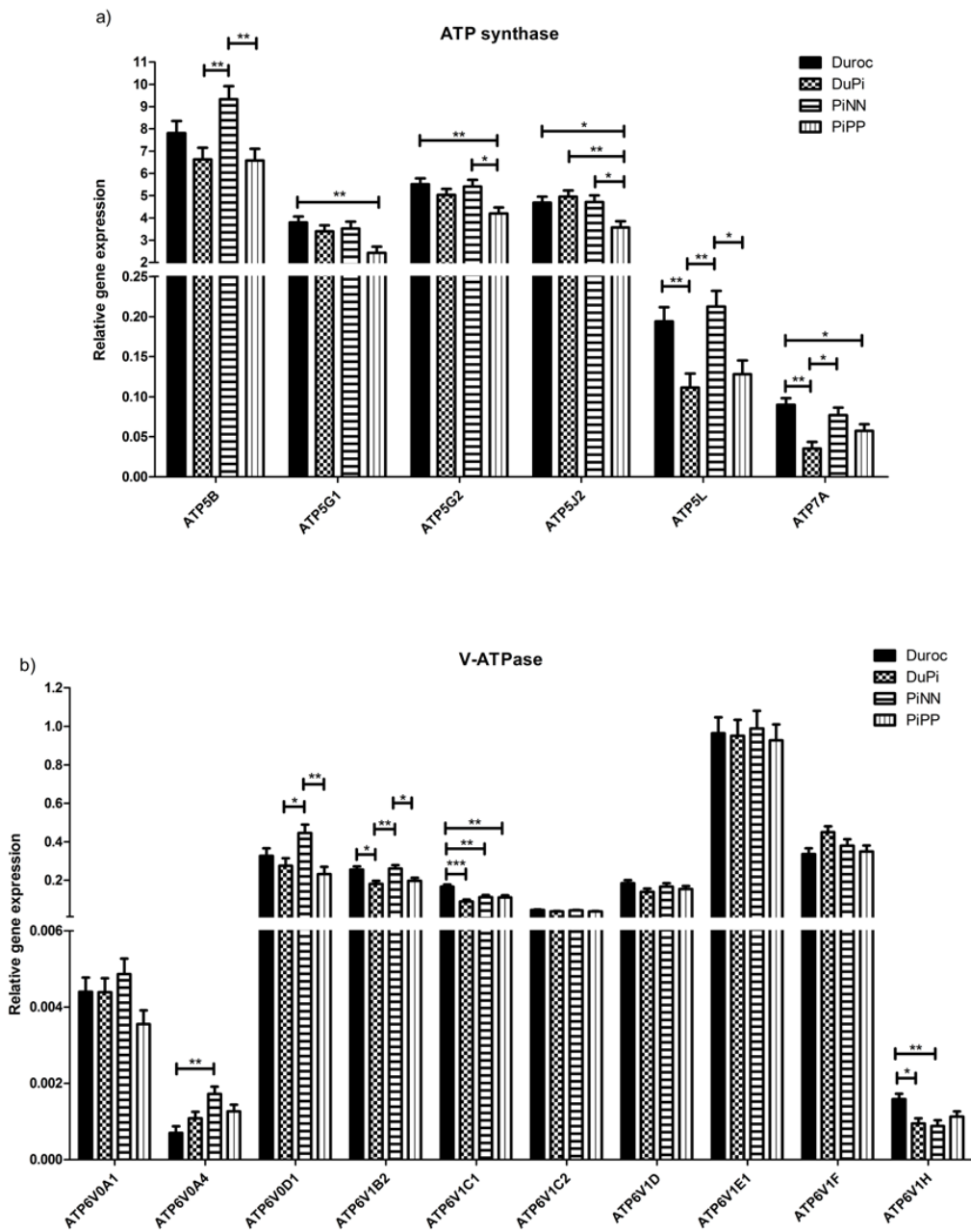
Fig. 3 Relative mRNA expression of a) ATP synthase isoforms (*ATP5B, ATP5G1, ATP5G2, ATP5J2, ATP5L,* and *ATP7A*) and b) V-ATPase isoforms (*ATP6V0A1, ATP6V0A4, ATP6V0D1, ATP6V1B2, ATP6V1C1, ATP6V1C2, ATP6V1D, ATP6V1E1, ATP6V1F,* and *ATP6V1H*) in longissimus muscles of Duroc, DuPi, PiNN, and PiPP pig breeds was determined using quantitative real time PCR (qPCR). Relative gene expression was normalized to reference genes *ACTB, RPL32,* and *RPS11* using 2^ (-ΔCt). Each column represents the least square means with standard error represented by bars. *$p <$ 0.05; **$p <$ 0.01; ***$p <$ 0.001

17

Table 1 Relative gene expression of complex I in Duroc, DuPi, PiNN, and PiPP pig breeds

Gene	Duroc (n=12) Lsmean$_{SE}$	DuPi (n=12) Lsmean$_{SE}$	PiNN (n=10) Lsmean$_{SE}$	PiPP (n=12) Lsmean$_{SE}$	*p*					
					Duroc –DuPi	Duroc –PiNN	Duroc –PiPP	DuPi– PiNN	DuPi– PiPP	PiNN– PiPP
NDUFA1	$0.013_{0.023}$	$0.107_{0.022}$	$0.011_{0.025}$	$0.068_{0.022}$	**0.027**	1	0.322	**0.032**	0.613	0.331
NDUFA2	$1.401_{0.081}$	$1.432_{0.08}$	$1.643_{0.089}$	$1.258_{0.08}$	0.993	0.202	0.594	0.307	0.421	**0.013**
NDUFA3	$0.032_{0.002}$	$0.036_{0.002}$	$0.041_{0.003}$	$0.026_{0.002}$	0.532	0.051	0.382	0.503	**0.024**	**0.001**
NDUFA4	$2.174_{0.128}$	$1.97_{0.126}$	$2.284_{0.141}$	$1.363_{0.126}$	0.669	0.939	**3E-04**	0.359	**0.008**	**1E-04**
NDUFA4L2	$0.048_{0.003}$	$0.044_{0.003}$	$0.042_{0.003}$	$0.033_{0.003}$	0.792	0.55	**0.004**	0.967	**0.045**	0.166
NDUFA5	$0.077_{0.007}$	$0.045_{0.007}$	$0.042_{0.008}$	$0.04_{0.007}$	**0.011**	**0.007**	**0.003**	0.987	0.949	0.998
NDUFA6	$0.034_{0.004}$	$0.021_{0.004}$	$0.042_{0.004}$	$0.028_{0.004}$	0.074	0.446	0.661	**0.002**	0.525	0.06
NDUFA8	$0.065_{0.008}$	$0.084_{0.008}$	$0.066_{0.009}$	$0.05_{0.008}$	0.318	1	0.568	0.408	**0.02**	0.557
NDUFA9	$0.455_{0.033}$	$0.451_{0.032}$	$0.514_{0.036}$	$0.333_{0.032}$	1	0.628	0.053	0.575	0.061	**0.003**
NDUFA10	$0.232_{0.022}$	$0.272_{0.021}$	$0.312_{0.024}$	$0.209_{0.021}$	0.544	0.076	0.873	0.602	0.167	**0.013**
NDUFA11	$1.593_{0.085}$	$1.729_{0.084}$	$1.907_{0.094}$	$1.249_{0.084}$	0.669	0.079	**0.032**	0.496	**0.001**	**<.0001**
NDUFA12	$0.09_{0.049}$	$0.36_{0.049}$	$0.47_{0.054}$	$0.348_{0.049}$	**0.002**	**<.0001**	**0.003**	0.446	0.998	0.355
NDUFA13	$2.979_{0.175}$	$2.733_{0.172}$	$3.462_{0.193}$	$2.249_{0.172}$	0.748	0.262	**0.025**	**0.036**	0.21	**2E-04**
NDUFAB1	$0.586_{0.052}$	$0.635_{0.052}$	$0.622_{0.058}$	$0.435_{0.052}$	0.91	0.968	0.184	0.998	**0.044**	0.091
NDUFB1	$0.808_{0.068}$	$1.028_{0.067}$	$0.877_{0.074}$	$0.724_{0.067}$	0.11	0.902	0.811	0.438	**0.013**	0.428
NDUFB2	$0.343_{0.041}$	$0.471_{0.041}$	$0.321_{0.046}$	$0.289_{0.041}$	0.142	0.983	0.789	0.083	**0.016**	0.955
NDUFB4	$1.002_{0.085}$	$1.139_{0.084}$	$1.234_{0.094}$	$0.836_{0.084}$	0.669	0.279	0.517	0.875	0.07	**0.016**
NDUFB7	$0.611_{0.068}$	$0.721_{0.067}$	$0.817_{0.075}$	$0.533_{0.067}$	0.66	0.194	0.843	0.776	0.21	**0.036**
NDUFB8	$1.626_{0.102}$	$1.855_{0.101}$	$1.714_{0.113}$	$1.327_{0.101}$	0.394	0.939	0.176	0.787	**0.004**	0.067
NDUFS3	$0.372_{0.044}$	$0.391_{0.043}$	$0.485_{0.048}$	$0.308_{0.043}$	0.99	0.321	0.726	0.478	0.531	**0.045**
NDUFS5	$2.129_{0.101}$	$1.848_{0.1}$	$2.239_{0.111}$	$1.699_{0.1}$	0.215	0.884	**0.022**	0.059	0.716	**0.005**
NDUFS6	$0.196_{0.019}$	$0.268_{0.019}$	$0.21_{0.021}$	$0.197_{0.019}$	**0.045**	0.959	1	0.174	**0.048**	0.969
NDUFS8	$0.873_{0.042}$	$0.712_{0.042}$	$0.882_{0.046}$	$0.654_{0.042}$	**0.046**	0.999	**0.004**	**0.045**	0.756	**0.004**
NDUFV1	$0.385_{0.037}$	$0.372_{0.036}$	$0.508_{0.041}$	$0.294_{0.036}$	0.994	0.129	0.303	0.075	0.435	**0.002**
Total genes with *p* < 0.05					**5**	**2**	**8**	**4**	**10**	**13**

Lsmean = least squares mean; SE = standard error

Table 2 Correlation between gene expression and enzyme activity

Enzyme activity	Gene	Duroc		DuPi		PiNN		PiPP		All breeds	
		r	p	r	p	r	p	r	p	r	p
Complex I	NDUFA2	0.37	0.230	-0.17	0.616	0.88	**0.002**	-0.47	0.170	0.38	**0.014**
	NDUFA3	0.25	0.439	0.30	0.369	0.27	0.486	-0.30	0.397	0.35	**0.023**
	NDUFA4	0.13	0.687	0.38	0.256	-0.19	0.629	-0.26	0.468	0.34	**0.026**
	NDUFA4L2	0.33	0.298	-0.08	0.807	0.43	0.246	0.15	0.670	0.45	**0.003**
	NDUFA9	0.39	0.209	0.11	0.742	0.41	0.277	0.02	0.964	0.45	**0.003**
	NDUFA11	0.33	0.294	-0.17	0.623	0.74	**0.023**	-0.34	0.330	0.41	**0.007**
	NDUFA12	-0.39	0.209	0.31	0.350	-0.73	**0.025**	0.62	0.056	-0.26	0.099
	NDUFA13	0.47	0.127	-0.22	0.507	0.73	**0.024**	-0.52	0.126	0.45	**0.003**
	NDUFB8	0.50	0.101	-0.26	0.443	0.70	**0.037**	-0.05	0.889	0.38	**0.012**
	NDUFS1	0.41	0.187	0.05	0.884	0.37	0.328	0.18	0.609	0.36	**0.018**
	NDUFS5	0.31	0.330	0.17	0.617	0.54	0.132	-0.69	**0.029**	0.43	**0.004**
	NDUFS8	0.50	0.101	-0.28	0.409	0.48	0.186	-0.34	0.337	0.41	**0.006**
Complex II	SDHC	0.22	0.499	0.65	**0.031**	0.58	0.132	-0.62	0.055	0.28	0.073
Complex IV	COX10	-0.10	0.757	0.58	**0.047**	-0.07	0.844	0.32	0.342	0.15	0.310
	COX15	0.25	0.437	0.48	0.112	0.27	0.446	-0.35	0.295	0.36	**0.015**
	COX5B	0.66	**0.021**	0.18	0.584	0.40	0.248	-0.46	0.150	0.29	0.051
	COX6C	0.37	0.238	0.65	**0.023**	0.26	0.462	-0.51	0.110	0.54	**0.0001**
	COX7A1	0.59	**0.041**	0.39	0.212	0.21	0.556	-0.60	**0.049**	0.37	**0.013**
	COX7A2	0.41	0.189	0.79	**0.002**	0.16	0.661	0.07	0.831	0.63	**<.0001**

Table 3 Correlation between gene expression and muscle fiber-type by breed

Breed	Gene		STO		FTO		FTG	
			r	*p*	r	*p*	r	*p*
Duroc	Phospho-fructokinase	*PFKM*	0.87	**0.024**	-0.29	0.571	-0.80	0.054
	Citrate synthase	*CS*	0.51	0.304	-0.98	**0.001**	0.10	0.855
	Complex I	*NDUFA2*	0.82	**0.048**	-0.25	0.634	-0.78	0.070
		NDUFA3	0.86	**0.030**	-0.82	**0.047**	-0.42	0.411
		NDUFA9	0.82	**0.045**	-0.60	0.205	-0.53	0.282
		NDUFA10	0.83	**0.040**	-0.42	0.412	-0.67	0.143
		NDUFA11	0.83	**0.041**	-0.53	0.282	-0.60	0.211
		NDUFA13	0.86	**0.028**	-0.37	0.473	-0.75	0.088
		NDUFB7	0.84	**0.038**	-0.75	0.086	-0.44	0.383
		NDUFB8	0.68	0.134	0.10	0.855	-0.87	**0.026**
		NDUFS1	0.64	0.168	0.13	0.813	-0.84	**0.038**
		NDUFS7	0.84	**0.035**	-0.37	0.471	-0.71	0.111
		NDUFS8	0.92	**0.009**	-0.74	0.095	-0.55	0.258
		NDUFV1	0.93	**0.008**	-0.62	0.192	-0.64	0.168
	Complex II	*SDHA*	0.86	**0.029**	-0.51	0.307	-0.64	0.170
		SDHB	0.83	**0.039**	-0.58	0.223	-0.55	0.253
		SDHC	0.66	0.153	0.17	0.741	-0.89	**0.017**
	Complex IV	*COX5B*	0.88	**0.021**	-0.59	0.222	-0.61	0.203
	ATP synthase	*ATP5G1*	0.99	**<.0001**	-0.52	0.295	-0.79	0.061
	V-ATPase	*ATP6V1E1*	0.42	0.405	0.50	0.314	-0.84	**0.037**
		ATP6V1F	0.82	**0.048**	-0.23	0.657	-0.78	0.067
DuPi	Phospho-fructokinase	*PFKM*	0.32	0.531	-0.83	**0.040**	0.11	0.842
	Complex I	*NDUFA8*	0.09	0.870	-0.93	**0.008**	0.32	0.531
		NDUFA10	0.03	0.954	-0.87	**0.023**	0.34	0.505
		NDUFS6	-0.30	0.566	-0.89	**0.016**	0.66	0.155
		NDUFS7	-0.31	0.550	-0.85	**0.033**	0.62	0.186
	Complex II	*SDHA*	-0.17	0.749	-0.90	**0.014**	0.52	0.290
	Complex IV	*COX6A1*	-0.91	**0.012**	0.03	0.958	0.73	0.098
PiNN	ATP synthase	*ATP5L*	0.20	0.575	0.47	0.172	-0.68	**0.031**
	V-ATPase	*ATP6V1B2*	0.16	0.650	0.55	0.099	-0.72	**0.018**
PiPP	Lactate dehydrogenase	*LDHC*	-0.91	**0.011**	-0.55	0.257	0.92	**0.010**
	Complex I	*NDUFA3*	0.83	**0.043**	0.29	0.575	-0.69	0.131
		NDUFA11	0.82	**0.048**	-0.02	0.968	-0.63	0.178
	V-ATPase	*ATP6V0D1*	0.92	**0.009**	0.48	0.335	-0.85	**0.032**
		ATP6V1C1	-0.48	0.333	-0.92	**0.009**	0.76	0.081

STO = slow-twitch oxidative; FTO = fast-twitch oxidative; FTG = fast-twitch glycolytic

20

SCIENTIFIC REP⚙RTS

Mitochondrial-nuclear crosstalk, haplotype and copy number variation distinct in muscle fiber type, mitochondrial respiratory and metabolic enzyme activities

Xuan Liu[1], Nares Trakooljul[2], Frieder Hadlich[1], Eduard Murani[2], Klaus Wimmers [2] & Siriluck Ponsuksili[1]

Genes expressed in mitochondria work in concert with those expressed in the nucleus to mediate oxidative phosphorylation (OXPHOS), a process that is relevant for muscle metabolism and meat quality. Mitochondrial genome activity can be efficiently studied and compared in Duroc and Pietrain pigs, which harbor different mitochondrial haplotypes and distinct muscle fiber types, mitochondrial respiratory activities, and fat content. Pietrain pigs homozygous-positive for malignant hyperthermia susceptibility (PiPP) carried only haplotype 8 and showed the lowest absolute mtDNA copy number accompanied by a decrease transcript abundance of mitochondrial-encoded subunits *ND1*, *ND6*, and *ATP6* and nuclear-encoded subunits *NDUFA11 and NDUFB8*. In contrast, we found that haplotype 4 of Duroc pigs had significantly higher mitochondrial DNA (mtDNA) copy numbers and an increase transcript abundance of mitochondrial-encoded subunits *ND1*, *ND6*, and *ATP6*. These results suggest that the variation in mitochondrial and nuclear genetic background among these animals has an effect on mitochondrial content and OXPHOS system subunit expression. We observed the co-expression pattern of mitochondrial and nuclear encoded OXPHOS subunits suggesting that the mitochondrial-nuclear crosstalk functionally involves in muscle metabolism. The findings provide valuable information for understanding muscle biology processes and energy metabolism, and may direct use for breeding strategies to improve meat quality and animal health.

Mitochondria are involved in many key cellular processes such as apoptosis, calcium homeostasis, reactive oxygen species production, and most importantly, adenosine triphosphate (ATP) generation by oxidative phosphorylation (OXPHOS). In addition, these organelles contain their own DNA distinct from the nuclear genome. In pigs, mitochondrial DNA (mtDNA) is 16,613 base pairs in length and encodes two ribosomal RNA (rRNA), 22 transfer RNA (tRNA), and 13 protein-coding genes involved in the OXPHOS system. Since OXPHOS subunits are encoded by both the nuclear and mitochondrial genome, the two genome systems interact intricately to form the fully assembled functional OXPHOS complexes.

Mitochondrial genetic variation can affect fertility, longevity, and evolutionary trajectories and acts as a human health indicator[1]. mtDNA haplotype variation affects metabolic performance in many species, such as raccoons, dogs, cows, and pigs[2], and mitochondrial DNA (mtDNA) copy number has been associated with extensive exercise, age-related hearing impairment, disordered antioxidant capacity, and heart failure[3–6]. In *Drosophila*, mtDNA copy number is proposed to be modulated by mtDNA genome variation[7]. Mitochondrial DNA haplotypes are potential targets for manipulating phenotypes including tolerance to heat, growth, and milk quality in farm animals[8]. Hence, an understanding of the influence of mitochondrial haplotypes on energy metabolism in pigs would provide valuable information on mitochondrial function and inform farming practices to improve

[1]Research Unit 'Functional Genome Analysis', Leibniz Institute for Farm Animal Biology (FBN), Wilhelm-Stahl-Allee 2, D-18196, Dummerstorf, Germany. [2]Research Unit 'Genomics', Leibniz Institute for Farm Animal Biology (FBN), Wilhelm-Stahl-Allee 2, D-18196, Dummerstorf, Germany. Correspondence and requests for materials should be addressed to S.P. (email: ponsuksili@fbn-dummertorf.de)

meat quality and animal health. Since pigs share many similarities with humans in terms of genetics and physiology, this knowledge is also potentially applicable to human diseases.

In addition to variation in mitochondrial density among muscle types, mitochondria are functionally optimized and specialized in glycolytic and oxidative fibers[9]. Mitochondria isolated from muscle immediately after slaughter are similar to those found in intact muscle, whereas some mitochondria from pale, soft, exudative (PSE) muscle are already swollen and show a decreased matrix density[10]. With an emphasis placed on glycolysis, mitochondrial content and function may be important factors contributing to postmortem muscle metabolism[11]. Duroc and Pietrain are two commercial pig breeds known for divergent meat quality and muscular energy metabolism. Muscle from Duroc pigs typically contains more slow-twitch oxidative (STO) fibers and intramuscular fat, whereas Pietrain pigs are leaner and their muscles contain more fast-twitch glycolytic (FTG) fibers[12-14]. The content of different muscle fibers types, their size and structure largely contribute to differences in growth performance and carcass traits as well as postmortem meat quality traits[15]. Lipids are stored mainly in STO fibers, which can improve the tenderness and juiciness of the meat[16]. The selection of a high percentage of FTG fibers may result in altered meat quality possibly due to the lower capillarization, insufficient delivery of oxygen and glycogen depletion[17,18]. Indeed, the meat quality parameters such as color of the meat, drip loss and shear force were measured in muscle of the same pigs[12,14]. PiPP pigs showed increased drip loss and shear force comparing to other three pig breeds. These results directly supported the association between muscle fiber type and meat quality. In Pietrain pigs, mutations within the ryanodine receptor 1 (RYR1) are associated with malignant hyperthermia susceptibility (MHS), reduced water holding capacity, and increased PSE meat[19-21]. Thus, Duroc and Pietrain pigs are unique models in which to study mitochondrial properties and energy metabolism influencing muscle metabolism and meat quality.

We have previously shown the transcriptional signatures in muscle from these pigs to be related to metabolic properties and mitochondrial respiration[22-24]. Furthermore, we wanted to know the mtDNA variation of these pigs and investigate whether mtDNA variation preferentially modifies the expression of mitochondria-associated OXPHOS gene from both mitochondria and nuclear genomes. Finally, we investigated mtDNA variation genes involved in mtDNA copy number in conjunction with muscle fiber types and metabolic enzyme activities in postmortem longissimus muscles (LM) from four different pig breeds: Duroc, Pietrain homozygous-negative for MHS (PiNN), Pietrain homozygous-positive for MHS (PiPP), and an F2 crossbred Duroc-Pietrain homozygous-negative for MHS (DuPi).

Results

Phenotypic differences among breeds. To illustrate breed differences in muscle metabolism, muscle fiber composition, metabolic activities, and pH were compared among the four breeds. Duroc pigs had the highest percentage of STO muscle fibers and lower fast-twitch oxidative (FTO) fibers (Supplementary Fig. S1). PiPP pigs had a significantly higher percentage of FTG fibers (80.8%) compared to PiNN pigs (74.9%, $p = 0.02$), while Duroc and DuPi were in between the two Pietrain pigs.

The activities of key metabolic enzymes for energy metabolism were measured for all four pig breeds. PiNN pigs had the highest activity of phosphofructokinase (PFK), whereas no significant differences in the activities of glycogen phosphorylase (GP) and lactate dehydrogenase (LDH) were detected among breeds. Duroc pigs had the highest complex I activity (12.5 U/g protein) compared to other breeds. Moreover, PiPP had significantly lower pH than the other three breeds.

All measured phenotypic traits were compared at time 0 and 30 min postmortem (Supplementary Fig. S2). Most of the phenotypes, except complex IV activity, were significantly different between time points. The enzyme activities of PFK and LDH were increased from 475 to 859 U/g protein ($p = 0.0002$) and from 10.9 to 15 U/g protein ($p < 0.0001$), respectively, whereas the oxidative enzyme activities of CS, complex I and complex II, together with GP activity and pH, were decreased at 30 min postmortem compared to immediately after slaughter (p values ranging from < 0.0001 to 0.02).

Different mitochondrial haplotypes among pig breeds. The D-loop regions in 53 animals were sequenced and eight haplotypes were identified. For statistical reasons, five haplotypes identified in at least three animals were included in subsequent data analysis. Detailed haplotype information is shown in Supplementary Table 1 and Fig. S3. In brief, haplotypes 4 (Duroc: 10, DuPi: 6) and 6 (Duroc: 5, DuPi: 1) were present in mainly Duroc and DuPi pigs whereas haplotype 1 was present in five DuPi pigs only. Haplotype 7 was present in three PiNN pigs, while haplotype 8 was found in 14 PiPP and four PiNN pigs. Muscles from pigs with haplotype 7 contained significantly more FTO muscle fibers than haplotypes 4, 6, and 8 ($p < 0.05$, Fig. S4). Interestingly, haplotype 8 showed the lowest complex I activity among all the haplotypes and had significantly lower activity than haplotypes 4 and 6 ($p < 0.05$). All other phenotypic traits were comparable between haplotypes.

Duplication of the porcine mitochondrial genome in the nuclear genome. Using BLASTN, the pig mitochondrial genome was compared to the pig nuclear genome. Many regions among 18 somatic chromosomes and the X chromosome of the porcine nuclear genome matched to the mitochondrial genome (Fig. 1).

Comparison of mtDNA copy number. PiPP pigs had the lowest mtDNA copy number (368 copies per nuclear genome) among the four breeds, especially compared to Duroc pigs (435 copies per nuclear genome, $p = 0.02$, Fig. 2a). Further, mtDNA copy number in longissimus muscle was decreased from 420 copies per nuclear genome at 0 min postmortem to 389 copies at 30 min postmortem ($p = 0.01$, Fig. 2b). Finally, muscle from pigs with haplotype 8 contained the lowest mtDNA copy number. Pigs with haplotype 8 had 375 copies per nuclear genome in their muscle tissue, which was significantly less than the 435 copies per nuclear genome seen in pigs with haplotype 4 ($p = 0.02$, Fig. 2c). There were no significant effects of sex on mtDNA copy number.
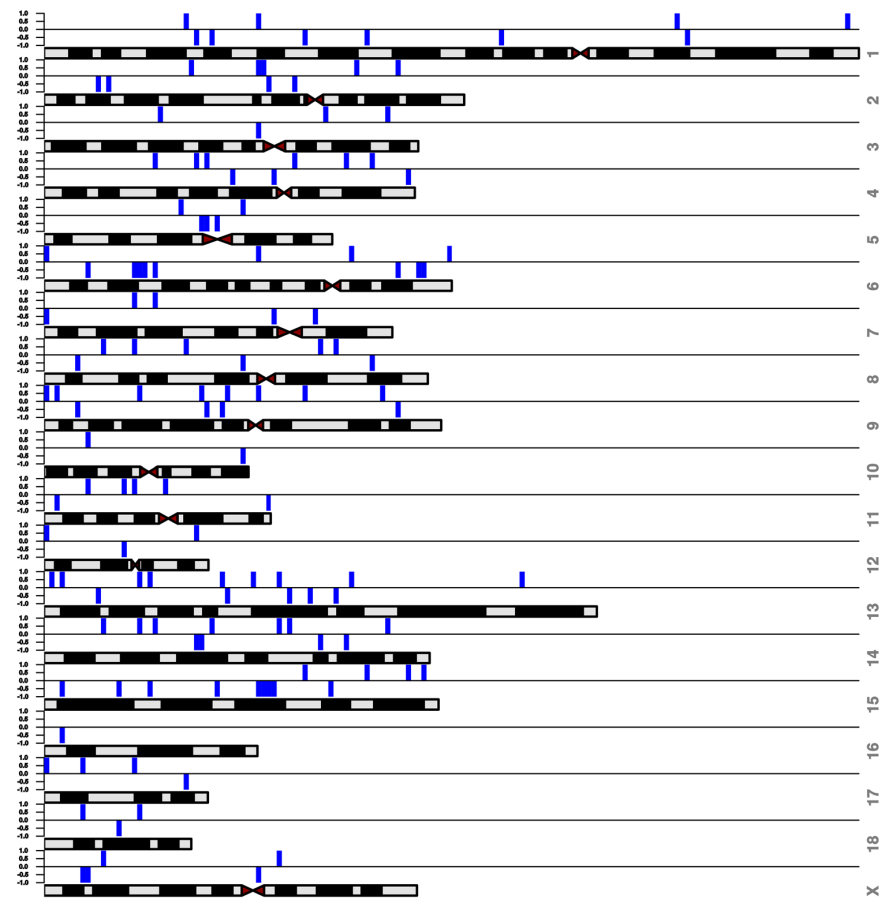
Figure 1. Duplication of mitochondrial genome in the nuclear genome. Blue bars represent the locations of duplicated mitochondrial genome against the porcine chromosomes.

Correlation between mtDNA copy number, phenotype, and gene expression. As shown in Fig. 2d, mtDNA copy number was significantly correlated with muscle fiber type (STO: r = 0.263 p = 0.031; FTG: r = −0.292 p = 0.017) and enzyme activities (CS: r = 0.249 p = 0.009; complex I: r = 0.43 p = < 0.0001). Moreover, the expression of mitochondria-encoded genes (*ND1, CYB, COX1,* and *ATP6*) and nuclear-encoded OXPHOS genes (*NDUFA3, NDUFA11, NDUFA13, NDUFB8, NDUFS8, NDUFV1, ATP5G1,* and *ATP5L*) were significantly correlated with mtDNA copy number (p values ranged from 0.006 to 0.031 and < 0.0001 to 0.015, respectively. MtDNA copy number was weakly correlated with PPARG coactivator 1 alpha (*PGC-1α*) mRNA (p = 0.156).

Comparison of mitochondrial and nuclear encoded OXPHOS genes expression. To further examine breed and time differences in postmortem muscular energy metabolism at a molecular level, both mitochondrial and nuclear encoded gene expression was profiled at 0 and 30 min postmortem using qPCR in all four pig breeds. No mitochondrial-encoded genes were differently expressed between 0 and 30 min postmortem (Table 1). The mRNA levels of 4 nuclear-encoded genes, NDUFB8, COX7A2 and ATP5L were significantly lower at 30 min postmortem than 0 min (p values < 0.0001 to 0.02).

Out of the sixteen genes investigated, ten genes including mitochondrial-encoded *ND1, ND2, ND6, ATP6* were differently expressed between breeds (Fig. 3a). PiPP pigs had the most differentially expressed genes, especially compared to the Duroc and DuPi breeds: complex I subunits ND1 and ND6 and the ATP synthase subunit ATP6 were all significantly upregulated in Duroc pigs (p values < 0.0001 to 0.003). Nuclear-encoded *NDUFA11, NDUFB8, NDUFS8, NDUFV1, ATP5G1* and *ATP5L* showed significant differences among breeds (p < 0.05, Supplementary Table 2) (Fig. 3b). All six differentially expressed were down-regulated in PiPP pigs compared to the three other breeds.

Eleven genes including *ND1, ND2, ND6, CYB, COX1, ATP6* and nuclear-encoded *NDUFA11, NDUFA13, NDUFB8, ATP5G1* and *ATP5L* showed significant differences in haplotypes (Supplementary Table 3). Only three genes including nuclear-encoded *NDUFB8, COX7A2* and *ATP5L* demonstrated that they were significantly influenced by time. No gene expression was affected by sex.
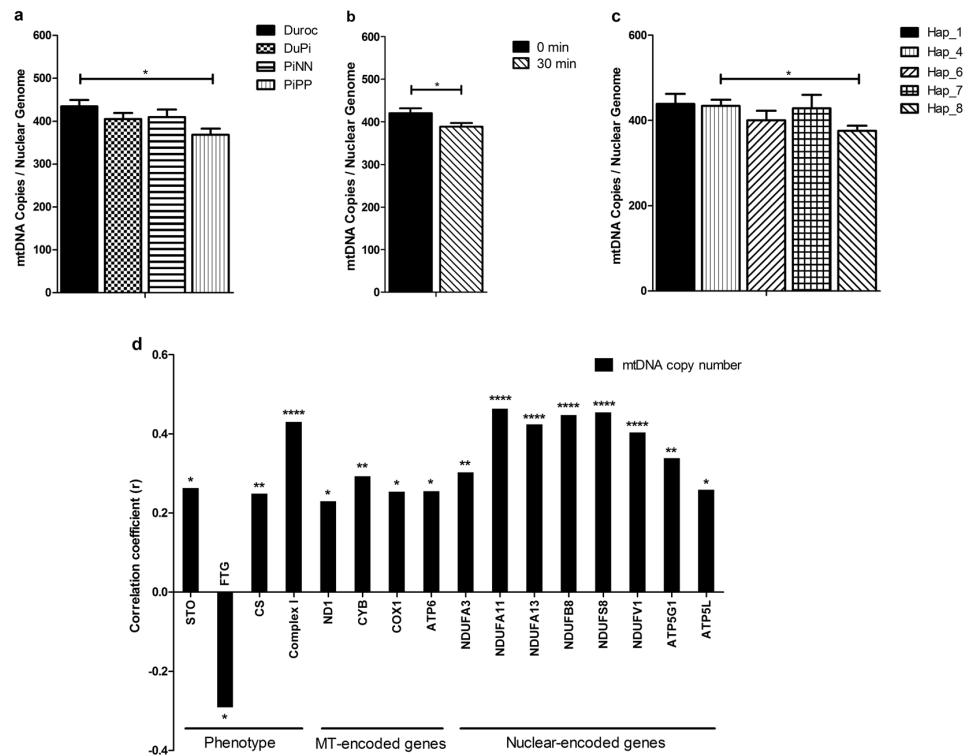
Figure 2. Absolute mitochondrial DNA copy number in porcine *longissimus* muscles. Least-square means with standard error (Lsmeans ± SE) of mtDNA copy number (**a**) in Duroc, DuPi, PiNN, and PiPP pigs (**b**) at 0 min and 30 min postmortem (**c**) in different mitochondrial haplotypes (**d**). The correlation coefficient of mtDNA copy number and OPXHOS gene expression with phenotypes of traits. *p < 0.05; **p < 0.01****p < 0.0001. See also Table S3 and S4.

Gene		0 min (n = 58) Lsmean$_{SE}$	30 min (n = 58) Lsmean$_{SE}$	0 vs 30 min p-value
Mitochondrial-encoded	ND1	$9.978_{0.316}$	$10.126_{0.401}$	0.768
	ND2	$7.528_{0.416}$	$7.025_{0.484}$	0.433
	ND4	$13.780_{0.435}$	$13.449_{0.669}$	0.680
	ND6	$6.641_{0.316}$	$6.262_{0.443}$	0.462
	CYB	$0.007_{0.0004}$	$0.008_{0.0005}$	0.213
	COX1	$20.677_{0.580}$	$21.731_{0.854}$	0.306
	ATP6	$17.539_{0.658}$	$16.849_{0.770}$	0.507
Nuclear-encoded	NDUFA3	$0.022_{0.002}$	$0.024_{0.002}$	0.367
	NDUFA11	$0.257_{0.009}$	$0.264_{0.008}$	0.549
	NDUFA13	$0.333_{0.012}$	$0.336_{0.010}$	0.858
	NDUFB8	$0.639_{0.020}$	$0.348_{0.013}$	**<0.0001**
	NDUFS8	$0.320_{0.013}$	$0.304_{0.011}$	0.326
	NDUFV1	$0.175_{0.007}$	$0.188_{0.006}$	0.105
	COX7A2	$0.132_{0.006}$	$0.086_{0.004}$	**<0.0001**
	ATP5G1	$0.521_{0.025}$	$0.566_{0.022}$	0.071
	ATP5L	$0.036_{0.003}$	$0.029_{0.002}$	**0.016**

Table 1. OXPHOS gene expression at 0 and 30 min postmortem.

All PiPP pigs had haplotype 8, which showed significantly lower gene expression than haplotypes 1, 4, and 6 for *ND1*, *ND2*, *ND6*, *CYB*, *COX1*, and *ATP6* (*p* values from *p* < 0.0001 to 0.048; Fig. 4a and b). Complex I subunits *NDUFA11*, *NDUFA13*, and *NDUFB8* showed significantly lower gene expression in haplotype 8 than haplotype 1 pigs (*p* values < 0.0001 to 0.029, Fig. 4c and d).
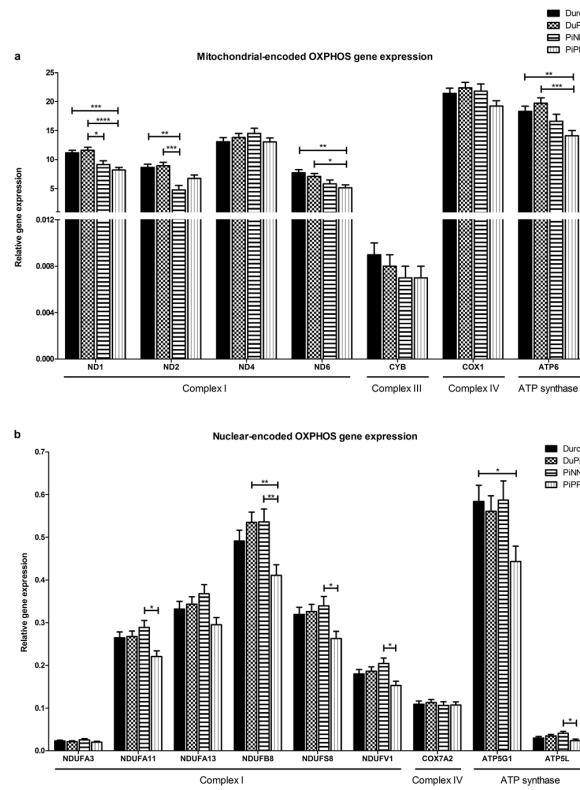
Figure 3. Relative mRNA expression of OXPHOS subunits in *longissimus* muscles of Duroc, DuPi, PiNN, and PiPP pigs. Least-square means with standard error (Lsmeans ± SE) of relative gene expressions for (**a**) mitochondrial-encoded complex I subunits (*ND1, ND2, ND4,* and *ND6*), complex III subunit (*CYB*), complex IV subunit (*COX1*) and ATP synthase subunit (*ATP6*) (**b**) nuclear-encoded complex I subunits (*NDUFA3, NDUFA11, NDUFA13, NDUFB8, NDUFS8,* and *NDUFV1*), complex IV subunit (*COX7A2*) and ATP synthase subunits (*ATP5G1* and *ATP5L*). Relative gene expression was normalized to reference genes *ACTB, RPL32* and *RPS11* using $2^{(-\Delta Ct)}$. *p < 0.05; **p < 0.01; ***p < 0.001; ****p < 0.0001. See also Table S3.

Correlation between expression levels of mitochondrial, nuclear encoded genes and phenotype. Pairwise correlation was calculated and plotted for each individual OXPHOS gene (Fig. 5a). All included genes were significantly correlated with at least one of the other genes. Further, all mitochondrial-encoded OXPHOS subunits tended to be more tightly co-expressed while nuclear-encoded OXPHOS subunits were in a tight co-expressed relationship. Figure 5b shows the correlation between the expression of OXPHOS genes and phenotype. The expression of mitochondrial encoded OXPHOS subunits *ND2, ND6,* and *ATP6* and the nuclear encoded subunit *NDUFV1* were highly correlated with muscle fiber type (*ND2*: FTO r = −0.49 p = 0.0002; *ND6*: STO r = 0.286 p = 0.042; *ATP6*: STO r = 0.342 p = 0.014; *NDUFV1*: FTG r = −0.346 p = 0.013). The nuclear encoded OXPHOS subunits *NDUFA3, NDUFA11, NDUFB8, NDUFS8,* and *COX7A2* were significantly correlated with at least one of the activities of oxidative enzymes CS, complex I, complex II, and complex IV. The expression of *ND2* (r = −0.239 p = 0.026) and *ND6* (r = −0.221 p = 0.04) were negatively correlated with PFK activity. The expression of *NDUFB8 and COX7A2* were highly correlated with the activities of GP (*NDUFB8*: r = 0.304 p = 0.007; *COX7A2*: r = 0.236 p = 0.037), PFK (*NDUFB8*: r = −0.309 p = 0.004; *COX7A2*: r = −0.305 p = 0.004), and LDH (*NDUFB8*: r = −0.354 p = 0.001; *COX7A2*: r = −0.376 p = 0.0003). The mRNA levels of *ATP6, NDUFB8, COX7A2,* and *ATP5L* were positively correlated with pH (*p* values < 0.0001 to 0.028).

The expression of the master regulator of mitochondrial biogenesis and oxidative phosphorylation *PGC-1a* was significantly correlated with the phenotypes of CS, complex I, complex II, complex IV, and pH (Table 2). The mRNA levels of *PGC-1a* were also significantly correlated with the expression of mitochondrial-encoded genes *ND1, ND2, ND4, ND6, CYB, COX1,* and *ATP6*. Among these genes, *ATP6, ND6,* and *ND2* showed the top three most significant correlations with *PGC-1a* (*ATP6*: r = 0.415 p < 0.0001; *ND6*: r = 0.372 p = 0.0003; *ND2*: r = 0.361 p = 0.0004). The expression of *PGC-1a* showed a significant correlation with the nuclear-encoded genes *NUDFA11, NDUFA13, NDUFB8, COX7A2, ATP5G1,* and *ATP5L* (*p* values < 0.0001 to 0.036).

Discussion

We compared the mitochondrial DNA content, gene expression pattern of mitochondrial and nuclear encoded OXPHOS subunits, metabolic enzyme activities and mitochondrial respiration in four pig breeds distinct in
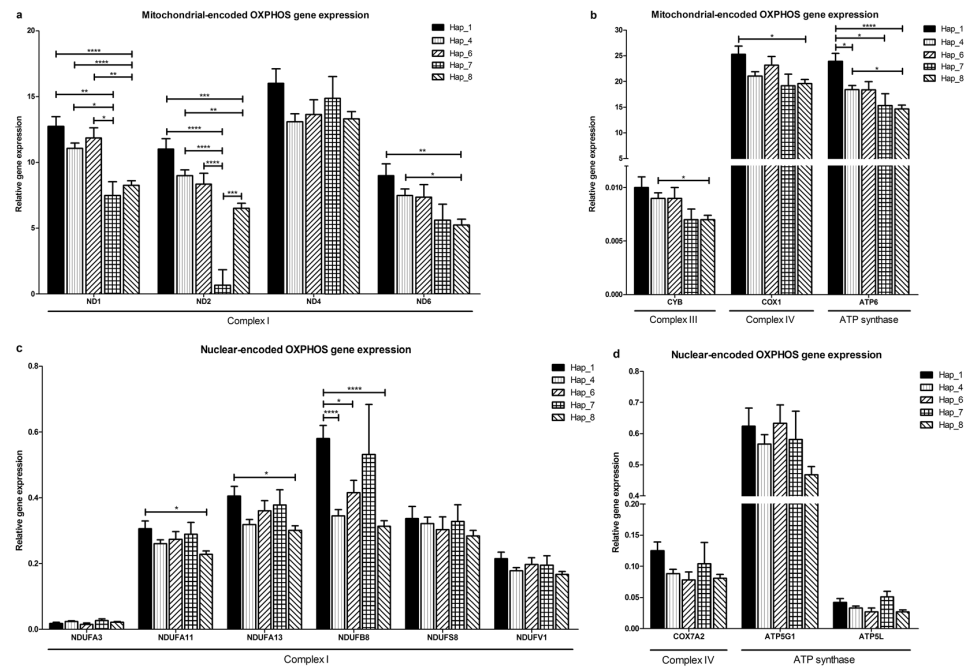
Figure 4. Relative mRNA expression of OXPHOS subunits in *longissimus* muscles of different mitochondrial haplotypes. Least-square means with standard error (Lsmeans $\pm$ SE) of relative gene expression for (**a**) mitochondrial-encoded complex I subunits (*ND1, ND2, ND4,* and *ND6*). (**b**) complex III subunit (*CYB*), complex IV subunit (*COX1*) and ATP synthase subunit (*ATP6*). (**c**) nuclear-encoded complex I subunits (*NDUFA3, NDUFA11, NDUFA13, NDUFB8, NDUFS8* and *NDUFV1*). (**d**) complex IV subunit (*COX7A2*) and ATP synthase subunits (*ATP5G1* and *ATP5L*). Relative gene expression was normalized to reference genes *ACTB, RPL32* and *RPS11* using $2^{(-\Delta Ct)}$. *p < 0.05; **p < 0.01; ***p < 0.001; ****p < 0.0001. See also Table S4.

muscle phenotype. The effect of mitochondrial haplotypes on mitochondrial DNA copy number and OXPHOS gene expression were also examined since there were different haplotypes among the investigated pig breeds.

Muscle samples were collected from the fat-type Duroc pigs with a higher proportion of STO fibers and greater oxidative enzyme activities. Pietrain pigs are muscular and lean, and their muscles contain more FTG fibers. DuPi pig is a Duroc-Pietrain F2 crossbred. Mutations within ryanodine receptor 11 (RYR1) are frequently detected in Pietrain pigs. This leads to abnormal Ca^{2+} homeostasis and result in increased excitability of the muscle associated with MHS. This genetic defect consequently leads to reduction of water holding capacity, loss of stress resistance and PSE meat[19–21].

Reduced mtDNA copy number in PiPP pigs. Previous studies have demonstrated the relative mtDNA copy number in porcine muscle[25,26]. In this study we quantified the absolute mtDNA copy number by qPCR and found that PiPP pigs contained the lowest amount of mtDNA copies in muscle cells compared to PiNN, DuPi, and particularly Duroc pigs. mtDNA copy number was positively correlated with STO fibers and negatively correlated with FTG fibers and indicated a strong association between mtDNA copy number and muscle fiber types.

The underlying cause of the mtDNA copy number variation between pig breeds remains unknown. In other case, changes in cytosolic Ca^{2+} and pH could influence the amount of ROS produced at the mitochondrial respiratory complex I and III[27]. The abnormal Ca^{2+} homeostasis in PiPP pigs may result in oxidative stress associated with elevated ROS production. The elevated ROS could increase mitophagy to remove damaged mitochondria and leads to mitochondrial degradation[28,29]. The copy number depletion associated with increased mitochondria turnover is caused by a burst of ROS production[30]. Indeed, the burst of ROS and mtDNA depletion have been observed in cell-culture experiments. All together, these may partially explain the copy number variation of mtDNA in pig breeds. However, supporting evidence under physiological situation is still needed.

Decreased transcript levels of mitochondrial and nuclear encoded OXPHOS genes in PiPP pigs. Decreased abundance of many nuclear-encoded OXPHOS subunits transcripts was found in PiPP pigs compared to other breeds. This phenomenon is very likely caused by the abnormal Ca^{2+} homeostasis in PiPP pigs since MHS knock-in mice show a clear Ca^{2+} overload in the mitochondrial matrix and a switch to a compromised bioenergetics state characterized by low OXPHOS[31]. Similarly, transcript abundance of mitochondrial-encoded genes was decreased in PiPP pigs including subunits of complex I and ATP synthase. The previous study reported that ATP concentration has been significantly reduced in PiPP pigs compared to other breeds because of their accelerated energy consumption[14]. ATP sensing by transcriptional machinery has been proposed to regulate the
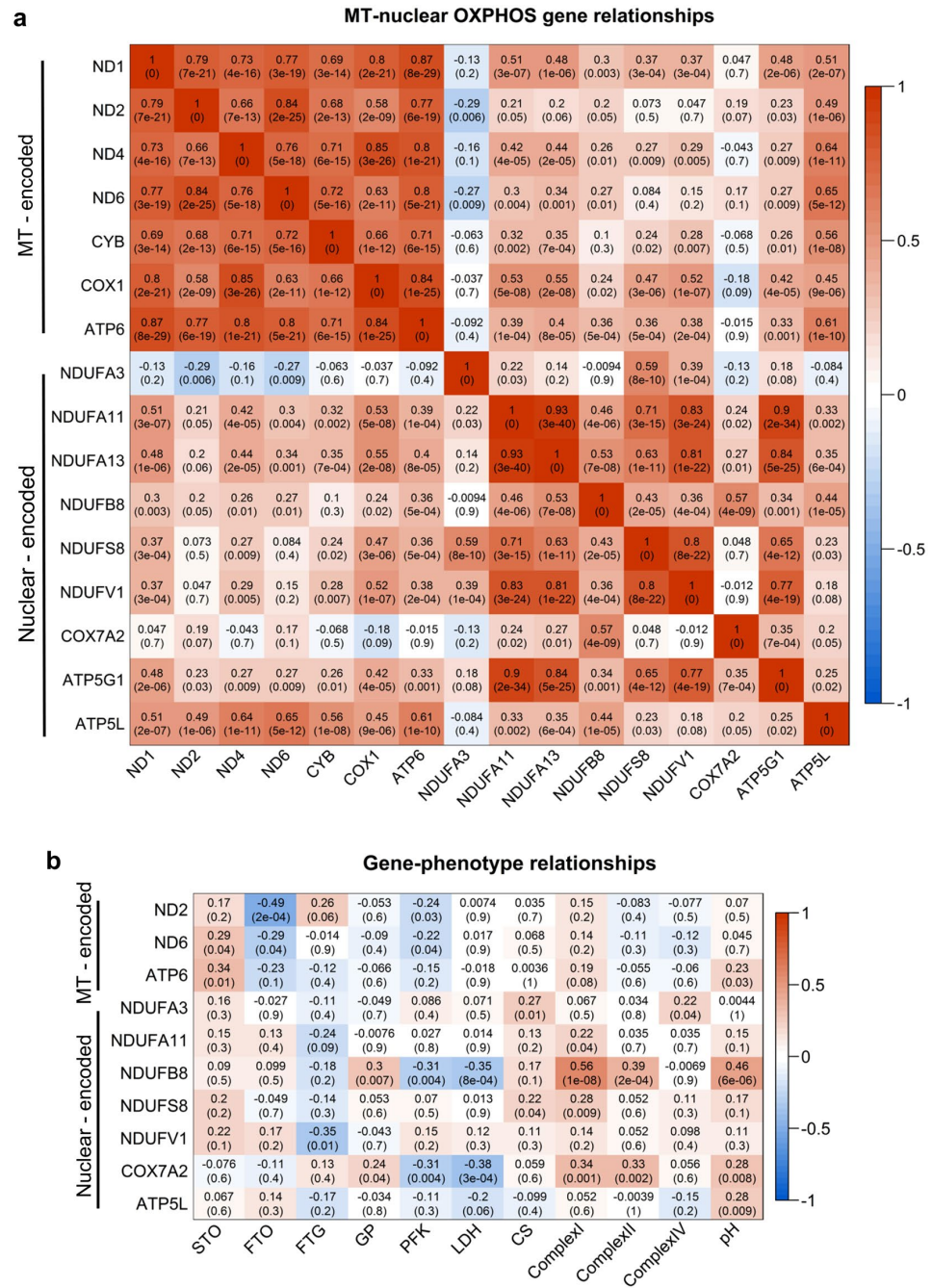
112

Figure 5. Correlation matrix of OXPHOS gene expression and phenotypes. (**a**) correlation matrix between mitochondrial and nuclear encoded OXPHOS gene expressions. (**b**) correlation matrix between OXPHOS gene expression and phenotype. Number in each cell represents the value of correlation coefficients and the corresponding p-values. Cell color indicates correlation (red, positive correlation; blue, negative correlation).

initiation of mitochondrial transcription and promotor usage[32–34]. Therefore, the lower ATP availability in PiPP pigs may influence their mitochondrial transcription and function.

Recent work has established that glucocorticoid receptor (GR) is translocated from cytosol to the mitochondria and binds to the D-loop control region while stress and corticosteroids have a direct influence on hippocampal mtDNA gene expression in rats[35]. Since *RYR1* mutated PiPP pigs are stress susceptible, it is speculated that the abundance of mtDNA transcripts may be decreased in those pigs.

Phenotype/mRNA		*PGC-1a*	
		r	p
Phenotype	CS	0.382	**0.0003**
	Complex I	0.405	**<0.0001**
	Complex II	0.234	**0.030**
	Complex IV	0.309	**0.004**
	pH	0.285	**0.007**
MT gene	*ND1*	0.346	**0.001**
	ND2	0.361	**0.0004**
	ND4	0.282	**0.007**
	ND6	0.372	**0.0003**
	CYB	0.246	**0.019**
	COX1	0.220	**0.036**
	ATP6	0.415	**<0.0001**
Nuclear gene	*NDUFA11*	0.266	**0.011**
	NDUFA13	0.220	**0.036**
	NDUFB8	0.341	**0.001**
	COX7A2	0.397	**<0.0001**
	ATP5G1	0.298	**0.004**
	ATP5L	0.358	**0.001**

Table 2. Correlation between *PGC-1a*, phenotype, and OXPHOS gene expression.

The early postmortem period had no effect on the expression of mitochondrial-encoded OXPHOS genes, but the mtDNA copy number was decreased from 0 min to 30 min postmortem. In other words, the early phase of hypoxia triggered mitochondrial genome instability while transcript abundance was maintained in porcine muscle. This disparity is of interest and might provide valuable information toward the understanding of mitochondrial mechanisms in muscle tissue under hypoxia, which has been linked to oxidative stress, ischemia, and cancer[36]. In addition, the identified postmortem mitochondrial properties are relevant to muscle injury, also caused by oxygen depletion[37].

The effect of haplotype on mtDNA copy number and OXPHOS gene expression. Our study showed for the first time the effect of different mitochondrial haplotypes on muscle fiber types and mitochondrial respiration at both the phenotypic and molecular level in pigs. Among different haplotypes, our results showed variations in complex I activity and mtDNA copy number. At the molecular level, six of the mitochondrial-encoded and three of the nuclear-encoded OXHPOS genes were differentially expressed. These findings suggest that mitochondrial haplotypes could contribute to variations in mitochondrial content and OXPHOS system function.

The mitochondrial haplotype has been found to affect mtDNA copy number, OXPHOS respiration, and mitochondrial molecular function in *Drosophila*[1,7,38]. In porcine transmitochondrial cybrids, the mitochondrial haplotype is linked to metabolic traits including ROS production, ATP content, and complex II activity[39]. The assembly kinetics of OXPHOS complexes is proposed to be modulated by mitochondrial DNA background[40].

Coordination of the nuclear and mitochondrial genomes contribute to phenotype. Our results showed that all mitochondrial-encoded OXPHOS subunits were highly co-expressed; moreover also the nuclear-encoded OXPHOS subunits tended to be in a tight co-expressed relationship. This observation reflects the fact that the mitochondrial genome has its own transcription machinery distinct from the nuclear genome. Although mitochondrial- and nuclear-encoded OXPHOS genes are expressed separately via different transcription machineries in different cellular locations, they are not completely independent. The observed association between mitochondrial- and nuclear-encoded OXPHOS genes is in line with the theory of mitochondrial-nuclear crosstalk. PPARG coactivator 1 alpha (PGC-1α) is a nuclear-encoded transcription factor that acts as a master coordinator to mediate mitochondrial biogenesis and oxidative phosphorylation[41]. In this study, the mRNA level of *PGC-1α* significantly correlated with all investigated mitochondrial-encoded OXPHOS subunits, six nuclear-encoded subunits and enzyme activities of complex I, II, and IV. In fact, the nuclear-encoded subunits need to be imported into the mitochondria together with mitochondrial-encoded subunits to form a fully assembled functional OXPHOS system in the mitochondrial inner membrane. Accordingly, the absence of the mtDNA-encoded subunits COX1 and COX2 has been shown to affect the stability of some subunits of nuclear encoded respiratory chain proteins[42].

In our results, different mitochondrial haplotypes showed variation of the expression of mitochondrial-encoded subunits *ND2*, *ND6* and *ATP6* as well as nuclear-encoded subunits *NDUFA11* and *NDUFB8*. These genes were co-expressed and not only highly correlated to *PGC-1α* but also highly associated with different muscle fiber types and enzyme activities of complex I and II. Therefore, we propose that mitochondrial haplotype contributes to muscle fiber type and energy metabolism in porcine via altering the gene expression of OXPHOS subunits mediated by the nuclear-mitochondrial crosstalk. In addition, different haplotypes showed variation in complex I activity. It directly supported the link between haplotype and energy metabolism.

The disrupted Ca^{2+} homeostasis affects mitochondrial membrane biogenesis and hence metabolic stress[43]. Under conditions of oxidative stress, the expression of *ND6* is suppressed through methylation[44]. Consistent with our results, downregulated *ND6* expression in PiPP pigs has been associated with mutant *RYR1*-induced mitochondrial injury and oxidative stress[45]. These evidences supported the possibility of haplotype 8 could be linked to oxidative stress with altered mitochondrial transcription in PiPP pigs.

Our results showed some of the mitochondrial and nuclear-encoded OXPHOS transcripts were significantly correlated to at least one of the phenotypes including muscle fiber type, metabolic enzyme activities and pH. The mtDNA encoded OXPHOS gene expression was highly associated with muscle fiber types, which is consistent with the fact that STO muscle fibers in general contain more mitochondria[46]. It is worth mentioning that the mRNA levels of *ATP6, ND6*, and *ND2*, which were the top three genes correlated with *PGC-1α*, also significantly correlated with muscle fiber type. Hence, it raised the possibility that mitochondrial-encoded subunits with high correlation with *PGC-1a* showed effects on muscle fiber types. The muscle oxidative capacity not only relies on mitochondrial function but also on mitochondrial density[46]. Our measured mtDNA copy number was correlated positively with STO fibers and oxidative enzyme activity while negatively correlated with FTG fibers. The mtDNA copy number is related to mitochondrial oxidative capacity and adipocyte lipogenesis[47].

Conclusions

In summary, we investigated the mitochondrial DNA content and the expression of both mitochondrial and nuclear encoded OXPHOS genes in conjunction with post-mortem muscle phenotype, and metabolic enzyme activities in distinct haplotypes of pig breeds including Duroc, DuPi, PiNN, and PiPP. The most significant link between haplotypes or breeds to the muscle phenotype was found between the muscle fibers type and complex I. Specific expression pattern of mt transcript including ND1, ND6, and ATP6 and nuclear-encoded subunits NDUFA11 and NDUFB8 was identified and in turn play a role in muscle fibers type and enzyme activities of complex I. All of these changes in the PiPP haplotype 8 pigs may partially contribute to negative outcomes of meat quality such as pale soft exudative pork. PiPP pigs showed the lowest mtDNA copy number and reduced gene expression of many mitochondrial and nuclear encoded OXPHOS subunits compared to the other breeds. Our results provide valuable information on haplotype and breed-specific mitochondrial content variation as well as the molecular basis of mitochondrial respiration. Haplotypes could be linked to porcine energy metabolism at a functional level by altering gene expression of mitochondrial and nuclear OXPHOS subunits. Since haplotype 7 Pietrain pigs demonstrate a high ratio of FTO muscle fibers, while haplotype 8 pigs show the lowest complex I activity among all other haplotypes, implementing a selection of the favorable haplotype 7 along with the RYR1 locus in marker assisted selection program may further improve meat quality. Selection of the favorable haplotype can be used in marker assisted selection in pig breeding strategy.

Material and Methods

Sample collection and phenotypic measurement. The experiment and muscle collection were approved and authorized by the German and European animal welfare regulations for animal husbandry, transport, and slaughter[12–14]. All experimental procedures, including animal care and tissue sample collection, followed guidelines for safeguarding and good scientific practice in accordance with the German Law of Animal Protection, officially authorized by the Animal Care Committee and authorities [Niedersächsischen Landesamt für Verbraucherschutz und Lebensmittelsicherheit (LAVES) 33.42502/01-47.05].

Duroc, PiNN, PiPP, and DuPi pigs were raised to the age of 180 days at the University of Bonn. Muscle samples from each breed (Duroc, n = 15; DuPi, n = 16; PiNN, n = 12; PiPP, n = 15) were collected immediately (0 min postmortem) and 30 min after stunning (30 min postmortem) from LM between the 13th and 14th thoracic vertebrae. Samples were frozen in liquid nitrogen and stored at −80 °C until analysis.

We used the samples and all phenotypical traits from previously study which were measured as described[12–14]. In brief, the cryopreserved muscle samples were cutting into slices of 12 μm thickness. NADH tetrazolium reductase and Myofibrillar ATPase were stained to identify the muscle fiber types. 3 sections were used for calculating the percentage of the slow-twitch-oxidative (STO), fast-twitch-oxidative (FTO) and fast-twitch glycolytic (FTG) fibers by relating the number of counted fibers of each type to the total counted fiber number. For measurement of Metabolic Enzyme Activities, muscle samples were homogenized and all the experiments were finished within 2 h in duplicate. GP catalyzed the degradation of glycogen (2 mg/ml) to glucose-1-phosphate followed by the isomerization to glucose-6-phosphate (G-6-P) 2. GP activity was determined spectrophotometrically by the reduction of NADP+ (1.6 mM) to NADPH at 340 nm and pH 6.8 when G-6-P dehydrogenase (5 U/ml) catalyzed G-6-P to gluconate-6-phosphate. PFK catalyzes fructose-6-phosphate (3.0 mM) to fructose 1,6-bis-phosphate, which is split to glyceraldehyde-3-phosphate and dihydroxyacetonephosphate (DHAP). PFK activity was determined by the oxidation of NADH (1.6 mM) to NAD+ at 340 nm and pH 8.0 when glycerol-3-phosphate dehydrogenase (10 U/ml) /triosephosphate isomerase (100 U/ml) catalyzed DHAP to glycerol-3-phosphate. LDH activity was determined by the oxidation of NADH (150 μM) to NAD+ at 340 nm when LDH catalyzed pyruvate (1.2 mM) to lactate. CS catalyzes acetyl-CoA (0.1 mM) and oxaloacetate (0.5 mM) to citrate to liberate CoA. CS activity was determined by the irreversible reaction of CoA with 5,5′-Dithiobis-(2-nitrobenzoic acid; 0.1 mM) to thionitrobenzoic acid at 412 nm 3. Complex I was spectrophotometrically determined by following the oxidation of NADH (0.2 mM) to NAD+ at 340 nm. Complex II was determined at 600 nm following the reduction of 2, 6-dichlorophenolindophenol (DCPIP) by ubiquinol resulting from this reaction. Complex IV was determined by following the oxidation of reduced cytochrome c to the oxidized form at 550 nm and pH 7.0.

DNA and RNA extraction. Genomic DNA from LM samples was extracted. Total RNA was isolated from muscle samples using Tri-reagent and RNeasy Minikit (Qiagen, Hilden, Germany) with an on-column DNase

treatment according to the manufacturer's protocol. RNA integrity was assessed by 1% agarose gel electrophoresis. DNA and RNA concentration was measured on a NanoDrop ND-1000 spectrophotometer.

Mitochondria-specific primer design. Primers for the detection of mitochondrial DNA (mtDNA) copy number were carefully designed avoiding co-amplification of mitochondrial duplicated regions in the nuclear genome. Duplication of the mitochondrial genome in the nuclear genome was detected using BLASTN (http://www.ncbi.nlm.nih.gov)[48]. The mitochondrial sequence (Sus scrofa 10.2 download from NCBI: http://www.ncbi.nlm.nih.gov/ on 1.9.2015) was split into fragments of 150 bps in length with a 50 bps overlap and blasted against the reference genome to identify a 'unique' mitochondrial sequence based on a significant threshold of E-value < 0.1 and length > 100 bps. The result of duplicated regions was demonstrated using R package IdeoViz[49] and a cytogenetic map of pig chromosomes was extracted from ArkDB (http://www.thearkdb.org/arkdb)[50].

Absolute quantification of mtDNA copy number. The absolute quantification approach was used to determine mtDNA copy number. The mitochondrial genes ND1, ND2, and COX1 were used to quantify mtDNA copy number, whereas the nuclear gene glucagon gene (GCG), which is highly conserved between species and presents as a single copy, was used as the single-copy reference gene[25,51]. Primer sequences were presented in Supplementary Table 4 online. Mitochondrial and nuclear DNA standards were prepared separately using PCR products in seven serial dilutions at a dilution factor of 10. The amplified DNA fragments were purified with the QIAquick PCR Purification kit (Qiagen, Hilden, Germany). The purified products were quantified using a NanoDrop ND-1000 spectrophotometer (Peqlab, Erlangen, Germany). The copy number was calculated according to the following equation[52]:

$$copies/\mu l = \frac{ng/\mu l}{m} \tag{1}$$

$$m = n \times [1.096 \times 10^{-12}] \tag{2}$$

where m is the mass of a single copy and n is the target size in base pairs.

The absolute copy numbers of *ND1*, *ND2*, *COX1* and *GCG* were calculated based on their standard curves using the following equation:

$$copies = 10^{(Ct-b)/a} \tag{3}$$

where a is the slope and b is the intercept of the regression line.

Since *GCG* is a single copy nuclear gene, the mtDNA copies per nuclear genome were calculated as follows:

$$mtDNA\ copies/nuclear\ genome = \frac{mtDNA\ copies}{nuclearDNA\ copies} \tag{4}$$

The mtDNA copy number per nuclear genome was calculated separately using *ND1*, *ND2*, and *COX1*. The data was reported as a mean.

Measurement of gene expression. High-throughput gene-expression analysis with EvaGreen dye on a BioMark HD real-time PCR system was used to measure gene expression according to manufacturer's recommendations (Fluidigm, San Francisco, CA, USA). All reagents were purchased from Fluidigm unless otherwise indicated. Briefly, cDNA was synthesized from 2 µg of total RNA using Superscript II reverse transcriptase and oligo-dT (Invitrogen) with specific target amplification and exonuclease I (New England Biolabs) treatment. qPCR reactions were performed using a 96 × 96 dynamic array and integrated fluidic circuit. Each sample inlet was loaded with 2.5 µL of 2 × SsoFast EvaGreen supermix with low ROX (Biorad), 0.25 µL of 20×DNA-binding dye sample loading reagent, and 2.25 µL of specific target amplification and exonuclease-I-treated sample. Assays were performed for mitochondrial-coded complex I subunits *ND1, ND2, ND3,* and *ND4*, complex III subunit *CYB*, complex IV subunit *COX1*, ATP synthase subunit *ATP6*, and nuclear-encoded complex I subunits *NDUFA3, NDUFA11, NDUFA13, NDUFB8, NDUFS8,* and *NDUFV1*, complex IV subunit *COX7A2*, ATP synthase subunits *ATP5G1* and *ATP5L*, and master regulator *PGC-1α*. All measurements were performed in duplicate. Primer sequence information is available in Supplementary Table 4. Reference genes *ACTB, RPL32,* and *RPS11* were used to normalize expression values.

Sequence analysis. DNA from muscle samples of 53 animals (Duroc: N = 15, DuPi: N = 15, PiNN: N = 9, PiPP: N = 14) were sequenced using an ABI 3500 sequencer (Applied Biosystems Inc, Foster City, CA, USA). The D loop region was amplified using forward primer 5′-CTCCGCCATCAGCACCCAAAG-3′ and reverse primer 5′-GCACCTTGTTTGGATTRTCG-3′[53]. All sequences were aligned using Clustal × 2.1[54]. DNASP 5.1 software was used to analyze the haplotypes of all sequences[55]. The detailed information of haplotypes is shown in Supplementary Table 2. Only the haplotypes with at least three animals were included in the subsequent statistical analysis.

Statistical analysis. Data were analyzed using SAS 9.4 statistical software (SAS Institute) and the MIXED procedure. The statistical model included the effects of breed (Duroc, PiNN, PiPP, and DuPi), sex (male and female), time (0 and 30 min postmortem). With the same model, we also calculated with haplotype (Haplotypes 1, 4, 6, 7, and 8) instead of breeds. The model was combined with a repeated statement for the time component to take into account correlations among measurements made on the same animal at time 0 and 30 min postmortem.

Post hoc Tukey–Kramer method was used for multiple comparison adjustments. Results were reported as least-squares means (Lsmeans) with standard error (SE) and considered to be statistically significant if $p < 0.05$. Data were plotted using GraphPad Prism 5. The correlation coefficient (r) between gene expression and phenotypic measurement was calculated for all individuals. The correlation plots were generated in R.

References

1. Camus, M. F., Wolf, J. B., Morrow, E. H. & Dowling, D. K. Single Nucleotides in the mtDNA Sequence Modify Mitochondrial Molecular Function and Are Associated with Sex-Specific Effects on Fertility and Aging. *Curr Biol* **25**, 2717–2722 (2015).
2. Shi, Y., Buffenstein, R., Pulliam, D. A. & Van Remmen, H. Comparative studies of oxidative stress and mitochondrial function in aging. *Integr Comp Biol* **50**, 869–879 (2010).
3. Baykara, O., Sahin, S. K., Akbas, F., Guven, M. & Onaran, I. The effects of mitochondrial DNA deletion and copy number variations on different exercise intensities in highly trained swimmers. *Cell Mol Biol (Noisy-le-grand)* **62**, 109–115 (2016).
4. Falah, M. *et al.* The potential role for use of mitochondrial DNA copy number as predictive biomarker in presbycusis. *Ther Clin Risk Manag* **12**, 1573–1578 (2016).
5. Gao, Y. *et al.* Changes of the mitochondrial DNA copy number and the antioxidant system in the PBMC of hepatocellular carcinoma. *Chinese journal of applied physiology* **32**, 1–5 (2016).
6. Huang, J. *et al.* Decreased Peripheral Mitochondrial DNA Copy Number is Associated with the Risk of Heart Failure and Long-term Outcomes. *Medicine (Baltimore)* **95**, e3323 (2016).
7. Salminen, T. S. *et al*. Mitochondrial genotype modulates mtDNA copy number and organismal phenotype in Drosophila. *Mitochondrion* (2017).
8. Tsai, T. & St John, J. C. The role of mitochondrial DNA copy number, variants, and haplotypes in farm animal developmental outcome. *Domest Anim Endocrinol* **56**(Suppl), S133–146 (2016).
9. Picard, M., Hepple, R. T. & Burelle, Y. Mitochondrial functional specialization in glycolytic and oxidative muscle fibers: tailoring the organelle for optimal function. *Am J Physiol Cell Physiol* **302**, C629–641 (2012).
10. Greaser, M. L., Cassens, R. G., Briskey, E. J. & Hoekstra, W. G. Post-Mortem Changes in Subcellular Fractions from Normal and Pale, Soft, Exudative Porcine Muscle. 1. Calcium Accumulation and Adenosine Triphosphatase Activities. *Journal of Food Science* **34**, 120–124 (1969).
11. Scheffler, T. L., Matarneh, S. K., England, E. M. & Gerrard, D. E. Mitochondria influence postmortem metabolism and pH in an *in vitro* model. *Meat science* **110**, 118–125 (2015).
12. Werner, C., Natter, R., Schellander, K. & Wicke, M. Mitochondrial respiratory activity in porcine longissimus muscle fibers of different pig genetics in relation to their meat quality. *Meat science* **85**, 127–133 (2010).
13. Werner, C., Natter, R. & Wicke, M. Changes of the activities of glycolytic and oxidative enzymes before and after slaughter in the longissimus muscle of Pietrain and Duroc pigs and a Duroc-Pietrain crossbreed. *Journal of animal science* **88**, 4016–4025 (2010).
14. Krischek, C., Natter, R., Wigger, R. & Wicke, M. Adenine nucleotide concentrations and glycolytic enzyme activities in longissimus muscle samples of different pig genotypes collected before and after slaughter. *Meat science* **89**, 217–220 (2011).
15. Wimmers, K. *et al.* Relationship between myosin heavy chain isoform expression and muscling in several diverse pig breeds. *Journal of animal science* **86**, 795–803, https://doi.org/10.2527/jas.2006-521 (2008).
16. Essen-Gustavsson, B., Karlsson, A., Lundstrom, K. & Enfalt, A. C. Intramuscular fat and muscle fibre lipid contents in halothane-gene-free pigs fed high or low protein diets and its relation to meat quality. *Meat science* **38**, 269–277 (1994).
17. Karlsson, A. H., Klont, R. E. & Fernandez, X. Skeletal muscle fibres as factors for pork quality. *Livestock Production Science* **60**, 255–269 (1999).
18. Karlsson, A., Essen-Gustavsson, B. & Lundstrom, K. Muscle glycogen depletion pattern in halothane-gene-free pigs at slaughter and its relation to meat quality. *Meat science* **38**, 91–101, https://doi.org/10.1016/0309-1740(94)90098-1 (1994).
19. Yue, G. *et al.* Linkage and QTL mapping for Sus scrofa chromosome 6. *Journal of Animal Breeding and Genetics* **120**, 45–55 (2003).
20. Shen, Q. W., Underwood, K. R., Means, W. J., McCormick, R. J. & Du, M. The halothane gene, energy metabolism, adenosine monophosphate-activated protein kinase, and glycolysis in postmortem pig longissimus dorsi muscle. *Journal of animal science* **85**, 1054–1061 (2007).
21. Fujii, J. *et al.* Identification of a mutation in porcine ryanodine receptor associated with malignant hyperthermia. *Science* **253**, 448–451 (1991).
22. Liu, X. *et al.* Muscle Transcriptional Profile Based on Muscle Fiber, Mitochondrial Respiratory Activity, and Metabolic Enzymes. *Int J Biol Sci* **11**, 1348–1362 (2015).
23. Liu, X. *et al.* MicroRNA-mRNA regulatory networking fine-tunes the porcine muscle fiber type, muscular mitochondrial respiratory and metabolic enzyme activities. *BMC Genomics* **17**, 531 (2016).
24. Liu, X. *et al.* Molecular changes in mitochondrial respiratory activity and metabolic enzyme activity in muscle of four pig breeds with distinct metabolic types. *J Bioenerg Biomembr* **48**, 55–65 (2016).
25. Xie, Y. M. *et al.* Quantitative changes in mitochondrial DNA copy number in various tissues of pigs during growth. *Genet Mol Res* **14**, 1662–1670 (2015).
26. Shen, L. *et al.* Transcriptome Analysis of Liangshan Pig Muscle Development at the Growth Curve Inflection Point and Asymptotic Stages Using Digital Gene Expression Profiling. *PLoS One* **10**, e0135978 (2015).
27. Lindsay, D. P., Camara, A. K., Stowe, D. F., Lubbe, R. & Aldakkak, M. Differential effects of buffer pH on Ca(2+) -induced ROS emission with inhibited mitochondrial complexes I and III. *Front Physiol* **6**, 58 (2015).
28. Lana, A. & Zolla, L. Apoptosis or autophagy, that is the question: Two ways for muscle sacrifice towards meat. *Trends in Food Science & Technology* **46**, 231–241 (2015).
29. Dagda, R. K., Zhu, J., Kulich, S. M. & Chu, C. T. Mitochondrially localized ERK2 regulates mitophagy and autophagic cell stress: implications for Parkinson's disease. *Autophagy* **4**, 770–782 (2008).
30. Fukuoh, A. *et al.* Screen for mitochondrial DNA copy number maintenance genes reveals essential role for ATP synthase. *Mol Syst Biol* **10**, 734 (2014).
31. Giulivi, C. *et al.* Basal bioenergetic abnormalities in skeletal muscle from ryanodine receptor malignant hyperthermia-susceptible R163C knock-in mice. *J Biol Chem* **286**, 99–113 (2011).
32. Bonawitz, N. D., Clayton, D. A. & Shadel, G. S. Initiation and beyond: multiple functions of the human mitochondrial transcription machinery. *Mol Cell* **24**, 813–825 (2006).
33. Zollo, O., Tiranti, V. & Sondheimer, N. Transcriptional requirements of the distal heavy-strand promoter of mtDNA. *Proceedings of the National Academy of Sciences of the United States of America* **109**, 6508–6512 (2012).
34. Amiott, E. A. & Jaehning, J. A. Mitochondrial transcription is regulated via an ATP "sensing" mechanism that couples RNA abundance to respiration. *Mol Cell* **22**, 329–338 (2006).
35. Hunter, R. G. *et al.* Stress and corticosteroids regulate rat hippocampal mitochondrial DNA gene expression via the glucocorticoid receptor. *Proceedings of the National Academy of Sciences of the United States of America* **113**, 9099–9104 (2016).
36. Semenza, G. L. Hypoxia-inducible factor 1: oxygen homeostasis and disease pathophysiology. *Trends Mol Med* **7**, 345–350 (2001).
37. Ponsuksili, S. *et al.* Correlated mRNAs and miRNAs from co-expression and regulatory networks affect porcine muscle and finally meat properties. *BMC Genomics* **14**, 533 (2013).

38. Wolff, J. N. *et al*. Evolutionary implications of mitochondrial genetic variation: mitochondrial genetic effects on OXPHOS respiration and mitochondrial quantity change with age and sex in fruit flies. *J Evol Biol* **29**, 736–747 (2016).

39. Yu, G. *et al*. Mitochondrial Haplotypes Influence Metabolic Traits in Porcine Transmitochondrial Cybrids. *Sci Rep* **5**, 13118 (2015).

40. Pello, R. *et al*. Mitochondrial DNA background modulates the assembly kinetics of OXPHOS complexes in a cellular model of mitochondrial disease. *Hum Mol Genet* **17**, 4001–4011 (2008).

41. LeBleu, V. S. *et al*. PGC-1alpha mediates mitochondrial biogenesis and oxidative phosphorylation in cancer cells to promote metastasis. *Nat Cell Biol* **16**(992-1003), 1001–1015 (2014).

42. Marusich, M. F. *et al*. Expression of mtDNA and nDNA encoded respiratory chain proteins in chemically and genetically-derived Rho0 human fibroblasts: a comparison of subunit proteins in normal fibroblasts treated with ethidium bromide and fibroblasts from a patient with mtDNA depletion syndrome. *Biochim Biophys Acta* **1362**, 145–159 (1997).

43. Biswas, G. *et al*. Retrograde Ca2+ signaling in C2C12 skeletal myocytes in response to mitochondrial genetic and metabolic stress: a novel mode of inter-organelle crosstalk. *EMBO J* **18**, 522–533 (1999).

44. Shock, L. S., Thakkar, P. V., Peterson, E. J., Moran, R. G. & Taylor, S. M. DNA methyltransferase 1, cytosine methylation, and cytosine hydroxymethylation in mammalian mitochondria. *Proceedings of the National Academy of Sciences of the United States of America* **108**, 3630–3635, https://doi.org/10.1073/pnas.1012311108 (2011).

45. Jin, O. *et al*. RyR1 mutation associated with malignant hyperthermia facilitates catecholaminergic stress-included arrhythmia via mitochondrial injury and oxidative stress (893.8). *The FASEB Journal* **28**, 893.898 (2014).

46. Gueguen, N., Lefaucheur, L., Fillaut, M., Vincent, A. & Herpin, P. Control of skeletal muscle mitochondria respiration by adenine nucleotides: differential effect of ADP and ATP according to muscle contractile type in pigs. *Comp Biochem Physiol B Biochem Mol Biol* **140**, 287–297 (2005).

47. Kaaman, M. *et al*. Strong association between mitochondrial DNA copy number and lipogenesis in human white adipose tissue. *Diabetologia* **50**, 2526–2533 (2007).

48. Altschul, S. F., Gish, W., Miller, W., Myers, E. W. & Lipman, D. J. Basic local alignment search tool. *J Mol Biol* **215**, 403–410 (1990).

49. IdeoViz: Plots data (continuous/discrete) along chromosomal ideogram v. R package version 1.6.0 (2014).

50. Hu, J. *et al*. The ARKdb: genome databases for farmed and other animals. *Nucleic Acids Res* **29**, 106–110 (2001).

51. Wang, J. *et al*. A genome-wide detection of copy number variations using SNP genotyping arrays in swine. *BMC Genomics* **13**, 273 (2012).

52. Chan, S. W., Chevalier, S., Aprikian, A. & Chen, J. Z. Simultaneous quantification of mitochondrial DNA damage and copy number in circulating blood: a sensitive approach to systemic oxidative stress. *Biomed Res Int* **2013**, 157547 (2013).

53. Jin, L. *et al*. Mitochondrial DNA evidence indicates the local origin of domestic pigs in the upstream region of the Yangtze River. *PLoS One* **7**, e51649 (2012).

54. Thompson, J. D., Gibson, T. J., Plewniak, F., Jeanmougin, F. & Higgins, D. G. The CLUSTAL_X windows interface: flexible strategies for multiple sequence alignment aided by quality analysis tools. *Nucleic Acids Res* **25**, 4876–4882 (1997).

55. Librado, P. & Rozas, J. DnaSPv5: a software for comprehensive analysis of DNA polymorphism data. *Bioinformatics* **25**, 1451–1452 (2009).

Acknowledgements

Author Contributions

X.L. analysed the data and drafted the manuscript; F.H. helped in analyzing duplicated region of the mitochondrial genome in the nuclear genome. N.T., E.M., and K.W. helped in sampling and data collection and drafting the manuscript; S.P. discussed and contributed to data interpretation and helped in drafting the manuscript. All authors have read and approved the final manuscript.

Additional Information

Supplementary information accompanies this paper at https://doi.org/10.1038/s41598-017-14491-w.

Competing Interests: The authors declare that they have no competing interests.

Publisher's note: Springer Nature remains neutral with regard to jurisdictional claims in published maps and institutional affiliations.

ANNEX B

List of figures

List of figures

ANNEX C

List of abbreviations

List of abbreviations

Abeta	amyloid beta
ADP	adenosine diphosphate
AMP	adenosine 5'-monophosphate
AMPK	AMP-activated protein kinase
ANT	adenine nucleotide translocators
APP	amyloid precursor protein
AR	androgen receptor
ATP	adenosine triphosphate
ATP5I	ATP synthase, mitochondrial F0 complex, subunit E
BMP7	bone morphogenetic protein 7
BMPR2	bone morphogenetic protein receptor type II
CAPN3	calpain-3
CAPN6	calpain-6
CDs	coding sequences
CMYA5	cardiomyopathy associated 5
CPT1a	carnitine palmitoyltransferase 1a
CS	citrate synthase
CYP24A1	cytochrome P450, family 24, subfamily A, peptide 1
DABG	detection above background
DEGs	differentially expressed genes
DuPi	F2 crossbred Duroc–Pietrain homozygous-negative for MHS
ECM	extracellular matrix
FDR	false discovery rate
FTG	fast-twitch glycolytic
FTO	fast-twitch oxidative
GCG	glucagon
GO	gene ontology.
GP	glycogen phosphorylase
GR	glucocorticoid receptor
GSK3A	glycogen synthase kinase 3 alpha
GYS1	glycogen synthase 1
Hb	Hemoglobin
HSPA2	heat shock 70kDa protein 2
IGF-1R	insulin-like growth factor 1 receptor
IMP	inosine 5'-monophosphate
INSR	insulin receptor
IRS1	insulin receptor substrate 1
IRS2	insulin receptor substrate 2
LDH	lactate dehydrogenase
LGMD2A	limb-girdle muscular dystrophy type 2A
LM	longissimus muscle
LRPPRC	Leucine-rich pentatricopeptide repeat containing
Lsmeans	least-squares means
Mb	Myoglobin
MCU	mitochondrial calcium uniporter
ME3	malic enzymes 3

MHS	malignant hyperthermia susceptibility
miRNA	microRNA
MRA	mitochondrial respiratory activity
MSTN	myostatin
mt	mitochondrial
MTCH1	mitochondrial carrier 1
mtDNA	mitochondrial DNA
NRFs	nuclear respiratory factors
OXPHOS	oxidative phosphorylation
PDHA1	pyruvate dehydrogenase alpha 1
PEKFB2	fructose 2, 6–bisphosphatase 2
PFK	phosphofructokinase
PGC-1α	PPARG coactivator 1 alpha
PHB2	prohibitin 2
PiNN	malignant hyperthermia syndrome (MHS)-negative Pietrain
PiPP	malignant hyperthermia syndrome (MHS)-positive Pietrain
PPARGC1A	peroxisome proliferator-activated receptor gamma coactivator 1 alpha
PPP3CA	protein phosphatase 3 catalytic subunit alpha isoform
pre-miRNA	precursor miRNA
PSAP	presenilin 1-associated protein
PSE	pale soft exudative
qPCR	quantitative polymerase chain reaction
RB1	retinoblastoma 1
RCI	respiratory control index
RISC	RNA-induced silencing complex
RMA	robust multichip average
ROS	reactive oxygen species
rRNA	ribosomal RNA
RYR1	ryanodine receptor 1
SE	standard error
SERCA	sarcoplasmic reticulum Ca2+ ATPase
SR	sarcoplasmic reticulum
SRL	sarcalumenin
STA	specific target amplification
STO	slow-twitch oxidative
TFAM	mitochondrial transcription factor A
Th	thoracic vertebrae
THRB	thyroid hormone receptor beta
TOM	topological overlap matrix
tRNA	transfer RNA
UBFD1	ubiquitin family domain containing 1
UPS	ubiquitin proteasome system
UQCC	ubiquinol-cytochrome c reductase complex chaperone
USP24	ubiquitin specific peptidase 24
UTR	untranslated region
VDAC	voltage-dependent anion channel
WGCNA	weighted gene co-expression network analysis

ANNEX D

Acknowledgements

Acknowledgements

The PhD study is a precious experience in my whole life and I love every minute of it. Firstly, I would like to express my very great appreciation to my dear supervisor at Leibniz Institute for Farm Animal Biology (FBN), PD. Dr. Siriluck Wimmers, for giving me the opportunity to pursue a Ph.D degree in Germany. Her profound knowledge, rigorous academic attitude, kindness, encouragement, patience and excellent supervision guided and supported me throughout my entire study, for which I will always be grateful. She set a good example as an excellent scientist, for which I will always learn from her.

With my deepest gratitude, I would also like to thank Prof. Dr. Karl Schellander, the Institute of Animal Science, Animal Breeding and Husbandry Group, University of Bonn, for his willingness to be my co-supervisor.

My sincerely appreciation goes to Prof. Dr. Klaus Wimmers for his valuable advices, helpful discussions and proof reading throughout the manuscript. It has been a great learning opportunity for me.

I would also like to sincerely acknowledge Prof. Dr. Karl-Heinz Südekum, the Institute of Animal Science, Animal Nutrition Group, University of Bonn and Prof. Dr. Brigitte Petersen, the Institute of Animal Science, Preventive Health Management Group, University of Bonn for their agreement to be in the thesis committee.

My grateful thanks are also extended to Dr. Nares Trakooljul and Dr. Eduard Murani, for their kind support and proof reading for the manuscript.

I would also like to sincerely thank PD. Dr. Carsten Krischek, the Institute of Food Quality and Food safety, University of Veterinary Medicine Hannover and Prof. Dr. Michael Wicke, Department of Animal Science, Quality of Food of Animal Origin, Georg-August-University Goettingen for providing the phenotypical measurement data which is significantly important in this study. Measurements of phenotypic traits were supported by the German Research Foundation (Deutsche Forschungsgemeinschaft, DFG) in a project initiated and led by Prof. Dr. Michael Wicke (Department of Animal Science, Quality of Food of Animal Origin, Georg-August-University Goettingen) who has left us forever.

Many thanks are to Mrs. Annette Jugert, Mrs. Joana Bittner, Mrs. Nicole Gentz and Mrs. Marlies Fuchs for their excellent technical help, to Dr. Yang Du and Mr. Frieder Hadlich